TP 10845E

Prepared for:

Transportation
Development Centre

Transport Canada

CA1
DTR290-
91
R26

41.D

FTL FLEET TECHNOLOGY LIMITED

92-01007/

CA1
DTR290-
91
R26

469173

41.D

Resistance and Propulsive Performance Trials of the MV Terry Fox and MV Ikaluk in Level Ice

TP 10845E

February 1991

Prepared for:

The Transportation Development Centre
Policy and Coordination Group
Transport Canada

AUG 27

Prepared by:

Fleet Technology Limited
#16 - 6325 11th. Street S.E.
Calgary, Alberta
T2H 2L6

D.N. Bruce Cowper

469173

DSN 469168

DISCLAIMER

The contents of this report reflect the views of Fleet Technology Limited and not necessarily the official view or opinions of the Transportation Development Centre of Transport Canada, Policy and Coordination Group.

Un sommaire en français de ce rapport est inclus avant la table des matières.

Approved by:

Ian Glen, President

Transport Canada / Transports Canada

PUBLICATION DATA FORM

1. Transport Canada Publication No.	2. Project No.	3. Recipient's Catalogue No.
TP 10845E	7622	

4. Title and Subtitle	5. Publication Date
Resistance and Propulsive Performance Trials of the M.V. Terry Fox and M.V. Ikaluk in Level Ice	February 1991
	6. Performing Organization Document No. C3622C
7. Author(s)	8. Transport Canada File No.
D.N.B. Cowper, G. Comfort, I.F. Glen, R. Ritch	ZCD 1460 - 305
9. Performing Organization Name and Address	10. DSS File No.
Fleet Technology Limited 16, 6325 11th Street S.E. Calgary, Alberta T2H 2L6	048SZ.T8200-0-0507
	11. DSS or Transport Canada Contract No. T8200-0-0507/01-SZ
12. Sponsoring Agency Name and Address	13. Type of Publication and Period Covered
Transportation Development Centre 200 René Lévesque Blvd. West, West Tower, Suite 601 Montreal, Quebec H2Z 1X4	Final Report
	14. Project Officer P. L. Sémery

15. Supplementary Notes (Funding programs, titles of related publications, etc.)

16. Abstract

It has always been recognized that the key to a full understanding of icebreaker powering performance is an accurate knowledge of its constituent parts; ship resistance, propulsor performance and the hydrodynamic (including ice) interaction between the two. To obtain more information in this regard a unique set of full-scale resistance and propulsive performance tests was carried out by Fleet Technology Limited in association with Gulf Canada Resources. The main objectives of this project were to measure and report on the full-scale resistance and propulsive performance, and on the shaftline vibration responses during ice-propeller interaction.

Two CASPPR Arctic Class IV vessels, the M.V. Terry Fox and the M.V. Ikaluk were selected for testing. One has ducted propellers, the other open propellers, and both are operated by Gulf Canada Resources Limited. Three days of dedicated tests were conducted in Herschel Basin, Yukon from June 11-13, 1990.

The results of this study indicated the following for each of the vessels:

- The resistance vs speed relationship
- The self-propulsion power and thrust vs speed relationship
- The thrust deduction vs speed relationship
- The shaftline vibrational response (torque and thrust) of an open and ducted propeller during ice-propeller interaction, in the same ice conditions.

The results from the full-scale towing tests and the self-propulsion tests can be used to verify or revise scaling laws for icebreaker powering performance. In addition, the results provide data for the calibration of empirical, model test, and numerical model methods of performance prediction. Further insight into the problem of ice/propeller interaction and the corresponding shaftline response was also attained for both open and ducted controllable pitch side-by-side operation of the vessels.

17. Key Words	18. Distribution Statement
Propeller-Ice Interaction, propulsion shaftline vibration, ice resistance, hydrodynamic forces	Limited number of copies available from the Transportation Development Centre on request.

19. Security Classification (of this publication)	20. Security Classification (of this page)	21. Declassification (date)	22. No. of Pages	23. Price
Unclassified	Unclassified	—	xv, 195,App	—

TDC/CDT 79-005 Rev 88

Canada

Transports Canada / Transport Canada

FORMULE DE DONNÉES POUR PUBLICATION

1. N° de la publication de Transports Canada	2. N° de l'étude	3. N° de catalogue du destinataire
TP 10845E	7622	

4. Titre et sous-titre	5. Date de la publication
Resistance and Propulsive Performance Trials of the MV Terry Fox and MV Ikaluk in Level Ice	Février 1991
	6. N° du document de l'organisme exécutant: 3622C

7. Auteur(s)	8. N° de dossier — Transports Canada
D.N.B. Cowper, G. Comfort, I.F. Glen, R. Ritch	ZCD 1460-305

9. Nom et adresse de l'organisme exécutant	10. N° de dossier — ASC
Fleet Technology Limited #16 - 6325 11th Street S.E. Calgary (Alberta) B3J 2Y3	048SZ.T8200-0-0507
	11. N° de contrat — ASC ou Transports Canada: T8200-0-0507/01-SZ

12. Nom et adresse de l'organisme parrain	13. Genre de publication et période visée
Centre de développement des transports (CDT) 200 ouest, boul. René-Lévesque Tour ouest, suite 601 Montréal (Québec) H2Z 1X4	Rapport final
	14. Agent de projet: P.L. Sémery

15. Remarques additionnelles (Programmes de financement, titres de publications connexes, etc.)

16. Résumé

On a toujours su que la puissance développée d'un navire dépendait de trois facteurs qu'il fallait connaître avec précision : la résistance de carène, le rendement du système propulsif et l'interaction hydrodynamique entre le navire et le milieu dans lequel il évolue. Des essais uniques en leur genre ont été menés conjointement par la Fleet Technology Limited et Gulf Canada Resources dans le but de réaliser les deux grands objectifs suivants: mesurage en vraie grandeur de la résistance de carène et du rendement du système propulsif et réponse vibratoire des lignes d'arbres durant les opérations de déglaçage.

Deux navires de cote arctique IV aux termes de la Loi sur la prévention de la pollution des eaux arctiques, le M.M. Terry Fox et le M.M. Ikaluk, ont été sélectionnés et préparés aux essais, l'un équipé d'hélices sous tuyère, l'autre pas, et tous deux exploités par la Gulf Canada Resources Ltd. Pendant trois jours, du 11 au 13 juin 1990, des essais ont été menés à bord, dans le bassin Mackenzie au Yukon.

La recherche a débouché sur des résultats montrant, pour chacun des navires, ce qui suit:

- la résistance de carène en fonction de la vitesse,
- la puissance d'autopropulsion et la poussée en fonction de la vitesse,
- la force de succion en fonction de la vitesse,
- la réponse vibratoire des lignes d'arbres aux sollicitations des glaces (couple et poussée) dans le cas d'hélices avec et sans tuyère et dans des conditions glacielles identiques.

Les résultats des essais de remorquage et d'autopropulsion en mer serviront à vérifier ou à affiner les facteurs de similitude applicables au mesurage de la puissance développée par des brise-glace. Ils peuvent également servir au calage des données tirées des méthodes de prévision empiriques, numériques ou par des essais sur maquettes. La recherche a également permis d'approfondir le phénomène d'interaction dynamique hélice-glaces et la réponse de la ligne d'arbres aux sollicitations correspondantes, dans le cas des hélices à pas variable protégées ou non par tuyère, par des essais menés sur les deux navires placés côte à côte et avançant à vitesse égale.

17. Mots clés	18. Diffusion
Interaction hélice-glaces, vibrations de la ligne d'arbres, résistance des glaces, propulsion, forces hydrodynamiques.	Le Centre de développement des transports dispose d'un nombre limité d'exemplaires.

19. Classification de sécurité (de cette publication)	20. Classification de sécurité (de cette page)	21. Déclassification (date)	22. Nombre de pages	23. Prix
Non classifiée	Non classifiée	--	--	--

CDT/TDC 79-005 Rév 88

Canada

PROJECT TEAM

This program has been conducted with the support and on behalf of four contributory participants: the Transportation Development Centre - Policy and Coordination Group, BeauDril Limited a Division of Gulf Canada Resources Limited, the Canadian Coast Guard, and NRC's Institute of Marine Dynamics.

Fleet Technology Limited acted as principal contractor to the project with overall responsibility for the design and installation of the instrumentation, the collection of the data in the field, and the subsequent analysis and reporting of the results. The following subcontractors were commissioned by Fleet Technology Limited:

BeauDril Limited

Acted as the principal subcontractor to the project with responsibility for the operation of the M.V. Ikaluk and M.V. Terry Fox.

AKAC Inc.

Assisted with certain aspects of the program design, testing, and data analysis.

MT&T Testing Ltd.

Assisted with the instrumentation installation and specification.

Kristi Maritime

Assisted with the towing design and collection of data.

The personnel involved in the management and execution of this project were:

Fleet Technology Limited:

Mr. Bruce Cowper	Project Manager
Mr. Ian Glen	Project Auditor
Mr. Ron Ritch	Project Engineer
Mr. Mike Steele	Computer Programmer
Mr. George Comfort	Ice Engineer
Mr. Mike Deparois	Technician
Mr. Brad Percival	Technician
Ms. Kathleen Irvine	Secretary

AKAC Inc.:

Dr. Robin Browne
Dr. Arno Keinonen

MT&T Testing Ltd.: Mr. Nick DeRuiter

Kristi Maritime: John Carter

ACKNOWLEDGEMENTS

This project was conducted under the auspices of the Transportation Development Centre (TDC), Policy and Coordination Group, Transport Canada, and the Canadian Coast Guard. The TDC Project Officer for this work was Mr. Pierre Sémery and the authors wish to acknowledge Mr. Sémery's contribution in helping to define the project and in providing very valuable scientific direction to the program. The Coast Guard Project Officer was Ernst Radloff whose input was very much appreciated. Mr. David Cumming and Mr. Robert Pallard of the Institute for Marine Dynamics (IMD) assisted in the various aspects of the trials program in the Arctic, and deserve special acknowledgement.

SUMMARY

It has always been recognized that the key to a full understanding of ship powering performance is an accurate knowledge of its constituent parts; ship resistance, propulsor performance and the hydrodynamic (including ice) interaction between the two. This, however, requires direct measurement of ship resistance, which has historically proved very difficult on technical, logistic and cost grounds. As a result of this requirement, a unique set of full-scale resistance and propulsive performance tests was carried out by Fleet Technology Limited in association with Gulf Canada Resources. The two main objectives of this project were to measure and report on:

1. The full-scale resistance and propulsive performance in level ice of two modern icebreakers (M.V. Ikaluk and M.V. Kalvik), incorporating both open and ducted propulsion.
2. The effect of the presence of ice on the interaction forces between the hulls and propulsion systems.

Two CASPPR Arctic Class IV vessels, the M.V. Terry Fox and the M.V. Ikaluk were selected for testing. One has ducted propellers, the other open propellers, and both are operated by Gulf Canada Resources Limited. Each vessel has two shafts, both of which were instrumented for torque, thrust, and rpm. Propeller pitch, engine fuel rack, and rudder angle positions were recorded. Two strain gauges on the port nozzle of the M.V. Ikaluk, which had been installed for tests conducted in 1989, were re-connected to measure the thrust contribution from the nozzle. A micro-wave positioning system was deployed in the test area to measure the position and speed of the vessels. An instrumented shackle in the towing cable was used to measure the towing force during dedicated towing tests. All measurements, including the ships' positions were recorded on the same time base by digital data acquisition systems installed on each vessel.

Three days of dedicated tests were conducted in Herschel Basin, Yukon from June 11-13 , 1990. Five towing trials and over fifty self-propulsion tests were performed. The average ice thickness was a uniform 1.55 m with negligible snow cover, and a flexural strength of 150 kPa. Hull roughness and ice-hull friction factors were measured during the tests. For "lead ship" towing trials, the vessels were positioned 700 m apart with an unbroken ice sheet between them, with a towing cable connecting them. In addition towing tests were conducted with both vessels in a broken channel. Testing the vessels in the same ice conditions enabled the response of the two different propulsion systems to be compared directly.

The following key results were obtained by the analysis of the data collected:

1. The maximum resistance for the M.V. Terry Fox was measured to be 0.95 MN at 3.3 knots. The maximum resistance for the M.V. Ikaluk was measured to be 0.77 MN at 2.77 knots.

2. The maximum self-propulsion speed attained was 3.6 knots (thrust of 1.34 MN) for the M.V. Terry Fox, and 2.3 knots (thrust of 0.89 MN) for the M.V. Ikaluk.

3. The resistance and power of the two vessels varied linearly with velocity over the tested speed ranges (0.5- 3.6 knots).

4. The thrust deduction fraction in ice is approximately the same as that for the open water overload condition at the corresponding speed and resistance for the M.V. Terry Fox. It ranged from 0.05 at 0.5 knots to 0.25 at 3.6 knots.

5. The thrust deduction fraction for the M.V. Ikaluk was much higher in ice than in open water. It ranged from 0.05 at 0.5 knots to 0.16 at 2.0 knots in ice, and was low (in the range of 0.02 to 0.05) in the open water overload condition. In the open water overload condition the thrust deduction was approximately equal to the hydrodynamic thrust provided by the nozzle.

6. The shaftline of the ducted propeller (M.V. Ikaluk) was measured to have significantly higher axial (thrust) vibrations than the open screw propeller (M.V. Terry Fox).

7. There was not a significant difference in the relative peak shaft torques measured between the nozzled and open screw propellers. The peak shaft torque during ice milling was measured to be 150% and 134% of the MCR torque for the M.V. Ikaluk and the M.V. Terry Fox respectively.

8. Generally more ice-propeller interaction was noticed on the nozzled vessel than the open screw vessel. Both types of shaftlines had approximately the same high damping present in the axial and torsional modes.

The results from the full-scale towing tests and the self-propulsion tests can be used to verify or revise scaling laws for icebreaker powering performance. In addition the results provide data for the calibration of empirical, model test, and numerical model methods of performance prediction. Further insight into the phenomenon surrounding ice/propeller interaction and the corresponding shaftline response was also attained for both open and ducted controllable pitch propellers, by direct, side by side operation of the vessels.

SOMMAIRE

On a toujours su que la puissance développée d'un navire dépendait de trois facteurs qu'il fallait connaître avec précision: la résistance de carène, le rendement du système propulsif et l'interaction hydrodynamique entre le navire et le milieu dans lequel il évolue. Le plus difficile à mesurer directement a depuis toujours été la résistance de carène pour des raisons techniques, logistiques et financières. Des essais uniques en leur genre ont été menés conjointement par la Fleet Technology Limited et Gulf Canada Resources dans le but de réaliser les deux objectifs suivants:

1. Mesurage en vraie grandeur de la résistance de carène et du rendement du système propulsif dans une glace uniforme à bord de deux brise-glace modernes (N.M. Ikaluk et Kalvik), l'un équipé d'hélices sous tuyère, l'autre pas.

2. Mesurage de l'effet produit par les glaces sur le rendement du système propulsif.

Deux navires de cote arctique IV aux termes de la Loi sur la prévention de la pollution des eaux arctiques, ont été sélectionnés et préparés aux essais: les N.M. Terry Fox et Ikaluk, l'un équipé d'hélices sous tuyère, l'autre pas, et tous deux exploités par la Gulf Canada Resources Ltd. Les deux lignes d'arbres de ces navires avaient été instrumentés pour le mesurage du couple moteur, de la poussée et du régime moteur. Ont aussi été enregistrés le pas des hélices, la position de la rampe d'injection et les angles de braquage du gouvernail. Afin de pouvoir mesurer l'apport des tuyères à l'effort propulsif total, les deux capteurs extensométriques sur la tuyère bâbord de l'Ikaluk ont été remis en oeuvre (ils avaient été déconnectés à l'issue des essais de 1989). La position et la vitesse des navires ont été enregistrés grâce à un système de radionavigation hyperfréquences. Enfin, la manille de remorque a été instrumentée, permettant de déterminer l'effort de remorquage exercé lors des essais dédiés. Toutes ces mesures ainsi que les points observés ont été enregistrés sur la même base de temps par la chaîne de mesure numérique à bord des navires.

Durant les essais dédiés d'une durée de trois jours, les 11, 12 et 13 juin 1990, dans la baie Herschel au Yukon, cinq essais de remorquage et plus de cinquante essais d'autopropulsion ont été menés dans une glace uniforme de 1,55 m d'épaisseur moyenne, presque pas recouverte de neige et d'une résistance à la rupture en flexion de 150 kPa. Les coefficients de rugosité de la coque et de frottement coque-glace ont été mesurés. Durant les essais de remorquage, les deux navires à 700 m de distance et reliés par une remorque étaient séparés par un champ de glace encore intact. D'autres essais de remorquage ont eu lieu, durant lesquels les deux navires se trouvaient dans un chenal ouvert. Ces essais dans des conditions glacielles identiques ont permis de comparer le rendement des deux systèmes propulsifs, qui ne se ressemblent pas.

L'analyse des données recueillies a permis de faire les principales constatations suivantes:

1. La résistance de carène maximale mesurée a été de 0,95 MN à 3,3 noeuds pour le Terry Fox et de 0,77 MN à 2,77 noeuds pour l'Ikaluk.

2. La vitesse d'autopropulsion maximale a été de 3,6 noeuds à 1,34 MN de poussée, et de 2,3 noeuds à 0,89 MN de poussée, respectivement.

3. Tant la résistance de carène que la puissance développée ont varié de manière linéaire avec la vitesse sur toute la plage des vitesses pratiquées (0,5 à 3,6 noeuds).

4. Dans le cas du Terry Fox, le coefficient de succion dans la glace et dans des conditions de surcharge en eau libre a été à peu près le même, à vitesse et résistance de carène égales. Il a varié entre 0,05 à 0,5 noeud et 0,25 à 3,6 noeuds.

5. Dans le cas de l'Ikaluk, le coefficient de succion a été plus élevé dans la glace que dans l'eau libre, ayant varié entre 0,05 à 0,5 noeud et 0,16 à 2 noeuds dans la glace; et faible (entre 0,02 et 0,05) dans des conditions de surcharge en eau libre. Dans ces conditions, la force de succion a été à peu près égale à la poussée hydrodynamique produite par la tuyère.

6. Les vibrations axiales de la ligne d'arbres dues à la poussée ont été beaucoup plus fortes dans le cas de l'Ikaluk (hélice sous tuyère) que dans celui du Terry Fox (hélice sans tuyère).

7. Aucune différence marquée dans les valeurs maximales du couple, mesurées dans les deux cas. En situation de broyage des glaces, la valeur maximale du couple a atteint 1,5 et 1,34 fois le couple correspondant à la puissance maximale continue, pour l'Ikaluk et le Terry Fox, respectivement.

8. Règle générale, les interactions hélice-glaces ont été plus fortes avec les hélices sous tuyère, tandis que la ligne d'arbres dans les deux navires a produit à peu près le même niveau d'amortissement des vibrations tant axiales que de torsion.

Les résultats des essais de remorquage et d'autopropulsion en mer serviront à vérifier ou à affiner les facteurs de similitude applicables au mesurage de la puissance développée par des brise-glace. Ils peuvent également servir au calage des données tirées des méthodes de prévision empiriques, numériques ou par des essais sur maquettes. La recherche a également permis d'approfondir le phénomène d'interaction dynamique hélice-glaces et la réponse de la ligne d'arbres aux sollicitations correspondantes, dans le cas des hélices à pas variable protégées ou non par tuyère, par des essais menés sur les deux navires placés côte à côte et avançant à vitesse égale.

TABLE OF CONTENTS

		Page
1.	INTRODUCTION	1
2.	INSTRUMENTATION	
	2.1 Vessel Instrumentation	7
	2.2 Towline Instrumentation	7
	2.3 Ship Positioning System	11
	2.4 Data Acquisition	11
		12
3.	ICE CONDITIONS	
	3.1 Test Location and Ice Cover Description	14
	3.2 Ice Thickness	15
	3.3 Ice Salinity and Temperature Profile and Mechanical Properties	19
	3.3.1 Ice Salinity and Temperature Profile	22
	3.3.2 Predicted Mechanical Properties of Ice	22
	3.4 Ice-Hull Friction Factor	26
	3.4.1 Measurement Technique	39
	3.4.2 Hull Surface Condition and Friction Factor Test Locations	39
	3.4.3 Test Results	39
	3.5 Ice Breaking Pattern	45
		52
4.	FULL-SCALE TESTS	
	4.1 Trials Planning and Design	56
	4.2 Towing Design and Execution	56
	4.3 Data Collection	73
	4.4 Trials Description	79
		80
5.	DATA AND RESULTS	
	5.1 Summary of Trials Results	85
	5.2 Comparisons of Results With Other Methods	85
	5.3 Data Processing	88
	5.4 Towing Tests	92
	5.5 Self Propulsion Tests	97
	5.6 Open Water Overload Tests	118
	5.7 Thrust Deduction Fractions	145
	5.8 Shaftline Response to Ice/Propeller Interaction	155
		161
6.	CONCLUSIONS	186
7.	BIBLIOGRAPHY	188
APPENDIX	M.V Terry Fox and M.V. Ikaluk Trials Log	

List of Figures

Figure 1.1	General Arrangement of M.V. Ikaluk		3
Figure 1.2	General Arrangement of M.V. Terry Fox		4
Figure 2.1.1	M.V. Ikaluk Shaftline Instrumentation		8
Figure 2.1.2	M.V. Terry Fox Shaftline Instrumentation		9
Figure 2.3.1	Arrangement of Microwave Positioning System Base Stations		13
Figure 3.1.1	Test Area Location Map		16
Figure 3.2.1	Ice Thickness Measurement Location Map		21
Figure 3.3.1	Ice Temperature - Salinity - Brine Volume Profile		23
Figure 3.3.2.1	Sea Ice Strength - In - Situ Cantilever Beam Test (after Lane, 1980)		29
Figure 3.3.2.2	Sea Ice Elastic Modulus as Measured by Dynamic Tests		32
Figure 3.3.2.3	Effective In-Situ Elastic Modulus		32
Figure 3.4.1.1	Tribometer Schematic		40
Figure 3.4.3.1	Sample Output from Tribometer Test		46
Figure 3.4.3.2	Friction Factor versus Hull Surface Roughness		51
Figure 4.1.1	Determination of Propulsion Performance Parameters		57
Figure 4.1.2	Propulsion Performance Characteristics		58
Figure 4.1.3	Trials Configurations		59
Figure 4.1.4	Components of Thrust During ice Transit		63
Figure 4.1.5	Power to Thrust Ratio Comparisons		63
Figure 4.1.6	M.V. Terry Fox Level Ice Resistance Estimate		68
Figure 4.1.7	M.V. Ikaluk Level Ice Resistance Estimate		69
Figure 4.1.8	M.V. Ikaluk and M.V. Terry Fox Tow Rope Pull Estimates		70
Figure 4.1.9	Towing Diagram: M.V. Terry Fox Towing M.V. Ikaluk		71
Figure 4.1.10	Towing Diagram: M.V. Ikaluk Towing M.V. Terry Fox		72
Figure 4.2.1	Details of Smit Bracket		75
Figure 4.4.1	Trials Testing Area		81
Figure 4.4.2	Planned Towing Trials		82
Figure 4.4.3	Towing and Self-Propulsion Trials Conducted		84
Figure 5.3.1	Unfiltered and Filtered Ship Speed Time History		95
Figure 5.3.2	Unfiltered and Filtered Towline Force Time History		96
Figure 5.4.1	Resistance in Ice vs Velocity: M.V. Terry Fox and M.V. Ikaluk		98
Figure 5.4.2	Resistance in Ice vs Velocity: M.V. Terry Fox		100
Figure 5.4.3	Speed and Towing Force: M.V. Terry Fox	Tow No. 1	102
Figure 5.4.4	Total Shaft Thrust: M.V. Terry Fox	Tow No. 1	103
Figure 5.4.5	Port Shaft Thrust and Torque: M.V. Terry Fox	Tow No. 1	104
Figure 5.4.6	Speed and Towing Force: M.V. Terry Fox	Tow No. 2	105
Figure 5.4.7	Speed and Towing Force: M.V. Terry Fox	Tow No. 2 (500-800 sec.)	106
Figure 5.4.8	Total Shaft Thrust: M.V. Terry Fox	Tow No. 2	107
Figure 5.4.9	Resistance in Ice vs Velocity: M.V. Ikaluk		110
Figure 5.4.10	Speed and Towing Force: M.V. Ikaluk	Tow No. 1	111
Figure 5.4.11	Total Shaft and Nozzle Thrust: M.V. Terry Fox	Tow No. 1	112
Figure 5.4.12	Port Shaft Thrust and Torque : M.V. Ikaluk	Tow No. 1	113
Figure 5.4.13	Speed and Towing Force: M.V. Ikaluk	Tow No. 2	114
Figure 5.4.14	Port Shaft Thrust and Torque : M.V. Ikaluk	Tow No. 2	115
Figure 5.4.15	Speed and Towing Force: M.V. Ikaluk	Tow No. 3	116

Figure 5.4.16	Total Shaft and Nozzle Thrust: M.V. Terry Fox Tow No. 3	117
Figure 5.5.1	Total Shaft Thrust vs Speed: M.V. Terry Fox and M.V. Ikaluk Self Prop.	119
Figure 5.5.2	Total Shaft Power vs Speed: M.V. Terry Fox and M.V. Ikaluk Self Prop.	119
Figure 5.5.3	Total Shaft Thrust vs Speed: M.V. Terry Fox Self Propulsion	123
Figure 5.5.4	Total Shaft Power vs Speed: M.V. Terry Fox Self Propulsion	123
Figure 5.5.5	Total Shaft Thrust vs Speed: M.V. Ikaluk Self Propulsion Test 7	125
Figure 5.5.6	Total Shaft Power: M.V. Terry Fox Self Propulsion Test 7	126
Figure 5.5.7	Port Shaft Torque and Thrust : M.V. Terry Fox Self Propulsion Test 7	127
Figure 5.5.8	Port and Starb. Shaft Thrust and Rudder Angle: M.V. Terry Fox Self Propulsion Test 7	128
Figure 5.5.9	Port and Starb. Shaft RPM and Torque: M.V. Terry Fox Self Propulsion Test 7	129
Figure 5.5.10	Port and Starb. Propeller Pitch and Engine Fuel Rack: M.V. Terry Fox Self Propulsion Test 7	130
Figure 5.5.11	Ship Speed, Total Power and Total Shaft Thrust: M.V. Terry Fox Self Propulsion Test 1	131
Figure 5.5.12	Total Shaft Thrust vs Speed: M.V. Ikaluk Self Propulsion Test 7	135
Figure 5.5.13	Total Shaft Power vs Speed: M.V. Ikaluk Self Propulsion Test 7	135
Figure 5.5.14	Ship Speed, Nozzle Thrust, Total Thrust, Total Power: M.V. Ikaluk Self Propulsion Test 7	137
Figure 5.5.15	Ship Speed and Total Shaft Thrust: M.V. Ikaluk Self Propulsion Test 7	138
Figure 5.5.16	Port and Starboard Shaft Torque: M.V. Ikaluk Self Propulsion Test 7	139
Figure 5.5.17	Port and Starboard Shaft Torque and RPM: M.V. Ikaluk Self Propulsion Test 7	140
Figure 5.5.18	Port and Starboard Shaft Thrust and Rudder Angle: M.V. Ikaluk Self Propulsion Test 7	141
Figure 5.5.19	Port and Starb. Propeller Pitch and Engine Fuel Rack: M.V. Ikaluk Self Propulsion Test 7	142
Figure 5.5.20	Ship Speed, Port Pitch, Total Power and Total Shaft Thrust: M.V. Ikaluk Self Propulsion Test 8	143
Figure 5.5.21	Ship Speed, Port Pitch, Total Power and Total Shaft Thrust: M.V. Ikaluk Self Propulsion Test 9	144
Figure 5.6.1	Thrust and Towline vs Speed: M.V. Terry Fox O.W. Overload	146
Figure 5.6.2	Thrust Deduction vs Speed: M.V. Terry Fox O.W. Overload	147
Figure 5.6.3	Thrust Deduction Fraction vs Speed: M.V. Terry Fox O.W. Overload	147
Figure 5.6.4	Towline Force and (Ice Resistance): M.V. Terry Fox O.W. Overload	148
Figure 5.6.5	Ship Accleration and Total Shaft Thrust: M.V. Terry Fox O.W. Overload	149
Figure 5.6.6	Thrust and Towline vs Speed: M.V. Ikaluk O.W. Overload	151
Figure 5.6.7	Thrust Deduction vs Speed: M.V. Ikaluk O.W. Overload	152
Figure 5.6.8	Thrust Deduction Fraction vs Speed: M.V. Ikaluk O.W. Overload	152
Figure 5.6.9	Towline Force and (Ice Resistance): M.V. Ikaluk O.W. Overload	153
Figure 5.6.10	Ship Accleration and Total Shaft Thrust: M.V. Ikaluk O.W. Overload	154
Figure 5.7.1	Resistance and Thrust in Ice: M.V. Terry Fox	156
Figure 5.7.2	Thrust Deduction in Ice: M.V. Terry Fox	156
Figure 5.7.3	Thrust Deduction Fraction in Ice: M.V. Terry Fox	156
Figure 5.7.4	Thrust Deductions: M.V. Terry Fox	157
Figure 5.7.5	Thrust Deduction Fractions: M.V. Terry Fox	157
Figure 5.7.6	Resistance and Thrust in Ice: M.V. Ikaluk	159

Figure 5.7.7	Thrust Deduction in Ice: M.V. Ikaluk	159
Figure 5.7.8	Thrust Deduction Fraction in Ice: M.V. Ikaluk	159
Figure 5.7.9	Thrust Deductions: M.V. Ikaluk	160
Figure 5.7.10	Thrust Deduction Fractions: M.V. Ikaluk	160
Figure 5.8.1	Port Shaft Torque,Thrust, Pitch, and Fuel Rack: M.V. Ikaluk Test H1	165
Figure 5.8.2	Stbd. Shaft Torque,Thrust, Pitch, and Fuel Rack: M.V. Ikaluk Test H1	166
Figure 5.8.3	Port Shaft Torque,Thrust, Pitch, and Fuel Rack: M.V. Ikaluk Test H1	167
Figure 5.8.4	Starboard Shaft Torque and Thrust: M.V. Ikaluk Test H2	169
Figure 5.8.5	Stbd. Shaft Torque,Thrust, Pitch, and Fuel Rack: M.V. Ikaluk Test H3	170
Figure 5.8.6	Port Shaft Torque,Thrust, Pitch, and Fuel Rack: M.V. Ikaluk Test H3	171
Figure 5.8.7	Port Shaft Torque and Thrust: M.V. Ikaluk Test H3	172
Figure 5.8.8	Fourier Transforms of Port Shaft Torque and Thrust: M.V. Ikaluk Test H3	173
Figure 5.8.9	Port Shaft Torque: M.V. Ikaluk Test H4	174
Figure 5.8.10	Port Shaft Torque,Thrust, Pitch, and Fuel Rack: M.V. Terry Fox Test H8: 0-20 Seconds	177
Figure 5.8.11	Port Shaft Torque,Thrust, Pitch, and Fuel Rack: M.V. Terry Fox Test H8: 0-6 Seconds	178
Figure 5.8.12	Fourier Transforms of Port Shaft Torque and Thrust: M.V. Terry Fox Test H8	179
Figure 5.8.13	Starboard Shaft Torque and Fuel Rack: Test H8	180
Figure 5.8.14	Starboard and Port Shaft Pitch and RPM: M.V. Terry Fox Test H12	182
Figure 5.8.15	Port Shaft Torque and Thrust: M.V. Terry Fox Test H12: 0-20 Sec.	183
Figure 5.8.16	Port Shaft Torque and Thrust: M.V. Terry Fox Test H12: 17-20 Sec.	184
Figure 5.8.17	Port and Starboard Torque: M.V. Terry Fox Test H12: 5-15 Sec.	185

List of Tables

Table 1.1	Principal Characteristics of the M.V. Terry Fox and M.V. Ikaluk	5
Table 1.2	Shaftline Particulars of the M.V. Terry Fox and M.V. Ikaluk	6
Table 2.1	List of Signals Recorded	7
Table 3.2.1	Ice Thickness Summary	20
Table 3.3.1	Ice Core Summary	24
Table 3.3.2.1	Summary of Previous Flexural Strength Measurements Using the In-Situ Cantilever Beam Test (after Lane, 1980)	28
Table 3.3.2.2	Predicted Ice Flexural Strength	30
Table 3.3.2.3	Predicted Small Scale Uniaxial Crushing Strengths	36
Table 3.3.2.4	Summary of Predicted Small Scale Uniaxial Crushing Strengths	38
Table 3.4.1.1	Summary of Hull Surface Roughness Measurements	44
Table 3.4.3.1	Ice-Hull Friction Factors Measured for a Painted Inerta Surface	47
Table 3.4.3.2	Ice-Hull Friction Factors Measured for a Bare Hull Surface	48
Table 3.4.3.3	Ice-Hull Friction Factors Measured for an Inerta Surface	49
Table 4.2.1	List of Trials Performed	79
Table 5.3.1	Example of Statistics Calculated from Test Data	94
Table 5.4.1	Summary of Results from Ice Towing Trials	97
Table 5.4.2	M.V. Terry Fox Towing Test Results	99
Table 5.4.3	M.V. Ikaluk Towing Test Results	108
Table 5.5.1	Summary of Self Propulsion Test Data	118
Table 5.5.2	Self-Propulsion Data Summary: M.V. Terry Fox	121
Table 5.5.3	Selected Valid Self-Propulsion Data: M.V. Terry Fox	122
Table 5.5.4	Self-Propulsion Data Summary: M.V. Ikaluk	133
Table 5.5.5	Selected Valid Self-Propulsion Data: M.V. Ikaluk	134
Table 5.6.1	Open Water Data Summary: M.V. Terry Fox	146
Table 5.6.2	Open Water Data Summary: M.V. Ikaluk	151
Table 5.8.1	Summary of Shaftline Loads	161
Table 5.8.2	Summary of Shaftline Vibration Measurements: M.V. Ikaluk	164
Table 5.8.3	Summary of Shaftline Vibration Measurements: M.V. Terry Fox	176

List of Photographs

Plate 3.1.1	Ice Surface Conditions
Plate 3.1.2	Ice Surface Conditions
Plate 3.1.3	Ice Surface Conditions
Plate 3.1.4	Typical Ice Core
Plate 3.4.1.1	Ice-Hull Tribometer
Plate 3.4.1.2	Ice-Hull Tribometer
Plate 3.4.2.1	Section of Bare Hull where the Ice-Hull Friction Factor was Measured
Plate 3.4.2.2	Section of Bare Hull where the Ice-Hull Friction Factor was Measured
Plate 3.4.2.3	Section of Bare Hull where the Ice-Hull Friction Factor was Measured

SECTION 1

INTRODUCTION

1. INTRODUCTION

It has always been recognized that the key to a full understanding of ship powering performance is an accurate knowledge of its constituent parts; ship resistance, propulsor performance and the hydrodynamic (including ice) interaction between the two. This, however, requires direct measurement of ship resistance, which has historically proved very difficult on technical, logistic and cost grounds. Currently the majority of knowledge of resistance in ice and interaction between hulls and propulsion systems in the presence of ice has been obtained by deductions from full-scale measurement of powering performance or from physical and numerical models calibrated with the same indirect data. This is clearly unsatisfactory since it affects the credibility of all methods of performance prediction and restrains progress in our understanding of ship, propulsor and ice interaction. It was therefore recommended that more full-scale data be obtained for higher resistance values and ice thicknesses.

Direct measurements of full-scale icebreaking resistance were made by Fleet Technology on the USCGC Mobile Bay in February 1986 (Transport Canada Report No. TP8487E). This joint American and Canadian program provided the first full-scale verification of icebreaker resistance. Resistance and propulsion data were collected in ice thicknesses between 26 and 52 cm in Lake Michigan, with a resistance range of 49 kN to 169 kN over a horsepower range of 400 to 2500 HP. In planning the present tests it was recognized that more full-scale data was needed for higher resistance values and ice thicknesses to achieve a better understanding of icebreaking resistance and propulsive performance. In addition the ice-propeller interaction effects and full-scale overload tests should be measured and analyzed, as this had not been done before. As a result of this requirement, a unique set of full-scale resistance and propulsive performance tests was sponsored by the Canadian Coast Guard, the Transportation Development Centre (TDC) of Transport Canada, and the Institute of Marine Dynamics (IMD) and carried out by Fleet Technology Limited in association with Gulf Canada Resources. Two "Beaufort Sea" type icebreakers were selected for the trials. These offered the appropriate range of powers and thrusts, and provided an opportunity for direct comparison of an "open screw" and "ducted propeller" configurations.

The M.V. Ikaluk is an ASPPR Class IV icebreaking supply vessel fitted with two 3.75 *metre diameter nozzles and controllable pitch propellers transmitting* 7450 HP each (see Figure 1.1 and Table 1.1 & 1.2). The M.V. Kalvik is an ASPPR Class IV icebreaker with two 4.8 m open controllable pitch propellers delivering 11600 HP each (See Figure 1.2 and Table 1.1 & 1.2). In the winter of 1989/90 these vessels were harbored in Herschel Basin in the Yukon, N.W.T.. The ships are owned by Gulf Canada Resources Limited (GCRL) as part of their fleet of marine equipment operated by BeauDril and deployed to support oil exploration in the Beaufort Sea. In late May or early June of 1990 both vessels were available for charter at a favourable rate to conduct research.

In May and June Herschel Basin is an ideal testing location for icebreakers for several reasons. The ice cover is 100% with areas of relatively uniform properties. Testing can be conducted in uniform ice thicknesses ranging from 1.2 to 1.8 m in thickness. The icebreaking vessels are in the immediate area and, therefore, no time and expenditure is needed to find suitable ice for testing. The vessels are equipped with sophisticated towing equipment with the capacity for towing each other. The logistic support system provided by Gulf Canada Resources is excellent, as has been proven by the success of previous trials conducted on the M.V. Kalvik (1986) and the M.V. Ikaluk.(1989).

The two major objectives of the project reported herein were to measure and report on:

1. The full-scale resistance and propulsive performance in level ice of two modern icebreakers (M.V. Ikaluk and M.V. Kalvik), incorporating both open and ducted propulsion.
2. The effect of the presence of ice on the interaction forces between the hulls and propulsion systems.

M.V. "Ikaluk"

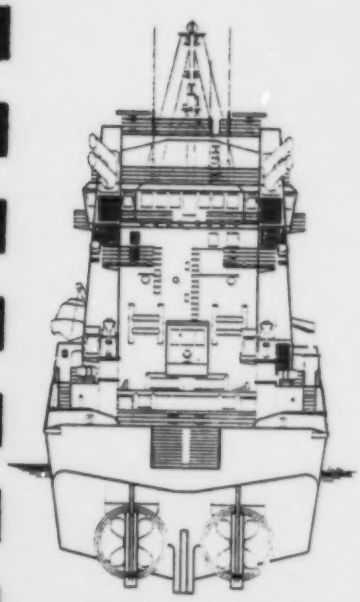

STERN ELEVATION

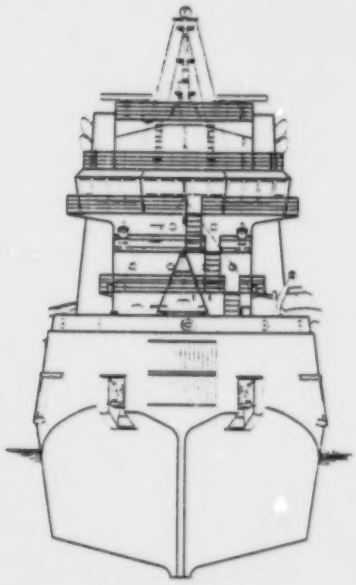

BOW ELEVATION

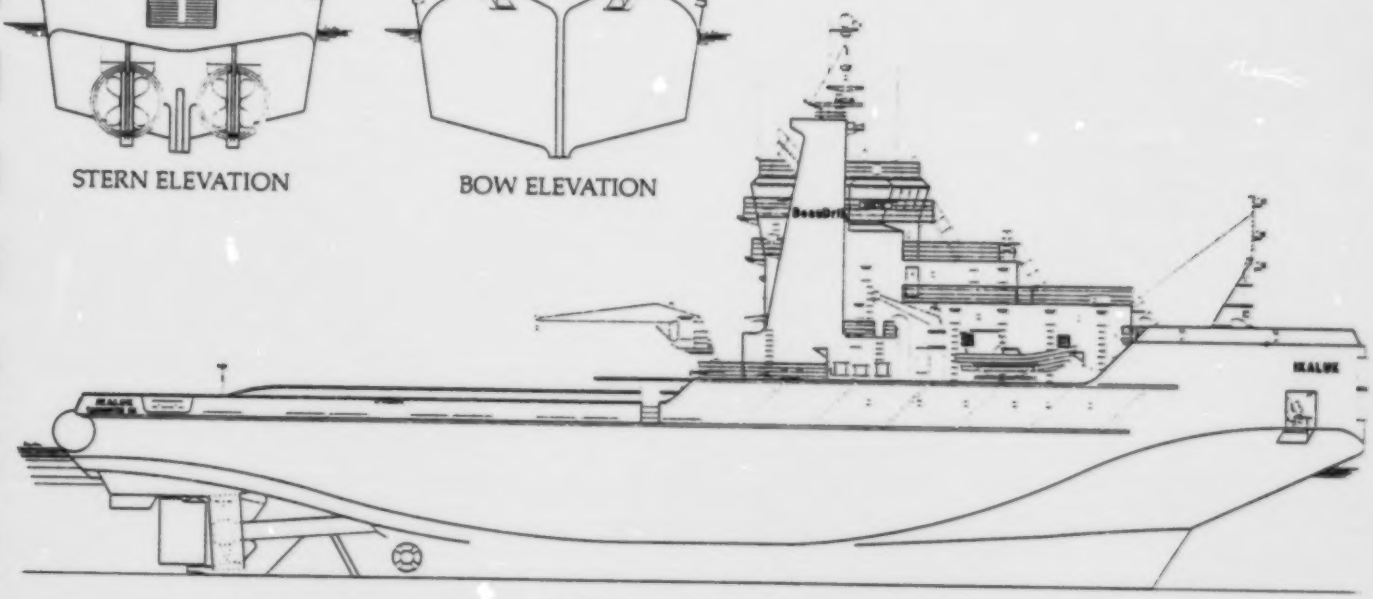

GENERAL ARRANGEMENT

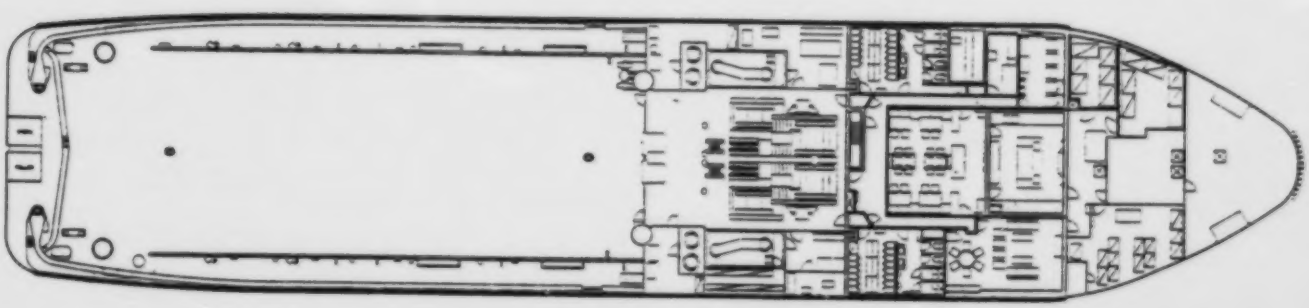

MAIN DECK

Figure 1.1 **General Arrangement of M.V. Ikaluk**

M.V. "Terry Fox"

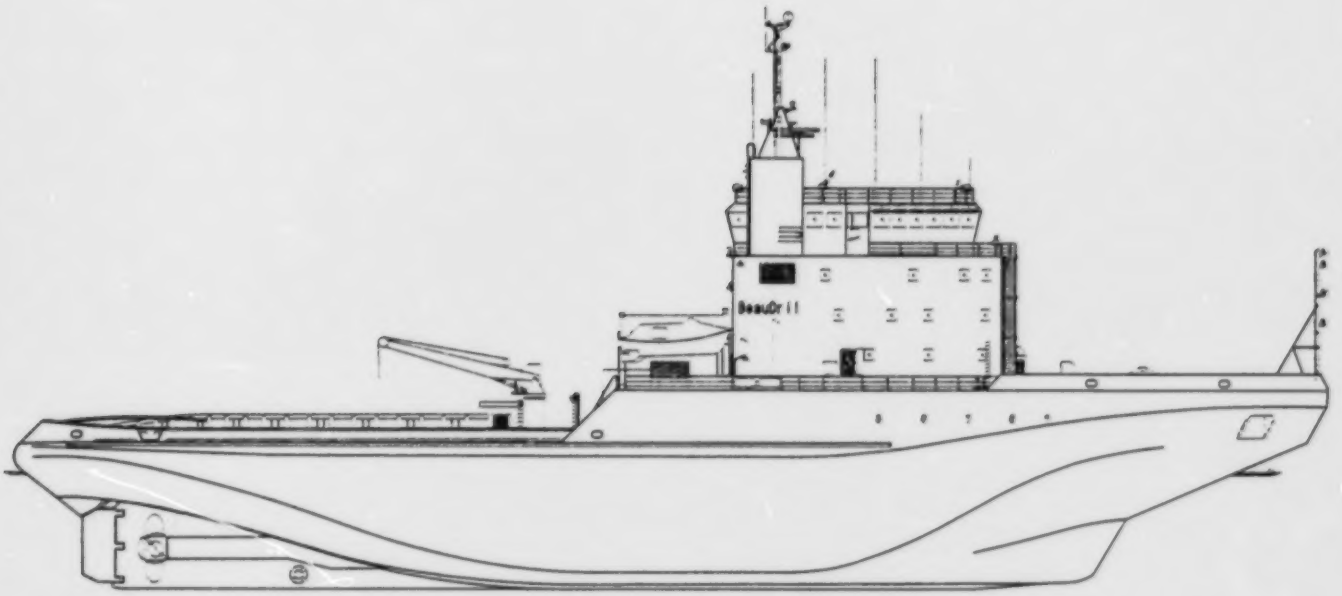

GENERAL ARRANGEMENT

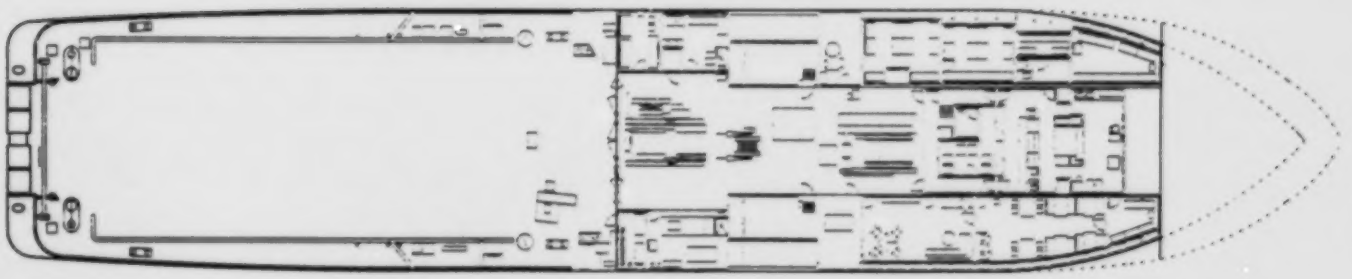

MAIN DECK

Figure 1.2 General Arrangement of M.V. Terry Fox

Table 1.1 Principal Characteristics of the M.V. Terry Fox and M.V. Ikaluk

Name	Miscaroo/Ikaluk	Kalvik/Terry Fox
Function	Icebreaking Supply Vessel	Icebreaker
Propeller System	Ducted	Open
Length OA	78.95 m	88 m
Length BP	70.0 m	75 m
Beam	17.22	17.82
Draft	7.5 m	8.3 m
Displacement	5107 tons	6825 tons
ASPPR Ice Class	4	4
BHP	14 900	23 200
SHP		
No. of Propellers	2 CPP	2 CPP
Manufacturer	Lips	Lips
Bollard Pull	150 tons	220 tons
Bow Thruster	1 200 HP	Air Bubbler Sys
Stern Thruster	800 HP	KaMeWa CPP
Open Water Speed (2 eng)	12 knots	13.28 knots
Open Water Speed (4 eng)	14.7 knots	15.57 knots
Crew	19	19
Berths	34	34

Table 1.2 Shaftline Particulars of the M.V. Terry Fox and M.V. Ikaluk

Description	Ikaluk	Terry Fox	Units
Diameter of Tail Shaft	0.426	0.775	m
Diameter of Intermediate Shaft	0.345	0.470	m
Weight of Tail Shaft	11,400	85,000	Kg
Weight of Intermediate Shaft	4,900	17,000	Kg
Weight of Flywheel	/	12,000	Kg
Shaft BHP	7,350	11,600	HP
Speed at MCR	165	130	rpm
Torque at MCR	317	595	KNm
Shaft Thrust at Bollard	500	900	kN
Shaft Rake	4.2	0	Deg.

NB. Both vessels are twin screw, controllable pitch, diesel - gear driven. The M.V. Ikaluk screw is nozzled and the M.V. Terry Fox is open.

The full scale trials program on the M.V. Ikaluk and M.V. Kalvik provide the following key information:

1. Data on directly measured full scale ice resistance for two modern icebreaking vessels.
2. Data on full scale propulsive performance for vessels with both open and ducted propellers.
3. Thrust deduction factors for vessels operating in ice covered waters.
4. Data for use in verifying or revising existing scaling laws for icebreaker powering performance.
5. Data for calibration of empirical formulae, model test and numerical model methods of performance prediction.
6. Data allowing comparison of the ice loads experienced on the shaftline on a nozzled CP propeller and an open CP propeller in the same ice conditions.

This report describes the trials program and the results obtained. It includes details on the intrumentation, ice conditions, full-scale tests, data, and results. Conclusions and recommendations are also provided.

SECTION 2

INSTRUMENTATION

2. INSTRUMENTATION

2.1 Vessel Instrumentation

The M.V. Ikaluk and M.V. Terry Fox were instrumented in a similar manner. Table 1 lists the signals recorded on the vessels.

Table 2.1
Ship Signals Recorded During Trials

	M.V. Ikaluk	M.V. Terry Fox
Propeller Pitch	2	2
RPM	2	2
Shaft Torque	2	2
Shaft Thrust	2	2
Rudder	2	1
Fuel Rack (Outboard engines)	2	2
Instrumented Towline shackle	1	1
Towing Winch		1
Port nozzle-inboard side	1	
Port nozzle-inboard side	1	
TOTAL	**15**	**13**

The instrumentation arrangements for the M.V. Ikaluk and the M.V. Terry Fox are shown in Figure 2.1.1 and Figure 2.1.2 respectively.

The propeller pitch, rpm, and torque were recorded by interfacing with the ASEA control system. The rudder angle was recorded by connecting directly to the control potentiometers attached to the rudder. The rudder angle was calibrated by moving the rudder a number of degrees, visual reading the rudder angle directly off the rudder stock, and then measuring the voltage at the computer. The propeller pitch was calibrated in a similar manner. The RPM and torque were calibrated using electrical shunts.

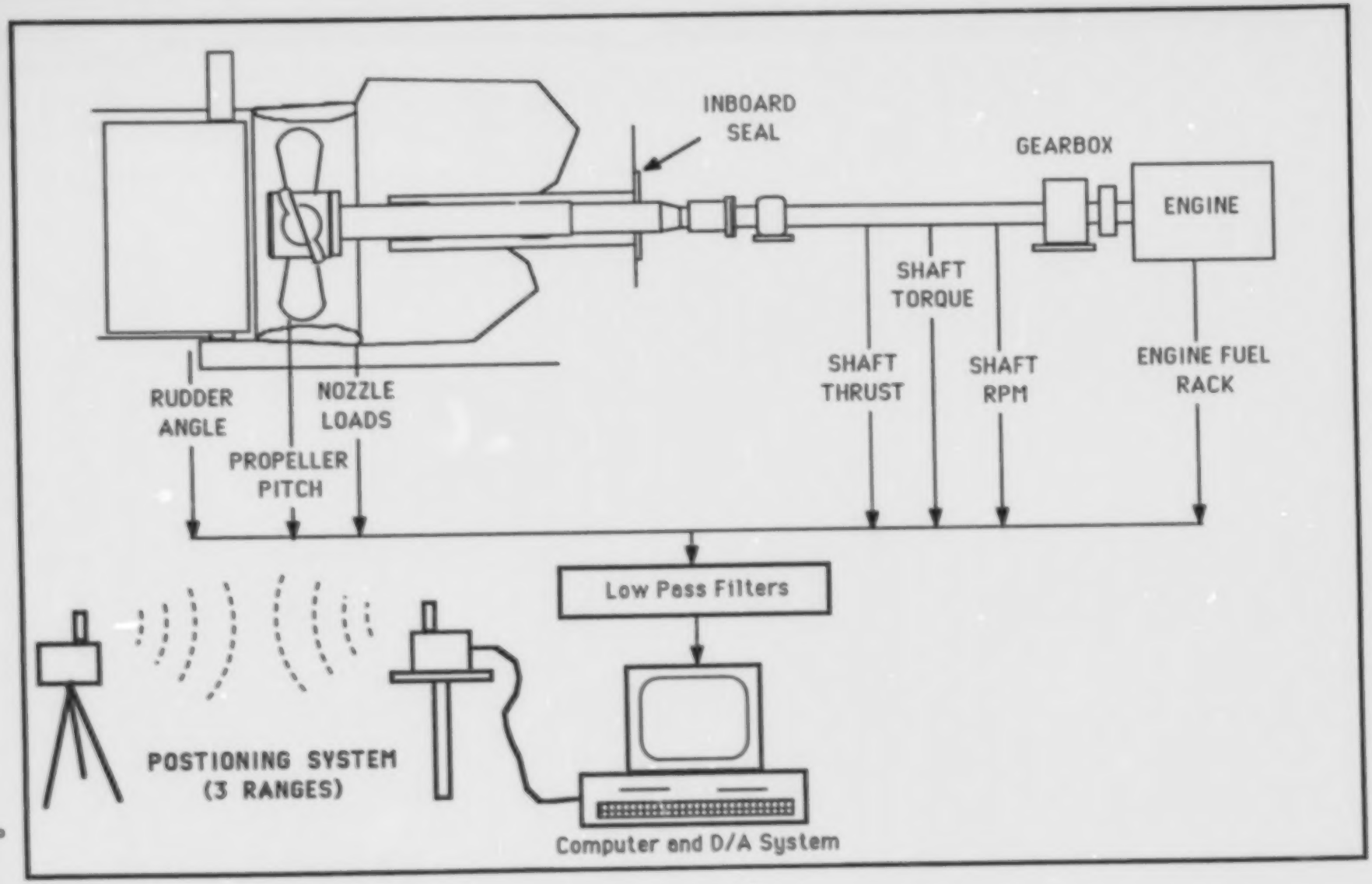

Figure 2.1.1
M.V. IKALUK SHAFTLINE INSTRUMENTATION
(Note: Both Port and Sterboard Sheftlines Instrumented)

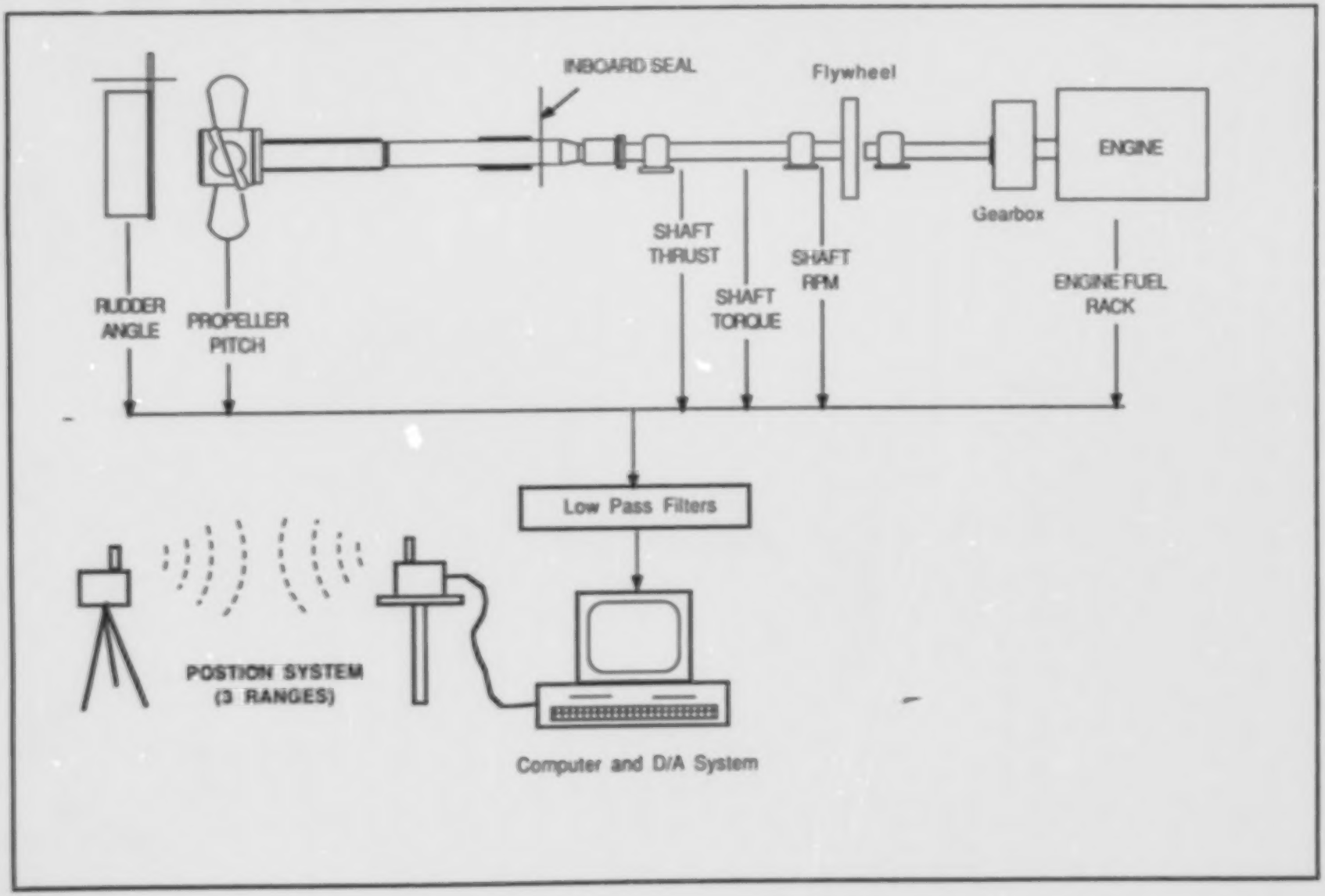

Figure 2.1.2 MV Terry Fox Shaftline Instrumentation

(Note: Both Port and Starboard shaftlines instrumented)

The engine fuel racks on the M.V. Ikaluk were measured by attaching a rotational potentiometer directly to the fuel rack control arm. The fuel racks were then calibrated by visually setting the rack to a specific height and then reading the voltage output by the potentiometer. The M.V. Terry Fox fuel rack was recorded from the ASEA control system output. Only the outboard engine fuel racks on each shaftline were measured as both engines on a shaftline operate at the same rpm and fuel rack position.

The shaft thrust on both vessels was measured by the use of strain gauges mounted on the shafts. Extra special care and consideration is required in measuring thrust due to the very low thrust strains and the cross coupling of shaft torque into the thrust signal. The cross coupling can occur due to very small strain gauge misalignments during installation. To avoid this cross coupling, a special strain gauge configuration known as Hylarides was used. The advantage of this configuration is that any gauge misalignment is automatically compensated for. This automatic compensation, however, has the disadvantage of further reducing the strain gauge bridge sensitivity. Special measures were taken to boost the sensitivity of the gauges by increasing the excitation and the amplification. The strain gauges were attached to Accurex frequency modulated (F.M.) transmitters to transfer the thrust signal from the revolving shaft to a stationary receiver located in the shaft tunnel.

To measure the thrust and drag contribution of the MV Ikaluk's nozzle, two shear gauges that were installed during the 1989 nozzle and shaftline instrumentation project were connected again. One gauge was located on the inboard, centre, upper side of the port nozzle and the other was at a similar position on the outboard side. Both of these strain gauges balanced when connected to the strain gauge amplifiers. However, due to the nature of the harsh environment and the period since the installation (over 1 year), the gauges tended to drift slowly over time. This was compensated by taking a baseline reading of all sensors prior to any tests.

Fleet Technology's software package (called "Ship Trial") used for conducting ship trials was used for this set of tests with only minor modification. The software, developed over the last six years, provides the user with the ability to continuously monitor and display key parameters such as shaft torque, shaft power, and ship speed. In addition the position of the vessel is plotted in plan view on a 2 axis coordinate system.

2.2 Towline Instrumentation

The towline force was measured by using an instrumented towing pin (strain gauge based). Two such towing pins complete with shackles were transported to the test site: one with a safe working load of 250 tons and another specified for 200 tons as a back up. Prior to the commencement of the trials, the towline measurement system for each towing winch onboard the vessels was calibrated against the instrumented towing pins. This provided a service to the ships, a test of this project's instrumentation system, and a check on the calibration factors given by the suppliers of the towing pins.

Figure 2.2.1 shows the arrangement of the ships during towing and the connection of the towing pin to the vessel and the towline. The instrumented pin was attached to a bracket located on the centreline of the forecastle (fo'c's'le) deck at the bow of the towed vessel. Figure 2.2.2 illustrates the details of the connection of the towing pin to the bracket. With this arrangement the instrumented shackle measured directly the load being applied to the towed vessel. While towing, the towline was lifted off the ice into a catenary. The angle of the catenary was such that very little vertical force was applied to the bow as shown in Figure 2.2.2.

2.3 Ship Positioning System

The vessel position was measured using a Racal Microfix positioning system. The positioning system measures in real time the distance from a mobile master station, located onboard a vessel, to fixed shore based "remote" stations. Three base stations were placed on the shore around Herschel Basin, with the aid of a Bell 206 helicopter. The locations of the stations were chosen such that an approximate equilateral triangle could be formed with two base stations and the vessel in the test area as shown in Figure 2.3.1. The distance between the shore based stations was measured using the mobile master unit, which was connected temporarily at each remote base station. A master unit antenna was placed on the top of the mast on each vessel. The mobile master central measuring unit (CMU) was placed on the bridge and connected with a serial interface to the data acquisition system. Therefore, the position of the vessel and the machinery signals (torque, thrust, etc.) were measured on the same time base with the same data acquisition system. The range measurements were taken with an error of ± 1.0 m every three seconds.

In principal only two remote stations are required to fix the position of a vessel. Three remotes were deployed for the following reasons:

a) Provide redundancy in cases were the master antenna on the mast may be shielded by the smoke stack
b) Provide a wider area of operation
c) From three remotes three separate positions can be calculated to form what mariners term a "cocked hat" as shown in the top of Figure 2.3.1. The three positions are then averaged to get the ship's position more accurately

A two axis (X, Y) coordinate system is specified with one axis defined by two remote base stations. For this deployment the origin (0,0) was defined as the remote base station at Collinson Point. The X axis was defined to run through the remote station at Calton Point. The vessel position from the origin was calculated by triangulation. Two sides of the triangle were formed by the measured distances from the remote base stations to the vessel, and the third side was the measured distance between the two remote base stations (constant value). Given these three lengths of the triangle the coordinates X and Y can be calculated by using standard trigonometric relationships.

The data acquisition system read the distances from the CMU. All the coordinate geometric processing was performed by Fleet Technology's ship trials software package in real time. The vessel speed was calculated by simply dividing the distance moved from one position to the next by the corresponding elapsed time.

2.4 Data Acquisition

The computer system used onboard both vessels was a HP 9816 with over two megabytes of RAM memory. An analog to digital converter card was installed into the computer to convert the ship's high level (± 5.0 V) analog voltage signals to digital format for storage and processing. During the self propulsion tests and resistance trials all analog channels were passed through a 1 Hz low pass filter and scanned at 10 Hz per channel. During the high speed data collection the filter was changed to a 60 Hz low pass filter and scanned at 500 Hz per channel. The ship position was measured every three seconds . The storage device used was a HP9122 double density floppy disk drive with a storage capacity of approximately 500 kBytes.

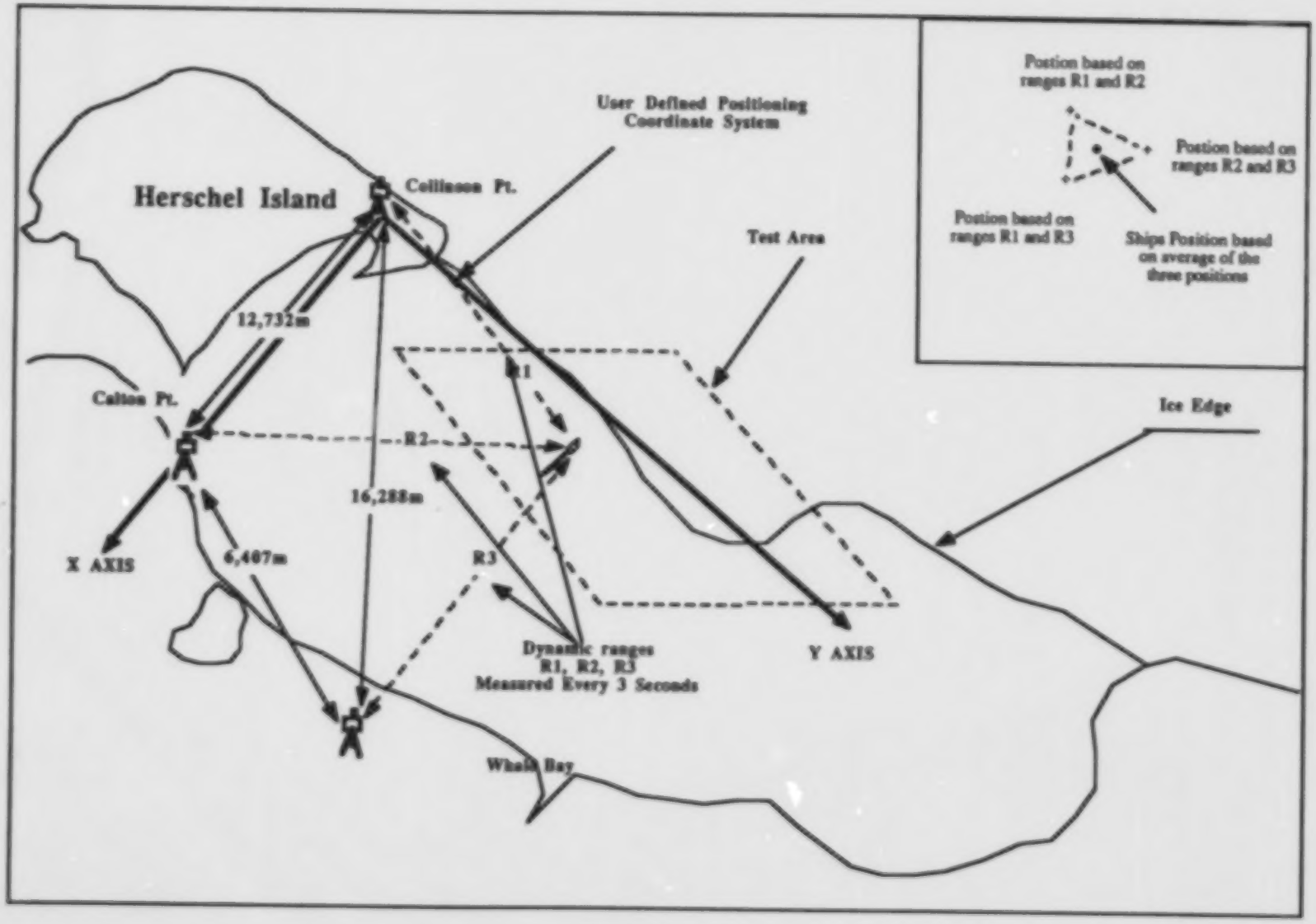

Figure 2.3.1
ARRANGEMENT OF MICROWAVE POSITIONG SYSTEM BASE STATIONS

SECTION 3

ICE CONDITIONS

3. ICE CONDITIONS

Measurements were made to provide a basic description of the ice in Herschel Basin at the time of the trials. The following ice parameters were measured:

(a) ice thickness.

(b) ice salinity-temperature profile. These data were used to estimate key in-situ mechanical properties of the ice.

(c) ice-hull friction factor.

Observations were also made of the icebreaking pattern around the ship.

The average ice thickness was measured at 1.55m ± 0.11m, and the average flexural strength was estimated to be 150 kPa. The average friction factor was measured to be 0.18.

Upon initial contract with the bow, the ice failed in cusps which were relatively large. The depth of these cusps was about one to two times the ice thickness while their length was about four times the ice thickness.

3.1 Test Location and Ice Cover Description

Prior to the start of the ship-testing phase of the field program, surveys were conducted using a helicopter and a snowmobile to locate a suitable test site. A test area was sought in which the ice cover consisted of an extensive level ice sheet with no ridges, with uniform ice thickness, and with no visible cracks or major flaws. As the nearshore portion of the Beaufort Sea was ice-free and it was desirable to minimize the travel distance for the ships to the test site, it was decided to conduct the field program in the Herschel Basin area where a level ice sheet was present.

Surveys were conducted to sample the ice thickness over most of the basin and to locate cracks, ridges and other flaws. Also, a trip was made to investigate ice conditions west of Herschel Island; this area was ice-free. A test area was selected in Herschel Basin as shown in Figure 3.1.1.

The ice cover in this test area, and over most of Herschel Basin, consisted of a level ice sheet with relatively uniform thickness. This sheet is believed to have consisted entirely of first year ice based on the measured thicknesses and salinities and on the fact that no incursions of old ice were observed for Herschel Basin over the 1989-90 winter (B. Wright, Gulf Canada Resources Ltd., personal communication). The ice sheet was in a deteriorated condition at the time of the ship trials. Although few thaw holes were present, it was extensively covered with melt pools and was free of snow. See plates 3.1.1 to 3.1.3. Considerable drainage of these melt pools had occurred with the result that the depth of water in the pools was reduced to a maximum of about 0.2m. Many melt pools were drained completely. This produced an ice sheet in which the upper 15 cm (approximate value) consisted of a matrix of weakly-bonded granules which had a consistency similar to that of snow particles. The remainder of the ice sheet consisted of more competent material. See plate 3.1.4.

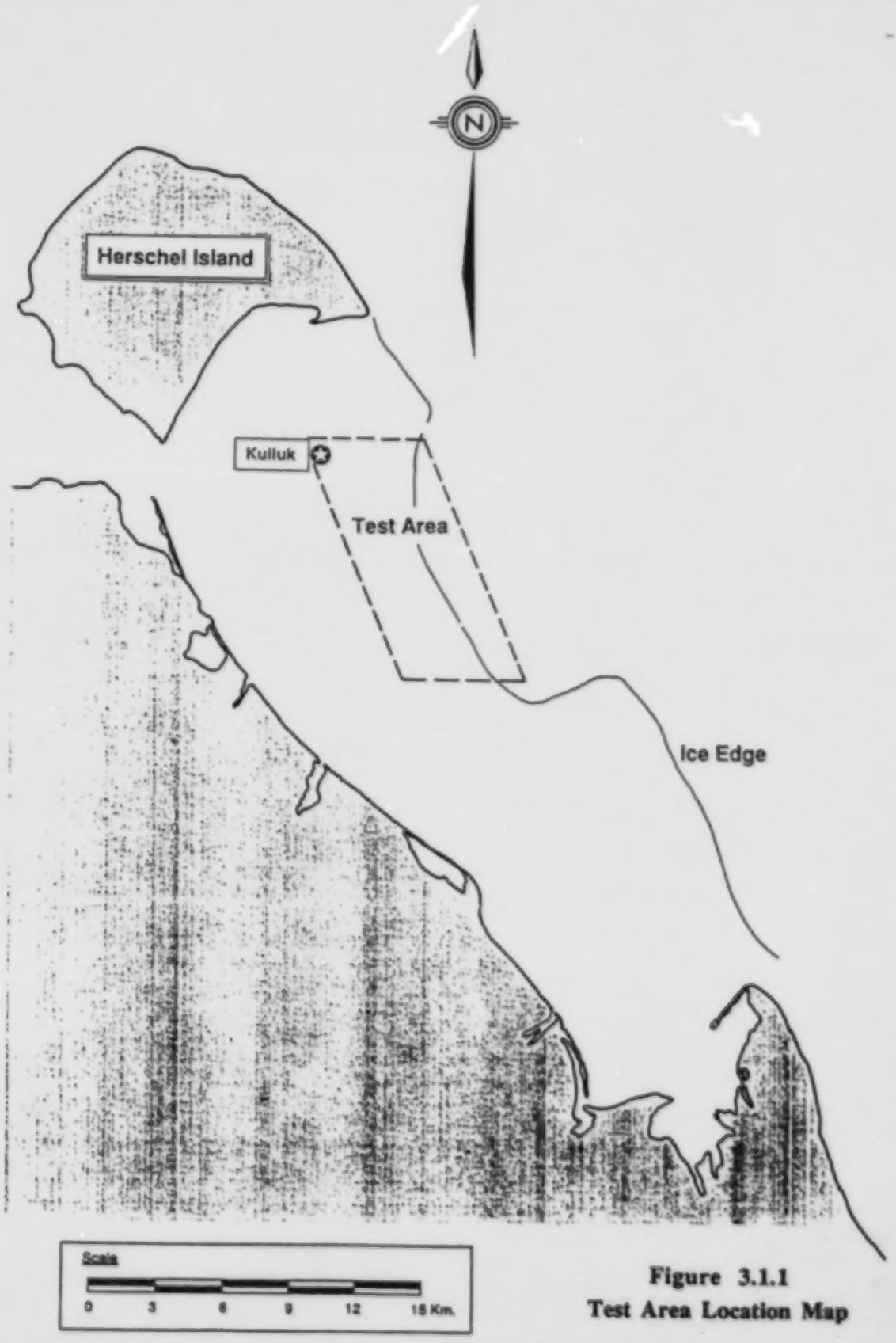

Figure 3.1.1
Test Area Location Map

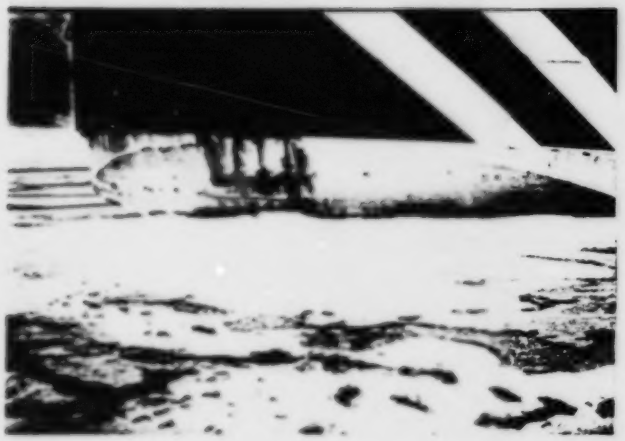

Plate 3.1.1
Ice Surface Conditions

Plate 3.1.2
Ice Surface Conditions

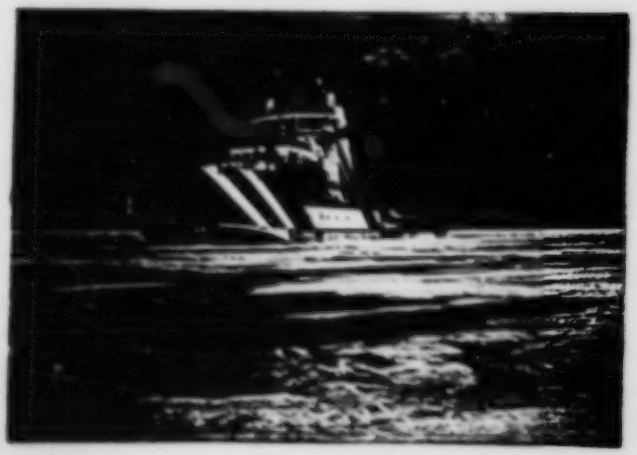

Plate 3.1.3
Ice Surface Conditions

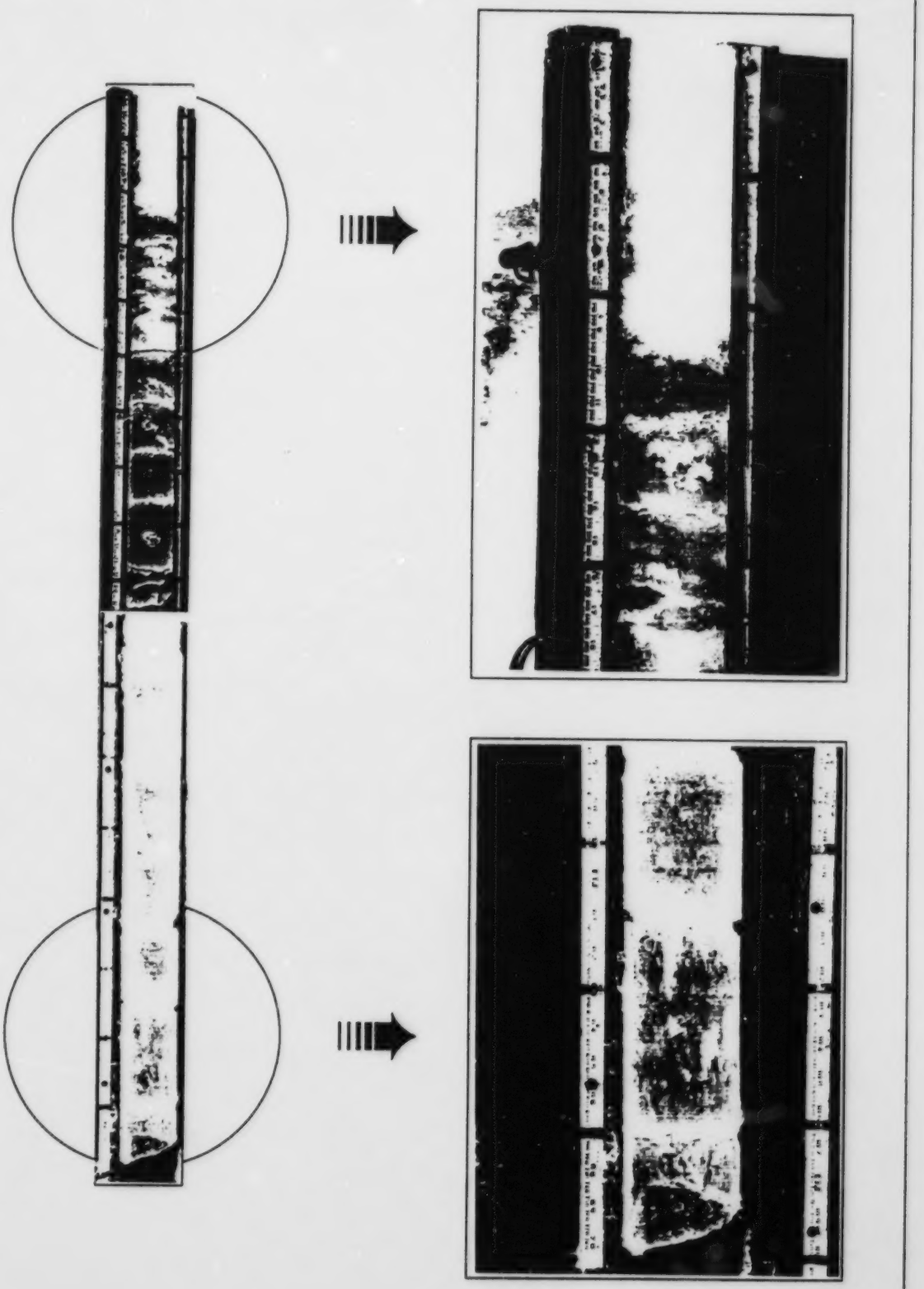

Plate 3.1.4 Typical Ice Core

3.2 Ice Thickness

Efforts were made to define the ice thickness well as this parameter is the most important ice property affecting ship resistance. The ice thickness was measured directly by inserting a survey tape and toggle into a hole drilled in the ice. Prior to the resistance trials, a grid of survey tracks was marked out in the test area and ice thicknesses were sampled at 100m intervals along several of these lines. This survey established that the ice thickness was relatively uniform over the test area.

Ice thicknesses were then measured along the tracks traversed by the ships during the resistance trials, which are shown in Figure 3.2.1. A total of 114 ice thickness measurements were made. These data are summarized in Table 3.2.1 and presented in raw form in Appendix A. The average of all ice thickness measurements over the test area was 1.55 ± 0.11m.

The ice thickness was sampled at preset intervals (of 50 to 100m) along the survey line. As the ice was extensively covered with melt pools, the dataset includes ice thicknesses for surface conditions ranging from hummocks to melt pools. This resulted in an ice thickness variation of about 0.4m for each survey line. See Table 3.2.1.

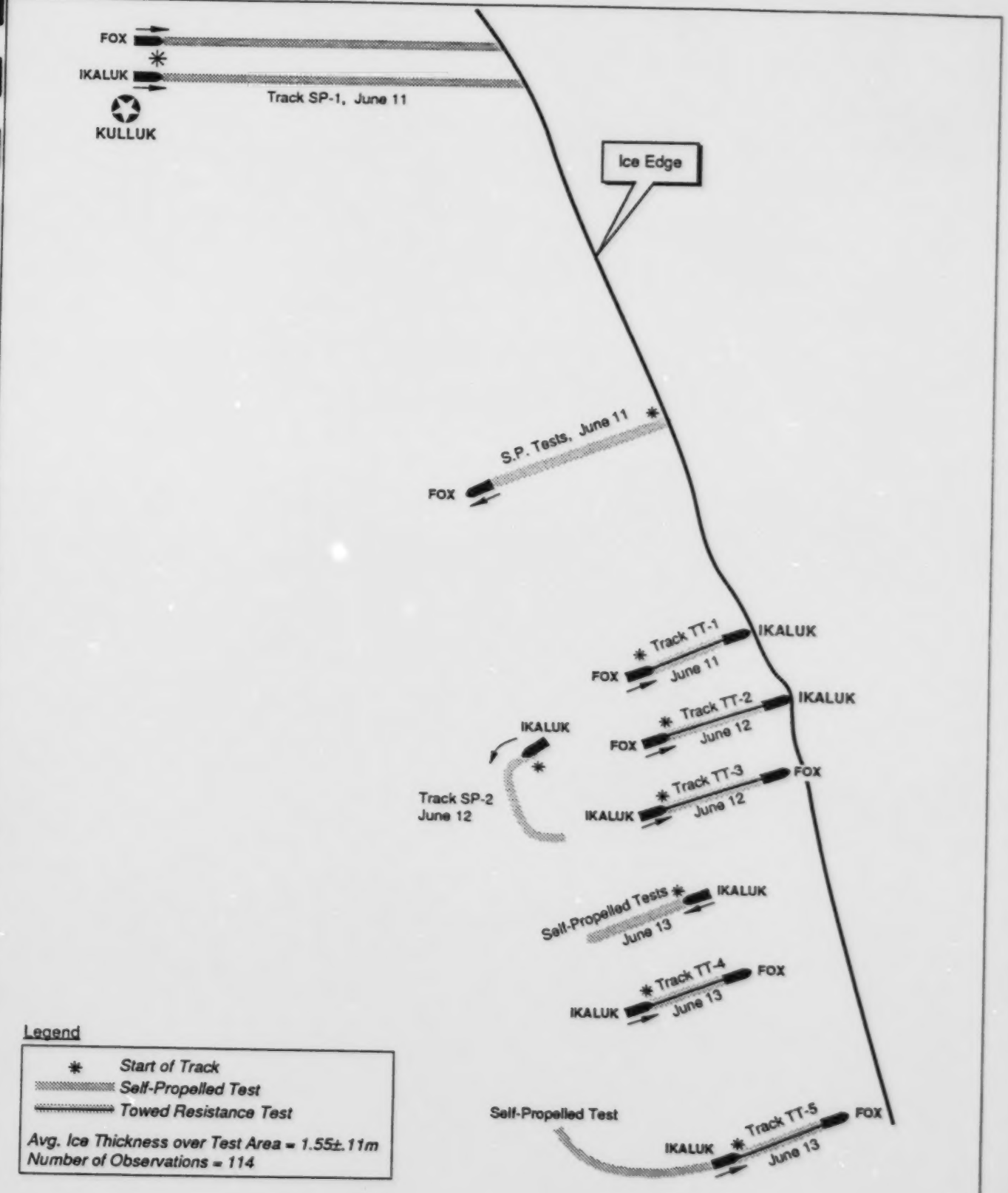

Figure 3.2.1 Ice Thickness Measurement Location Map

TABLE 3.2.1

ICE THICKNESS SUMMARY

Date	Track No. (see Fig 3.1)	Number of Observations	Avg Ice Thick. and Std Dev (m)	Maximum Ice Thick. (m)	Minimum Ice Thick. (m)
June 11	SP-1	14	1.59 ± 0.10	1.88	1.49
June 11	TT-1	15	1.58 ± 0.17	2.05	1.35
June 12	TT-2	19	1.55 ± 0.08	1.71	1.41
June 12	SP-2	10	1.48 ± 0.08	1.62	1.39
June 12	TT-3	21	1.57 ± 0.12	1.85	1.40
June 13	TT-4	15	1.51 ± 0.06	1.61	1.45
June 13	TT-5	20	1.53 ± 0.14	1.94	1.25

3.3 Ice Salinity and Temperature Profile and Mechanical Properties

3.3.1 Ice Salinity and Temperature Profile

Field Measurement Technique

The salinity and temperature profile of the ice was measured by analyzing 8 cm diameter cores that were extracted from the ice sheet. The ice temperature profile was measured immediately after extraction by inserting a direct-reading temperature probe into small holes about 3 mm in diameter that were drilled into the core. A model T53 Fisher thermometer was used to make these measurements.

The ice salinity profile was determined by measuring the conductivity of the brine produced by melting samples of the core. These measurements were made using a model RB-5 salinometer that was manufactured by Beckman Instruments Ltd. With this instrument, it was necessary to melt relatively large core samples (typically in excess of 10 cm in length) in order to provide a sufficient volume of brine to allow measurements to be made. Thus, the measured salinities represent the average value over the depth range from which the core sample was taken.

Raw Field Data

A total of nine cores were taken and analyzed over the duration of the field program. Figure 3.3.1 shows a typical profile of the ice salinity and temperature. Table 3.3.1 summarizes the measured ice temperatures and salinities. The minimum ice temperature and the maximum salinity measured for the nine cores ranged from -1.4°C to -2.3°C and 2.5 ppt to 4.0 ppt, respectively. Appendix B provides a complete set of the measured ice temperature and salinity profiles as well as a complete listing of the raw data.

As numerous investigators have correlated the mechanical properties of sea ice to its brine volume, the brine volume profile was determined for each core. See Figure 3.3.1 for a typical brine volume profile. The brine volume was determined using the following formulae which were developed by Frankenstein and Garner, 1967:

Core #: 1

Date: June 1, 1990

Core Location: Near M.V. Terry Fox

Ice Thickness: 1.8 m

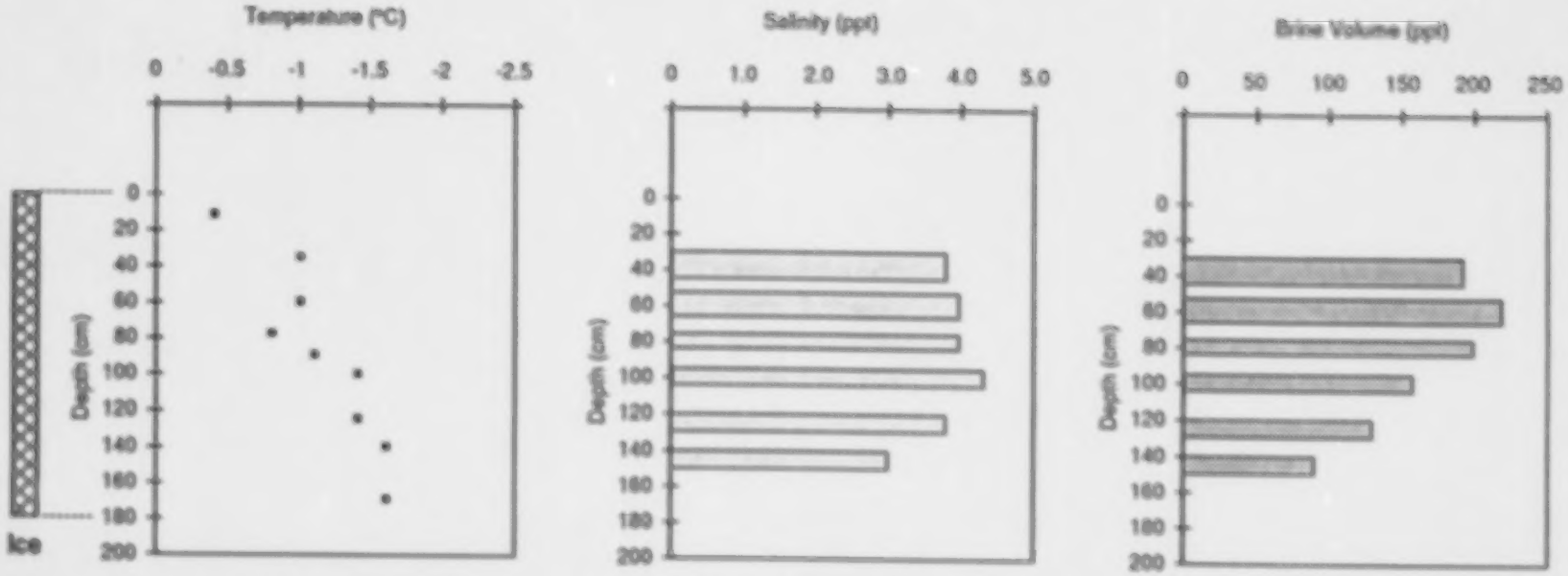

Note: The brine volume was computed using the formulae of Frankenstein and Garner, 1967

Figure 3.3.1
Ice Temperature - Salinity - Brine Volume Profile

TABLE 3.3.1

ICE CORE SUMMARY

Core #	Date Core Taken	Minimum Ice Temp (°C)	Maximum Salinity (ppt)
1	June 1	-1.6	4.0
2	June 3	-1.4	3.6
3	June 5	-2.3	4.0
4	June 7	-2.1	3.9
5	June 9	-1.5	2.8
6	June 11	-1.8	3.1
7	June 11	-1.8	3.2
8	June 12	-1.8	2.8
9	June 13	-1.6	2.5

Ice temperature range: -0.5°C to -2.06°C

$$\upsilon_b = S \left(\frac{-52.56}{t} - 2.28 \right) \qquad [3.1]$$

Ice temperature range: -2.06°C to -8.2°C

$$\upsilon_b = S \left(\frac{-52.56}{t} - 2.28 \right) \qquad [3.2]$$

where: υ_b = brine volume (ppt)

S = ice salinity (ppt)

t = ice temperature (°C)

3.3.2 Predicted Mechanical Properties of the Ice

"Cantilever Beam" Flexural Strength

Efforts were made to predict the ice flexural strength as many predictors of level ice resistance include this ice property as a parameter. In practice, the in-situ flexural strength is a difficult property to define as it is affected by the presence of a salinity and temperature gradient through the thickness of the ice sheet. This makes it difficult to apply the results of laboratory tests (which are typically conducted with ice that is isothermal and of constant salinity) to the in-situ strength of the sheet.

Several field tests have been carried out in the past to attempt to measure the in-situ flexural strength by failing cantilever beams cut in the ice sheet. However, it must be recognized that the interpretation of these test results is difficult as assumptions must be made regarding the material behaviour of the ice. Most of these test results have been interpreted by considering the ice to be an isotropic, linear-elastic material with uniform properties through its thickness.

This assumption is clearly inaccurate and hence, the "flexural strength" computed from cantilever beam tests should be taken as an index of the true in-situ flexural strength. However, a relatively large data base is available to define the "cantilever beam" flexural strength for a wide range of ice conditions. Also, empirical relationships have been developed to relate this index strength to the ice salinity and temperature. Furthermore, this index strength has been used both implicitly and explicitly as an ice parameter in the development of many level ice resistance predictors.

Therefore, it was decided to predict the "cantilever beam" flexural strength of the ice sheet in Herschel Basin. Table 3.3.2.1 and Figure 3.3.2.1 summarize most of the field tests that have been undertaken to measure the "cantilever beam" flexural strength and its observed relationship with the brine volume of the ice. The test data indicate a bilinear relationship. At low brine volumes, the flexural strength decreases linearly with the square root of the brine volume. At high brine volumes, (i.e., greater than about 120 ppt), it is independent of this parameter.

Lane, 1980 utilized most of these data to determine the following predictors for ice flexural strength:

Ice sheet brine volume range: 0 to 120 ppt

$$\sigma_f = 850\,(1 - 0.072\,\sqrt{v_b}) \qquad [3.3]$$

Ice sheet brine volume range: >120 ppt

$$\sigma_f = 150 \text{ kpa} \qquad [3.4]$$

where σ_f = ice "cantilever beam" flexural strength (kPa)

Using equations [3.3] and [3.4], the ice flexural strength is predicted to range from 150 kPa to 380 kPa. See Table 3.3.2.1. This variation is typical of the scatter of the field test data. See Figure 3.3.2.1. However, the flexural strengths predicted for the cores taken after June 7 are generally higher than for the previous cores. See Table 3.3.2.2. As the ice temperature profile was measured to be generally similar for all cores (see Table 3.3.2.1), the higher strengths predicted for the later cases mainly result from the lower salinities that were measured for these cores. As brine drainage occurred during extraction of the cores, particularly for the later cores, the measured salinities are expected to underestimate the true value. Therefore, the flexural strengths predicted for the later cores are considered to be suspect.

In order to investigate this discrepancy further, and as all of the data plotted on Figure 3.3.2.1 for brine volumes greater than 120 ppt were obtained for thin ice (i.e., less than 0.5 m thick), the literature was reviewed to locate other sources of data for thick ice of high brine volume. Noble and Comfort, 1979, conducted cantilever beam tests in relatively thick ice (i.e., 0.6 m to 1.2 m) of high brine volume in Strathcona Sound, N.W.T. These results agree well with Lane's, 1980 predictor, (see Figure 3.3.2.1), which supports the flexural strengths predicted from the earlier cores.

In our opinion, the flexural strengths predicted for the earlier cores are likely to be more reliable. Consequently, it is recommended that the ice "cantilever beam" flexural strength be taken as 150 kPa.

TABLE I

FLEXURAL STRENGTH
BY
IN-SITU CANTILEVER BEAM TEST

Author	Ref.	Date	Location	Top Ice Temperature °C	Strength Range kPa
Tabata	3	1964	Mombetsu Harbour	-1 to -2	98-265
Tabata	4	1965	Mombetsu Harbour	-1 to -2	49-353
Tabata	5	1966	Mombetsu Harbour	-1 to -3	150-400
Vaudrey	6	1976	Chukchi Sea McMurdo Sound	-18 to -28	385-765 207-335
Brown	7	1962	Wales, Alaska Thule, Greenland	-2 to -20	200-550
Frankenstein	8	1970			334-443
Weeks Anderson	9	1956	Thule, Greenland Hopedale, Labrador	-2 to -7	49-300
Dykins	10 11	1967	McMurdo Sound	-2 to -4	227-655
Kingery	12	1962	Thule, Greenland	-15 to -25	325-662

TABLE II

SUMMARY
FLEXURAL STRENGTH VERSUS $\sqrt{\text{BRINE VOLUME}}$
EQUATIONS FOR SEA ICE
AS DETERMINED BY
THE IN-SITU CANTILEVER BEAM TEST

Author	Ref.	No. of Samples	Equation
Vaudrey	6	12	$\sigma_f = 960\ (1 - 0.063\sqrt{v})$
Dykins	11	7	$\sigma_f = 1080\ (1 - 0.063\sqrt{v})$
Tabata	4	24	$\sigma_f = 520\ (1 - 0.035\ \sqrt{v})$
Weeks and Anderson	9	38	$\sigma_f = 360\ (1 - 0.052\ \sqrt{v})$
Weeks and Assur	2	26	$\sigma_f = 735\ (1 - 0.063\ \sqrt{v})$
Schwarz and Weeks	13		$\sigma_f = 750\ (1 - 0.070\ \sqrt{v})$

TABLE 3.3.2.1

SUMMARY OF PREVIOUS FLEXURAL STRENGTH MEASUREMENTS USING THE IN-SITU CANTILEVER BEAM TEST (AFTER LANE, 1980)

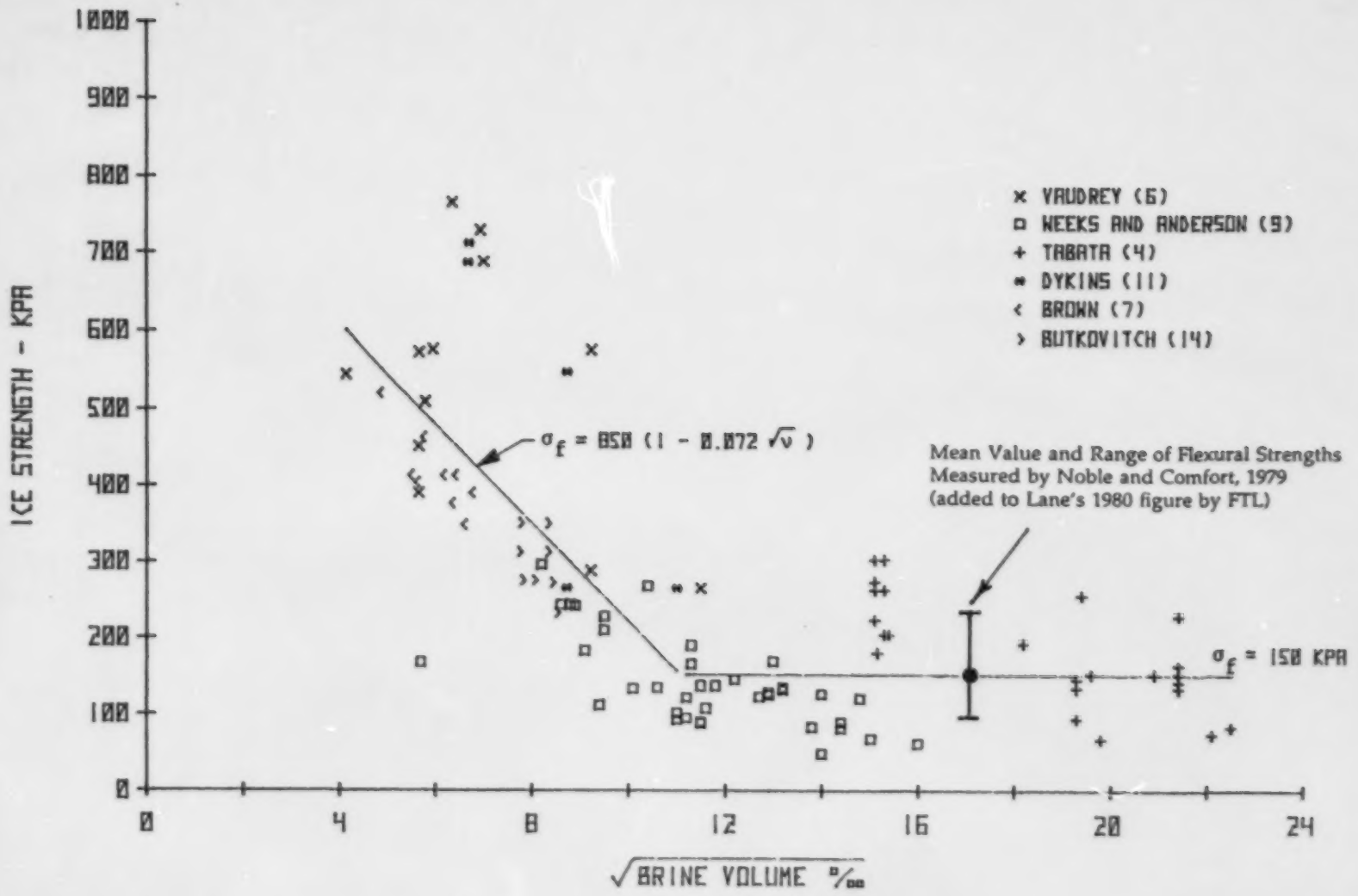

FIGURE 3.3.2.1

SEA ICE STRENGTH - IN-SITU CANTILEVER BEAM TEST
(AFTER LANE, 1980)

TABLE 3.3.2.2

PREDICTED ICE FLEXURAL STRENGTH

Core #	Date Core Taken	Depth Averaged Brine Volume (ppt)	Predicted "Cantilever Beam" Ice Flexural Strength (kPa)
1	June 1	158	150
2	June 3	257	150
3	June 5	90	270
4	June 7	126	150
5	June 9	79	300
6	June 11	67	350
7	June 11	76	320
8	June 12	92	260
9	June 13	58	380

NOTE: The "cantilever beam" flexural strength has been predicted using the formulae of Lane, 1980.

Elastic Modulus

Some predictors of level ice resistance include the ice elastic modulus as a parameter. As this parameter was not measured in the field, efforts were made to predict it based on the measured ice salinity and temperature profile. This is difficult as ice does not behave as an elastic material in many cases and ice defections are often time-dependent. Some key parameters affecting the behaviour of the ice are the loading rate, the magnitude of the applied stresses, and the ice temperature and salinity. For a more detailed discussion of this issue, the reader is referred to Weeks and Assur, 1967 and Mellor, 1983.

One approach for determining the elastic modulus is to measure the velocity of propagation of P, S, surface and flexural waves in the ice sheet. During this type of test, the ice behaviour can probably be assumed to be elastic with reasonable accuracy as there is little time for creep strains to become significant. Figure 3.3.2.2 shows the results of some previous dynamic tests. These test results indicate a value of 1 to 5 gPa for ice with a brine volume similar to that of the ice in Herschel Basin at the time of the test program.

Other tests have been done by applying static loads to an ice sheet or cantilever beam. As would be expected, these test results tend to indicate lower values for the elastic modulus than do the dynamic test results. Tabata et al, 1966 investigated the effect of stress rate on the in-situ elastic modulus for a cantilever beam. See Figure 3.3.2.3. The stress rate applicable to icebreaking is somewhat uncertain. However, for the tests in Herschel Basin, the loading rate during breakage of an individual ice cusp is expected to be of the order of 100 kPa/sec (based on a failure stress of 150-200 kPa and a time to failure of 1 to 2 sec). For this loading rate, a value of 0.1 to 0.5 gPa is suggested by Figure 3.3.2.3 for the in-situ elastic modulus of ice of similar temperature to that in Herschel Basin.

The above values provide guidelines for the elastic modulus for preliminary analyses. For more detailed analyses, it is recommended that the elastic modulus value be selected to suit the specific requirements (e.g., definition of in-situ versus purely elastic response) of the numerical model which is under evaluation and/or development.

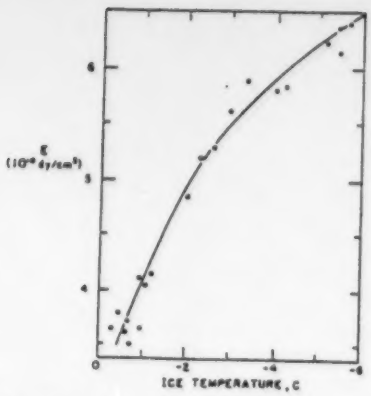

Figure 35. Decrease in elastic modulus E with increasing ice temperature as determined by in-situ seismic measurements; Laptev Sea, spring (data of Listov).[118]

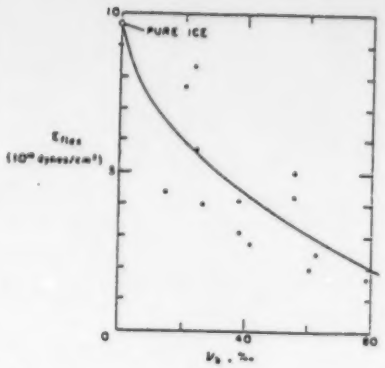

Figure 38. Elastic modulus E, as determined by seismic measurements, vs brine volume v_b (Anderson).[3]

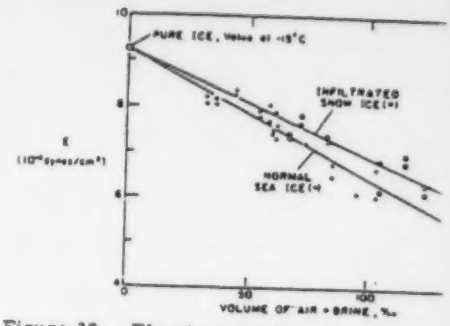

Figure 39. Elastic modulus, E, vs volur air plus brine, v; young sea ice (Tabata)

Figure 3.3.2.2
Sea Ice Elastic Modulus as Measured by Dynamic Tests
(figures cited by Weeks and Assur, 1967)

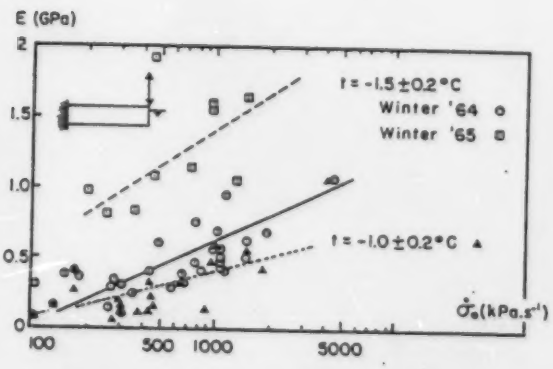

FIG. 47. Effective *in situ* elastic modulus versus stress rate (Tabata *et al.* 1966).

Figure 3.3.2.3
Effective In-Situ Elastic Modulus
(figure cited by Lainey and Tinawi, 1984)

Uniaxial Crushing Strength

Some predictors of level ice resistance include this ice property as a parameter as ice failure occurs initially by crushing, and subsequently by flexure during the breakage of an individual cusp. As this parameter was not measured in the field, efforts have been made to predict it based on the measured temperature and salinity profile of the ice.

The small-scale uniaxial compressive strength was predicted using the following equations which were developed by Timco and Frederking, 1989 a;b.

Vertically-loaded columnar-grained ice:

$$\sigma_c = 160\ (\dot{\varepsilon})^{0.22}\ [1 - (\upsilon_T/200)^{0.5}] \qquad [3.5]$$

Horizontally-loaded columnar-grained ice:

$$\sigma_c = 37\ (\dot{\varepsilon})^{0.22}\ [1 - (\upsilon_T/270)^{0.5}] \qquad [3.6]$$

Granular ice (σ_c independent of the loading direction):

$$\sigma_c = 49\ (\dot{\varepsilon})^{0.22}\ [1 - (\upsilon_T/280)^{0.5}] \qquad [3.7]$$

where: σ_c = uniaxial compressive strength (mpa)

$\dot{\varepsilon}$ = strain rate (sec^{-1})

T = total porosity (i.e., brine + air) of the ice (ppt)

As the available field data were insufficient to use these expressions directly, a number of assumptions had to be made as follows:

(a) **Ice grain size** - it is well known that the upper portion of the ice sheet is granular, while the lower part is columnar-grained (e.g., Michel, 1978). For this study, the upper 0.4 m of the level ice was assumed to be granular while the remainder of the sheet was considered to be columnar-grained. This grain size profile is typical of arctic sea ice.

(b) **Ice density and the volume of the air in the ice** - the density is affected by the volume of air in the ice which affects the total porosity of the ice. As the ice density was not measured, the uniaxial compressive strength has been predicted by assuming that no air was present in the ice sheet. This assumption is believed to be justified as the ice was in a deteriorated state and was saturated with seawater at the time of the trials.

The small scale uniaxial compressive strength has been predicted based on the temperatures and salinities measured for each core. As a combination of vertical and horizontal loading occurs during the contact of the ship's hull with ice, the uniaxial compressive strength has been predicted for both loading directions.

As the compressive strength also depends on the strain rate, these predictions need to be done for strain rates that are representative of ice-hull interactions. This is difficult to quantify reliably (and a detailed analysis of this issue was beyond the scope of the study). Strain rates of 10^{-4} and 10^{-3} sec^{-1} were selected for these computations as they are close to the transition point (where the ice behaviour changes from ductile to brittle). In the field, the ice is loaded relatively quickly by the hull and hence, it is expected that the ice will probably behave in a brittle manner. This suggests that a value of 10^{-3} sec^{-1}, or higher, would be appropriate for the strain rate. Unfortunately, the uniaxial compressive strength at high strain rates is poorly understood at present, as it is generally dependent upon many properties (such as the fracture toughness and the size and distribution of cracks and flaws in the ice). Timco and Frederking, 1989a caution the user that their formulae (i.e., equations 4.5 to 4.7) are expected to overpredict the uniaxial compressive strength for a strain rate of 10^{-3} sec^{-1}. Their formulae have been used in the absence of other more reliable methods and these results are expected to be adequate for preliminary analyses.

The average uniaxial compressive strength has been predicted for 40cm depth intervals in the ice sheet for each core, using the following two-step approach:

(a) predict the uniaxial compressive strength of the ice at each depth of interest in the ice sheet, based on the ice salinity-temperature profile,

(b) determine the average in-situ compressive strength of the ice over each 40cm depth range.

Step (a) has been accomplished using equations 3.5 to 3.7. Step (b) was accomplished by numerically averaging the small scale strengths predicted for each depth of interest. Timco and Frederking, 1989a, justify this approach based on the results of large scale field tests which were undertaken at Prudhoe Bay (Lee et al, 1986; Petrie et al, 1986; Wang et al, 1986). These field tests were undertaken by loading a floating ice block (about 2m x 5m in area) in uniaxial compression through its full thickness. Small-scale tests were also done in the laboratory to measure the profile of the ice uniaxial compressive strength for this ice block. The depth-averaged compressive strength predicted by the small-scale tests was found to correlate well with the field data.

Tables 3.3.2.3 and 3.3.2.4 summarize the uniaxial compressive strengths predicted for each core and on average, respectively. It should be noted that only the results of cores taken before June 9 were used to establish the average values as it is suspected that brine drainage occurred during extraction of the later cores. See Section 3.3.2 for further discussion. For a strain rate of 10^{-4} sec^{-1}, the average compressive strength is predicted to be 2.6 mpa for the upper 40cm of the ice sheet. The strength of the lower portion of the ice sheet is predicted to range from 1.5 to 1.7 mpa, and from 4.4 to 5.5 mpa, for horizontal and vertical loadings, respectively. These values are expected to be reliable for preliminary analyses. For more detailed analyses, it is recommended that the compressive strength be predicted for the strain rate range, depth range, and loading direction that is of specific interest to the numerical model which is under evaluation and/or development.

TABLE 3.3.2.3

PREDICTED SMALL SCALE UNIAXIAL CRUSHING STRENGTHS

Core #	Date Core Taken	Depth Range (cm)	Assumed Ice Grain Type	Crushing Strength (mPa) (see Note 1)			
				Vertical Loading		Horizontal Loading	
				Strain Rate = $10^{-4}sec^{-1}$	Strain Rate = $10^{-3}sec^{-1}$	Strain Rate = $10^{-4}sec^{-1}$	Strain Rate = $10^{-3}sec^{-1}$
1	June 1	0-40	Granular	1.1	1.9	Note 4	Note 4
		40-80	Columnar	0.5	0.8	0.6	1.0
		80-120	Columnar	2.4	3.9	0.9	1.4
		>120	Columnar	5.5	9.1	1.8	3.0
2	June 3	0-40	Granular	Note 2	Note 2	Note 2	Note 2
		40-80	Columnar	Note 3	Note 3	Note 3	Note 3
		80-120	Columnar	3.5	5.8	1.4	2.3
		>120	Columnar	6.4	11.5	2.0	3.3
3	June 5	0-40	Granular	4.0	6.6	Note 4	Note 4
		40-80	Columnar	9.5	15.8	2.6	4.3
		80-120	Columnar	7.4	12.0	2.2	3.5
		>120	Columnar	5.6	9.3	1.8	2.9
4	June 7	0-40	Granular	2.7	4.5	Note 4	Note 4
		40-80	Columnar	6.4	10.6	1.9	3.3
		80-120	Columnar	4.4	7.2	1.5	2.6
		>120	Columnar	2.0	4.0	1.2	1.9
5	June 9	0-40	Granular	3.5	5.9	Note 4	Note 4
		40-80	Columnar	6.8	11.3	2.0	3.4
		80-120	Columnar	7.0	11.7	2.1	3.5
		>120	Columnar	7.9	13.1	2.3	3.8

NOTES:

1. The above crushing strengths are the average predicted at each point in the salinity-temperature profile over the depth range of interest.
2. Brine volume out of range of equation 4.7.
3. Brine volume out of range of equations 4.5 and 4.6.
4. σ_c independent of loading direction.

TABLE 3.3.2.3 (cont'd)

Core #	Date Core Taken	Depth Range (cm)	Assumed Ice Grain Type	Crushing Strength (mPa) (see Note 1)			
				Vertical Loading		Horizontal Loading	
				Strain Rate = $10^{-4}sec^{-1}$	Strain Rate = $=10^{-6}sec^{-1}$	Strain Rate = $10^{-4}sec^{-1}$	Strain Rate = $10^{-6}sec^{-1}$
6	June 11	0-40	Granular	3.2	5.2	Note 4	Note 4
		40-80	Columnar	7.4	12.3	2.1	3.6
		80-120	Columnar	10.0	15.0	2.6	4.2
		>120	Columnar	8.9	14.7	2.5	4.1
7	June 11	0-40	Granular	3.3	7.0	Note 4	Note 4
		40-80	Columnar	7.9	13.0	2.2	3.7
		80-120	Columnar	6.7	11.1	2.0	3.4
		>120	Columnar	8.3	9.4	2.4	3.9
8	June 12	0-40	Granular	2.7	4.5	Note 4	Note 4
		40-80	Columnar	6.1	10.1	1.9	3.1
		80-120	Columnar	6.8	11.3	2.0	3.4
		>120	Columnar	10.2	17.0	1.7	4.5
9	June 13	0-40	Granular	4.5	7.5	Note 4	Note 4
		40-80	Columnar	9.1	15.0	2.5	4.1
		80-120	Columnar	8.4	14.0	2.4	3.9
		>120	Columnar	8.7	13.9	2.4	3.9

NOTES:

1. The above crushing strengths are the average predicted at each point in the salinity-temperature profile over the depth range of interest.
2. Brine volume out of range of equation 4.7.
3. Brine volume out of range of equations 4.5 and 4.6.
4. σ_c independent of loading direction.

TABLE 3.3.2.4

SUMMARY OF PREDICTED SMALL SCALE
UNIAXIAL CRUSHING STRENGTHS

Depth Range (cm)	Assumed Ice Grain Type	Average Crushing Strength (mpa) (See Note 1):			
		Vertical Loading		Horizontal Loading	
		Strain Rate = $10^{-4}sec^{-1}$	Strain Rate = $10^{-3}sec^{-1}$	Strain Rate = $10^{-4}sec^{-1}$	Strain Rate = $10^{-3}sec^{-1}$
0-40	Granular	2.6	4.3	Note 2	Note 2
40-80	Columnar	5.5	9.1	1.7	2.9
80-120	Columnar	4.4	7.2	1.5	2.5
> 120	Columnar	4.9	8.5	1.7	2.8

NOTE:

1. The above averages are based on the results of only the cores that were taken before June 9. See text for discussion.

2. The crushing strength is independent of the loading direction for granular ice.

3.4 Ice-Hull Friction Factor

3.4.1 Measurement Technique

The ice-hull friction factor was measured using a rotating arm tribometer which is depicted in plates 3.4.1.1 and 3.4.1.2 and Figure 3.4.1.1. It consists of a long arm that is rotated manually through an arc near the hull. An ice sample up to 10cm x 10cm in size is mounted at the end of the arm and is simultaneously crushed and slid past the hull as the tribometer is rotated. The tribometer is instrumented using force transducers to measure the time histories of the forces normal and parallel to the arm. Also, the speed and location of the tribometer during its arc near the hull are measured.

3.4.2 Hull Surface Condition and Friction Factor Test Locations

Ice-hull friction factor measurements were made at or near the waterline along the starboard side of the MV TERRY FOX. The ship was deballasted partially for these tests. Tests were done for a bare hull surface, an inerta-coated surface, and a painted inerta surface. See plates 3.4.2.1 and 3.4.2.2. These surfaces were selected for testing as they spanned the range of hull surface conditions which were in contact with the ice. See plates 3.4.2.3 to 3.4.2.7.

The friction factor of the MV IKALUK's hull was not measured due to time constraints imposed by the overall schedule of the project. However, the condition of its hull coating was generally similar to that of the MV TERRY FOX. For both ships, the inerta coating was intact over most of the bow and shoulder area. The area of exposed bare hull surface (which was visible) was small and was estimated to be less than 5% of the total.

The hull surface roughness was measured for both ships by staff from the Institute of Marine Dynamics (IMD) using a BSRA hull roughness analyzer. Table 3.4.2.1 summarizes these measurements.

Top View:

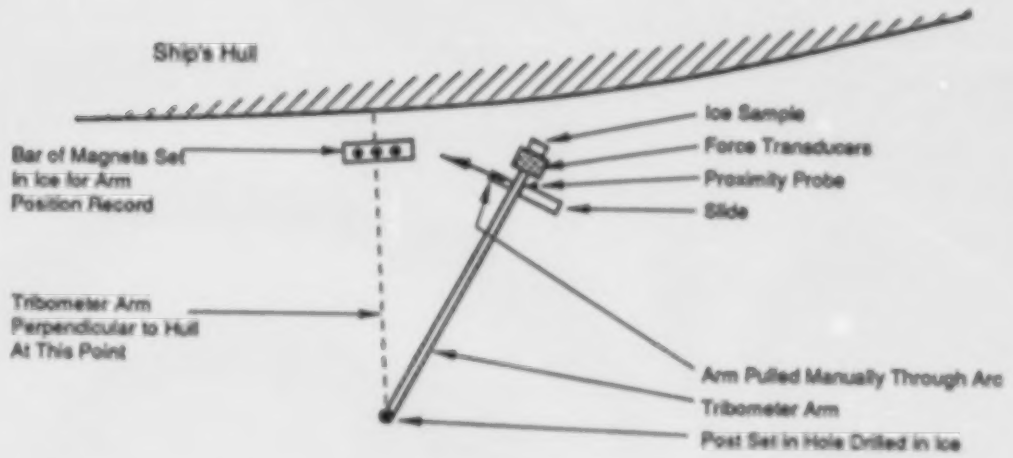
Ship's Hull
Ice Sample
Force Transducers
Proximity Probe
Slide
Bar of Magnets Set In Ice for Arm Position Record
Tribometer Arm Perpendicular to Hull At This Point
Arm Pulled Manually Through Arc
Tribometer Arm
Post Set in Hole Drilled in Ice

Side View:

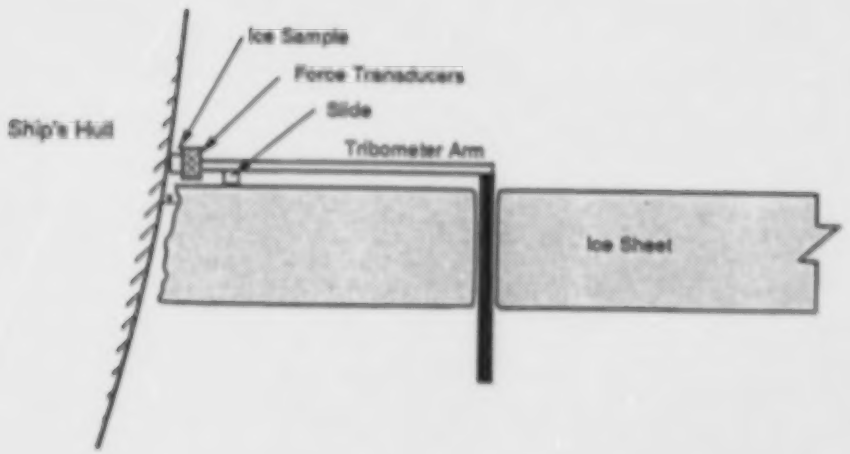

Figure 3.4.1.1 Tribometer Schematic

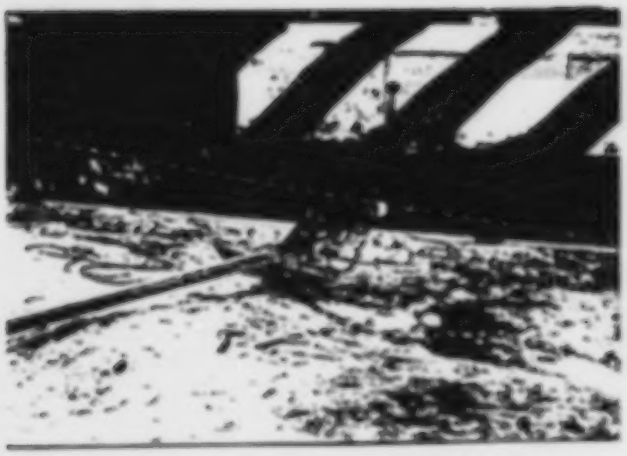

Plate 3.4.1.1
Ice-Hull Tribometer

Plate 3.4.1.2
Ice-Hull Tribometer

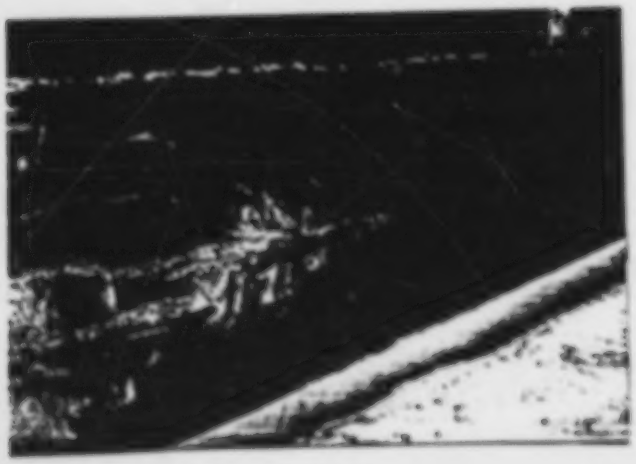

Plate 3.4.2.1
Section of Bare Hull Where
The Ice-Hull Friction Factor
Was Measured

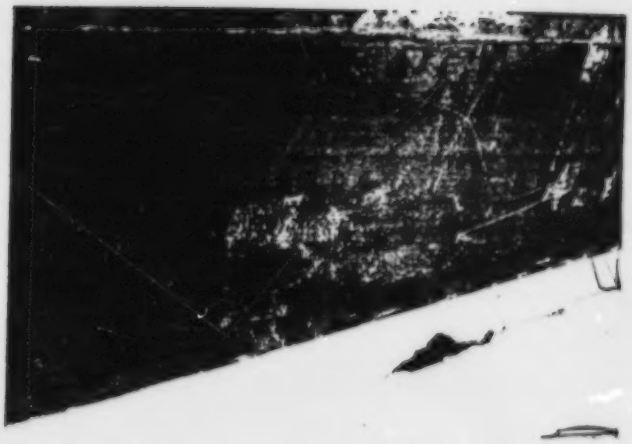

Plate 3.4.2.2
Inerta-Coated and Painted
Inerta Surfaces Where
Ice-Hull Friction Factor
Measurements Were Made

Plate 3.4.2.3
Starboard Side of
M.V. Terry Fox

Plate 3.4.2.4
Port Side of
M.V. Terry Fox

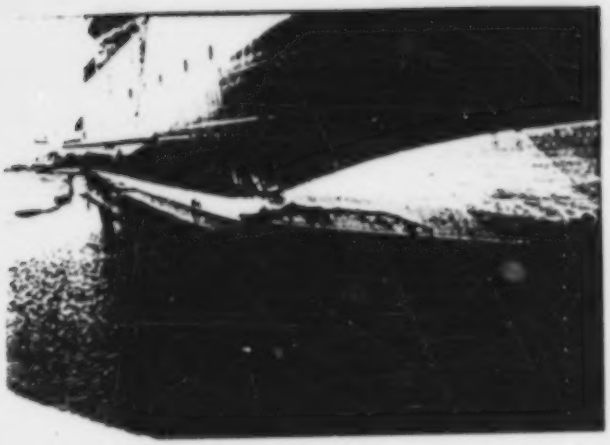

Plate 3.4.2.5
Starboard Bow of
M.V. Terry Fox

Plate 3.4.2.6
Starboard Bow of
M.V. Terry Fox

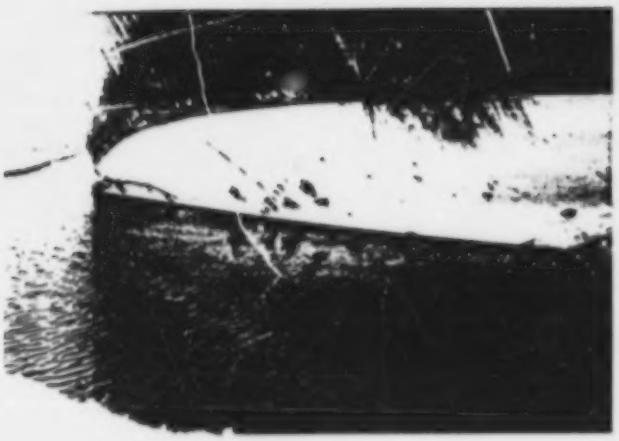

Plate 3.4.2.7
Bow of M.V. Terry Fox

TABLE 3.4.1.1

SUMMARY OF HULL SURFACE ROUGHNESS MEASUREMENTS
(DATA COLLECTED AND PROVIDED BY IMD)

Ship	Location		Average Surface Roughness (Microns)
MV IKALUK	Starboard Side:	0 m Aft of Stem	306
		1 m Aft of Stem	218
		2 m Aft of Stem	248
		3 m Aft of Stem	163
MV IKALUK	Port Side:	0 m Aft of Stem	408
		1 m Aft of Stem	203
		2 m Aft of Stem	217
		3 m Aft of Stem	248
		4 m Aft of Stem	314
		5 m Aft of Stem	297
		6 m Aft of Stem	239
		7 m Aft of Stem	223
		8 m Aft of Stem	221
MV TERRY FOX	Starboard Side:	0 m Aft of Stem	397
		1 m Aft of Stem	132
		2 m Aft of Stem	103
		3 m Aft of Stem	175
		4 m Aft of Stem	153
		5 m Aft of Stem	253
		6 m Aft of Stem	280
		7 m Aft of Stem	265
		8 m Aft of Stem	188
		9 m Aft of Stem	311
		10 m Aft of Stem	163
		11 m Aft of Stem	367
		12 m Aft of Stem	157
		13 m Aft of Stem	794
		14 m Aft of Stem	705
		15 m Aft of Stem	608
MV TERRY FOX	Port Side:	1 m Aft of Stem	841
		2 m Aft of Stem	769
		3 m Aft of Stem	628
		4 m Aft of Stem	584
		5 m Aft of Stem	492
MV TERRY FOX	Ice-Hull Friction Factor Measurement Locations:	• Bare Hull	212
		• Inerta	152
		• Painted Inerta	216

3.4.3 Test Results

Figure 3.4.3.1 shows raw output from a typical test. As the tribometer was rotated during the test, purely normal and tangential forces were only measured by the force transducers on the arm when it was perpendicular to the hull. The output of the proximity probe was used to establish this location on the force time history. Usually, the tribometer was setup such that it was perpendicular to the hull when it passed between the second and third magnets (which are denoted on the record by the second and third "spikes" respectively). See Figures 3.4.1.1 and 3.4.3.1.

The measured forces, and the ratio of these forces, show considerable variation during the test. See Figure 3.4.3.1. Changes in hull-arm geometry during the tribometer's arc are one source of this variation. Variations in ice failure processes are another source, particularly for the high frequency fluctuations that were recorded. Some tests were conducted by positioning the ice sample such that ice was "scraped" off the block during the tribometer's arc. As the ice sample was continuously pushed closer to the hull during the tribometer's arc, this produced a cyclical ice failure process of compression, shearing and/or pulverization, and sliding of the ice sample over the broken ice particles. These tests were categorized as "**sliding and crushing**" during subsequent data analyses.

Some other tests were conducted with the ice sample positioned such that little or no "scraping" occurred. In these tests, the ice sample was compressed without failure during the tribometer's arc. These tests were categorized as "**mainly sliding**" during subsequent analyses.

As the ratio of the measured forces shows considerable fluctuation (mainly reflecting variations in ice failure modes), the friction factor was established by averaging the ratio of the measured forces over a 15cm travel distance of the arm. This introduced some error as purely normal and tangential forces were not measured over this travel distance. However, this error is small (as the angle of the arm to the hull was less than two degrees from normal over this travel distance) and therefore the ratio of the measured raw forces was used directly without correction for changes in hull-arm geometry.

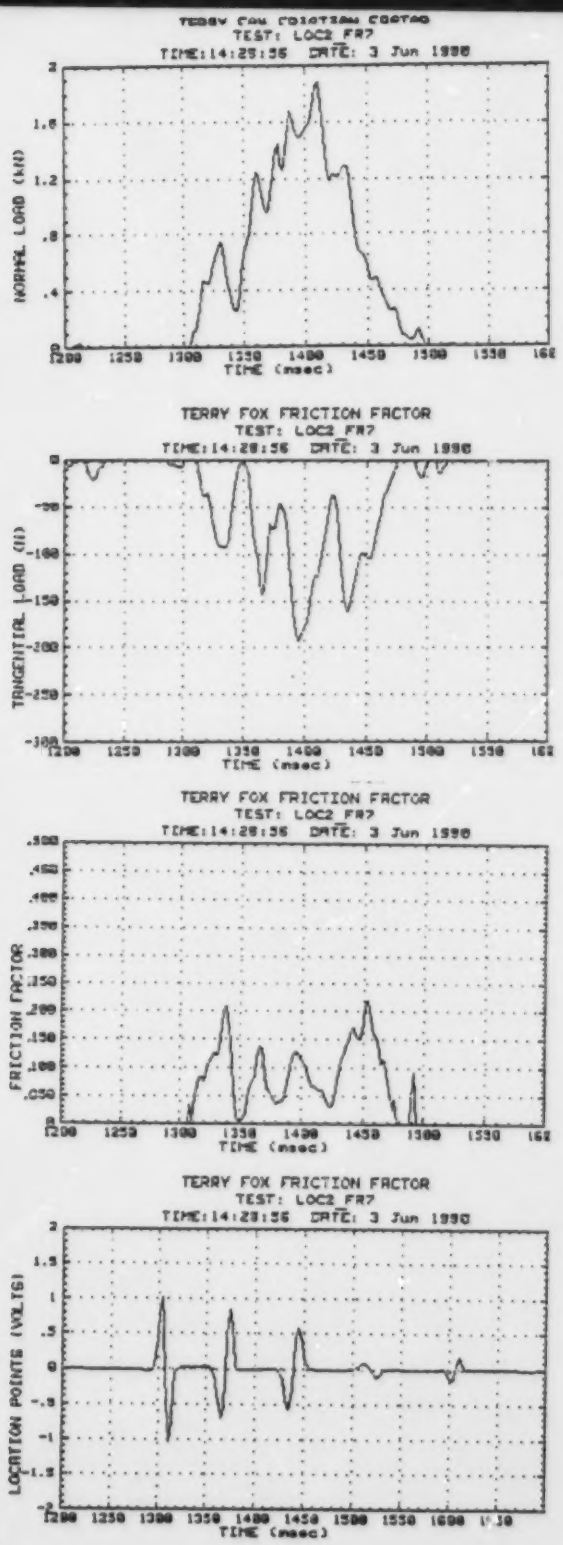

Figure 3.4.3.1

Sample Output from Tribometer Test

TABLE 3.4.3.1

Ice-Hull Friction Factors Measured For A Painted Inerta Surface

Ship: M.V. Terry Fox
Location: Starboard Side – Aft of Midship

Test Date: June 2
Air Temp.: –0.1°C
Ice Temp.: –0.2°C

Test #	Speed of Ice Sample (m/s)	Ice Failure Type	Friction Factor
Loc1–FR3	1.93	Sliding and Crushing	0.17
Loc1–FR4	1.55	Sliding and Crushing	0.19
Loc1–FR5	1.55	Sliding and Crushing	0.17
Loc1–FR6	1.66	Mainly Sliding	0.20
Loc1–FR7	2.08	Sliding and Crushing	0.18
Loc1–FR8	2.02	Sliding and Crushing	0.21
Loc1–FR9	1.60	Sliding and Crushing	0.20
Loc1–FR10	2.58	Mainly Sliding	0.17
Loc1–FR11	1.15	Sliding and Crushing	0.10
Loc1–FR12	2.21	Mainly Sliding	0.15
Loc1–FR13	2.44	Sliding and Crushing	0.20

Average Friction Factor For All Tests: 0.18 ± .03
Average Friction Factor For "Mainly Sliding" Tests: 0.18 ± .03
Average Friction Factor For "Sliding and Crushing" Tests: 0.17 ± .02

TABLE 3.4.3.2

Ice-Hull Friction Factors Measured For A Bare Hull Surface

Ship: M.V. Terry Fox
Location: Starboard Side – Aft of Midship

Test Date: June 3
Air Temp.: +4°C
Ice Temp.: –0.7°C

Test #	Speed of Ice Sample (m/s)	Ice Failure Type	Friction Factor
Loc2–FR1	2.28	Mainly Sliding	0.10
Loc2–FR2	1.29	Sliding and Crushing	0.15
Loc2–FR3	2.86	Mainly Sliding	0.15
Loc2–FR4	2.43	Sliding and Crushing	0.13
Loc2–FR5	1.65	Sliding and Crushing	0.21
Loc2–FR6	3.36	Sliding and Crushing	0.23
Loc2–FR7	2.65	Mainly Sliding	0.14
Loc2–FR8	1.35	Sliding and Crushing	0.21
Loc2–FR9	1.44	Sliding and Crushing	0.14
Loc2–FR10	2.79	Mainly Sliding	0.12
Loc2–FR11	2.00	Sliding and Crushing	0.14
Loc2–FR12	2.96	Mainly Sliding	0.18
Loc2–FR13	1.60	Sliding and Crushing	0.15
Loc2–FR14	2.43	Sliding and Crushing	0.18
Loc2–FR15	3.61	Mainly Sliding	0.19

Average Friction Factor For All Tests: $0.16 \pm .040$
Average Friction Factor For "Mainly Sliding" Tests: $0.14 \pm .040$
Average Friction Factor For "Sliding and Crushing" Tests: $0.17 \pm .035$

TABLE 3.4.3.3

Ice-Hull Friction Factors Measured For An Inerta Surface

Ship: M.V. Terry Fox
Location: Starboard Side – Aft of midship

Test Date: June 3
Air Temp.: +3.5°C
Ice Temp.: –0.6°C

Test #	Speed of Ice Sample (m/s)	Ice Failure Type	Friction Factor
Loc3–FR1	2.61	Mainly Sliding	0.09
Loc3–FR3	1.78	Sliding and Crushing	0.08
Loc3–FR4	2.23	Mainly Sliding	0.04
Loc3–FR5	2.35	Sliding and Crushing	0.07
Loc3–FR6	2.32	Mainly Sliding	0.05
Loc3–FR7	2.45	Sliding and Crushing	0.08
Loc3–FR8	2.19	Sliding and Crushing	0.06
Loc3–FR9	2.12	Sliding and Crushing	0.09
Loc3–FR10	2.49	Mainly Sliding	0.10
Loc3–FR11	2.26	Sliding and Crushing	0.04
Loc3–FR12	2.26	Sliding and Crushing	0.13
Loc3–FR13	2.04	Mainly Sliding	0.08
Loc3–FR14	2.09	Sliding and Crushing	0.04
Loc3–FR15	2.42	Sliding and Crushing	0.03

Average Friction Factor For All Tests: .070 ± .027
Average Friction Factor For "Mainly Sliding" Tests: .072 ± .023
Average Friction Factor For "Sliding and Crushing" Tests: .069 ± .029

Tables 3.4.3.1 to 3.4.3.3 summarize the test results. The average friction factor was 0.18, 0.16, and 0.07 for a painted inerta surface, a bare hull surface, and an inerta-coated surface respectively. The friction factors measured for "mainly sliding" tests were similar to those for "sliding and crushing" tests and differences were within the scatter of the individual test data.

Figure 3.4.3.2 shows the relationship of the friction factor to the hull surface roughness and compares these results to those of previous tests conducted with the same apparatus. The test results obtained in this study show reasonable correlation with previous results. All of these test data show that the friction factor increases with the hull surface roughness in a consistent manner. Figure 3.4.3.2 also shows that the ice type affects the friction factor as lower friction factors were measured for tests with cold fresh water ice than for warm saline arctic ice.

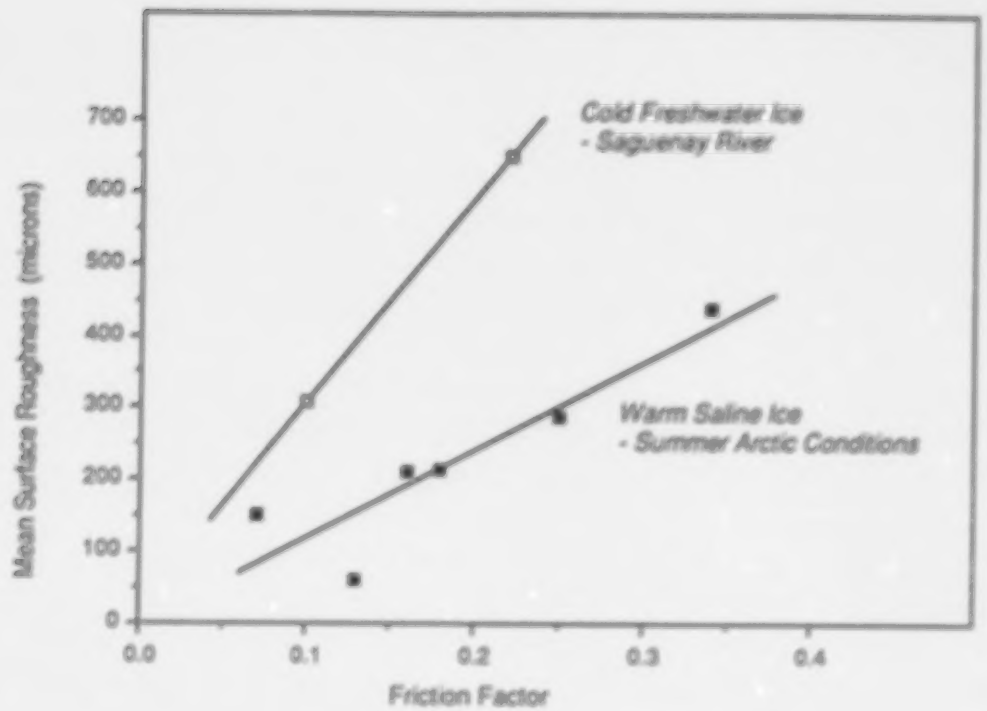

Legend:

Date of Trials	Hull Surface	Ship	Test Data: Friction Factor	Test Data: Surface Roughness (microns)	Data Source
June, 1990	Inerta	M.V. Terry Fox	.07	152	This Project
June, 1990	Bare Steel	M.V. Terry Fox	.16	212	This Project
June, 1990	Painted Inerta	M.V. Terry Fox	.18	216	This Project
July, 1979	Inerta	CCGS Louis S. St Laurent	.13	59	Noble & Comfort, 1979
July, 1979	Bare Steel	CCGS Louis S. St Laurent	.34	439	Noble & Comfort, 1979
Aug., 978	Bare Steel	CCGS Pierre Radisson	.25	287	Edwards et al, 1979
Feb., 1979	Bare Steel	CCGS Pierre Radisson	.22	649	Edwards et al, 1979
Feb., 1979	Painted Steel	CCGS Pierre Radisson	.10	308	Edwards et al, 1979

Figure 3.4.3.2 Friction Factor Versus Hull Surface Roughness

3.5 Icebreaking Pattern

Numerous photographs were taken to document the breaking pattern of the ice around the ship. This is important both for understanding the ice performance of the ship and for correlating the results of model scale tests to full scale. While a detailed description of the icebreaking pattern was beyond the scope of this project, some observations are presented in this section to provide a preliminary understanding of this issue.

Upon initial contact with the bow, the ice failed in cusps which were relatively large. The depth of these cusps was about one to two times the ice thickness while their length was about four times the ice thickness. See plates 3.5.1 to 3.5.5. In many cases, the ice failure location appeared to be unaffected by the presence of melt pools as it passed from a hummock to a melt pool with little change in direction. See plate 3.5.3. However, in some cases, the ice failure pattern changed abruptly at a melt pool (see plates 3.5.2 and 3.5.4) which indicates that the ice failure process was affected by the presence of melt pools on the ice surface.

The ice cusps which were initially broken and which passed under the ship were subsequently rebroken into much smaller pieces with dimensions of up to about one half the ice thickness. See plates 3.5.6 to 3.5.9. Plate 3.5.7 shows the broken ice pieces which were under the bow. (This picture was taken after the ship had been backed away from the ice sheet.) The majority of these pieces are small. Plates 3.5.8 and 3.5.9 show the ice pieces in the channel behind the ship. The channel is clogged with small pieces.

Plate 3.5.1
Cusp-breaking along the
mid-body of the M.V. Ikaluk

Plate 3.5.2
Cusp-breaking along the
mid-body of the M.V. Ikaluk

Plate 3.5.3
Cusp-breaking along the
mid-body of the M.V. Ikaluk

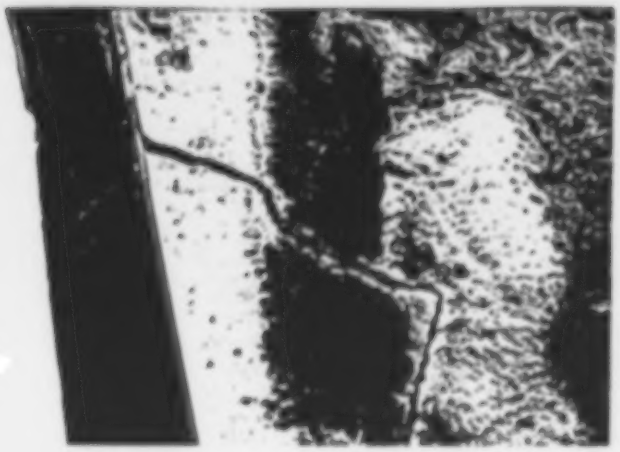

Plate 3.5.4
Cusp-breaking along the
mid-body of the M.V. Ikaluk

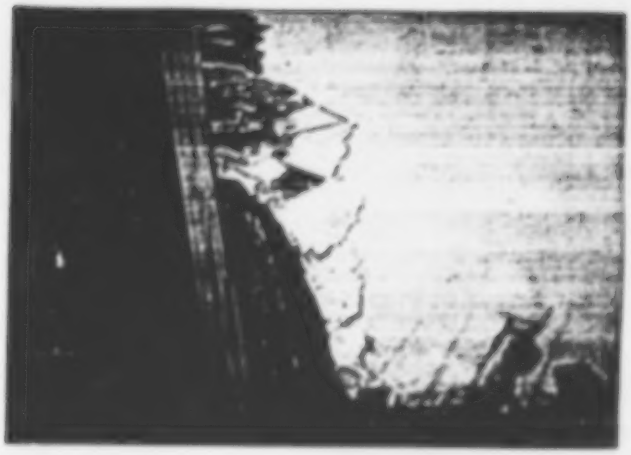

Plate 3.5.5
Cusp-breaking at the
aft end of the M.V. Ikaluk

Plate 3.5.6
Secondary Breaking of cusps
along mid-body of M.V. Ikaluk

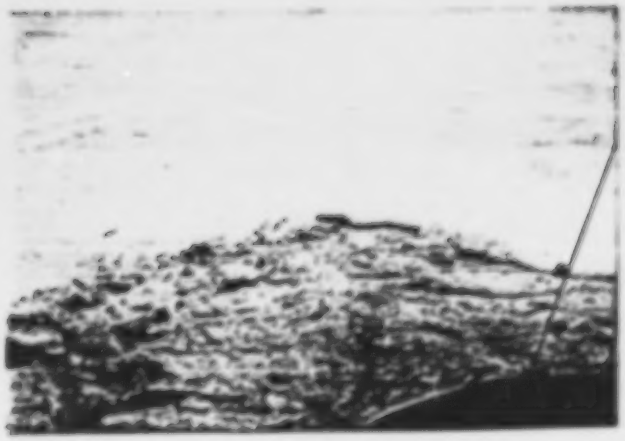

Plate 3.5.7
Broken Ice Pieces at Bow
of M.V. Terry Fox

Plate 3.5.8
Broken Channel

Plate 3.5.9
Broken Channel

SECTION 4

FULL-SCALE TESTS

4. FULL-SCALE TESTS

4.1 Trials Planning and Design

Objectives

The primary project objectives of the program were to determine the following propulsive performance characteristics for the two modern icebreakers:

1. Ship Resistance vs Velocity in Level Ice
2. Ship Power vs Velocity in Level Ice
3. Total Shaft Thrust vs Velocity in Level Ice and in Open Water Overload Conditions
4. Thrust Deduction Fraction vs Velocity in Level Ice and Open Water Overload Conditions

Figures 4.1.1 and Figure 4.1.2 illustrate the general form of the above.

An additional objective of the program was to obtain shaftline vibrational response data during ice-propeller interaction events, for both vessels in the same ice conditions in side by side tests.

Trials Required

In order to determine the propulsive performance characteristics it was necessary to carry out the following set of trials (see Figures 4.1.3a - 4.1.3d):

Ice Towing Tests: Tow each ship with the other and measure the net towing force (equal to resistance), for different steady towing speeds, in uniform unbroken level ice (Figure 4.1.3a). This includes the measurement of the towed ships' shaft thrust, which was equated to the drag of the propeller and was subtracted off of the towing force to obtain the net towing force.

Self Propulsion Tests in Ice: Self propel each vessel in as similar as possible ice conditions and at the same speeds as the towing tests (Figure 4.1.3b). Measure the shaft thrust and power required.

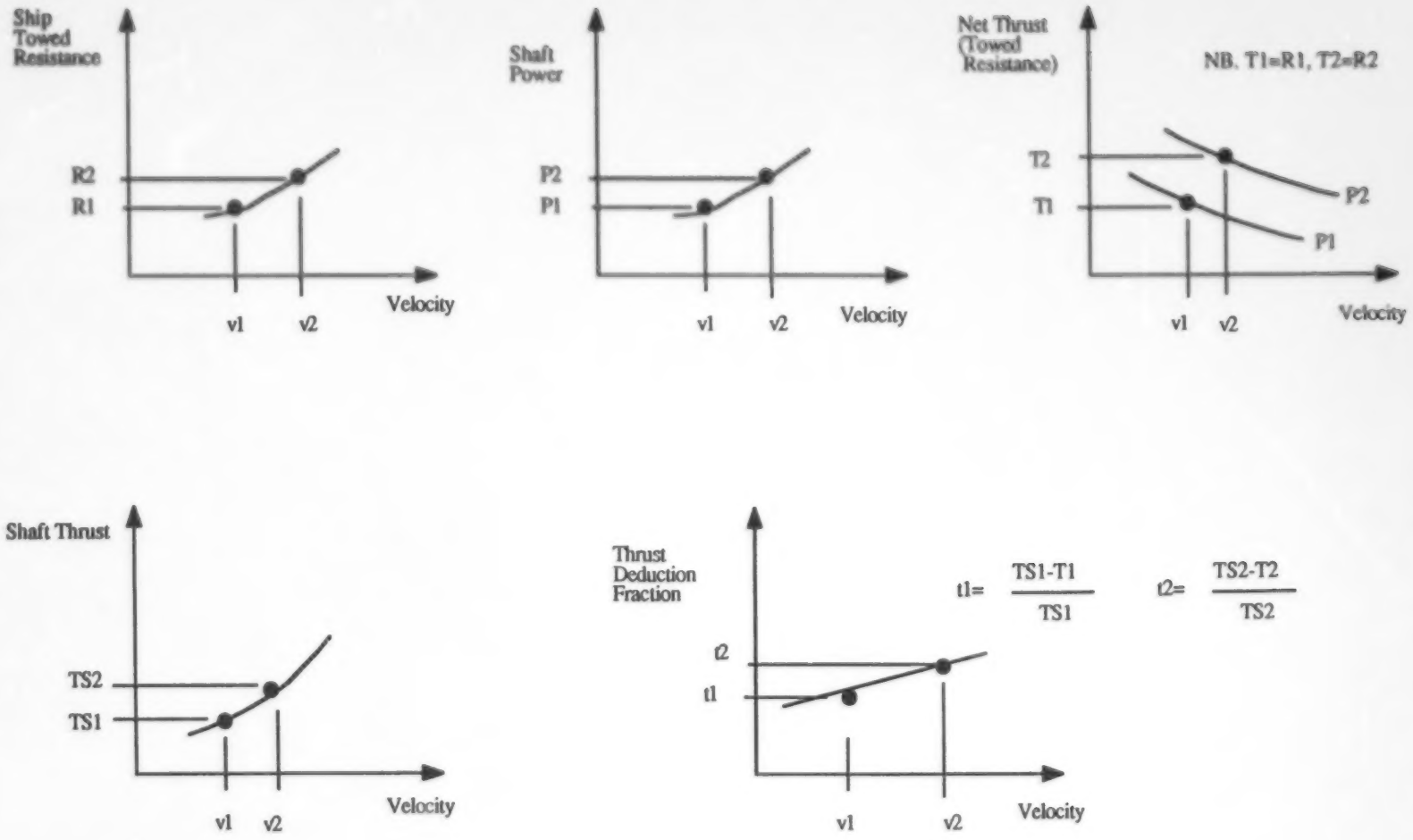

Figure 4.1.1 Determination of Propulsion PerformanceParameters

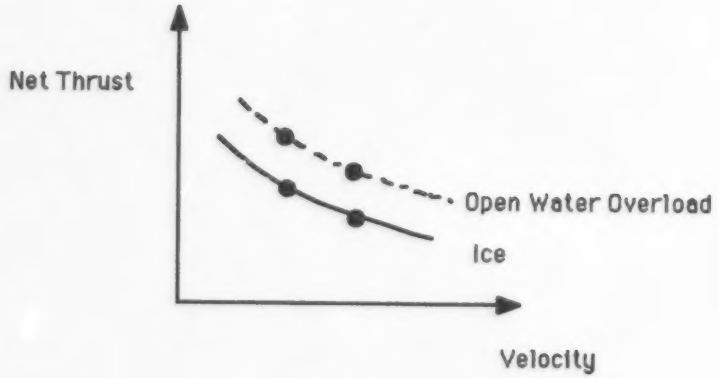

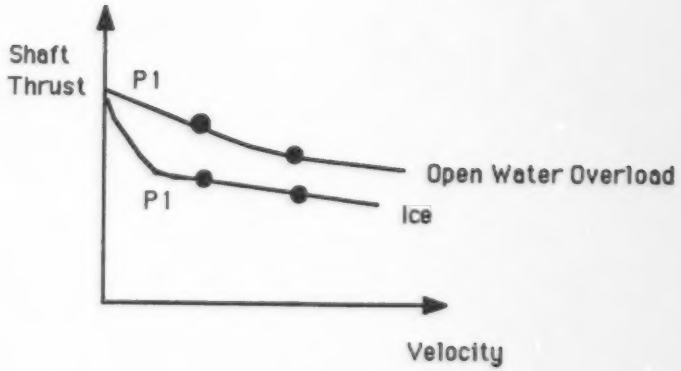

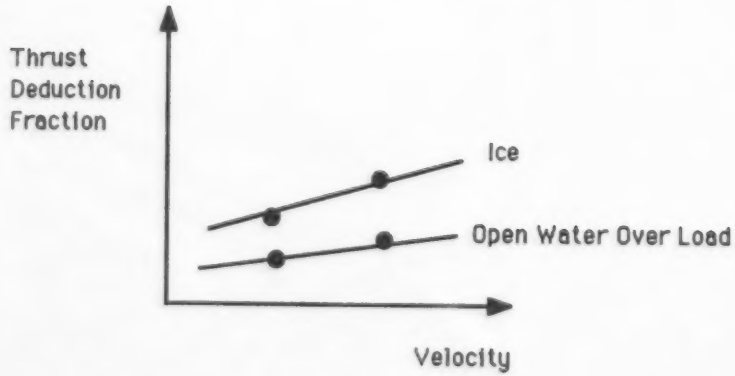

Figure 4.1.2 Propulsion Performance Characteristics

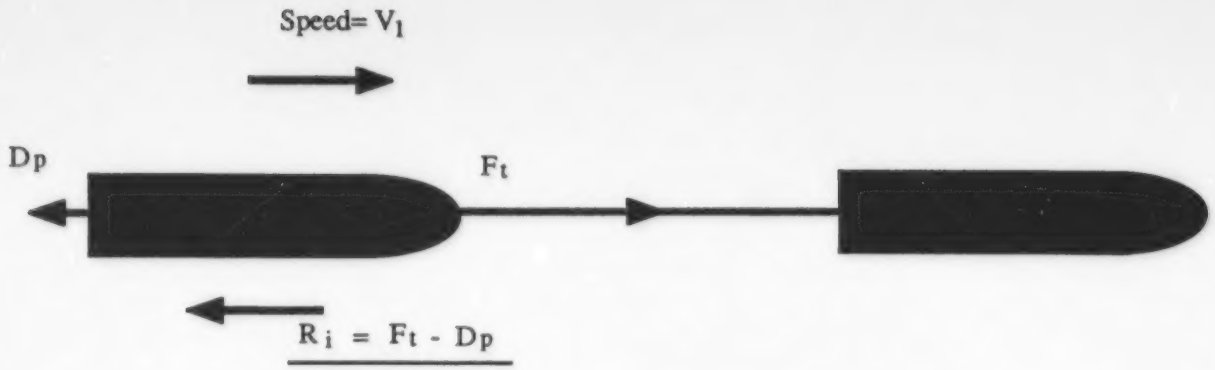

Figure 4.1.3a Towing Trials in Ice

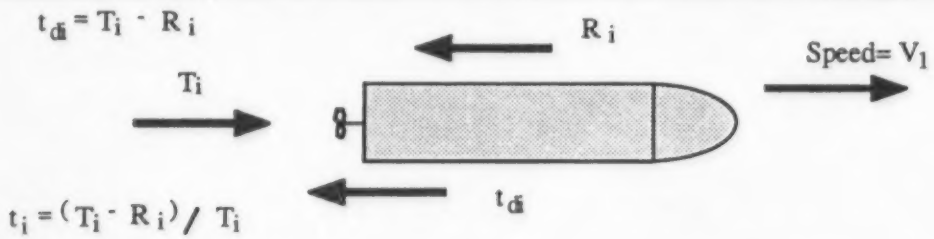

Figure 4.1.3b Self Propulsion Trials in Ice

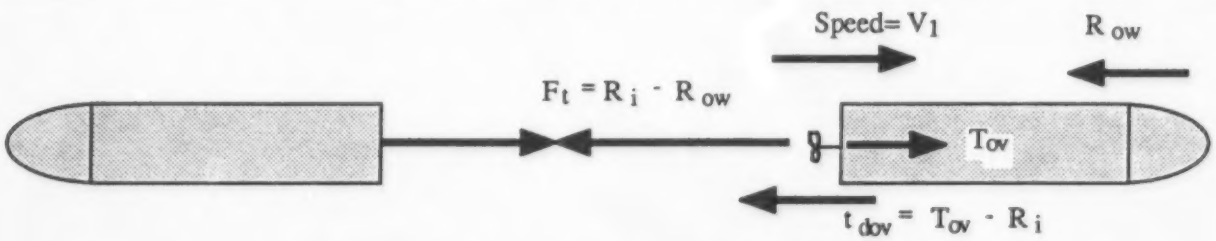

Figure 4.1.3c Overload Open Water Tests

MEASURE:

Shaft Thrust
Shaft Torque
Prop. Pitch
RPM
Fuel Rack
Rudder Angle

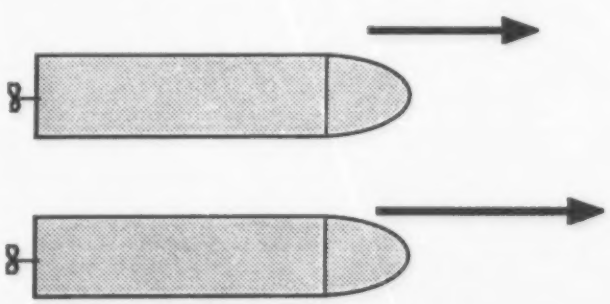

Figure 4.1.3d Level Icebreaking In Same Ice Sheet

Open Water Overload Tests: Self propel each vessel in open water, pulling against the other vessel (which provides added resistance), at the same speeds and tow rope pulls as those measured in the towing tests (Figure 4.1.3c). Measure the shaft thrust and power required.

Level Ice Breaking in the Same Ice Sheet: Manoeuvre both vessels through the same ice at the same time (Figure 4.1.3d). Measure the shaft torque and thrust as well as the machinery response at high data acquisition speed (500 readings/sec). Conducting these tests allows for a comparison of the response of two types of propulsion systems in the same ice conditions.

Propulsion Performance Parameters

Thrust Deduction

When a hull is towed, there is an area of high pressure over the stern which has a resultant forward component reducing the total resistance. With a self-propelled hull, however, the pressure over some of this area is reduced by the action of the propeller in accelerating the water flowing into it, the forward component is reduced, the resistance is increased and so also the thrust necessary to propel the model or ship. Common practice is to look upon this increase in resistance as a deduction from the thrust available at the propeller, so that although the screw provides a thrust of **T** tons, only $\mathbf{R_t}$ tons of thrust are available to overcome resistance. This 'loss of thrust' $(\mathbf{T - R_t})$ is called the **thrust deduction (td)**, and expressed as a fraction of the thrust is called the **thrust-deduction fraction, t**, where:

$$\mathbf{td = T - R_t = Thrust\ Deduction} \qquad (1)$$

$$\mathbf{t = (T - R_t) / T = 1 - (R_t / T) = Thrust\ Deduction\ Fraction} \qquad (2)$$

The expression **(1-t)** is called the **thrust-deduction factor**.

In Figure 4.1.3a, the required towing force (F_t) less the propeller drag (D_p = shaft thrust) for a steady speed (V_1) in ice is equal to the vessel resistance in ice (R_i). In Figure 4.1.3b, the vessel is in the same ice as in Figure 4.1.3a and is self-propelled at the same speed (V_1). The force balance equation yields:

$$R_i = F_t - D_p \quad (3)$$

$$td_i = T_i - R_i \quad (4)$$

$$t_i = (T_i - R_i) / T_i \quad (5)$$

where;

T_i = Total Shaft Thrust in Ice (Measured)

F_t = Tow Rope Pull (Measured)

D_p = Propeller Drag (Measured Shaft Thrust of Towed Vessel)

R_i = Vessel Resistance in Ice

td_i = Thrust Deduction in Ice

t_i = Thrust Deduction Fraction in Ice

Figure 4.1.c illustrates the method of conducting open water overload tests. One vessel is pulling against the other vessel with a tow rope force equal to the resistance in the ice towing trials (R_i), less the relatively small open water resistance R_o, and at the same speed (V_1) as that in the ice towing tests. The total resistance to vessel motion is therefore R_i. The force balance equation yields:

$$td_{ov} = T_{ov} - R_i \quad (6)$$

$$t_{ov} = (T_{ov} - R_i) / T_{ov} \quad (7)$$

where;

T_{ov} = Total Shaft Thrust in the Open Water Overload Condition (Measured)

R_i = Vessel Resistance in Ice (Measured)

td_{ov} = Thrust Deduction in the Open Water Overload Condition

t_{ov} = Thrust Deduction Fraction in the Open Water Overload Condition

It is useful to present a parameter called the ice thrust deduction factor (itdf), which is defined as follows:

$$itdf = (t_i - t_{ov}) / t_{ov} \quad \textbf{Ice Thrust Deduction Factor} \quad (8)$$

The lower the value of the itdf the less the influence the ice has on the thrust deduction.

The thrust which must be produced by the propulsion system of a vessel operating in ice is therefore built up by the components as shown in Figure 4.1.4. Knowledge of the nature and magnitude of the ice thrust deduction factor with respect to ice conditions, hull form and speed will allow for more accurate predictions of the thrust requirements for icebreaking vessels. If the thrust deduction fraction is known, the resistance at full-scale can be computed from the measurement of the shaft thrust, which is a significant cost advantage. In addition the knowledge of the thrust deduction in ice at full-scale will greatly assist in the scaling of model test results.

Ice Transit Power Factor

In the self-propulsion trial, Figure 4.1.3b, the shaft power P_i required to generate the thrust T_i is measured. In the open water overload trials, Figure 4.1.3c, the shaft power P_{ov}, required to generate the thrust T_{ov} is measured. From these trials the power to thrust ratio versus the thrust can be plotted as shown in Figure 4.1.5. Using this relationship the required open water power (P_{ov}) can be determined for a specified thrust needed in ice (T_i). The difference between the power required in ice transit and the power required in open water overload tests, to generate the same thrust, is the power absorbed through the interaction of ice with the propeller and wake, and is called the ice transit power factor, itpf such that;

$$itpf = (P_i - P_{ov}) / P_{ov} \qquad \text{Ice Transit Power Factor} \qquad (9)$$

where;

P_i = Power required in ice to produce T_i thrust

T_i = Thrust required in ice to produce speed V_i

P_{ov} = Power required in open water overload condition to produce T_i thrust

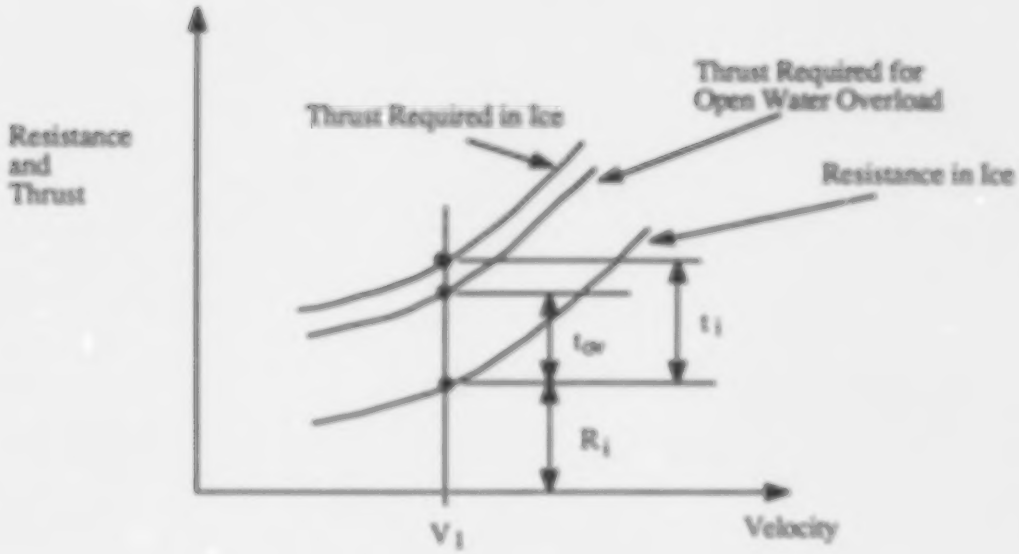

Figure 4.1.4 Components of Thrust During Ice Transit

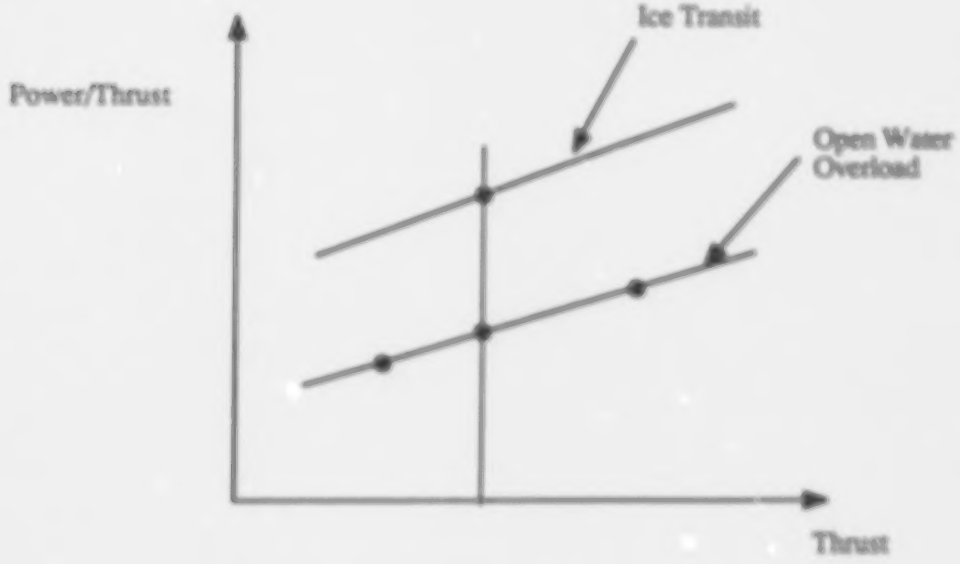

Figure 4.1.5 Power To Thrust Ratio Comparisons

Magnitude of Interaction Effects

Open water overload thrust deduction has not been measured previously for the vessels in either model tests or ship trials. However, based on data for other vessels, one would expect values of 5-10% at bollard, increasing by about 2-3% for each m/s increase in speed.

No data existed, prior to these tests, on the increase in thrust deduction due to the presence of ice,. The best guess, however, is an increase of about 10% of shaft thrust, for significant levels of interaction in ice of 1 m thickness or above. This means that interaction loads of about 10 tonnes must be discriminated from the difference of towing and shaft loads each in the region of 100 tonnes. In addition, the effect of ice milling might result in a maximum increase in average shaft power of about 5-10%. The high degree of control of trial conditions and accuracy in measurement required in the trials is evident from these numbers. The required degree of accuracy in the measurement of ship speed, shaft thrust and power and towing force is within current achievement levels. The matching of ship speed will call for considerable skill of the operator and cannot be expected to be achieved exactly. However, for small speed differences, data corrections can be made with some confidence.

Technical Issues

Ship trials with a similar objective were carried out on the Mobile Bay in 1986. The results of the towing trials are considered to have been successful, since resistance from these tests is in very good agreement with that analysed from propulsion trials on Katmai Bay in 1979. The propulsion aspect of these trials, however, was less successful. The reason for this has not been clearly determined, but the most likely explanation is that the ice conditions for the towed resistance tests and self propelled tests were not sufficiently well matched in terms of ice thickness and ice properties. In addition there may have been some pressure relief of the ice sheet ahead of the towed vessel. Any such pressure relieve would greatly reduce the resistance of the vessel, and therefore result in inaccurate estimates of thrust deduction.

From the above description of how the project objectives can be achieved, a number of issues arise as to the practical measures which must be followed in the trials in order to maximise success.

1. The ice sheet in front of the towed vessel must be infinite in nature, such that no pressure relief is evident during towing. This will require the positioning of the vessels 500 - 700m apart, with an unbroken sheet of ice between them.

2. The towed resistance and self-propulsion tests should be carried out in as nearly the same ice conditions as is possible. In early June in the Canadian Beaufort, landfast ice is in a state of deterioration. It is therefore imperative that companion towed resistance and self-propulsion tests be carried out in the same area and at almost the same time. The ideal situation is for these tests at each ice thickness and speed to be run consecutively.

3. The open water propulsion overload tests must be carried out after the ice tests. The towing force and speed combinations used should match those measured in the ice tests.

4. In order to have almost identical ice thicknesses in consecutive runs, tests should be carried out along iso-thickness ice contours. The first ice survey should map the available ice area in search of such constant thickness conditions.

5. The vessels were designed for 1.2 m of ice and the wedges under the bow do a good job of limiting ice interaction over much of the bottom of the vessel and the stern in the design ice. One ice thickness should therefore be close to this design thickness, say 1.0 to 1.2 m. The second ice thickness should be greater, such that the effect of significant interaction can be determined. Ice thicknesses of say 1.3 to 1.5 m., where the bow wedges are not sufficient to deflect the majority of ice, would be ideal. Determination of the actual trials ice thicknesses will of course be dependent upon many factors - the available ice thicknesses, aerial extent and degrees of uniformity, and the strength of the ice and subsequent ice resistance in relation to the tow rope pulls available.

6. Full analysis of the trials data for ice-hull and ice-propeller interaction factors, requires measurement of the total propulsive thrust. This equals shaft thrust, which will be recorded, for the open screw vessel. For the ducted screw vessel, however, part of the thrust is provided by the nozzle. Nozzle thrust should therefore be recorded if possible, or failing this, estimates based upon results from the trials conducted on the MV Ikaluk in the spring of 1989 could be done.

7. Ice properties will be changing throughout the trials. Measurements must therefore be taken as close to the tests as is possible.

8. Ship condition must be kept constant throughout the trials. This should only be changed after all tests at one draft have been completed and a requirement and opportunity exist to repeat a test at a different draft. Ship speed in companion resistance and propulsion tests must be controlled to be as similar as possible to one another. Small differences can be corrected for, but confidence in the end result decreases with each such correction.

9. It is considered that control of speed in the towed resistance tests will be more difficult than in the self-propulsion tests in ice. Consequently, the resistance test at any target speed should be carried out first and followed immediately, or very closely, by the self-propulsion test targeted at the speed measured in the resistance test.

Resistance and Tow Rope Pull Estimates

Resistance and tow rope pull estimates were calculated in order to determine the probable range of ice thicknesses and speeds which could be covered in the tests. It was assumed that ice physical properties would be typical of Spring Beaufort landfast ice. Level ice performance tests in Spring Beaufort landfast ice conditions, from which resistance predictions could be made directly, had not previously been carried out on M.V. Ikaluk and Terry Fox. It was therefore necessary to make predictions starting with Winter Beaufort performance data for the vessels. These data were modified for Spring conditions according to trends established from full-scale trials on Kigoriak and Robert Lemeur in both Winter and Spring conditions, and voyage performance data on the 1986 Summer Arctic trials of M.V. Kalvik.

The resistance estimates are given in Figures 4.1.6 and 4.1.7 for MV Ikaluk and Terry Fox respectively. They are for ice with a flexural strength of approximately 200 KPa. Winter Beaufort Sea data for speeds of 1,2 and 3 m/s and modified for spring conditions by increasing the ice thickness at any given resistance by 30%.

Tow rope pull estimates are based on data from full-scale bollard trials, model propulsion overload tests and open water performance trials. They are given in Figure 4.1.8 for both vessels. All data used in the estimates are drawn from the Transport Canada Report, "Icebreaker Design Synthesis - Analysis of Contemporary Icebreaker Performance", TP 9992E, 1990 and carried out be AKAC.

The resistance and tow rope pull estimates have been used to construct the towing diagrams for the MV Terry Fox and Ikaluk as shown in Figures 4.1.9 and 4.1.10 respectively. The towing limit curves are constructed by determining the ice thickness where the vessel's towed resistance at a given speed equals the towing vessel's tow rope pull at the same speed. Extrapolation of the resistance curve with respect to ice thickness has been necessary to complete the towing limit curves. An ice thickness exponent of 1.5 is used.

In Figure 4.1.9, it is seen that MV Terry Fox, working in a wide channel, can tow Ikaluk in thicker ice and at higher speeds than MV Ikaluk can manage under self-propulsion. In Figure 4.1.10, it is seen that Terry Fox can break ice under self-propulsion slightly better than when towed by Ikaluk.

Shallow Water Effects

The vessels have a maximum draft of 8 m and will be in water depths of about 16 m. Ship speeds will be from 0 to 6 knots. In these conditions, the effect of restricted depth of water upon resistance in ice will be negligible. In ICETECH 90, a paper entitled "Development of Ice Model Tests into a Reliable Tool for Icebreaking Ship Design", by H. Soininen, provided information on the effect of shallow water on ice resistance. At a depth/draft ratio of 2, the thickness of ice which can be broken by a vessel at a given power is reduced by 1.5%. This translates into a resistance increase of about 2%.

Figure 4.1.6

M.V. TERRY FOX
Level Ice Resistance Estimate

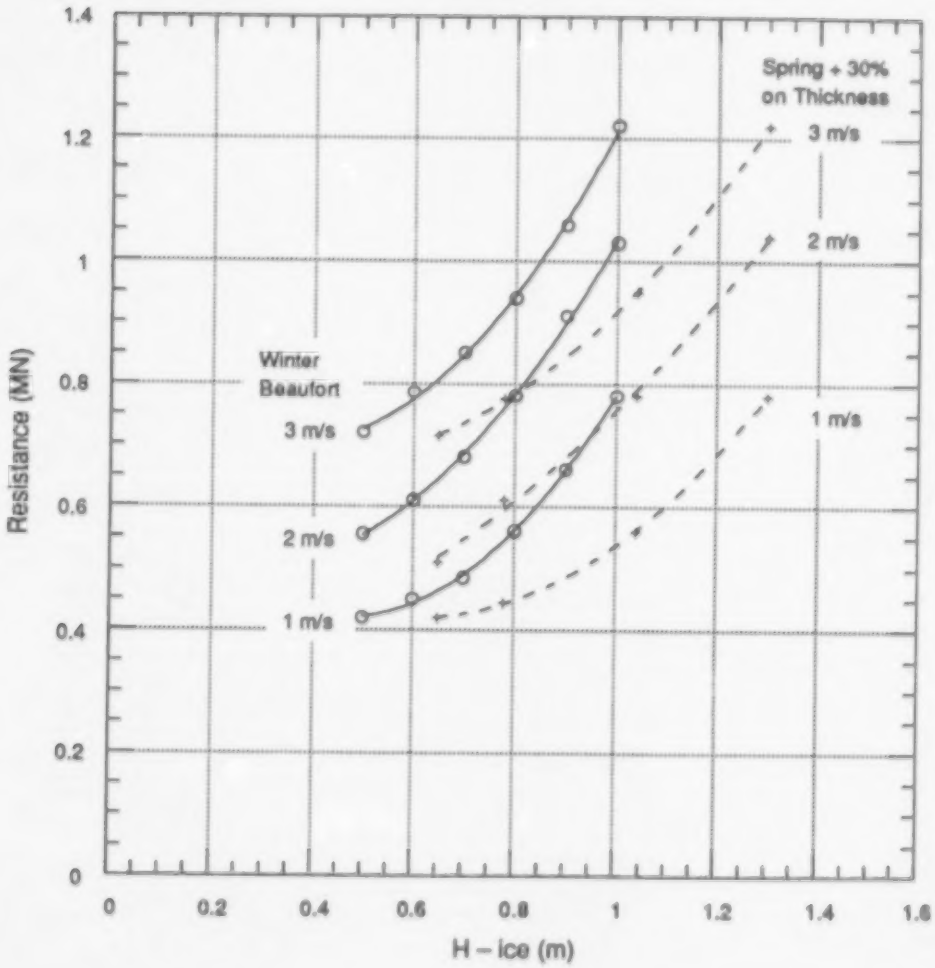

Figure 4.1.7

M.V. IKALUK
Level Ice Resistance Estimate

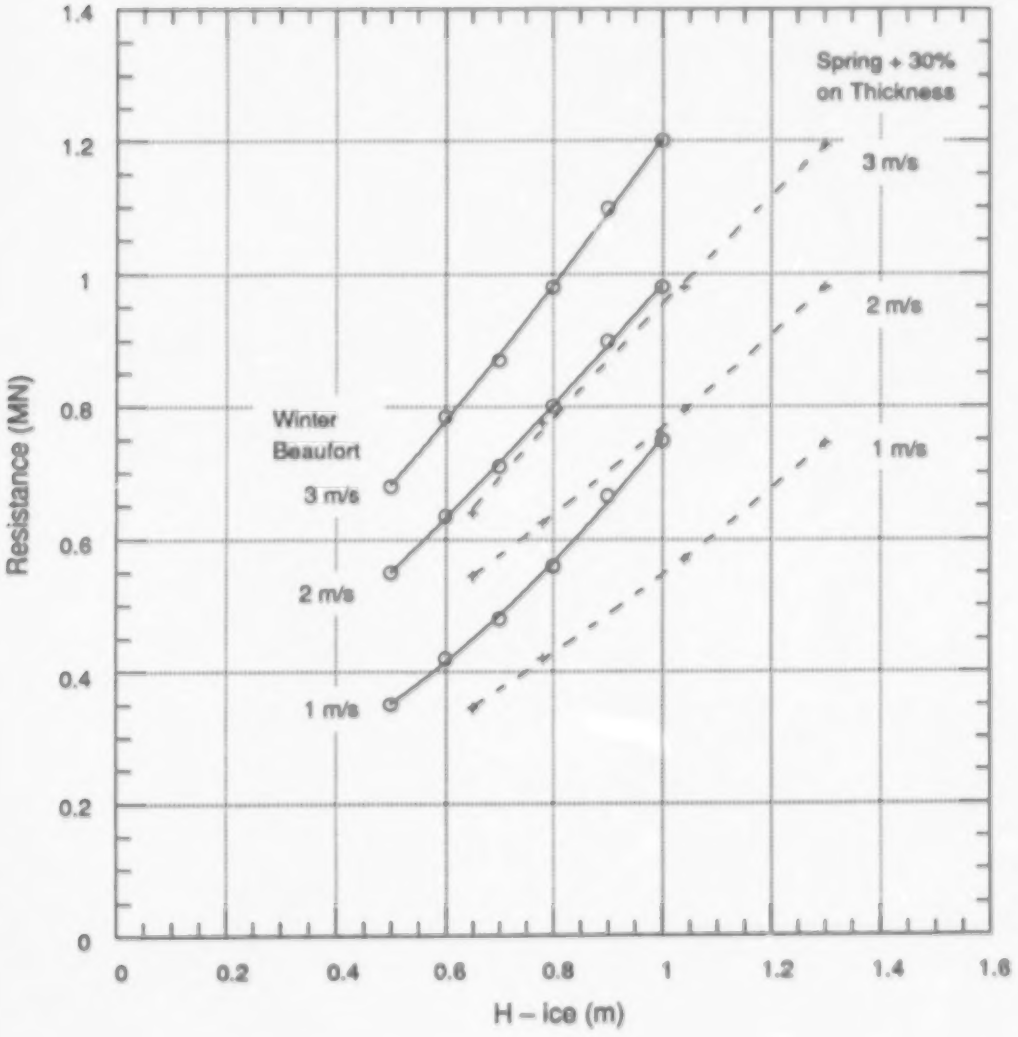

Figure 4.1.8

M.V. IKALUK and M.V. TERRY FOX
Tow Rope Pull Estimates

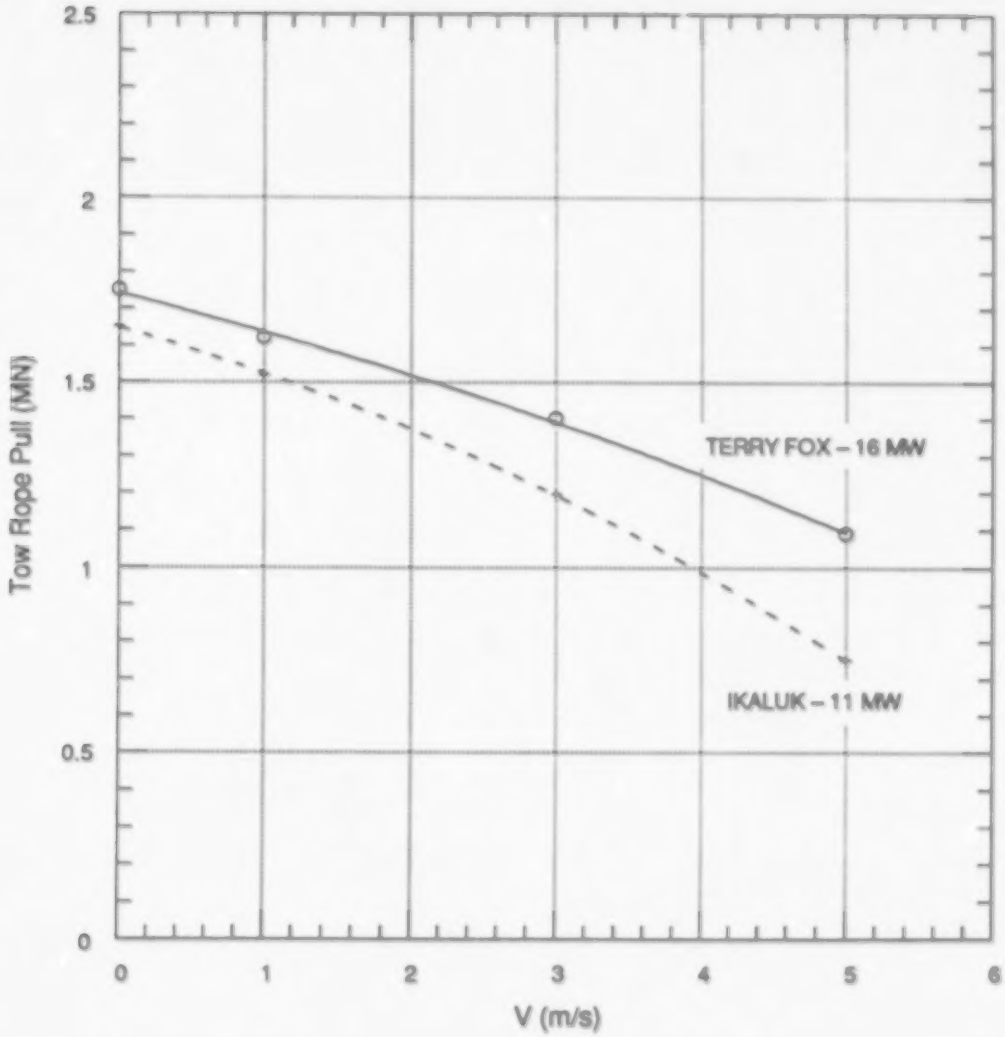

26 May, 1990

Figure 4.1.9

Towing Diagrams
M.V. TERRY FOX Towing M.V. IKALUK

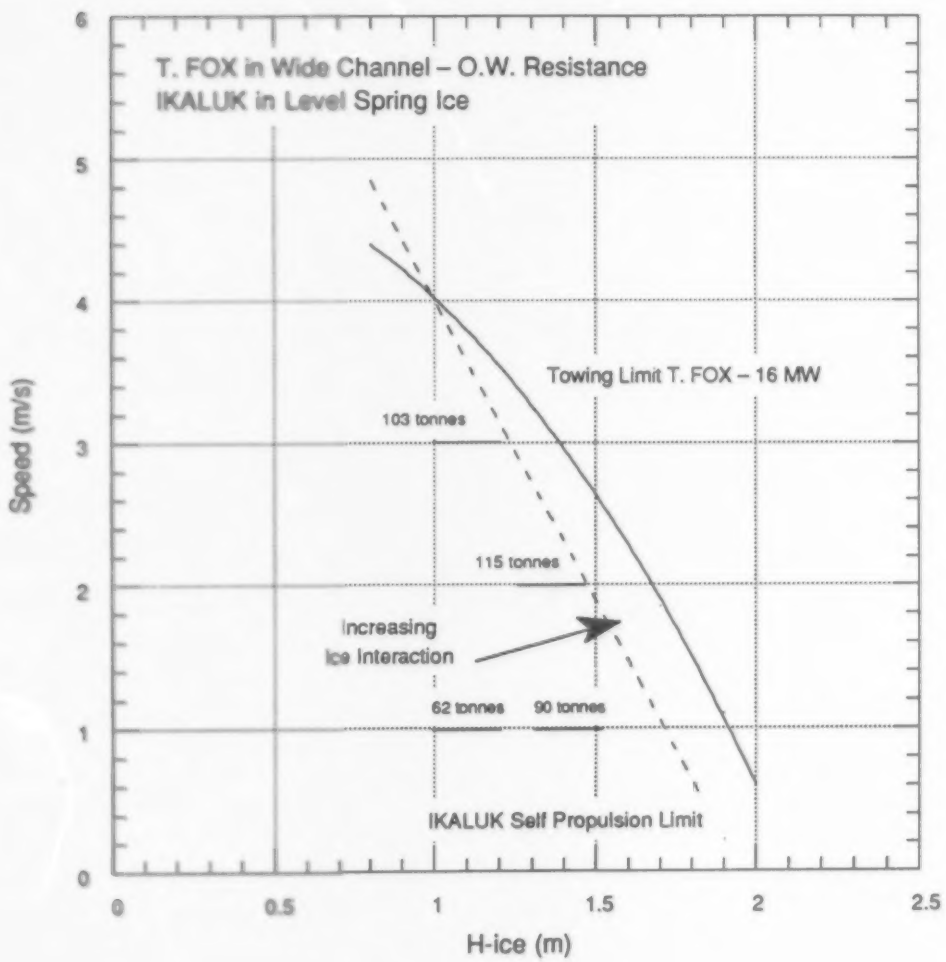

Figure 4.1.10

Towing Diagram
M.V. IKALUK Towing M.V. TERRY FOX

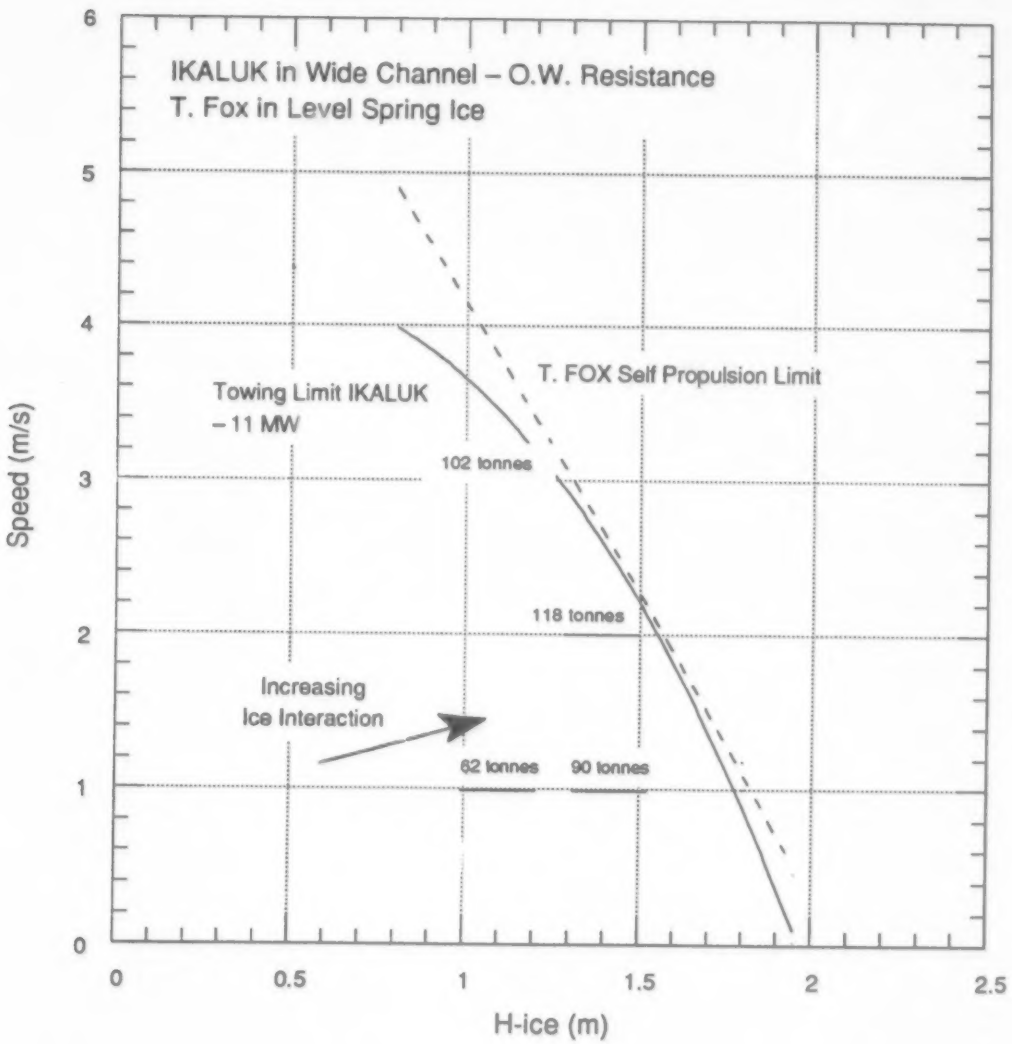

4.2 Towing Design and Execution (Contributed by Kristi Maritime Ltd.)

At the outset of this project it was realized that the logistics of the hook-up between the two test vessels and their capacity to tow each other was crucial to the successful completion of the full scale trial program. The towing capacity, towing equipment and powering characteristics for each vessel were carefully assessed during the planning stages. Since both vessels are equipped to meet their design operational roles, with heavy duty towing and anchor handling winches with capacity and towline strength substantially exceeding the expected resistance of the respective towed vessel, this equipment was judged more than adequate for the proposed trials. Examination of the foredeck however, showed that in both cases no suitable hook-up point could be made to existing mooring equipment.

The use of a towing bridle system which would result in the load cell outside of the vessel was rejected in view of the danger of submersion or damage during hook-up. Even if fitted with a prevention system to limit the drop below deck level it was still considered more advantageous to keep the load cell on deck.

Both vessels are fitted with closed chocks on centreline in the forward bulkwark. With the preference to keep the load cell on deck it was decided to fit a single point mooring in the form of a Smit bracket located on centreline forward with sufficient clearance for load cell and shackle between the bracket and bulwark.

This solution provided a very neat and unobtrusive additional piece of equipment to the vessels outfit and greatly simplified the hook-up procedure.

The bollard pull for MV Terry Fox is in the order of 180 tonnes and for MV Ikaluk about 150 tonnes.

For sizing of the Smit bracket the higher bollard pull was assumed as the maximum load which could be applied at the mooring point. Using a 100mm (4") diameter locking pin in mild steel gives a safety factor of 2.2 to yield which considering the nature of the test was considered adequate. Other scantlings of the bracket were sized accordingly.

A section of the Focsle Deck plate was cropped out in each case and the Smit bracket on its baseplate integrated into the bow structure being welded to the deck and to underdeck

structure at the interface providing sufficient weld material to ensure distribution of the tow load. Details of the Smit bracket ar shown in Fig 4.2.1.

Two methods of vessel deployment were considered for tow test trials: maneuvering with the vessels connected or maneuvering independently and with the vessels in position, transporting the tow cable over the ice.

The first approach was considered undesirable since it was believed that too much time would be involved due to interdependency of the vessels, and, more critically, the danger of destroying the ice sheet between the vessels prior to test.

The second approach was considered more practical in view of ice conditions, equipment and personnel available.

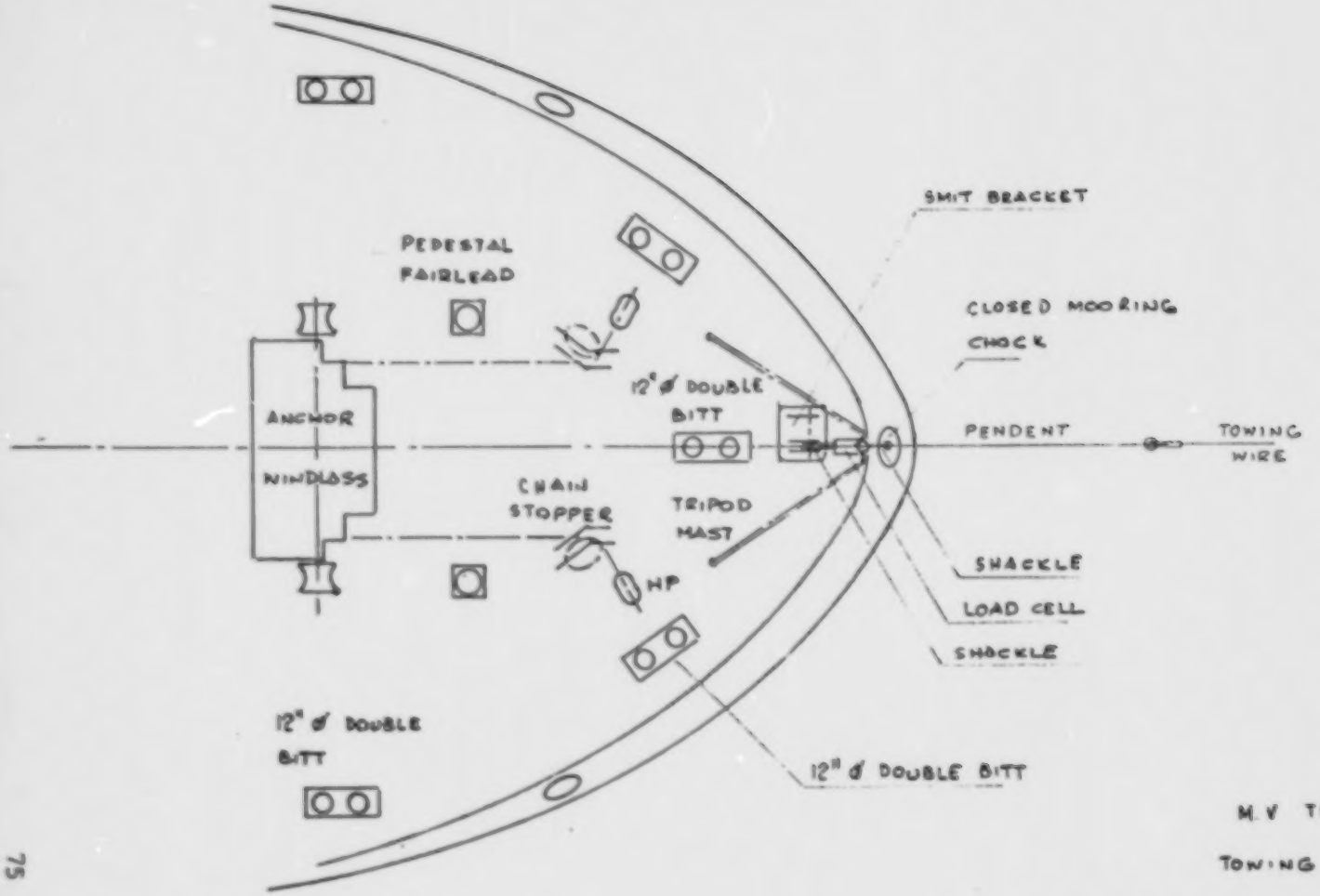

Figure 4.2.1 Details of Smit Bracket

Additionally, it was believed that there was a real danger of ice clogging the propulsion nozzles of the Ikaluk, therefore, it was preferable to have this vessel pull from an open water position rather than in a broken channel.

The procedure then was to manoeuvre both vessels into position independently with approximately 700m of undisturbed ice sheet between. In the tests with the Ikaluk towing, this vessel would back down from the open water into the ice sheet sufficient distance to provide a safe ice platform astern or alongside the vessel for personnel working the tow line messenger.

The messenger line consisted of lengths of ships polypropelene mooring ropes with soft eye splices each end. These lengths were run out over the ice and lashed at the eye splices.

Messenger was brought aboard using the anchor windlass warp ends, the tow line being payed out off the pulling vessel towing winch.

Initially some concern was expressed as to the effect of pulling the heavy tow wire over the ice, it being thought that this may result in a "sawn" slot in the ice surface thus weakening the ice sheet.

In preparation for the first test the messenger was run out well to port of the trial track, the tow line then being dragged laterally during run out and tensioning.

For subsequent tests the messenger was run directly between the vessels since it was observed that where the tow line had contacted the ice in the final run out and tensioning on the first test, this contact did not produce the saw-tooth effect anticipated and very little indentation of the ice sheet occurred.

The method of running the messenger was the subject of much deliberation and frustration.

Initially a snowmobile was utilized to deploy the lines, from the vessel to be towed out, over the ice to their respective positions along the track to the towing vessel and then lashed at each connection.

The snowmobile was limited in "towing" capacity such that only two lengths of mooring lines (messenger) could be deployed at a time.

The spring ice conditions had produced numerous melt pools (thus soft ice conditions in these areas) along the track which proved fatal to the operation of the snowmobiles attempting to manoeuvre towing the messenger lines. These conditions resulted in frequent stoppings and stalling of the vehicles. In the absence of any other means at this time, the ships' crew (including the female workers) cheerfully and willingly bent their backs to the task of manhandling (person handling) the ropes between the vessels.

For the last two tests the base helicopter was brought into service which air lifted the messenger lengths along the track substantially reducing deployment time.

With the load cell shackle already in place on the vessel to be towed and a pennant from this shackle out over the bow it was a relatively straightforward matter to make the final hook-up on the ice. For uncoupling after any given test run the vessels were brought in close proximity stem to stern and the towline released on deck of the towing vessel. Pennant was then brought back aboard the towed vessel ready for deployment and hook-up for the next test.

In order to minimize drag and to prevent any ice build-up forward of the propellers during a test run the ships were kept running at the normal operating RPM with pitch set at neutral (0 thrust).

For the first test run with Ikaluk towing Terry Fox, it was found that a substantial length of the track was used in accelerating the vessels to steady state.

For subsequent tests astern pitch was applied to the towed vessel to bring up tow line tension to a point where with pitch off, the vessel was accelerated more rapidly thus reaching required speed more quickly and hence minimizing loss in track length.

This method proved most effective, enabling an increased number of towing speeds to be achieved over each track length.

Preliminary power level requirements for each speed was estimated from existing model test and full scale data for each of the vessels. These power levels were adjusted, as necessary, based upon results generated as trials progressed.

Since instrumentation was monitored, in each case, aboard the towed vessel, power level incremental increases were initiated also at this point, these being radioed to the towing vessel when it was considered that sufficient steady state data had been recorded for any given speed.

The decisions taken as to method of deployment and hook-up of the test ships were fully vindicated in the successful completion of these unique trials.

The only negative aspect of the entire operation was in the time to deploy the messenger cable.

For future trials it would be recommended that a small diameter steel wire rope be employed to span the full track length in lieu of the mooring lines, at least as the lead connection, in order to expedite the initial hook-up.

4.3 Data Collection

Three days of dedicated testing were conducted from June 11-13, 1990, in Herschel Basin, Yukon. The tests were extremely successful with 5 towing trials performed and over 50 self-propulsion and ice/propeller interaction events recorded.

During the towing and self-propulsion trials, data was recorded digitally at a rate of 10 readings per second for each of the machinery signals, and 1 reading every three seconds for the each of the three ranges (to determine ship position and speed). For the ice/propeller interaction events data was recorded at 400 readings/sec/channel.

Table 4.3.1 shows the trials performed.

Table 4.3.1 List of Trials Performed

MV Terry Fox

Type	Description
Towing Level Ice	2 Tows, 3 - 4 speeds, 0.5 - 3.5 knots
Self Propulsion	23 Tests, 0.5 - 5.0 knots
Transient Response	12, 20 sec. events of ice propeller milling
Open Water Overload	5 tests, 30 - 105 tonnes, 0.5 - 4.0 knots

MV Ikaluk

Type	Description
Towing Level Ice	3 Tows, 3-4 speeds, 0.5 - 4.0 knots
Towing while lead vessel in Broken Channel and in Level Ice	2 Tows, 3 - 4 speed, 0.5 - 4.0 knots
Self Propulsion	13 Tests, 0 - 2.5 knots
Transient Response	10, 20 sec. events of ice propeller milling
Open Water Overload	6 tests, 30 - 100 tonnes, 0.5 - 3.5 knots

Over 60 disks of data were recorded (30 MBytes). Data was plotted and over 1,000 time history plots were produced and catalogued.

Ice property measurement was a significant part of the project. Section 3.0 described in detail the ice properties measured; this included:

- Ice thickness
- Ice salinity and temperature profile
- Ice-hull friction factor

Preliminary data analysis was conducted on the vessels during the trials program, to determine the status and validity of each sensor output. All sensor output was acceptable. Particular attention was required to analyse the nozzle strain gauge output on the MV Ikaluk. The total nozzle thrust was estimated from the output of one strain gauge. This value was compared to a calculation based upon the data collected from the tests conducted in the spring of 1989 on the MV Ikaluk, where the output of twenty strain gauges were used to determine the thrust contribution of the nozzle.

A detailed log was made during the trials on both vessels. In addition video tapes were recorded during the trials documenting the ice conditions, ship movement, and trials area.

4.4 Trials Description

Figure 4.4.1 illustrates the trials area. Several plans were developed and reviewed as the test dates approached. Consultation with the captains, chief engineers, and client representatives were conducted and a trials plan was produced. The plan called for seven towing trials as illustrated in Figure 4.4.2. The ice party laid out a test area by placing large orange flags as markers at each end of the 700 meter long tracks. The relatively long track length, allowed for the capability of towing the vessel at two to three constant speeds for two to three ship lengths each. The tracks were spaced 1,000 - 1,500 metres apart to prevent any pressure release of the ice while towing. Ice property measurements were conducted along the tracks prior to and during the testing, as described in section 3.0.

On the evening of June 10,1990 both the MV Terry Fox and MV Ikaluk manoeuvred away from the other BeauDril vessels and positioned themselves on the West side of the drilling rig "Kulluk". The following morning the two vessels proceeded to the ice edge, during which self-propulsion data was collected. It was decided that the MV Ikaluk would tow the MV Terry Fox for the first towing trial. After reaching the ice edge both vessels proceeded east in the open water, down the ice edge, for approximately 3 km. The MV Terry Fox broke into the land fast ice and conducted self-propulsion tests while manoeuvring to the start of the first towing track. The MV Ikaluk proceeded further down the ice edge to the

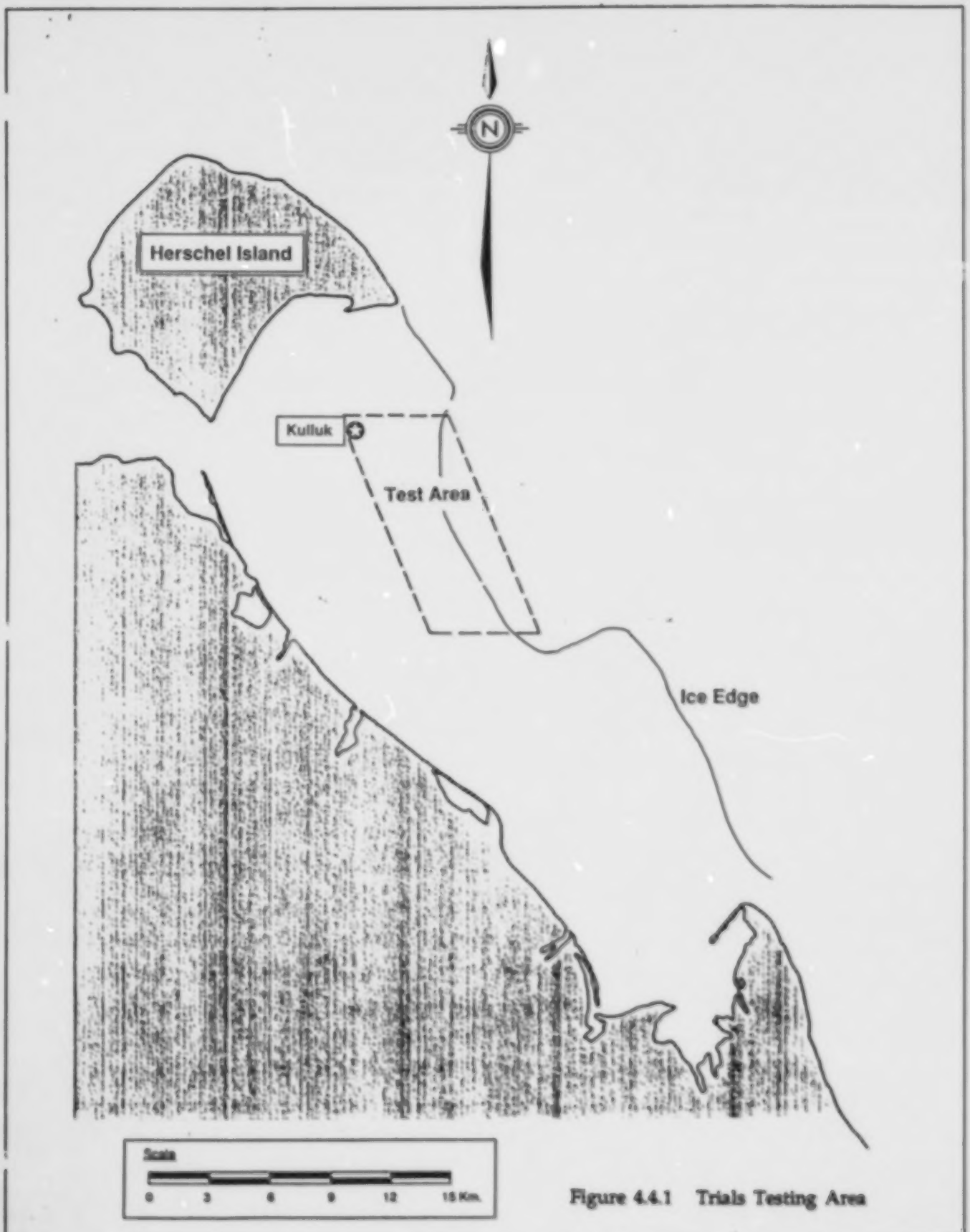

Figure 4.4.1 Trials Testing Area

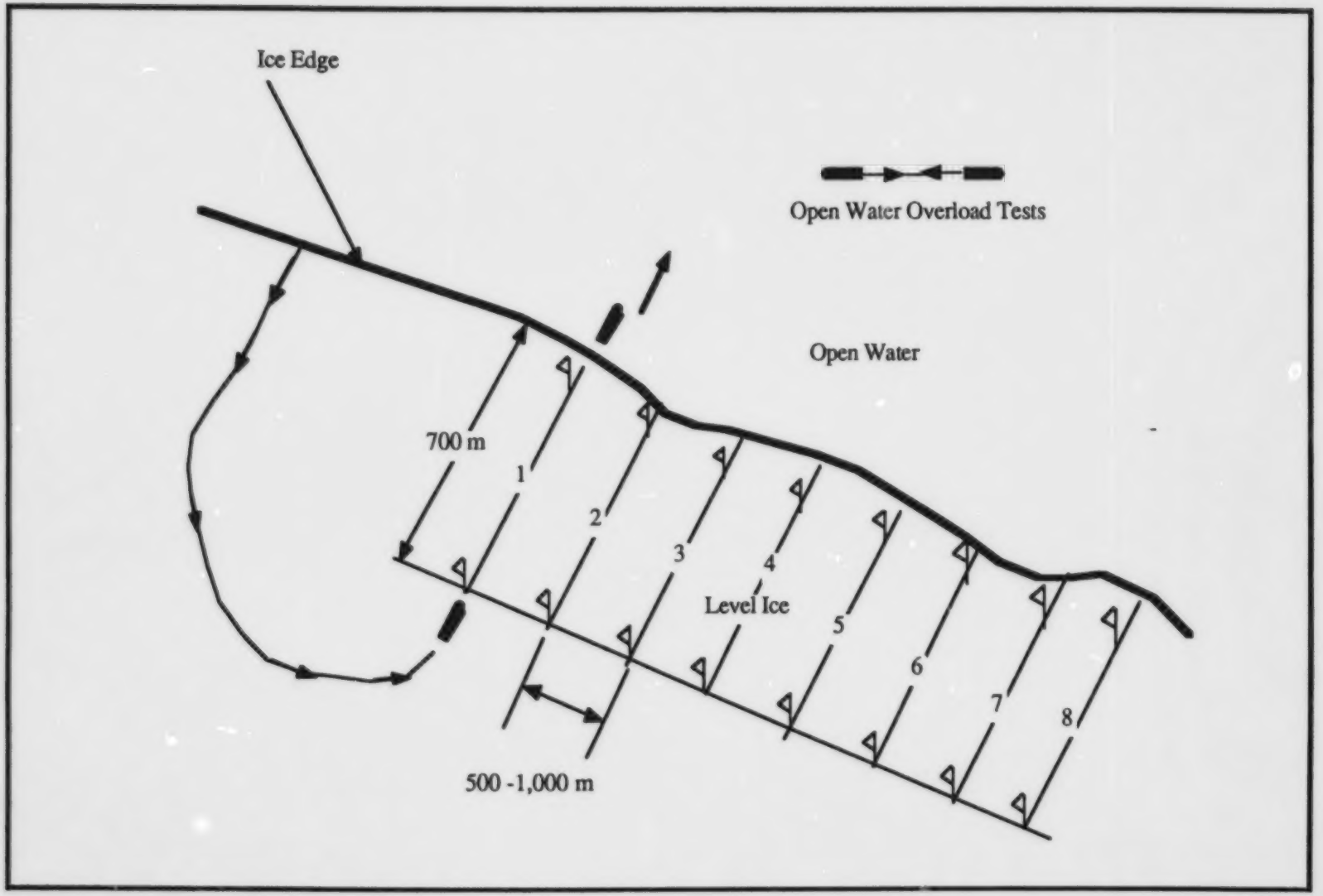

Figure 4.4.2 Planned Towing Trials

end of the towing track, and started hauling out a nylon rope lead line. One end of the lead line was connected to a winch on the MV Terry Fox, and the other end was connected to the towing line. The towing line was then pulled across the ice by winching in the lead line. It was then connected to a bracket located on the centre of the focsle deck at the bow. The MV Terry Fox was then pulled by the MV Ikaluk at two to three constant speeds. This procedure was repeated once more, and then the MV Terry Fox changed positions with the MV Ikaluk and towed the MV Ikaluk three times. After the towing tests were completed the open water overload tests were conducted, just outside the ice edge in clear open water. The two vessels were positioned stern on stern. One vessel provided the necessary resistance while the other propelled itself with approximately the same speed and towline force as that achieved during the ice towing trials. In addition towing tests were conducted with both vessels in a broken channel, and later with the MV Terry Fox breaking 1.5 metres of level ice while towing the MV Ikaluk at 2-3 knots. Figure 4.4.3 illustrates the actual trials conducted.

The estimated number of towing trials that could be conducted depended critically on the amount of time required to drag the towline across the ice and connect the two vessels. It required five hours for the first towing trial; this time was reduced to approximately three and a half hours by the last towing trial.

Fortunately the ice was relatively homogeneous from the ice edge to the shore line, and the end of the towing track could be located within a few metres of the ice edge. Therefore, the towing vessel could operate in the open water and did not have any ice resistance. This enabled it to achieve the maximum towing capability. In addition manoeuvring to the towing position was relatively simple in open water conditions. A total of 5 towing tests in ice were conducted as illustrated in Figure 4.4.3.

The trials log for the M.V. Terry Fox and the M.V. Ikaluk are contained in Appendix I.

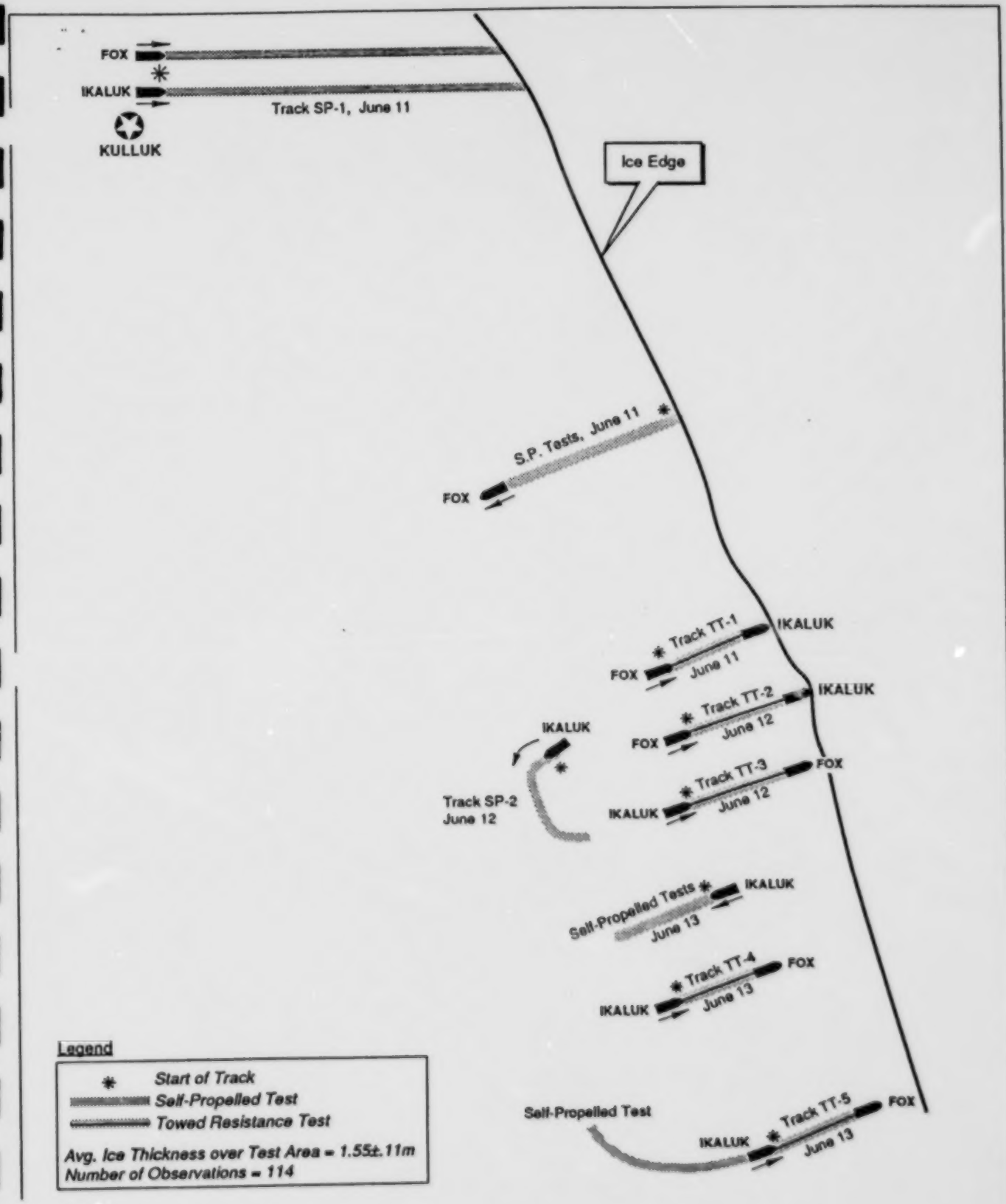

Figure 4.4.3 Towing and Self-Propulsion Trials Conducted

SECTION 5

DATA AND RESULTS

5. DATA AND RESULTS

5.1 Summary of Trials Results

Ice Conditions: 1.55 ± 0.11 metre level ice
Cantilever beam flexural strength of 150 kPa.
Hull Friction Factor: 0.18
Date: June 11-13, 1990
Location: Herschel Basin, N.W.T.

Results from Towing Tests

1. Resistance and corresponding constant speed values in unbroken ice sheet were:

M.V. TERRY FOX		M.V. IKALUK	
Velocity (knots)	Resistance* (MN)	Velocity (knots)	Resistance** (MN)
0.4	0.42	0.64	0.60
2.4	0.83	1.98	0.71
3.3	0.95	2.34	0.76
		2.77	0.77

* The M.V. Terry Fox resistance includes hull resistance and the single centreline rudder resistance. Propeller drag was accounted for.

** The M.V. Ikaluk resistance includes hull resistance, nozzle drag, propeller drag, and rudder drag.

2. The M.V. Terry Fox resistance varies approximately linearly with velocity over the speed range tested.

3. There was significant ice propeller interaction during the towing trials. Ice forces causing up to 100 kN drag on the propeller were recorded.

4. Cracks propogating to adjacent towing lanes indicated pressure relief during some towing tests. This resulted in an approximate decrease of 50% in resistance. This data was not included in the above results, but is useful in estimating icebreaking resistance in non-infinite ice sheets.

5. The M.V. Ikaluk could be towed by the M.V. Terry Fox at 3 knots, while the M.V. Terry Fox was breaking an infinite level ice sheet of 1.55 metres in thickness.

Results from Self Propulsion Tests

1. Total thrust and power required and the corresponding constant speed values in unbroken ice sheet were:

M.V. Terry Fox			M.V. Ikaluk		
Velocity (knots)	Power (MW)	Thrust (MN)	Velocity (knots)	Power (MW)	Thrust (MN)
1.5	5.5	0.75	0.9	5.9	0.69
2.3	8.5	0.97	0.9	6.0	0.65
2.9	10.6	1.16	1.5	8.6	0.80
3.6	14.0	1.34	2.2	9.5	0.85
			2.3	9.1	0.89

2. The power and thrust versus velocity relationship is linear over the speed range tested.

3. There was significant ice-propeller interaction for both vessels during the self-propulsion trials. The increase in power due to milling was no more than 7% over the time intervals analysed.

4. The M.V. Terry Fox required slightly less power (7%) than the M.V. Ikaluk at a speed of 2.3 knots. However, the power versus speed slope for the M.V. Terry Fox is approximately 1.7 times that of the M.V. Ikaluk - the corresponding ratio of displacements is 1.4.

Results from the Thrust Deduction Analysis

1. The thrust deduction fraction in ice is approximately the same as that for the open water overload condition at the corresponding speed and resistance for the M.V. Terry Fox. It ranged from 0.05 at 0.5 knots to 0.25 at 3.6 knots.

2. The thrust deduction fraction for the M.V. Ikaluk was much higher in ice than in open water. It ranged from 0.05 at 0.5 knots to 0.16 at 2.0 knots in ice, and was low (in the range of 0.02 to 0.05) in the open water overload condition. In the open water overload condition the thrust deduction was approximately equal to the hydrodynamic thrust provided by the nozzle.

Results from the Shaftline Vibration Analysis

1. There is not a significant difference in the relative peak torques measured between the nozzled and open screw propellers. The peak shaft torque during ice milling was measured to be 150% and 134% of the MCR torque for the M.V. Ikaluk and the M.V. Terry Fox respectively.

2. The shaftline of the nozzled propeller (M.V. Ikaluk) was measured to have significantly higher axial (thrust) vibrations than the open screw propeller (M.V. Terry Fox). The peak shaft thrust during ice milling was measured to be 310% and 110% of the bollard thrust for the M.V. Ikaluk and the M.V. Terry Fox respectively.

3. Generally more ice-propeller interaction was noticed on the nozzled vessel than the open screw vessel. Both types of shaftlines had approximately the same high damping present in the axial and torsional modes.

5.2 Comparison of Results with Other Methods (Contributed by AKAC Inc.)

The accomplishment of the full scale resistance and propulsive performance trials with all the complications associated when performing a variety of different kinds of Arctic trial is unique. It is warranted that such trials results be compared with data from other sources for performance predictions of these ships. The important issues to address in such comparisons are:

- check agreement between full scale resistance obtained directly from these trials with resistance obtained indirectly from other full scale trials
- compare the agreement between the established estimates for propulsive performance in overload conditions between these trials and other methods
- compare net ice resistance against analytical methods

In this project the scope is limited on this scale, and the following comparisons are considered justifiable:

- full scale data obtained from earlier trials with these ships versus level ice resistance in these trials
- analytical model predictions versus level ice resistance from these trials
- comparison with model test results of propulsion performance

The actual methods selected are the latest Canadian developments. These include the Carter model for level ice resistance, and the Icebreaker design synthesis based full scale correction method for correlating these full scale data with other test series with these ships.

Comparisons Against Full Scale Data

The data base to compare against is earlier full scale trials with these two classes of icebreakers. The following is the selected base:

- TERRY FOX winter trials, 1983
- IKALUK full scale trials in winter 1983

The comparison is made through taking the earlier results and correcting them to the full scale conditions for the current trials.

The method of correlation is from the Icebreaker Design Synthesis project. The corrections made are for:

-flexural strength of ice
- air temperature
- hull condition

The correction factors are for conversion between the winter trials, both ships were tested in the same location at the same time in similar ice, and the spring tests in this project. The following coefficients apply, based on Icebreaker Design Synthesis II:

- flexural strength, from 500 kPa to 150 kPa, factor 0.74 to correct the resistance from winter trials to current trials.
- air temperature, from -30°C to about -2°C, factor 0.77 to correct the resistance from winter trials to current trials.
- hull condition has been assumed to be identical, which is a close approximation based on knowledge of hull conditions.

There is another correction necessary to translate the winter trials results to current tests. The ice thickness for the winter trials was 1 m, whereas the current tests have a thickness of 1.55 m. The correction is made based on Icebreaker Design Synthesis I, using a thickness exponent of 1.45 for this purpose.

The results comparison in Figures 5.2.1 and 5.2.2 below gives an indication of the good agreement between the earlier, winter resistance tests and current tests, even though fairly major correction had to take place in terms of difference in environment.

Comparisons Against Analytical Formulations

There is only one recent Canadian analytical formulation for this comparison. This is the Carter formula for level ice resistance evaluation.

There are some shortcomings in this methodology which leave the comparison quite open to interpretation. There is no interpreted E/sigma value for the full scale data which would accurately reflect the properties of the field ice during these trials. It is only estimated that the range of E has been 0.1-0.5 GPa which will lead to E/sigma ratio 670-3300.

Carter's method is quite sensitive to the E/sigma ratio and thus predictions are made for both two extremes of this ratio.

Carter's method also has been shown to include only one of the two strengths, flexural strength/uniaxial compressive strength, and then ratio the other in proportion to the first. The ratios suggested by Carter have been in the range of having flexural strength of ice a set fraction of uniaxial compressive strength. This factor is in the range of 1.5-3. However, in these full scale trials, the estimates of uniaxial compressive strength of the ice and flexural respectively have been 2.6 MPa and 150 kPa (leaving a factor of 17 between these two strength components. Thus, the Carter comparison in this area seems to be in contradiction in terms of input data.

The results are shown on Figures 5.2.1 and 5.2.2 for these comparisons.

Comparisons with Model Test Data

Only three sets of model tests have been carried out on the TERRY FOX/KALVIK and IKALUK/MISCAROO vessel designs but they unfortunately do not offer comparisons of resistance and propulsive performance which are of any real value to this project.

During their design development, model tests were conducted at Hamburg Ship Model Basin. These concentrated on flow visualization and direct measurement of speed versus power in level ice. Resistance and propulsive performance data which might assist this project were not determined.

During the Polar 8 design project, model tests were carried out at IMD in order to correlate KALVIK's predicted level ice resistance and power loss due to propeller and ice interaction with that predicted in the ice basin using EGAD ice.

The full scale resistance data were the same as those used above in Section 5.2, so these correlation results do not add to our understanding.

Figure 5.2.1

M.V. TERRY FOX Level Ice Resistance For Conditions on Spring Trials 1990

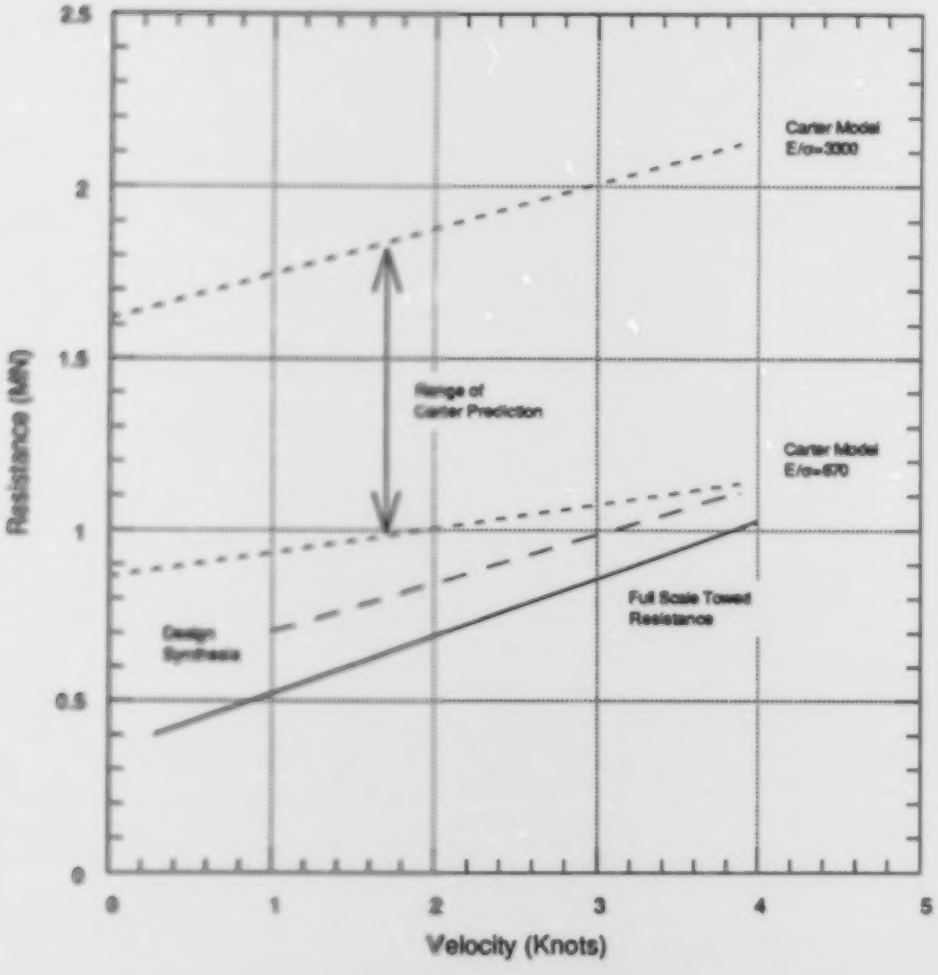

Figure 5.2.2

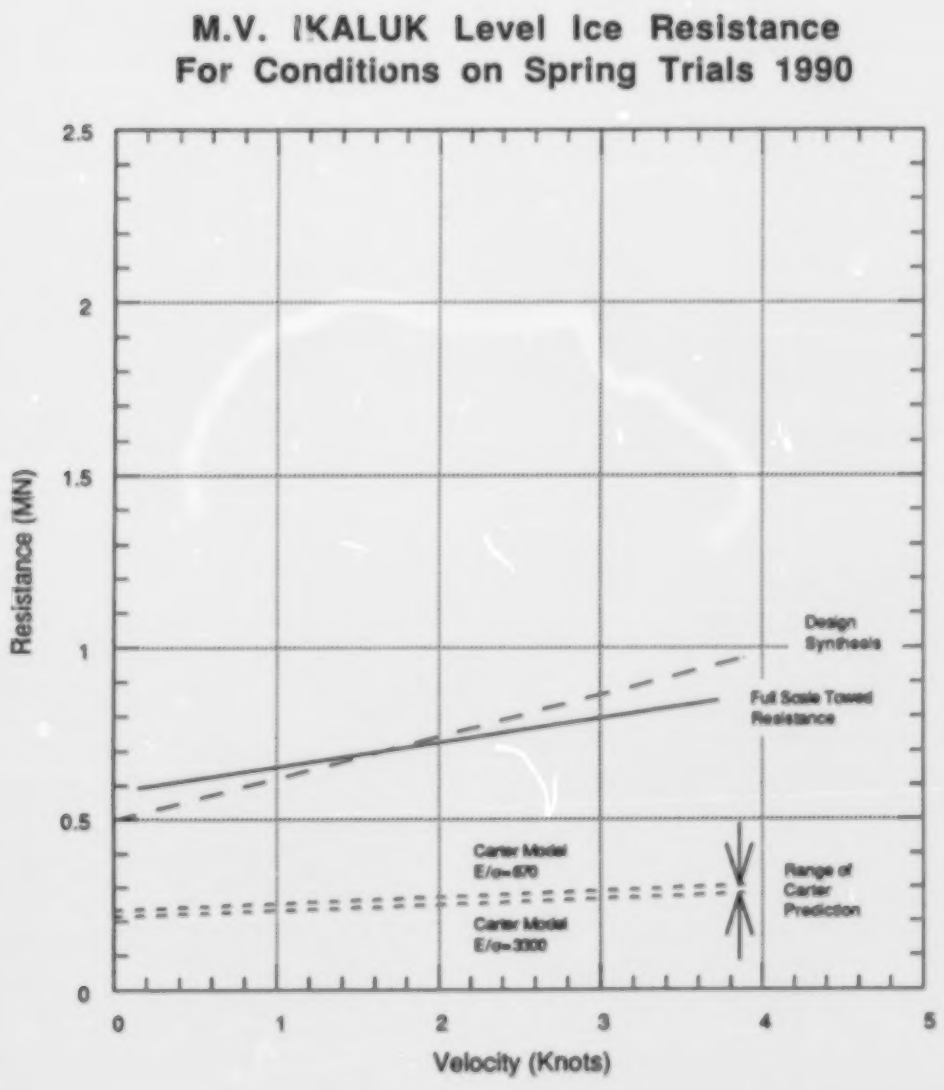
M.V. IKALUK Level Ice Resistance
For Conditions on Spring Trials 1990
Resistance (MN)
Velocity (Knots)
2.5
2
1.5
1
0.5
0
0
1
2
3
4
5
Design Synthesis
Full Scale Towed Resistance
Carter Model E/σ=870
Carter Model E/σ=3300
Range of Carter Prediction

Open water overload tests were also part of the project, but they were simply aimed at determining shaft revolutions versus thrust identity for subsequent tests in ice. The model boundary layer was not stimulated and the propeller pitch and RPM were well outside of the ranges covered in the full scale trials.

In summary, there are no model test data for TERRY FOX/KALVIK and IKALUK/MISCAROO which can be reliably correlated with the full scale trials.

Conclusions

The only reliable comparison which can be made between the results of the full scale resistance and propulsive performance trials '90 and data from other sources, is with respect to level ice resistance.

The Icebreaker Design Synthesis project analyzed ship level ice performance trials data for eighteen vessels worldwide and developed a performance prediction method which takes into account both ship design and environmental conditions.

TERRY FOX and IKALUK's winter ice Beaufort Sea performance has been corrected to the spring '90 environmental conditions using this predictor. The level of agreement is very good.

The comprehensive full scale trials project has, therefore, registered its first successful application in the improvement of ship performance prediction.

It is recommended that comprehensive open water overload model tests be carried out in order to investigate their correlation with full scale. For IKALUK, this should include nozzle thrust measurements.

It is recommended that propulsion tests simulating full scale conditions be carried out in an ice basin.

5.3 Data Processing

The data collected needed to be processed prior to any detailed analysis. This required the determination of zero offsets, confirmation of calibration factors, digital filtering of signals (if required), checking of all sensor output for each event, and the production of time history plots of all data. The zero offset is defined as the voltage given by a sensor at zero load. The sensors from the propeller pitch, shaft rpm, shaft torque, engine fuel rack, and rudder angle showed negligible changes in the zero offset (ie. negligible drift) during the trials. However, the shaft thrust signal indicated a change in the zero offset over a number of hours throughout the trials. Therefore, for each event the zero offset for thrust was calculated from portions of the recorded time series data when there was no load on the shaft or when it was stopped. Once these offsets were determined the data was plotted and hard copies were made.

The following calculated values were also plotted:

Port and Starboard Shaft Power
Total Shaft Power
Total Shaft Thrust
Speed
Distance travelled
Total Nozzle Thrust (for Ikaluk)

A total of over 1,000 plots (300 pages) were generated for each vessel.

The ship position was measured every 3 seconds and towline force was measured 10 times a second. The ship speed was calculated by dividing the distance traveled between two data points by the elapsed time (3 seconds). Because the speed of the vessels was less than 4 knots (approximately 2 metres/sec) the vessel would travel less than 6 meters each time interval. The positioning system had a resolution of ±1.0 metre, and therefore the speed time history plot showed a significant amount of noise when the speed was computed every 3 seconds.

The speed time history was filtered to cut out speed variations with less than a 10 second period. Figure 5.3.1 illustrates an unfiltered and the corresponding filtered towing speed time history plot (2nd Tow of M.V. Ikaluk). The towline force was also filtered at the same level, since it was compared directly to the speed time history, as illustrated in Figure 5.3.2. The variations of the towline force were well within the resolution of the system and the unfiltered towline force is a clear representation of the real towline force. The vessel is heaving and pitching as it is towed through the ice and the towline force varies correspondingly. However, the average towline force over the time interval of constant velocity is what is of concern when calculating the resistance velocity relationship.

A statistical analysis was also performed to calculate the minimum, maximum, average, and standard deviation of each signal, for each event, over a selected time interval of interest. Table 5.3.1 lists the statistics calculated for the time interval 450-600 seconds corresponding to Figures 5.3.1 and 5.3.2.

With the aid of the trials logs kept during the trials, portions of the time history data of constant speed were selected that corresponded to towing or self-propulsion tests in an essentially infinite ice sheet. Several occasions occurred when radial cracks propagated to open water leads in the ice sheet causing the resistance of the ship to be reduced by at least 50%. This data was discarded in the final analysis. The results from the various tests are described in detail in the following sections.

STATISTICS
1990 TRIALS - M.V. IKALUK
DATE:13 Jun 1990 FILE:I_F_P_IK2P
TIME:09:14:26 TO 09:16:56
ELAPSED TIME (Sec):450 TO 600

SIGNAL	AVG	MIN	MAX	STD
PORT FUEL RACK (mm)	1.282E+01	1.089E+01	1.783E+01	1.170E+00
PORT PITCH (Deg.)	1.033E+00	9.720E-01	1.090E+00	1.857E-02
PORT RPM (RPM)	1.718E+02	1.714E+02	1.721E+02	1.131E-01
PORT TORQUE (Nm)	4.749E+04	4.382E+04	6.808E+04	4.033E+03
PORT THRUST (N)	-2.524E+04	-5.495E+04	5.339E+03	8.706E+03
STBD FUEL RACK (mm)	1.236E+01	1.120E+01	1.618E+01	8.138E-01
STBD PITCH (Deg.)	8.671E-01	7.644E-01	9.315E-01	2.603E-02
STBD RPM (RPM)	1.691E+02	1.663E+02	1.694E+02	3.966E-01
STBD TORQUE (Nm)	4.246E+04	4.107E+04	5.197E+04	1.414E+03
STBD THRUST (N)	-5.418E+04	-2.762E+05	7.088E+02	4.078E+04
PORT RUDDER (Deg.)	2.148E+00	2.059E+00	2.241E+00	3.093E-02
STBD RUDDER (Deg.)	2.598E+00	2.565E+00	2.702E+00	3.483E-02
OUT. NOZZ. THRUST (N)	-3.752E+04	-1.471E+05	-1.290E+04	2.116E+04
IN. NOZZLE THRUST (N)	-4.655E+03	-1.268E+04	3.818E+03	2.638E+03
TOWLINE (N)	5.950E+05	3.709E+05	8.367E+05	1.151E+05
PORT POWER (W)	8.544E+05	7.877E+05	1.224E+06	7.220E+04
STBD POWER (W)	7.519E+05	7.277E+05	9.064E+05	2.386E+04
TOTAL POWER (W)	1.606E+06	1.523E+06	1.988E+06	8.038E+04
TOT. SHAFT THRUST(N)	-7.942E+04	-3.056E+05	-1.546E+04	4.325E+04
TOT. NOZZLE THRUST(N)	-1.862E+04	-5.073E+04	1.527E+04	1.055E+04
TOTAL THRUST (N)	-9.804E+04	-3.094E+05	-2.818E+04	4.199E+04
SPEED (kts)	6.375E-01			
Acc. (m/s)	3.561E-05			

TABLE 5.3.1

EXAMPLE OF STATISTICS CALCULATED FROM TEST DATA

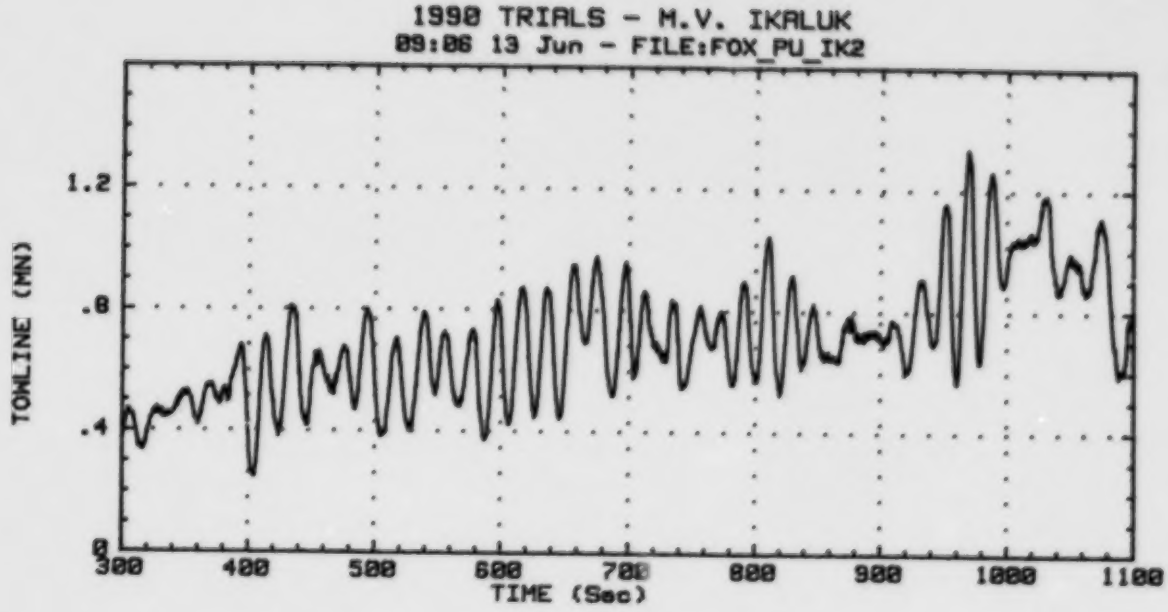

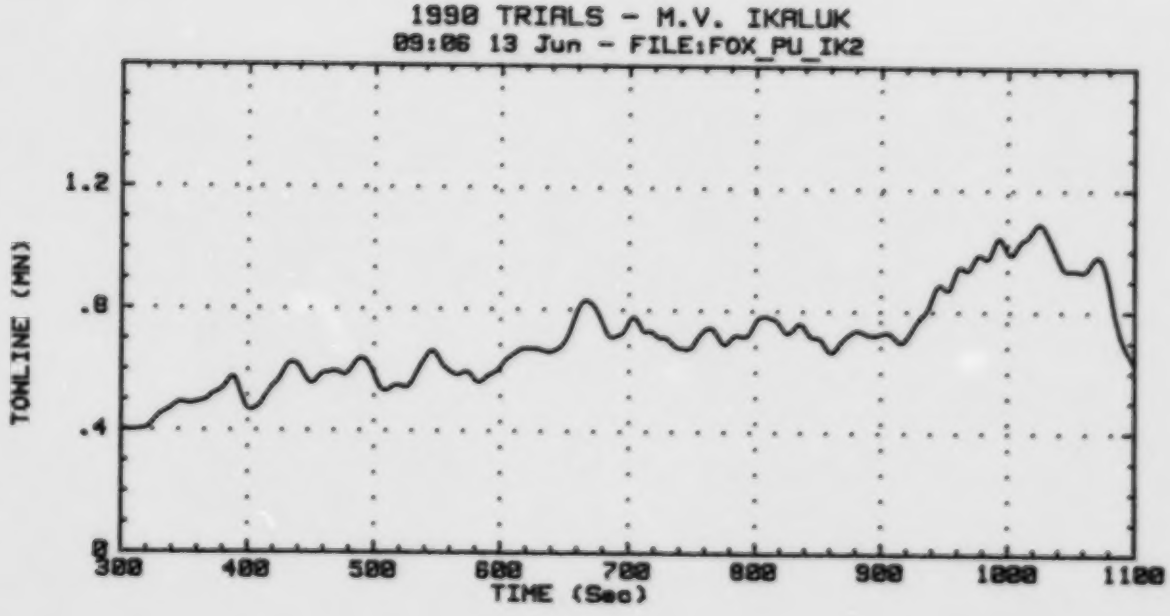

Figure 5.3.1 Unfiltered and Filtered Ship Speed Time History

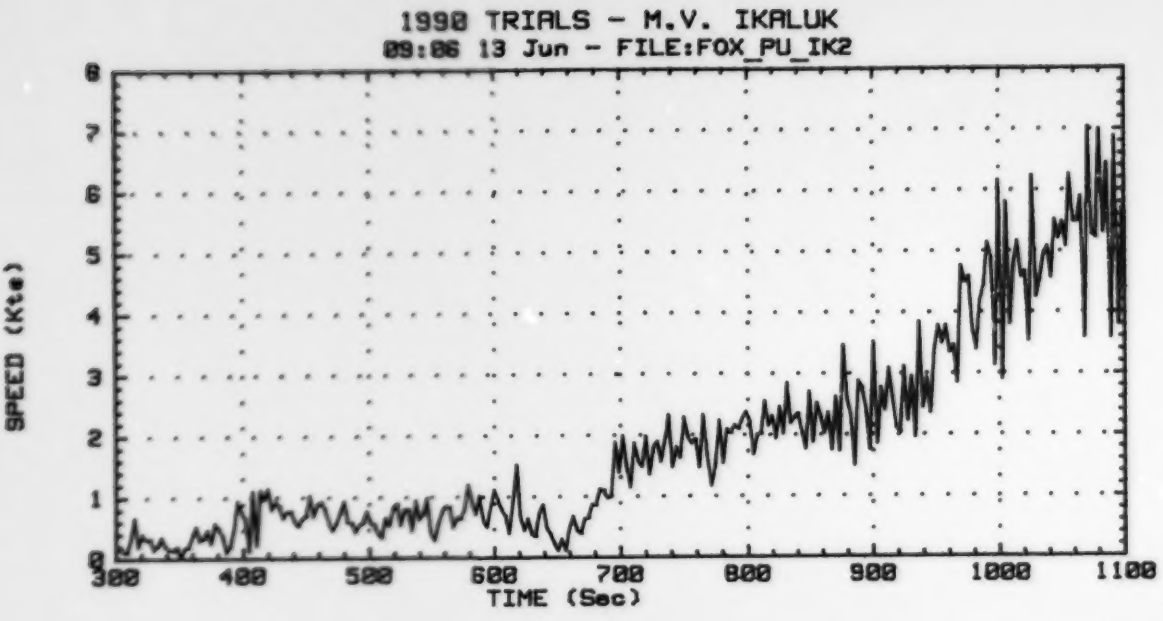

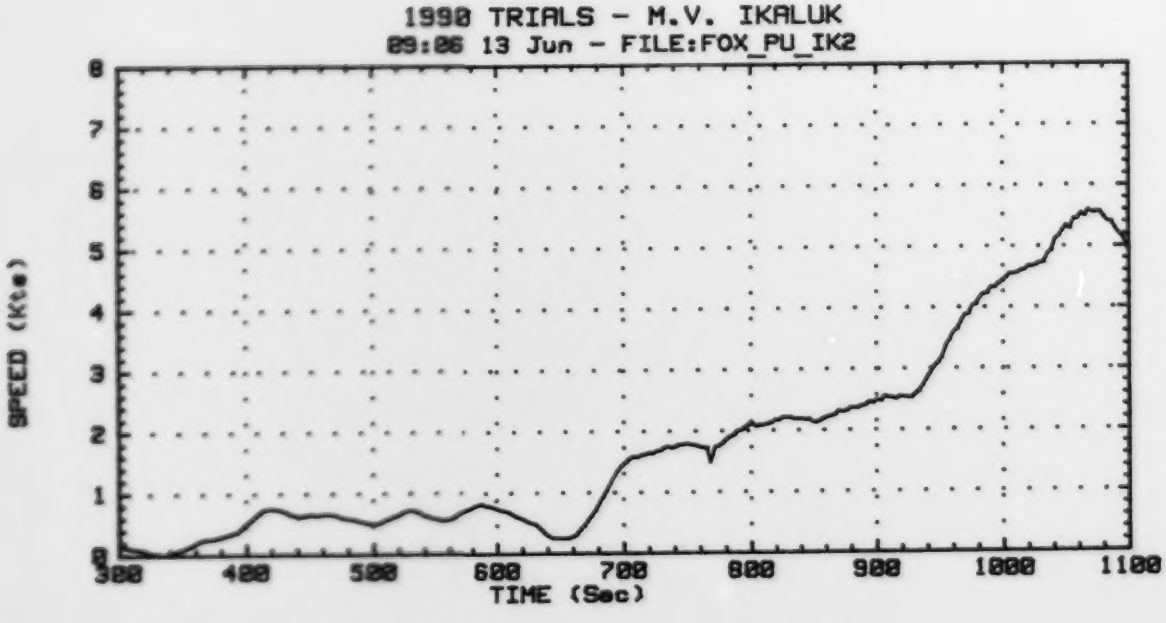

Figure 5.3.2 Unfiltered and Filtered Towline Force Time History

5.4 Towing Tests

Summary

This section summarizes the results of the towin test data analysis. The following sections describe the data and analysis in detail. Table 5.4.1 lists a summary of the results from the towing tests conducted.

Table 5.4.1 Summary of Results from Ice Towing Trials [1]

M.V. Terry Fox		M.V. Ikaluk	
Velocity (knots)	Resistance[2] (MN)	Velocity (knots)	Resistance[3] (MN)
0.4	0.42	0.64	0.60
2.4	0.83	1.98	0.71
3.3	0.95	2.34	0.76
		2.77	0.77

[1] Average Ice Properties: Thickness = 1.55 m; Flexural Strength = 150 kPa

[2] The M.V. Terry Fox resistance includes hull resistance and the single centreline rudder resistance. Propeller drag was accounted for.

[3] The M.V. Ikaluk resistance includes hull resistance, nozzle drag, propeller drag, and rudder drag.

Figure 5.4.1 is a plot of these results.

The following are the main findings of this study:

1. The M.V. Terry Fox resistance varies approximately linearly with velocity over the speed range tested.

2. There was significant ice propeller interaction during the towing trials. Ice forces causing up to 100 kN drag on the propeller were recorded.

3. The resistance decreases by approximately 50% when pressure relief was evident, such as cracks propagating through the ice sheet to open water leads.

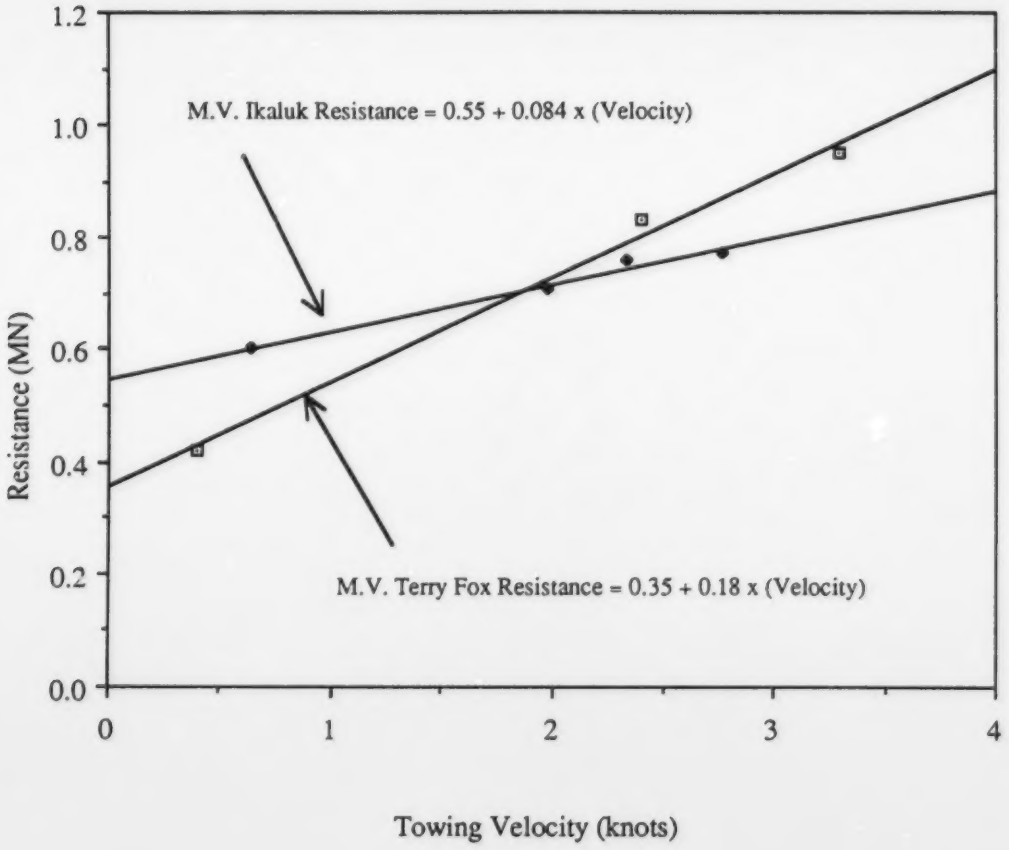

Figure 5.4.1 Resistance vs Velocity: M.V. Terry Fox and M.V. Ikaluk

Introduction

This section details the analysis of the data collected during the ice towing trials. Two towing trials were conducted on the M.V. Terry Fox, and three on the M.V. Ikaluk. The towing vessel was positioned at the shear zone with open water ahead of the vessel. The towed vessel manoeuvred to a position 700 metres into the ice such that there was an infinite ice sheet between the two vessels. A towing cable was dragged across the ice and the vessels were connected. The vessel was towed through the ice at two to three constant speeds, with the propeller turning at full rpm and zero pitch. Sections 4.2 and 4.4 describe the towing design and execution in detail. Section 5.3 describes how the data was processed.

M.V. Terry Fox Towing Test Results

Table 5.4.2 lists the data from the M.V. Terry Fox towing trials. The resistance is calculated by adding the shaft thrust (propeller drag), the inertial forces (mass x acceleration), and the towline force. Therefore, the only appendage drag not taken into account is the single rudder located on the centreline of the vessel, which should not contribute significantly to the towed resistance. The mass used in calculating the inertial forces was taken to be 1.1 times the mass of the vessel to include for added mass effects. The inertial forces were not significant for the these trials because time intervals of relatively constant velocity were chosen. Therefore, the error in the estimate of the effective mass of the vessel will not effect the results significantly. Three constant speeds through unbroken ice, with no pressure relief evident, were obtained from the two towing trials, one from the first towing test and two from the second.

Table 5.4.2 M.V. Terry Fox Towing Test Results

Tow	Time Interval (sec)	Vel. (knots)	Acc. (m/sec^2)	FORCES Towing (MN)	Thrust (MN)	Inertia (MN)	Resistance[1] (MN)
1	240-330	0.4	0.000	0.46	-0.04	-0.00	0.42
2	550-650	2.4	0.003	0.88	-0.03	-0.02	0.83
2	700-800	3.3	0.002	1.06	-0.09	-0.01	0.95

1. Resistance = Towing + Shaft Thrust (Propeller Drag) + Inertia

Figure 5.4.2 is a plot of the computed resistance versus the towed velocity. A linear regression line has been drawn through the data points. The fit is good and suggests that

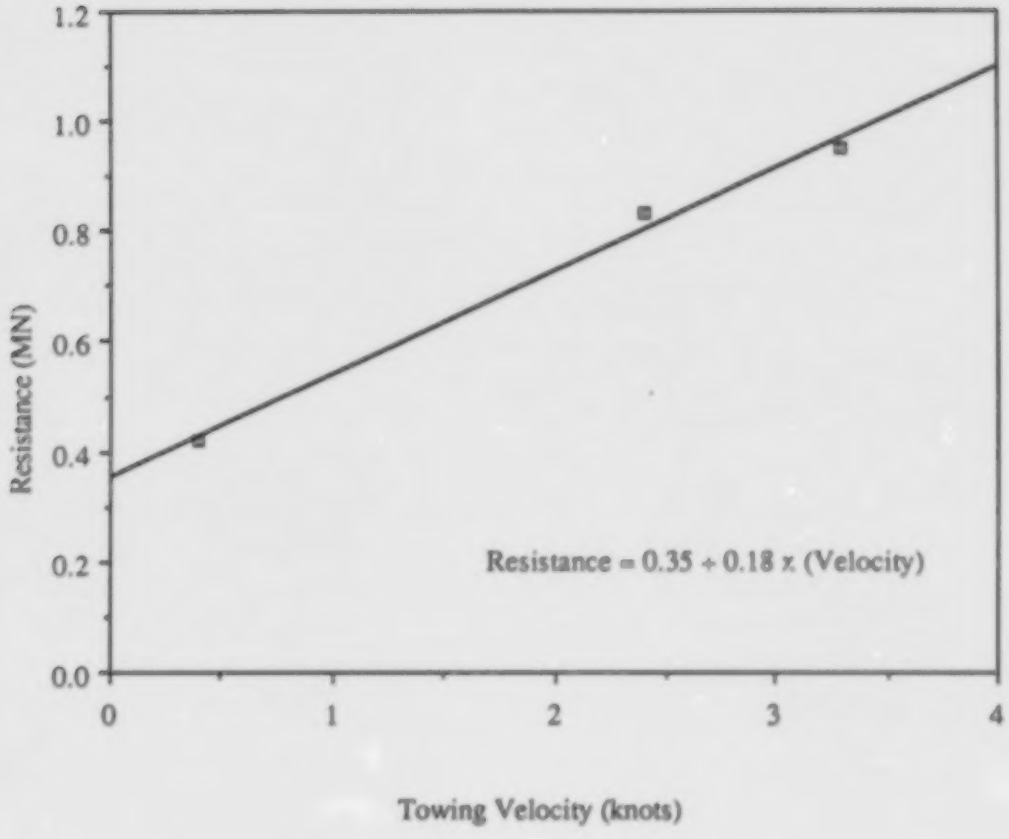

Figure 5.4.2 Resistance vs Velocity: M.V. Terry Fox

the resistance varies linearly with speed over the measured speed range of 0.4 to 3.3 knots. If the line is extrapolated to the vertical axis (zero speed) the resistance is 0.35 MN. This value is in agreement with the measured force required to start the vessel in motion at the beginning of a towing trial.

Tow Number 1

Figure 5.4.3 illustrates the vessel speed and towline force for the first towing trial conducted on the M.V. Terry Fox. Only one constant speed (0.4 knots) was achieved in uniform ice, which was from 240 to 330 seconds. Figure 5.4.4. is a plot of the total shaft thrust during this tow. The shaft thrust is relatively low and slightly negative indicating a slight drag force by the propeller. The towing force was increased at 300 seconds to attempt to attain a constant speed of 2 knots. However, significant ice propeller interaction occurred causing a high drag on the propeller which reduced the speed down to 1 knot. This is evident by the larger negative value of the total shaft thrust in Figure 5.4.4 above 400 seconds. Figure 5.4.5 indicates the ice-propeller interaction by the high torsional vibrations measured on both shaftlines.

Tow Number 2

Figure 5.4.6 illustrates the vessel speed and towline force for the second towing trial. Two relatively constant speeds were achieved in this trial. The first one at 2.4 knots from 550 to 650 seconds and the second one at 3.3 knots from 700 to 800 seconds. Figure 5.4.7 illustrates the vessel speed and towline force during the two constant speeds achieved. Figure 5.4.8 is a plot of the corresponding total shaft thrust. In the first 200 seconds the thrust is negative because of the negative pitch applied to the propellers. This was done to achieve a higher towline force prior to the vessel moving. This would cause the vessel to accelerate faster than the first tow, which enabled a higher tow speed to be achieved in a shorter track length. The shaft thrust was relatively small during the time period of constant speeds.

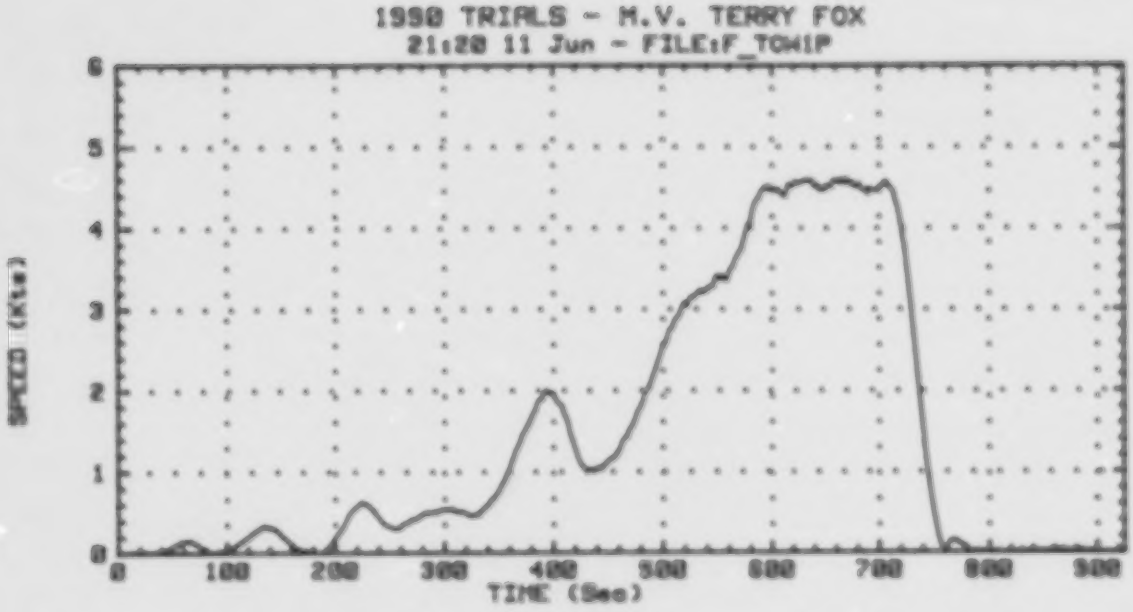

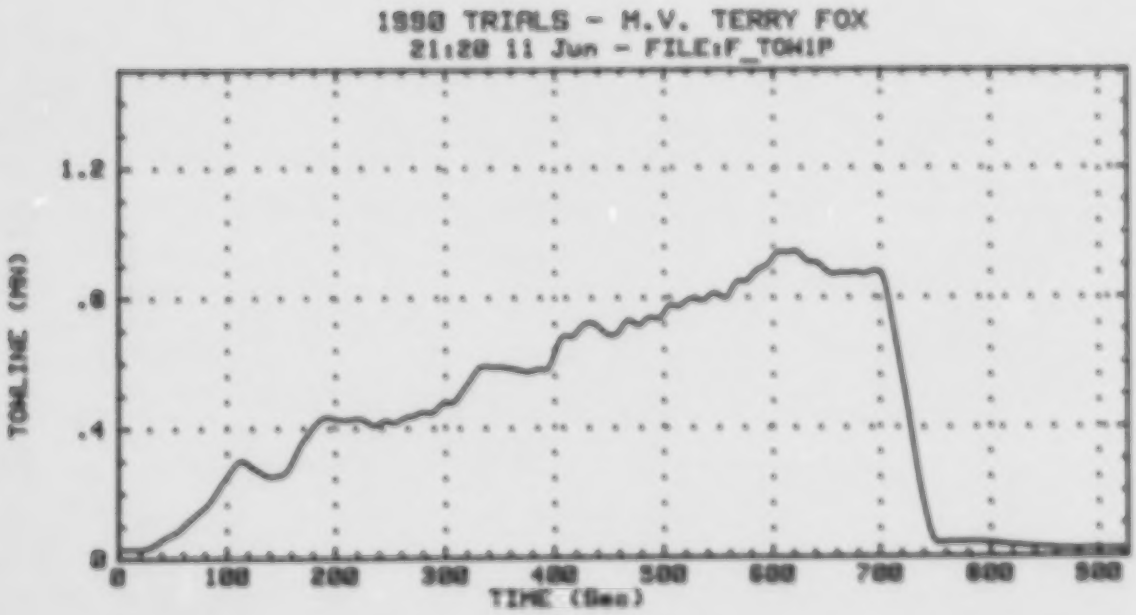

Figure 5.4.3 Speed and Towing Force: MV Terry Fox Tow No. 1

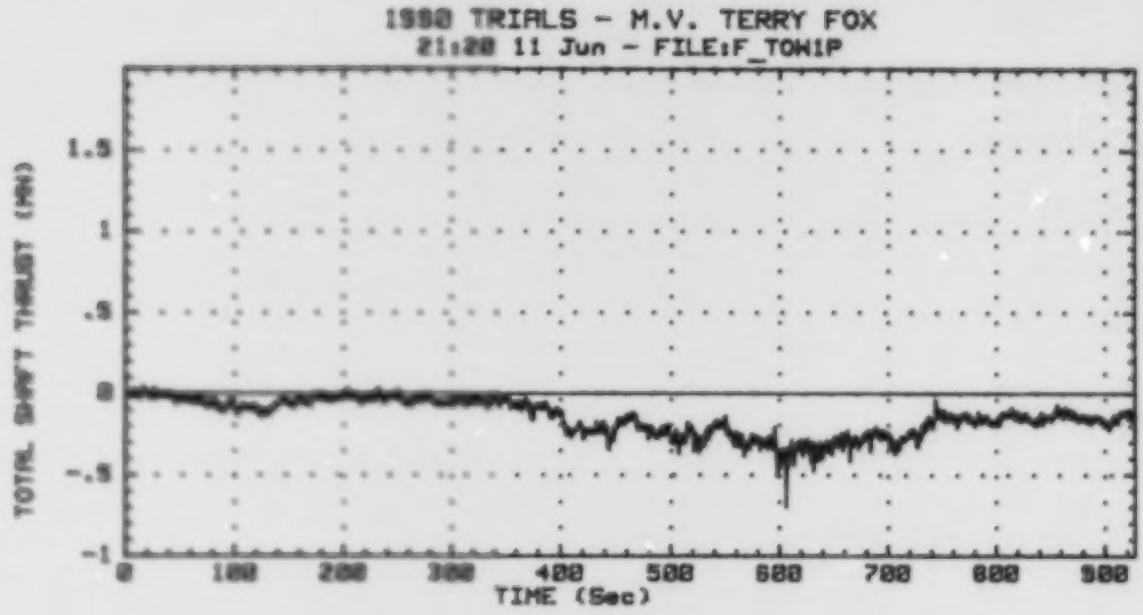

Figure 5.4.4 Total Shaft Thrust: MV Terry Fox Tow No. 1

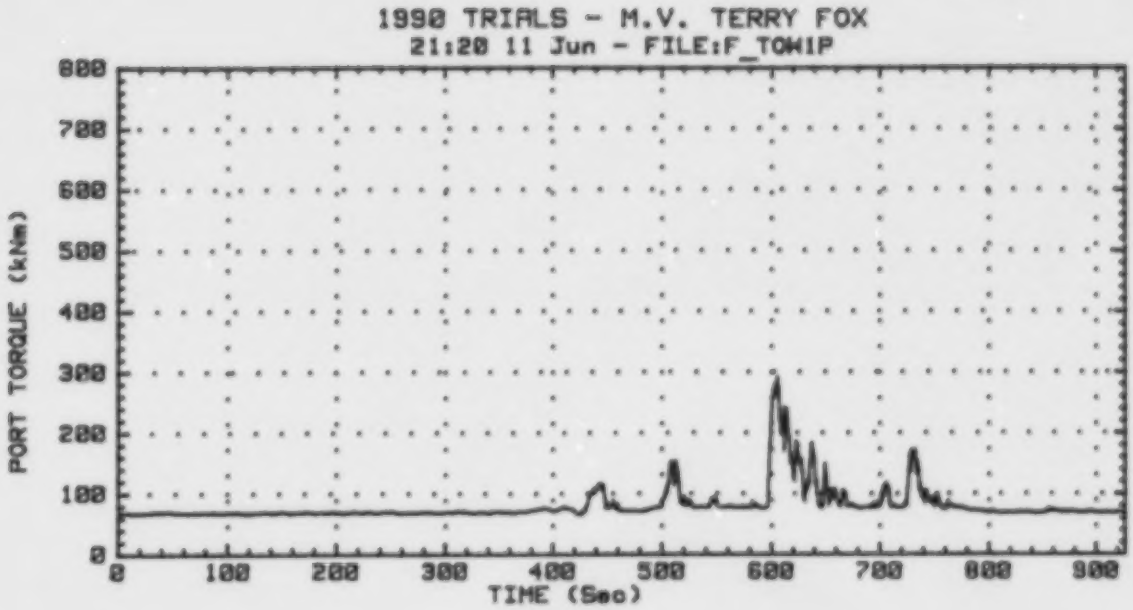

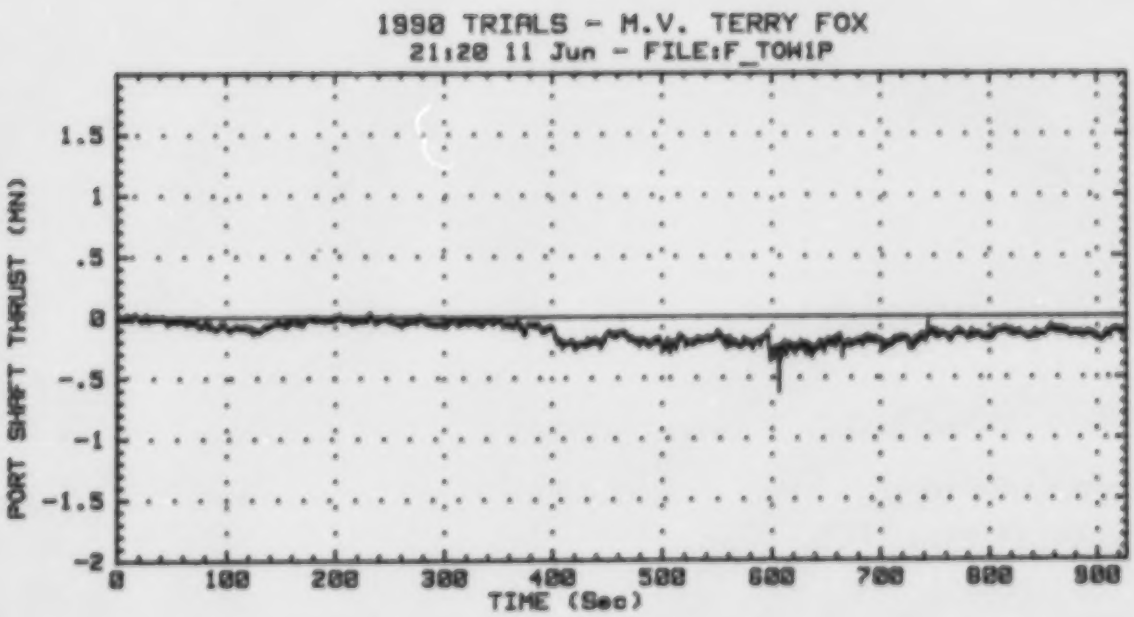

Figure 5.4.5 Port Shaft Thrust and Torque: MV Terry Fox Tow No. 1

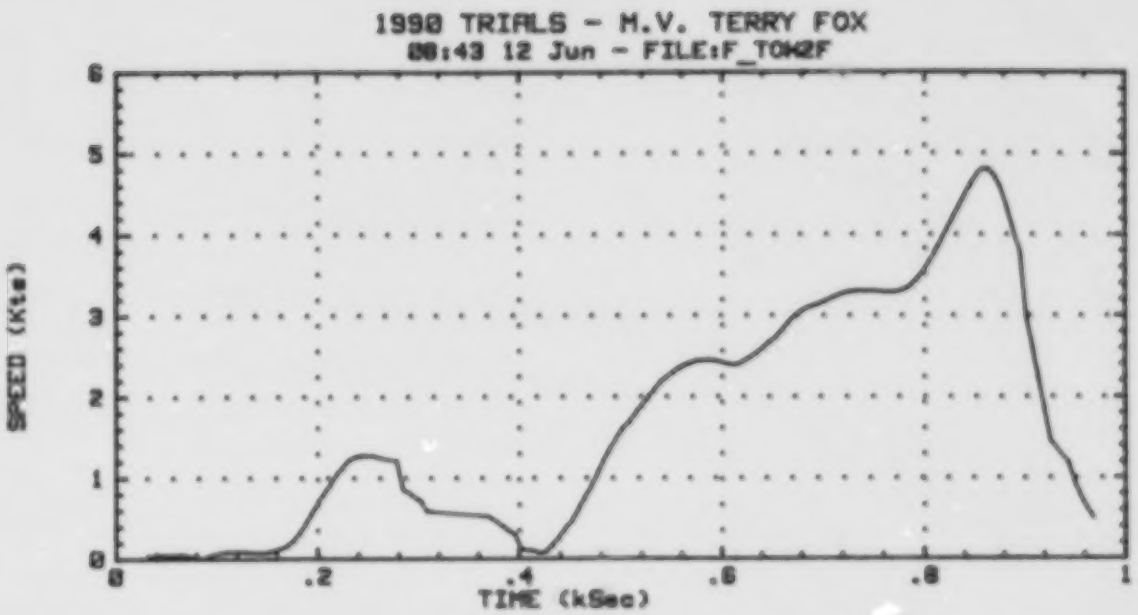

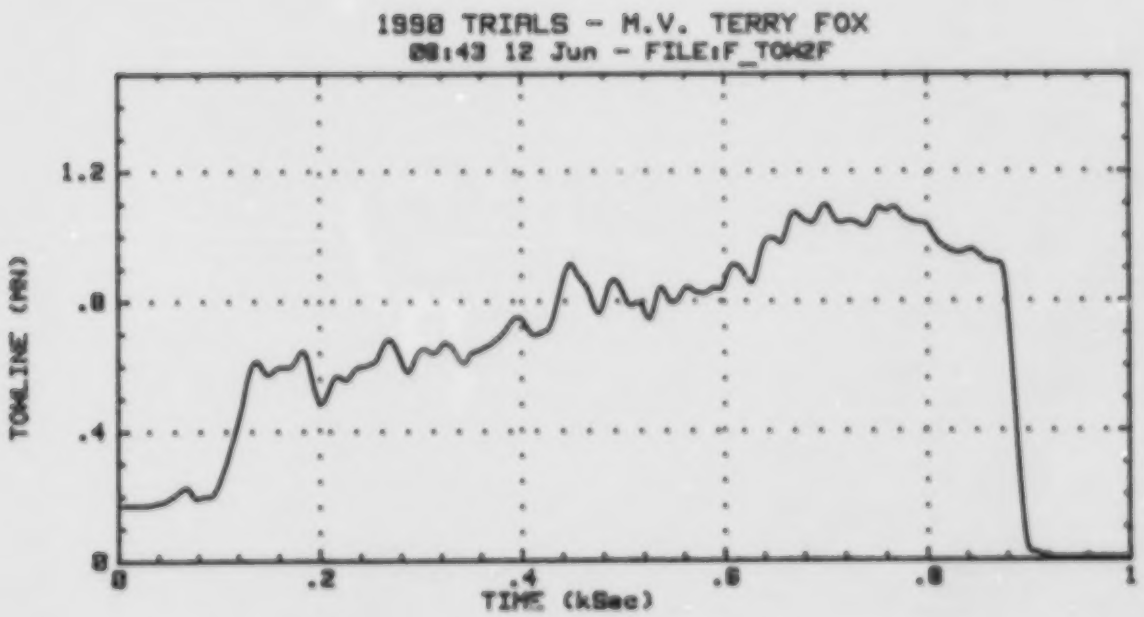

Figure 5.4.6 Speed and Towing Force: MV Terry Fox Tow No. 2

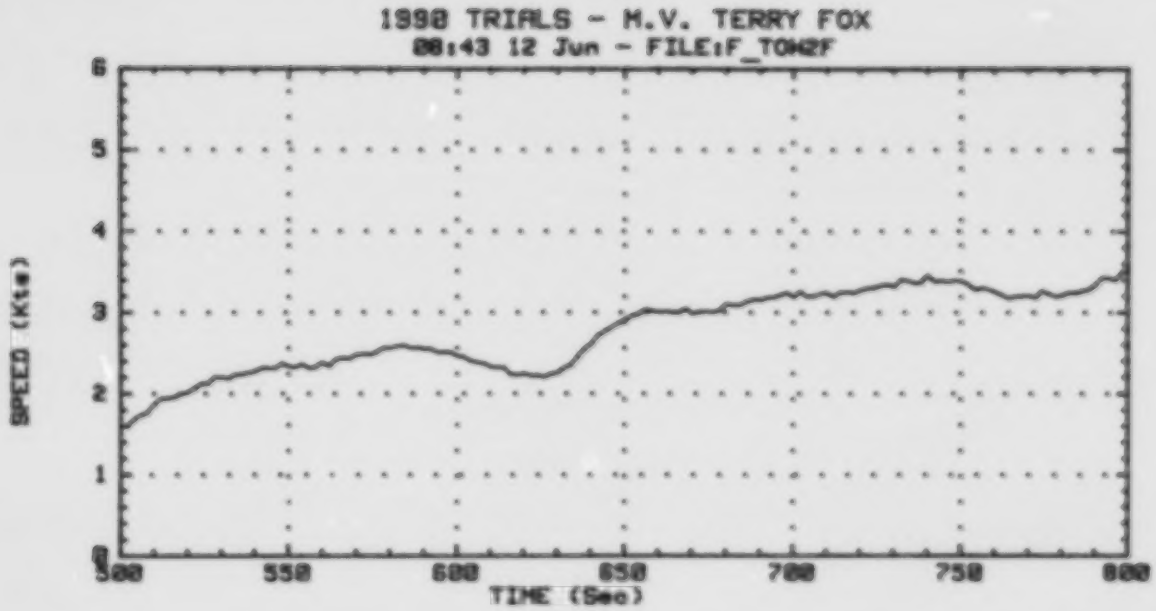

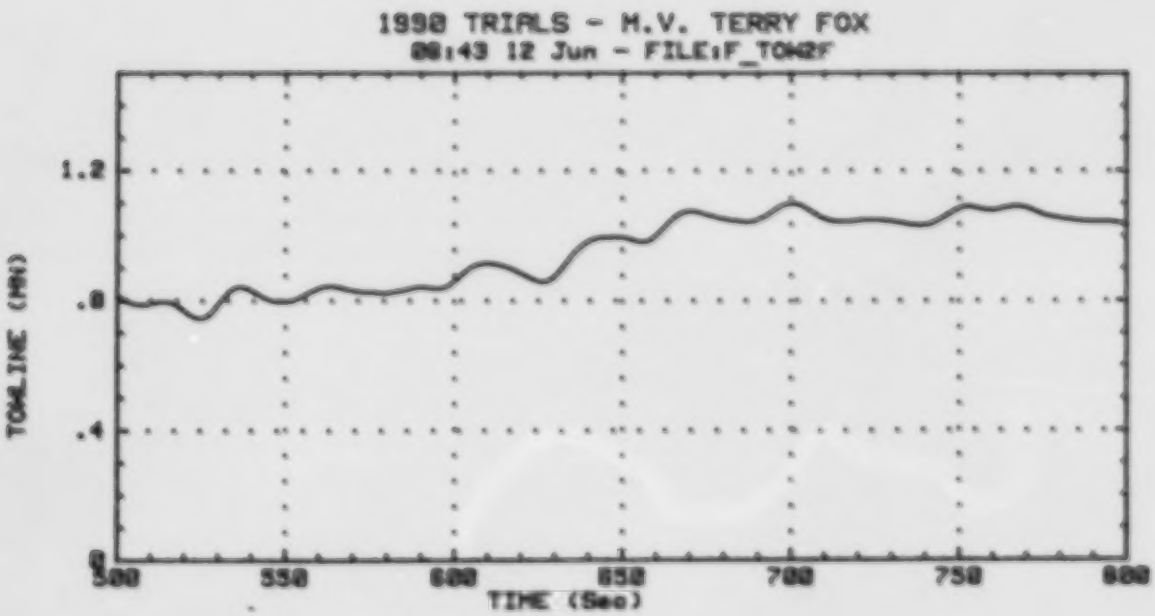

Figure 5.4.7 Speed and Towing Force: MV Terry Fox Tow No. 2 (500-800 sec.)

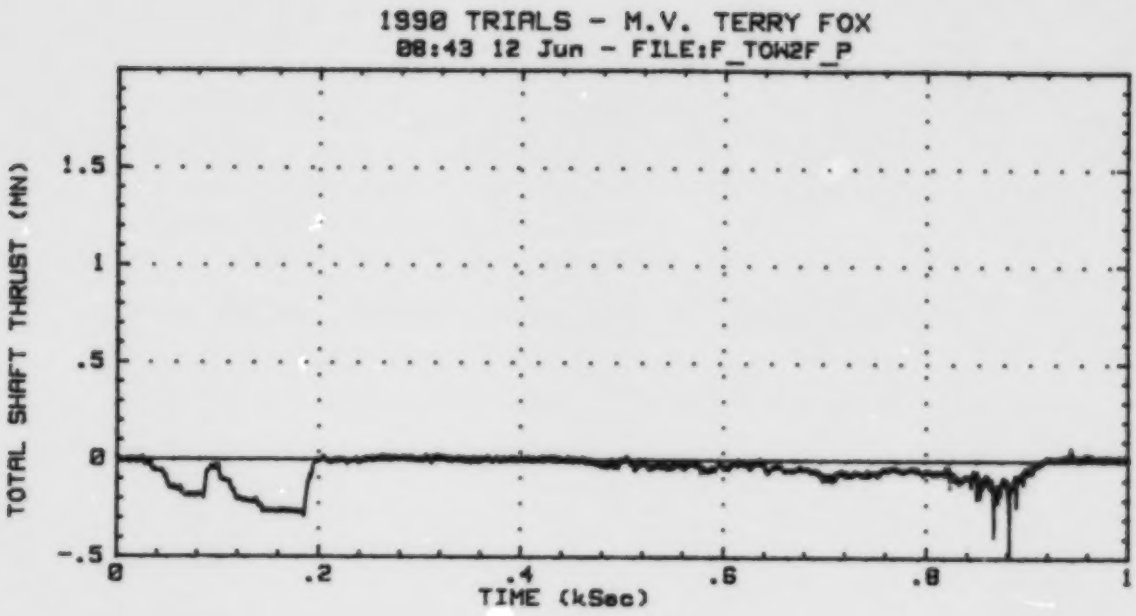

Figure 5.4.8 Total Shaft Thrust: MV Terry Fox Tow No. 2

M.V. Ikaluk Towing Test Results

Table 5.4.3 lists the data from the M.V. Ikaluk towing trials. The resistance is calculated by adding the inertial force (mass x acceleration) and the towline force. It was found that the nozzle measurement of thrust, from the output of the two strain gauges could not be used to estimate the nozzle thrust accurately; therefore, the contribution of the nozzle to the resistance is not included. In addition the propeller drag was not subtracted from the towing force. Therefore; the appendage drag from the two rudders, nozzles, and propeller were included in the towed resistance. However, it was estimated that these components did not contribute significantly to the towed resistance. The mass used in calculating the inertial forces was taken to be 1.1 times the mass of the vessel to include for added mass effects. The inertial forces were not significant for the these trials because time intervals of relatively constant velocity were chosen. Therefore, the error in the estimate of the effective mass of the vessel will not effect the results significantly. Four constant speeds through unbroken ice, with no pressure relief evident, were obtained from the three towing trials, one from the first, two from the second, and one from the third towing test .

Table 5.4.3 M.V. Ikaluk Towing Test Results

Tow	Time Interval (sec)	Vel. (knots)	Acceleration (m/sec^2)	FORCES Towing (MN)	FORCES Inertia (MN)	Resistance[1] (MN)
1	500-600	2.8	-0.001	0.77	0.00	0.77
2	450-650	0.6	0.000	0.60	-0.01	0.60
2	700-900	2.0	-0.003	0.72	-0.01	0.71
3	500-600	2.3	0.010	0.81	-0.05	0.76

1. Resistance = Towing + Inertia

Figure 5.4.9 is a plot of the computed resistance versus the towed velocity for the M.V Ikaluk. A linear regression line has been drawn through the data points. The fit is good and suggests that the resistance varies linearly with speed over the measured speed range of 0.6 to 2.8 knots. If the line is extrapolated to the vertical axis (zero speed) the resistance is 0.55 MN. This value is in agreement with the measured force required to start the vessel in motion at the beginning of a towing trial.

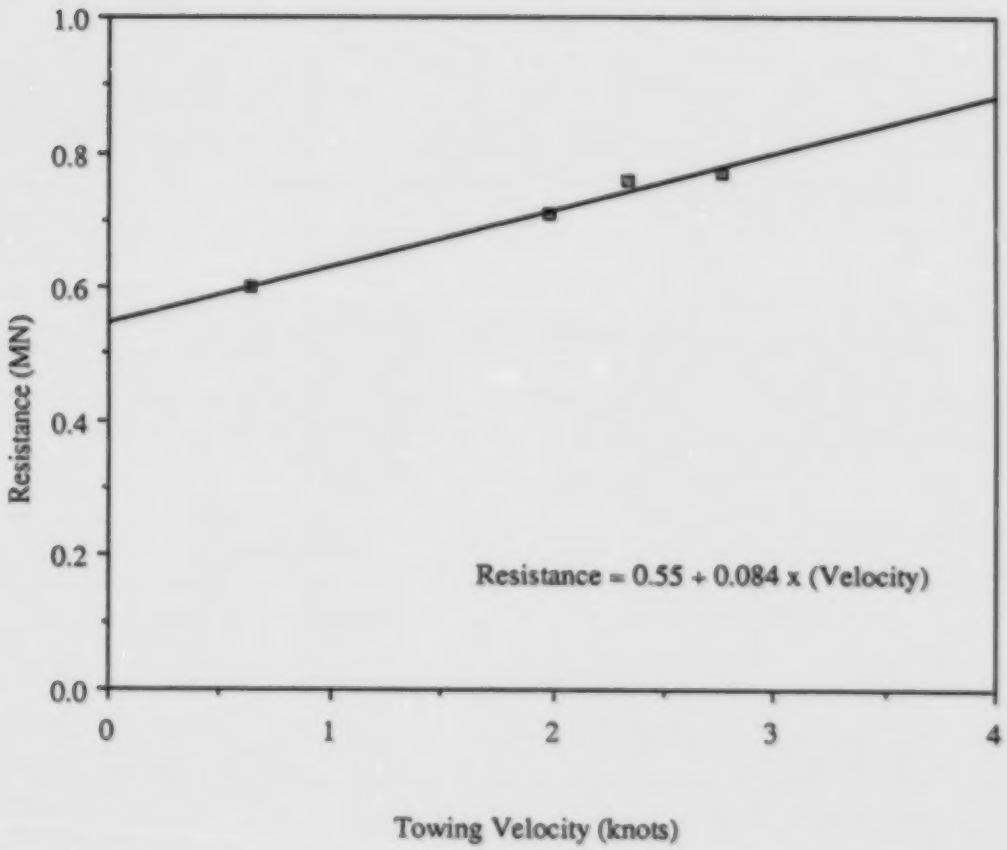

Figure 5.4.9 Resistance vs Velocity: M.V. Ikaluk

Tow Number 1

Figure 5.4.10 illustrates the vessel speed and towline force for the first towing trial conducted on the M.V. Ikaluk. Only one valid constant speed (2.8 knots) was achieved in uniform ice from 500 to 600 seconds. The constant speed of approximately 1.8 knots was discounted due to inconsistent ice features. Figure 5.4.11. is a plot of the total shaft thrust and measured nozzle thrust during this tow. Both plots indicate a relatively low drag over the time interval of interest. A negative thrust was applied to the vessel (astern command) so that the towline cable could reach reach approximately 0.4 MN prior to the vessel staring ahead motion, as was done on the M.V. Terry Fox. The Figure 5.4.12 illustrates the port shaft torque and thrust. The plots show relatively little dynamic vibrations, indicating that there was relatively little ice/nozzle/propeller interaction evident during this tow, .

Tow Number 2

Figure 5.4.13 illustrates the vessel speed and towline force for the second towing trial. Two valid constant speeds were achieved in this trial. The first one at 0.6 knots from 450-650 seconds and the second one at 2.0 knots from 700 to 900 seconds. Figure 5.4.14 illustrates plots of the corresponding port shaft torque and thrust. Both plot indicate negligible dynamic response and low magnitudes. In the first 300 seconds (not shown) the vessel was resisting the tow force to increase the towline force as in previous tows.

Tow Number 3

Figure 5.4.15 illustrates the vessel speed and towline force for the third towing trial. One valid constant speed of 2.3 knots, from 500-600 seconds, was achieved in this trial. Figure 5.4.16 illustrates plots of the corresponding port shaft torque and thrust. Both plots indicate negligible dynamic response and low magnitudes.

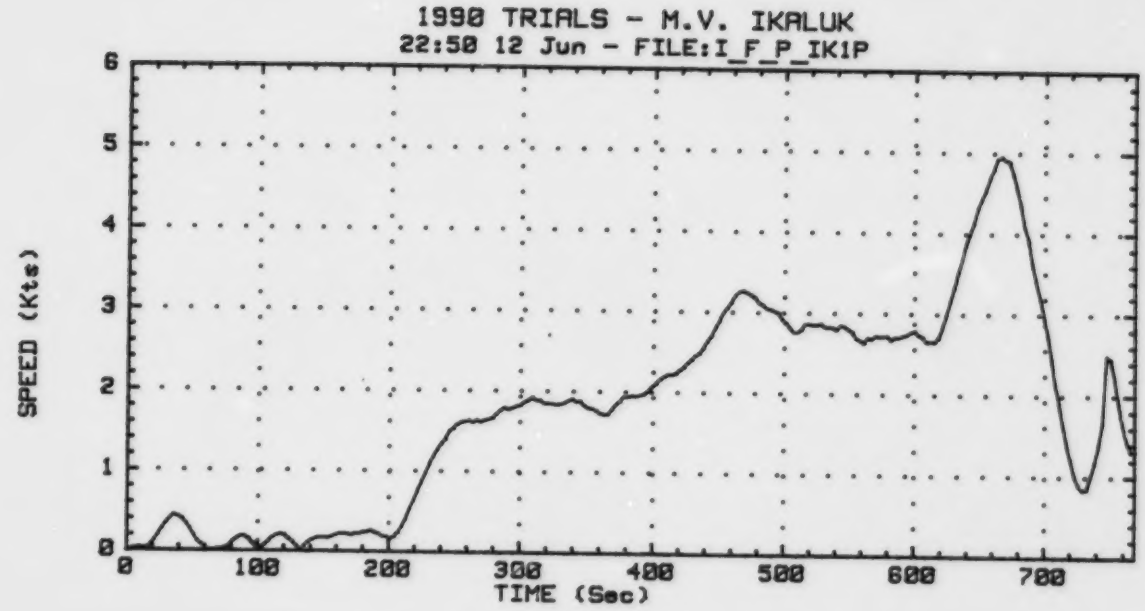

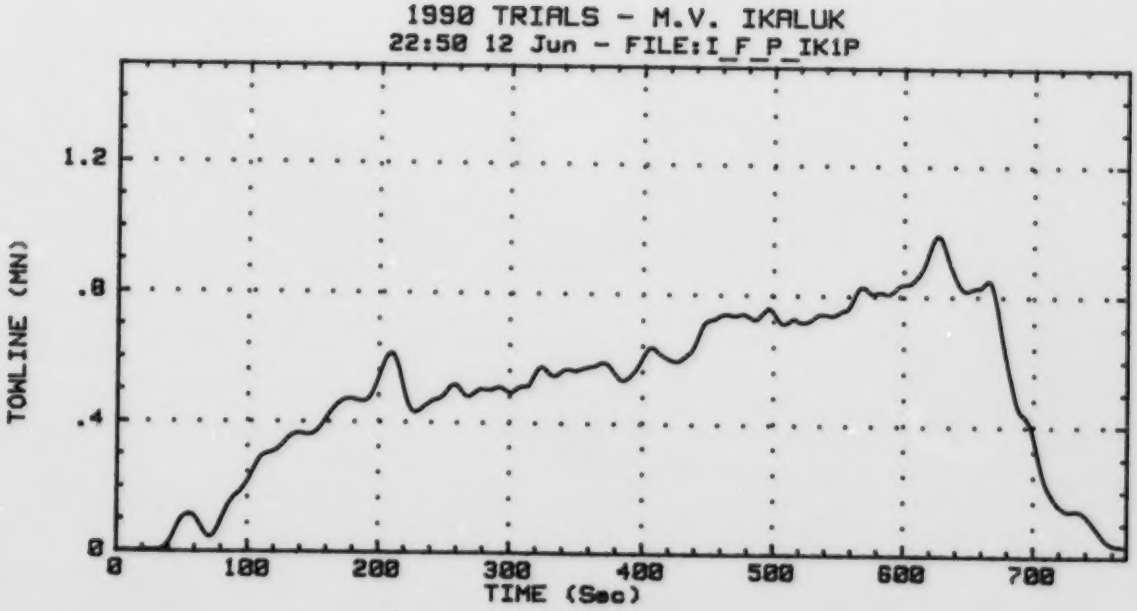

Figure 5.4.10 Speed and Towing Force: MV Ikaluk Tow No. 1

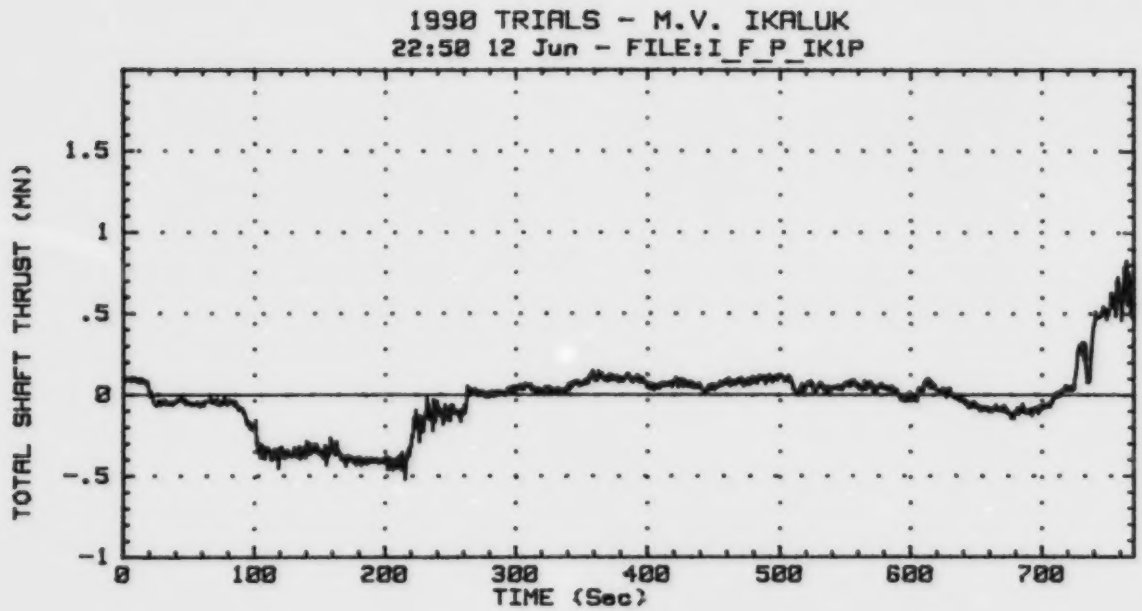

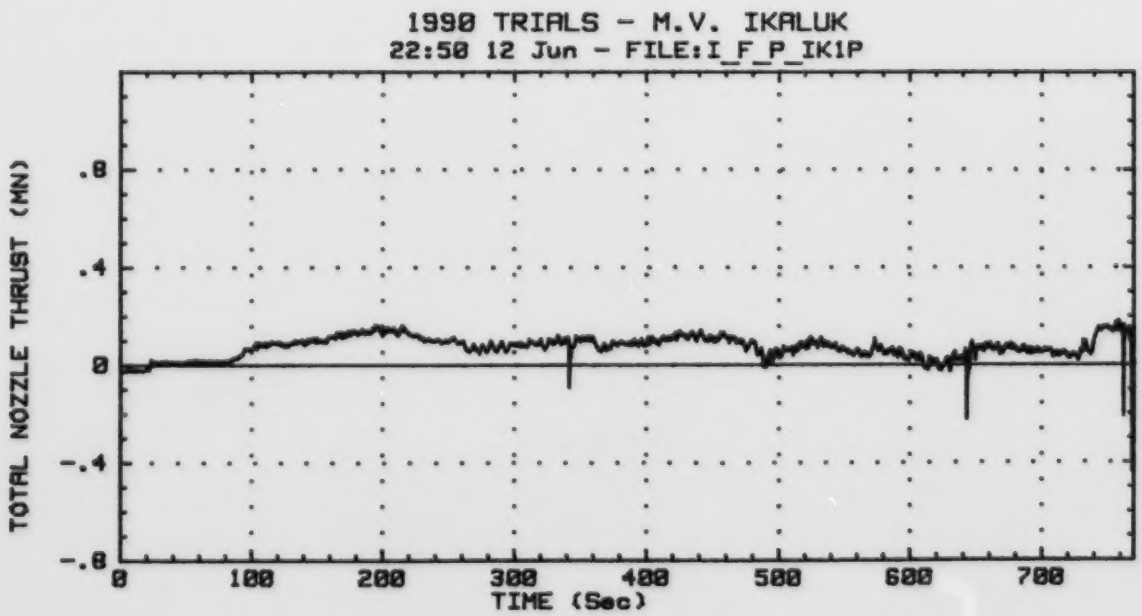

Figure 5.4.11 Total Shaft and Nozzle Thrust: MV Terry Fox Tow No. 1

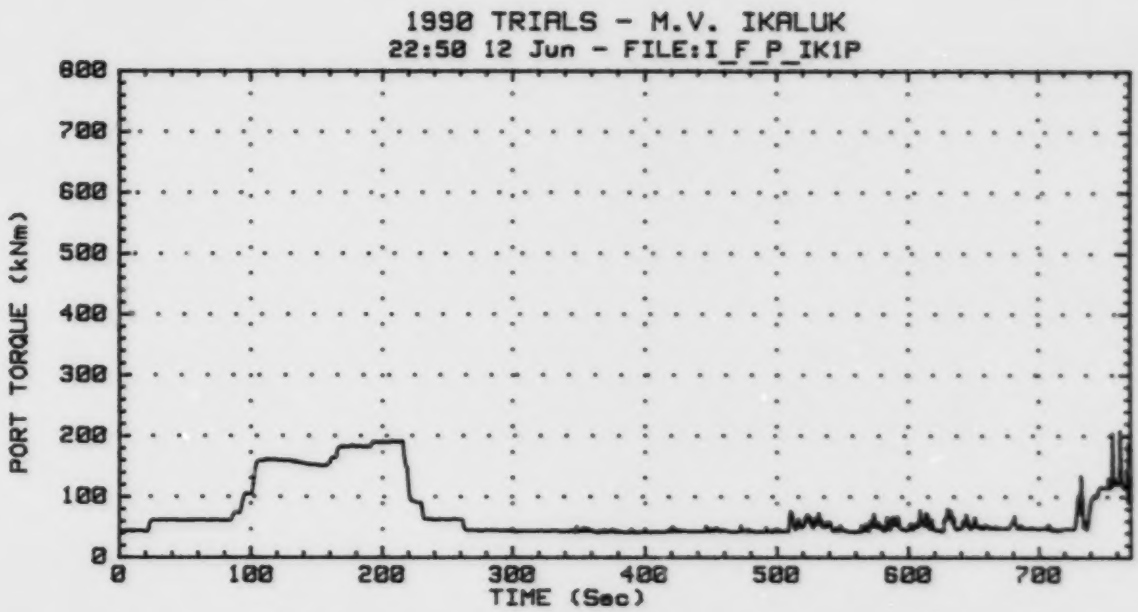

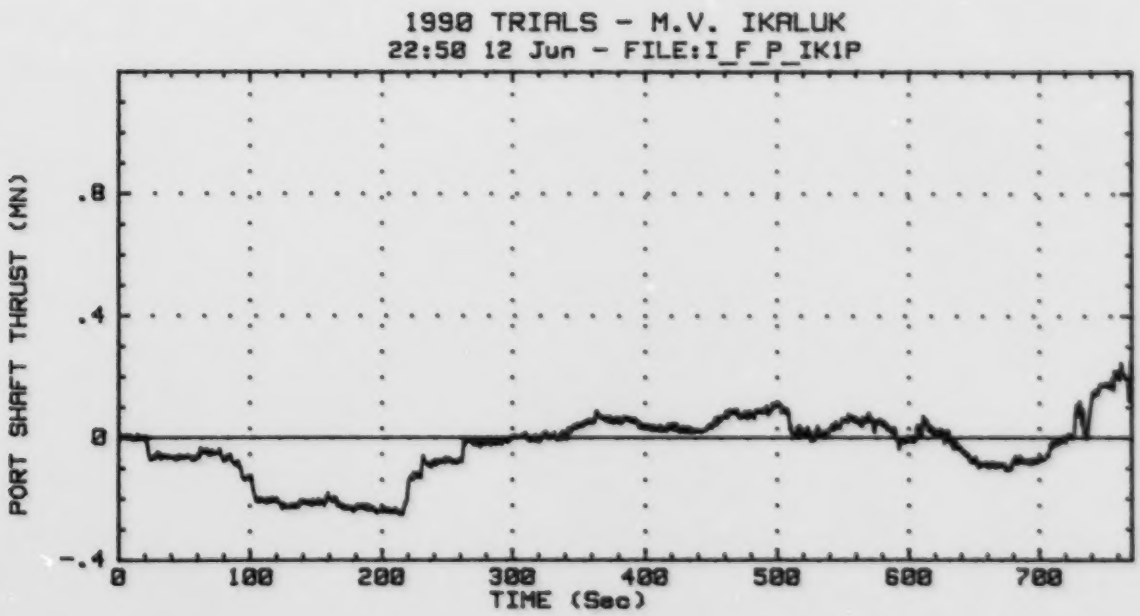

Figure 5.4.12 Port Shaft Thrust and Torque : MV Ikaluk Tow No. 1

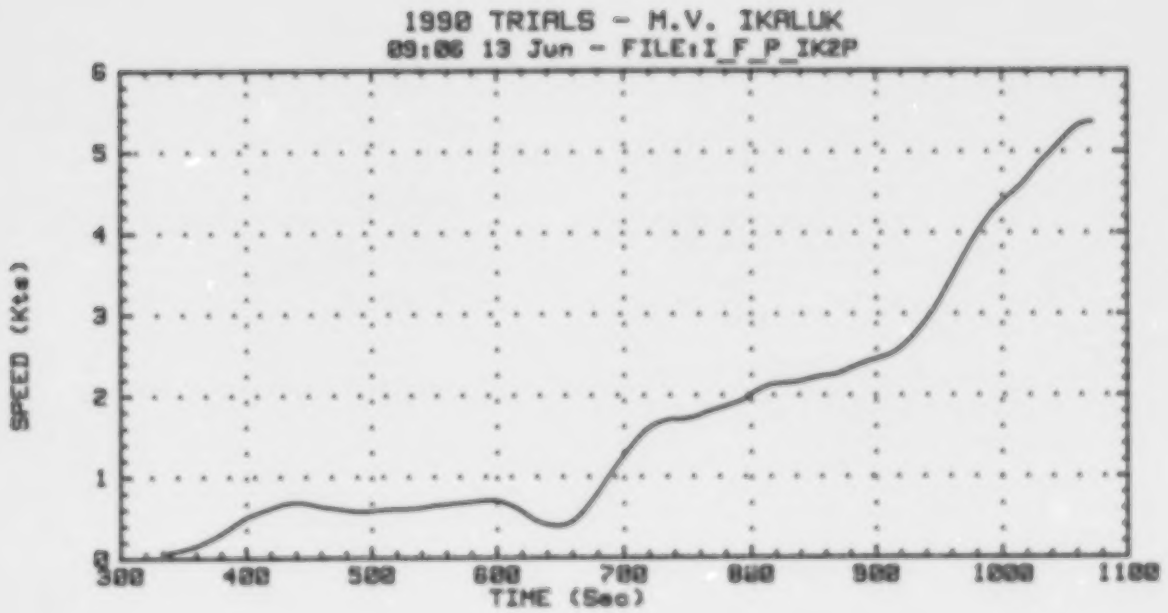

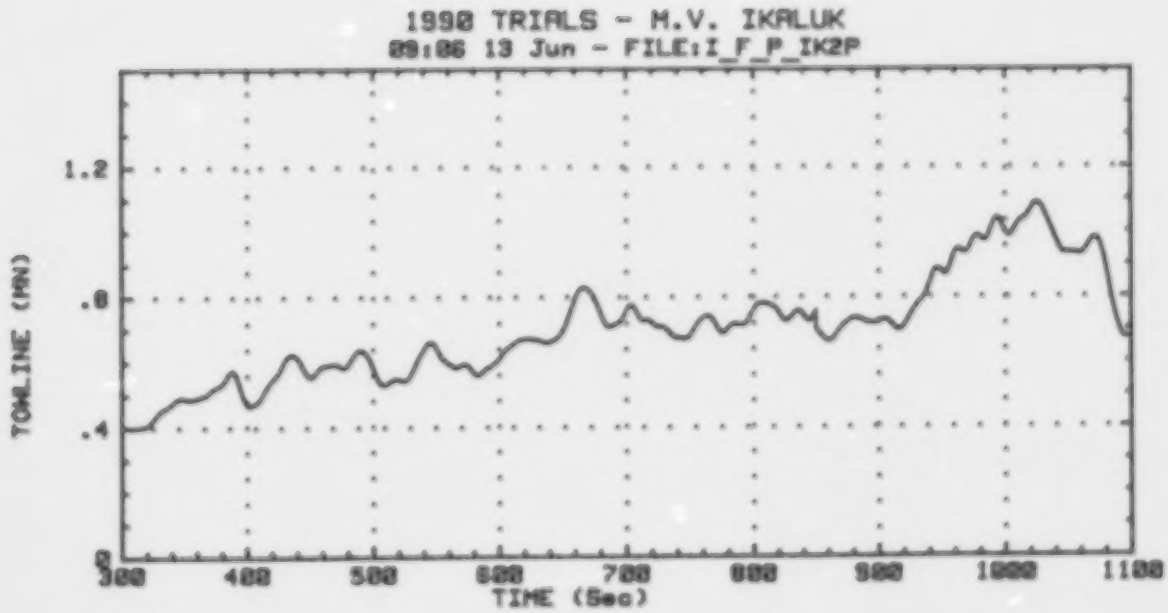

Figure 5.4.13 Speed and Towing Force: MV Ikaluk Tow No. 2

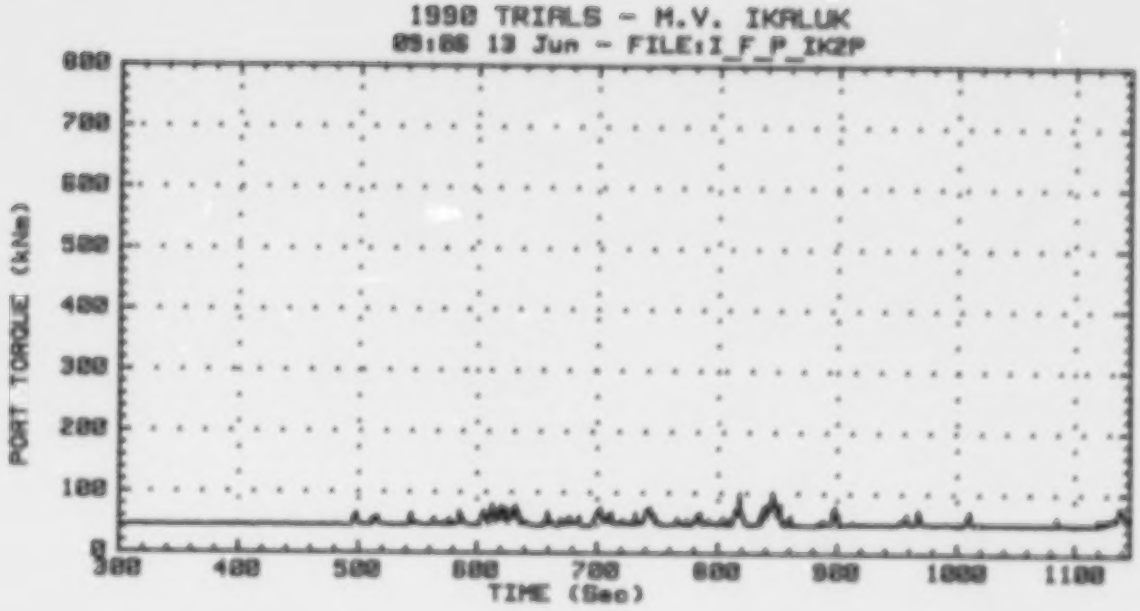

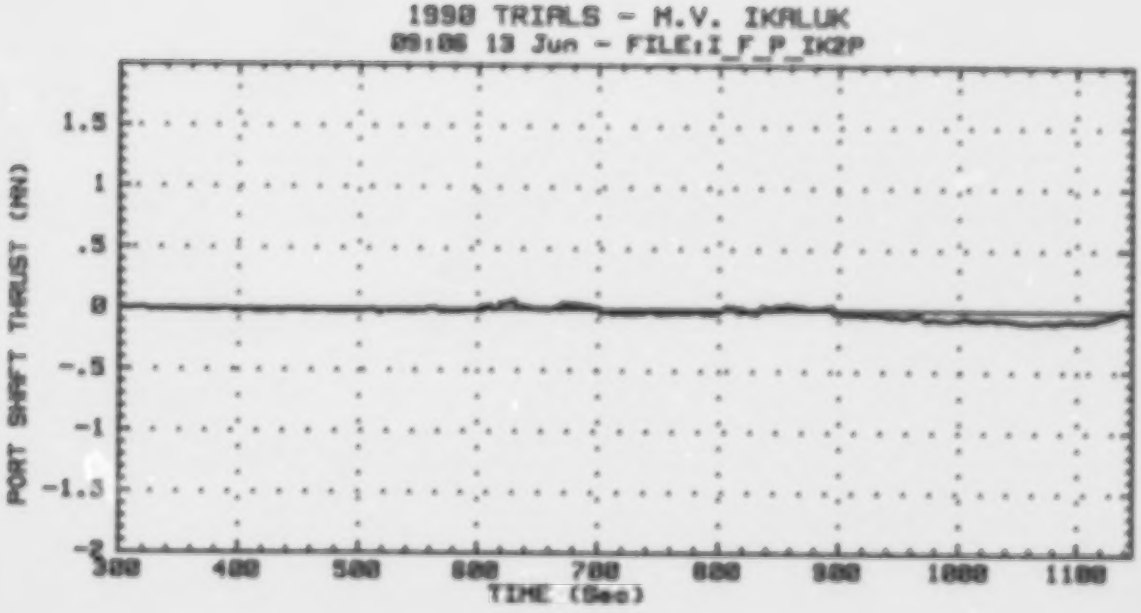

Figure 5.4.14 Port Shaft Thrust and Torque : MV Ikaluk Tow No. 2

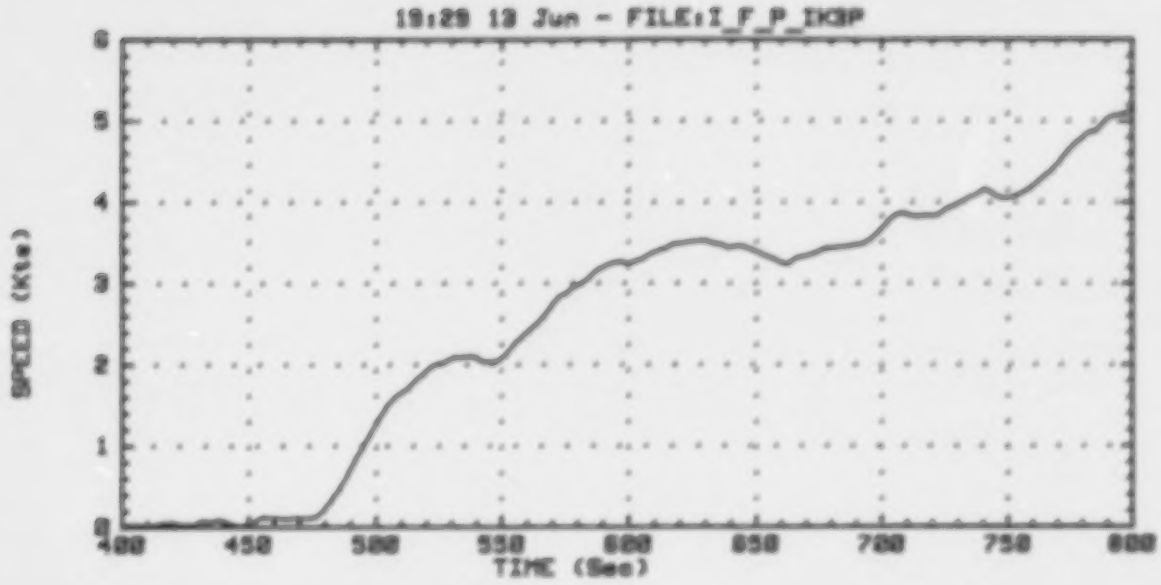

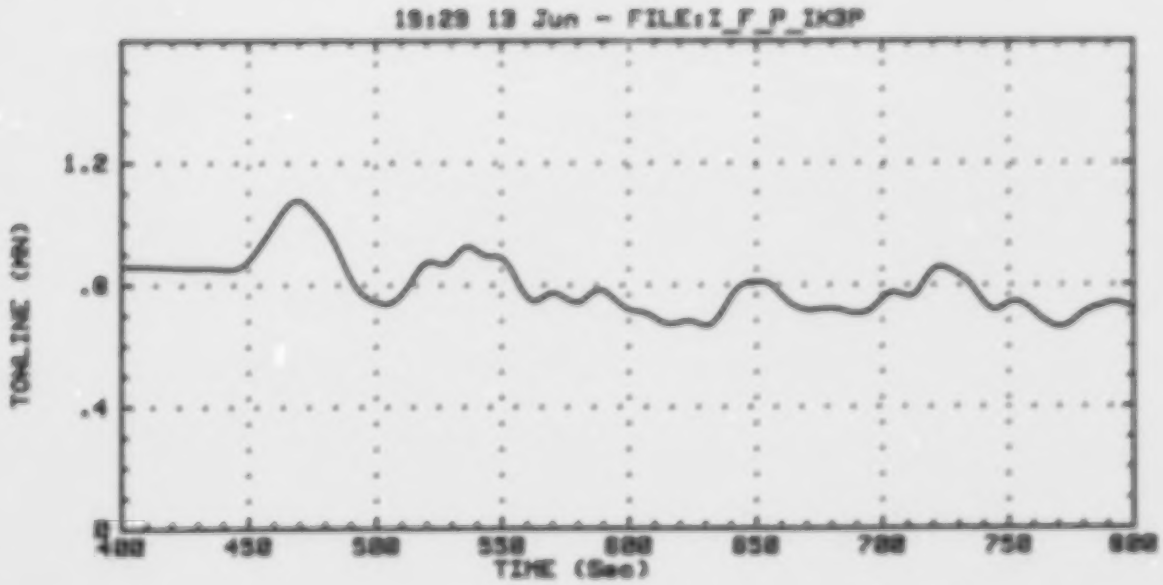

Figure 5.4.15 Speed and Towing Force: MV Ikaluk Tow No. 3

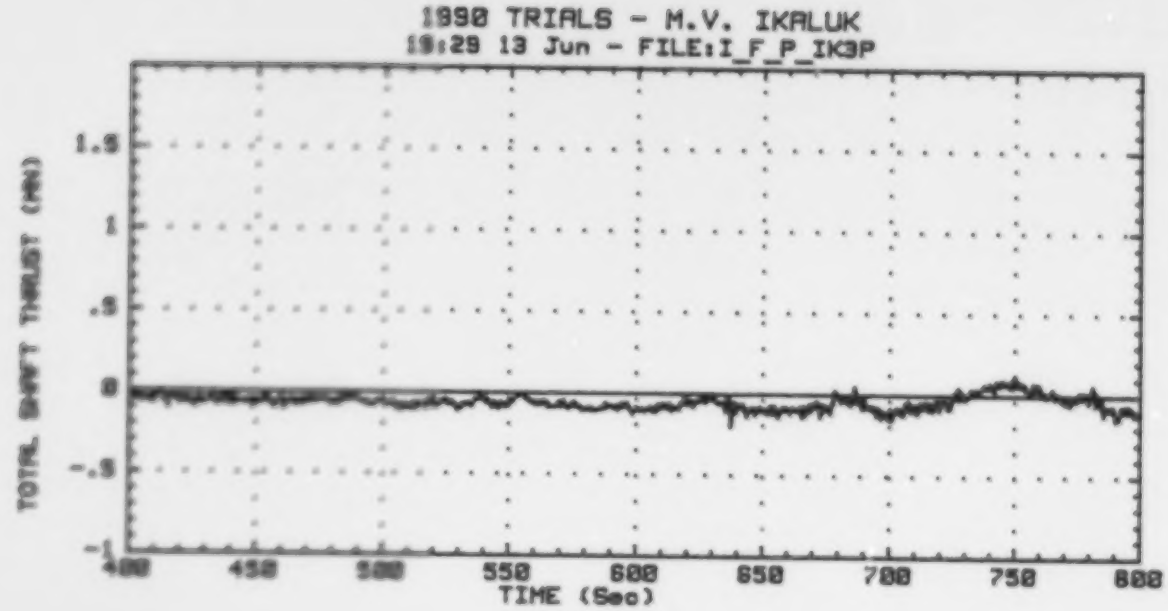

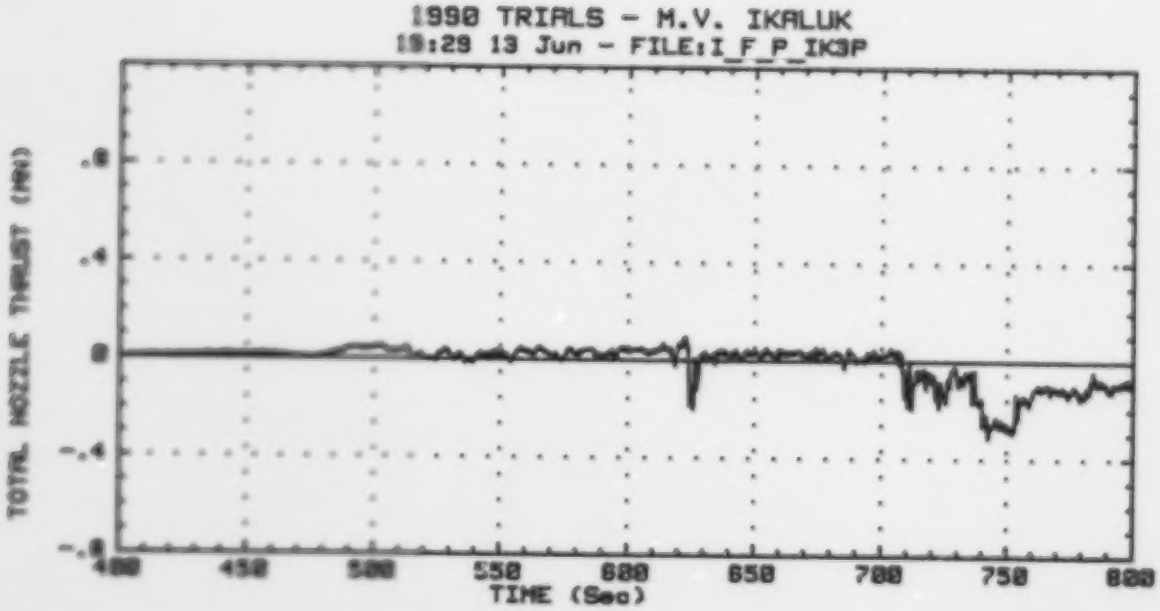

Figure 5.4.16 Total Shaft and Nozzle Thrust: MV Terry Fox Tow No. 3

5.5 Self-Propulsion Tests

Summary

This section summarizes the results of the data analysis of the self-propulsion tests, the following sections detail the analysis and present the data. Table 5.5.1 lists a summary of the results from the towing tests conducted.

Table 5.5.1 Summary of Self-Propulsion Test Data

M.V. Terry Fox			M.V. Ikaluk		
Velocity (knots)	Power (MW)	Thrust (MN)	Velocity (knots)	Power (MW)	Thrust (MN)
1.5	5.5	0.75	0.9	5.9	0.69
2.3	8.5	0.97	0.9	6.0	0.65
2.9	10.6	1.16	1.5	8.6	0.80
3.6	14.0	1.34	2.2	9.5	0.85
			2.3	9.1	0.89

Figure 5.5.1 is a plot of these results.

The following are the main findings of this study:

1. The power and thrust versus velocity relationship is linear over the speed range tested.

2. There was significant ice-propeller interaction for both vessels during the self-propulsion trials. The increase in power due to milling was no more than 7% over the time intervals analysed.

3. The M.V. Terry Fox required slightly less power (7%) than the M.V. Ikaluk at a speed of 2.3 knots. However, the power versus speed slope for the M.V. Terry Fox is approximately 1.7 times that of the M.V. Ikaluk - the corresponding ratio of displacements is 1.4.

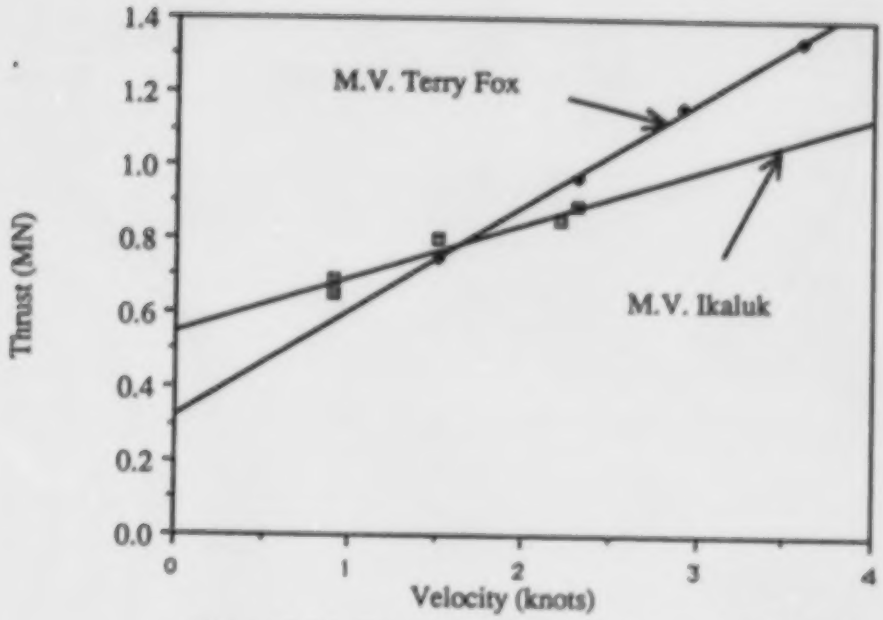

Figure 5.5.1 Thrust vs Speed: Self-Propulsion Trials

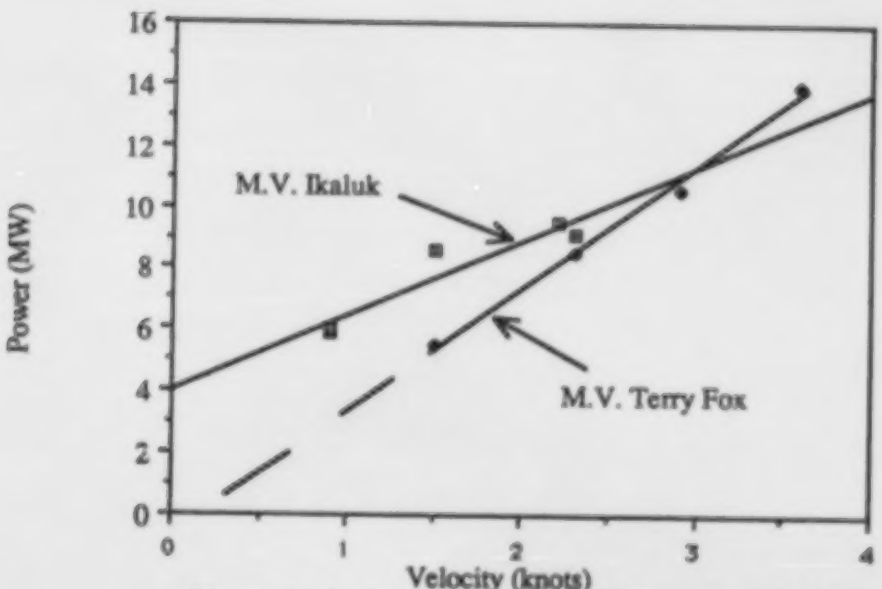

Figure 5.5.2 Power vs Speed: Self-Propulsion Trials

Introduction

This section details the analysis of the data collected during the self-propulsion trials. Seven trials were conducted on the M.V. Terry Fox, and thirteen on the M.V. Ikaluk. Each trial consisted of a number of speeds (power settings). By judicious selection of the available data four valid speeds were found for the M.V. Terry Fox and five for the M.V. Ikaluk. Data that was discounted included: non uniform ice, indications of pressure relief in the ice sheet (non-infinite ice sheet), and non-uniform velocities. Self-propulsion tests were conducted generally during manoeuvring to the towing test area, immediately prior to and after towing tests. This insured that the tests were conducted in the same ice conditions as the towing trials. Section 5.3 describes how the data was processed. The following describe in detail the data collected from selected tests.

NB. On all figures port pitch values should be 3° higher than illustrated. This has been corrected in the tables.

M.V. Terry Fox Self-Propulsion Results

Table 5.5.2 lists a number of the processed data sets from the M.V. Terry Fox self-propulsion trials. From this data set four tests were selected to be valid and the corresponding measurements are listed in Table 5.5.3. The inertial force (mass x acceleration) calculated, as was done during the towing trials. However, since the data selected consisted of relatively constant speed the inertial forces were negligible and did not effect the resulting thrust (ie. the shaft thrust = total net thrust).

Figures 5.5.3 and 5.5.4 illustrate the results in the form of plots of Thrust and Power versus speed. A linear regression line has been drawn through the data points. The fit is good and suggests that the power and thrust varies linearly with speed over the measured speed range of 1.5 to 3.6 knots. If the thrust curve is extrapolated to the vertical axis (zero speed) the thrust is 0.32 MN. This value is in close agreement with the measured towing force required to start the vessel in motion at the beginning of a towing trial.

Table 5.5.2 Self Propulsion Data Summary: M.V. Terry Fox

FILE	DAY	INTERVAL			PORT SHAFT				STBD SHAFT				TOTAL	
		Start (sec)	End (sec)	SPEED (kts)	Pitch (deg)	Torque (kNm)	Thrust (MN)	Power (MW)	Pitch (deg)	Torque (kNm)	Thrust (MN)	Power (MW)	Thrust (MN)	Power (MW)
2	11	60	150	6.6	23.6	557	0.56	7.50	24.1	543	0.54	7.20	1.11	14.76
2	11	300	350	4.0	20.5	479	0.59	6.48	20.1	430	0.47	5.74	1.07	12.21
2	11	400	600	2.7	17.0	342	0.48	4.60	17.5	346	0.42	4.60	0.90	9.20
3	11	250	500	1.8	15.5	308	0.52	4.17	15.5	287	0.50	3.83	1.02	8.00
4	11	170	2144	7.9	21.0	428	0.50	5.80	22.5	460	0.55	6.14	1.05	11.94
4	11	380	500	3.8	16.0	345	0.38	4.66	16.7	328	0.47	4.38	0.84	9.04
4	11	620	700	3.3	17.4	375	0.41	5.07	17.8	361	0.55	4.81	0.96	9.88
6	12	140	300	5.6	17.8	354	0.46	4.79	18.0	332	0.48	4.43	0.93	9.22
6	12	900	980	2.6	15.0	293	0.41	3.96	16.7	328	0.51	4.38	0.93	8.34
7	12	300	450	1.5	11.8	196	0.37	2.65	12.5	210	0.38	2.80	0.75	5.45
7	12	700	900	2.3	15.6	311	0.46	4.21	16.1	324	0.51	4.33	0.97	8.54
7	12	920	1000	2.9	17.1	347	0.53	4.70	19.0	446	0.63	5.96	1.17	10.66

Table 5.5.3 Selected Valid Self-Propulsion Data: M.V. Terry Fox

Data File		Self 7P	Self 7P	Self 7P	Self 1P
Date		13-Jun	13-Jun	13-Jun	14-Jan
Start Time		14:57	14:57	14:57	14:54
Interval		300 - 400	700 - 900	920 - 1000	530 - 700
Port Fuel Rack	(mm)	25	32	35	48
Port Pitch	(Deg.)	11.8	15.6	17.0	21.3
Port RPM	(RPM)	129	129	129	129
Port Torque	(kNm)	196	311	346	530
Port Thrust	(MN)	0.37	0.46	0.53	0.67
Stbd Fuel Rack	(mm)	23	30	39	42
Stbd Pitch	(Deg.)	12.5	16.1	19.0	21.1
Stbd RPM	(RPM)	127	127	128	127
Stbd Torque	(kNm)	210	320	446	513
Stbd Thrust	(MN)	0.38	0.513	0.63	0.67
Rudder	(Deg.)	3.5	3.5	3.5	3.4
Port Power	(MW)	2.6	4.2	4.7	7.1
Stbd Power	(MW)	2.80	4.30	6.00	6.80
Total Power	**(MW)**	**5.5**	**8.5**	**10.6**	**14**
Total Shaft Thrust	(MN)	0.75	0.97	1.16	1.34
Acceleration	(m/s^2)	-0.0001	-0.0002	0.0004	-0.0007
Inertial Thrust	(MN)	-0.001	-0.001	0.002	-0.004
(Mass x Acceleration)					
Net Thrust	**(MN)**	**0.75**	**0.97**	**1.16**	**1.34**
Velocity	**(knots)**	**1.5**	**2.3**	**2.9**	**3.6**

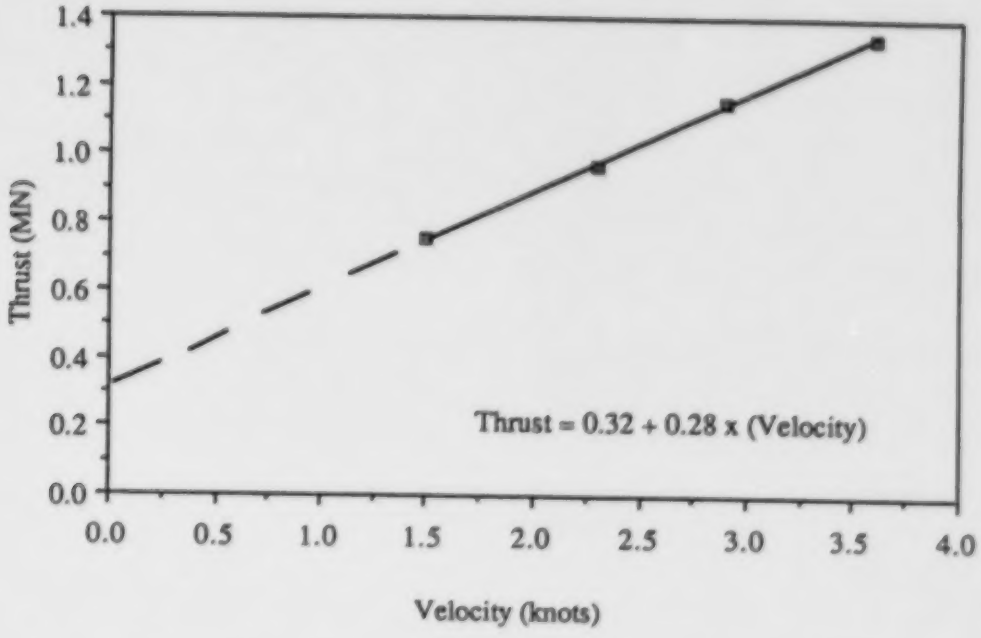

Figure 5.5.3 Thrust in Ice vs Velocity: M.V. Terry Fox

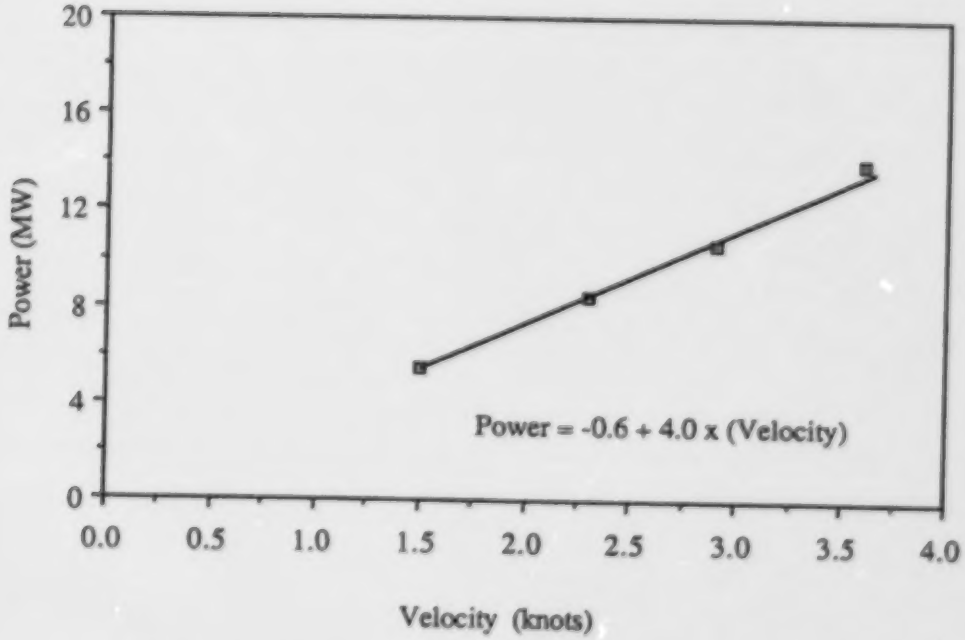

Figure 5.5.4 Power in Ice vs Velocity: M.V. Terry Fox

Self Propulsion Test 7: M.V. Terry Fox

Figure 5.5.5 illustrates the vessel speed and total shaft thrust for the seventh self-propulsion trial, and Figure 5.5.6 shows the corresponding total shaft power. The shaft rpm remained constant at 129-130 during all of the trials conducted.. Three relatively constant speeds in uniform ice were attained during this trial.

The ice interacted with the propeller throughout the test as indicated by the "spikes" in the shaft thrust and power time histories. This interaction is more evident in Figure 5.5.7 which illustrates the port shaft torque and thrust time histories. It is interesting to note that the shaft thrust "spikes" are in the negative direction, but the torque is in the positive direction. Therefore, during the ice interaction not only does the power requirement increase but the thrust developed decreases.

Figure 5.5.8 illustrates the port and starboard shaft thrust and the centreline rudder angle for this tests. As illustrated the rudder was kept approximately at the centreline position. Figure 5.5.9 shows the time history plots of the port and starboard shaft rpm and torque. The ice appears to interact with the starboard propeller more than the port one as illustrated by the higher degree of torsional "spikes" in the starboard shaft waveform

Figure 5.5.8 illustrates the port and starboard shaft thrust and the centreline rudder angle for this tests. As illustrated the rudder was kept approximately at the centreline position. Figure 5.5.9 shows the time history plots of the port and starboard shaft rpm and torque. The ice appears to interact with the starboard propeller more than the port one as illustrated by the higher degree of torsional "spikes" in the starboard shaft waveform. The rpm remains very constant during these interactions, which can largely be attributed to the high torsional inertia present in the shaftlines.

Figure 5.5.10 illustrates the port and starboard propeller pitch and engine fuel rack. The pitch remains relatively constant throughout the tests but the fuel rack time history indicates fluctuations corresponding to the shaft torsional "spikes".

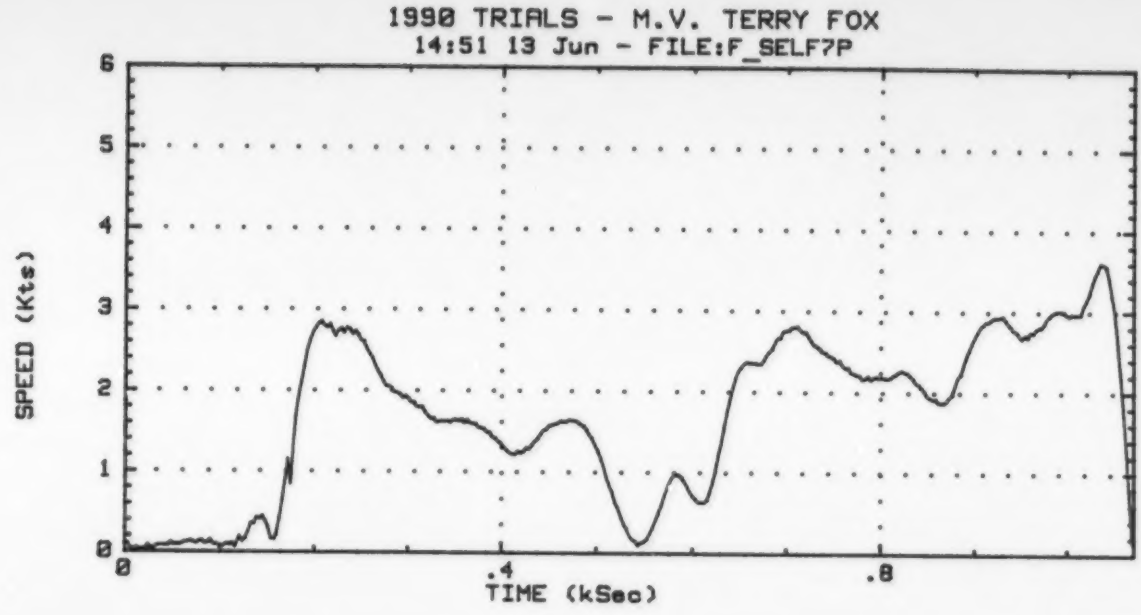

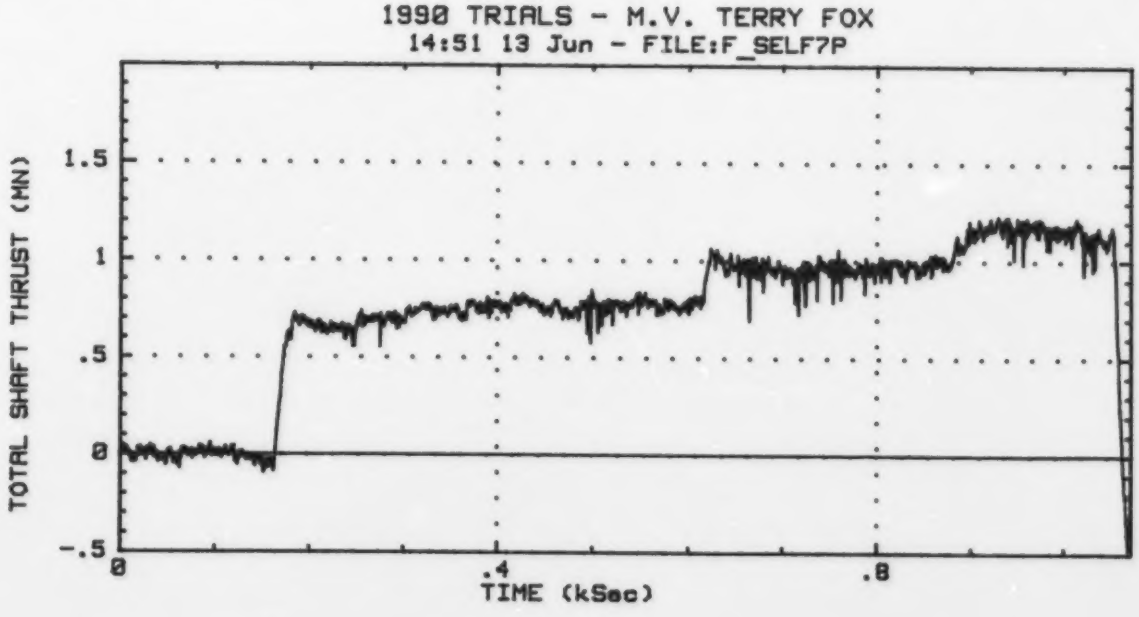

Figure 5.5.5 Total Shaft Thrust vs Speed: MV Ikaluk Self Propulsion Test 7

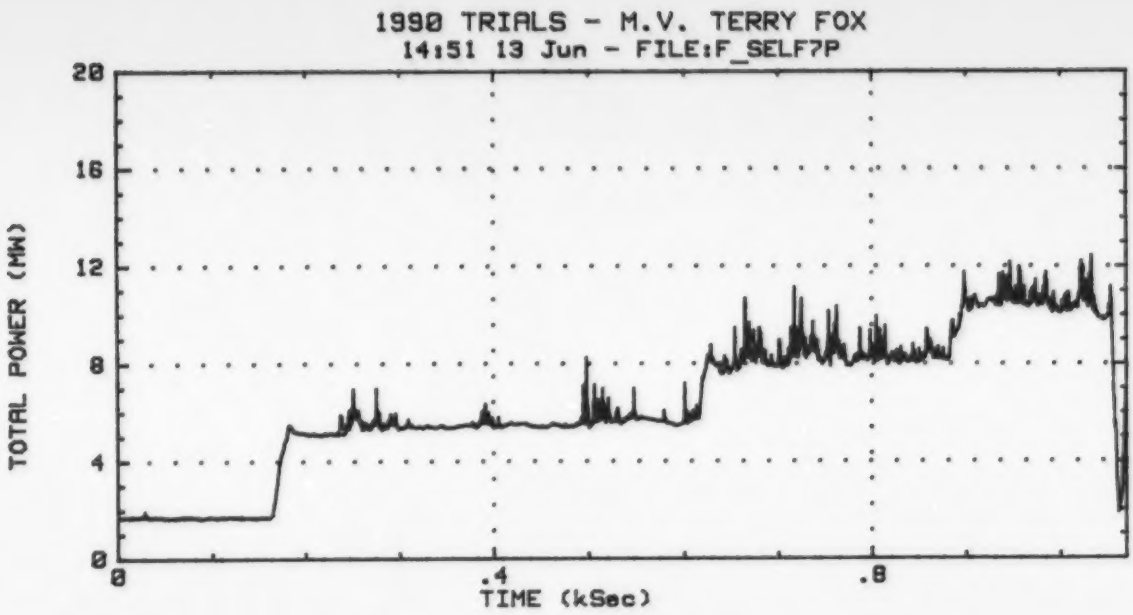

Figure 5.5.6 Total Shaft Power: MV Terry Fox Self Propulsion Test 7

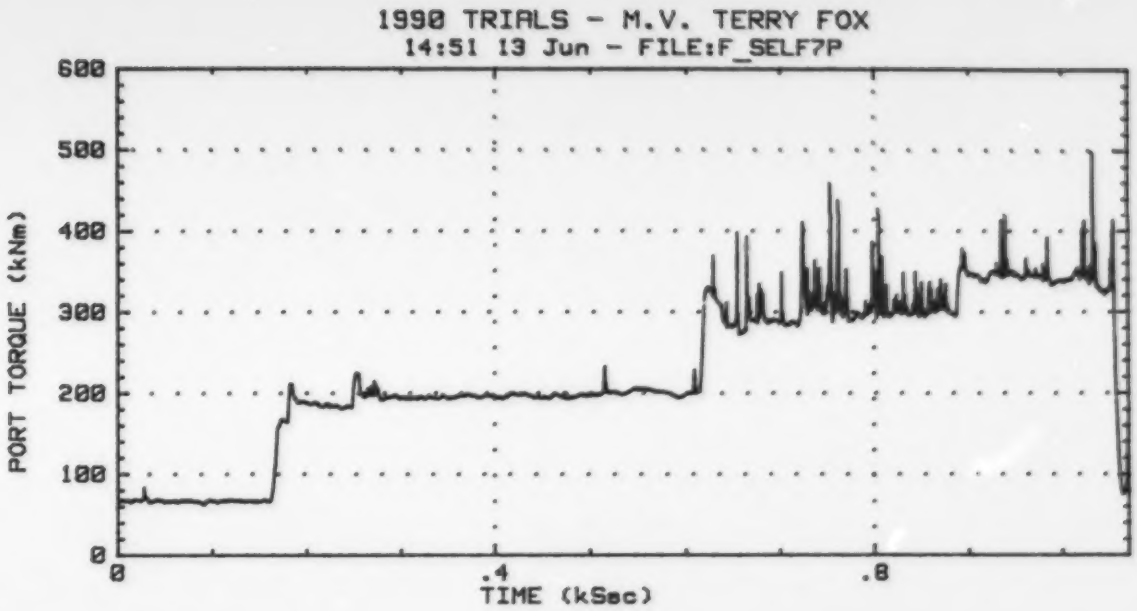

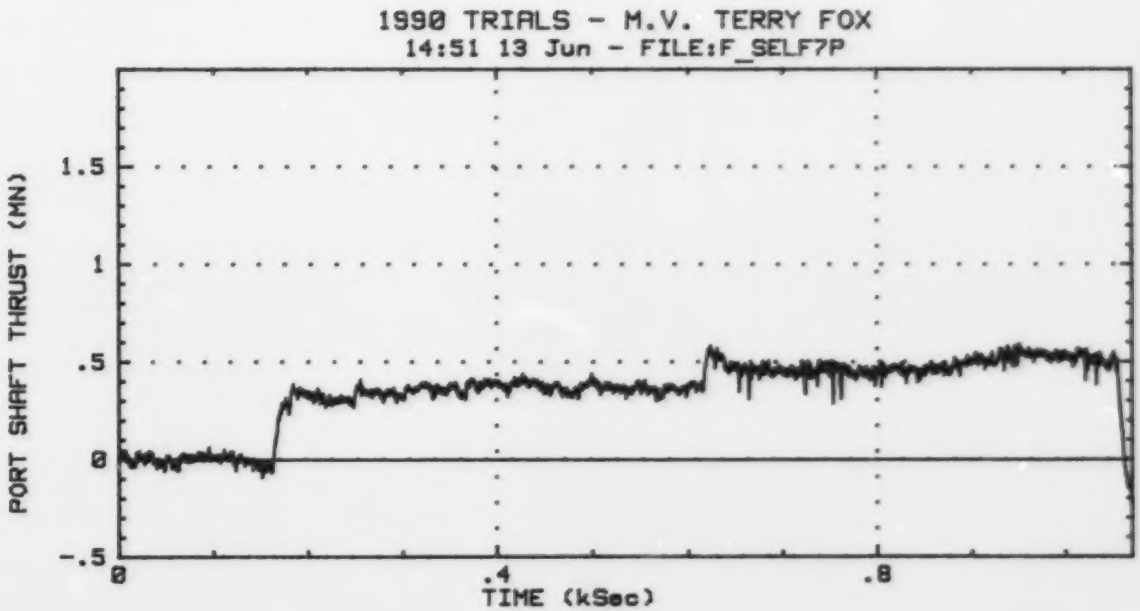

Figure 5.5.7 Port Shaft Torque and Thrust : MV Terry Fox Self Propulsion Test 7

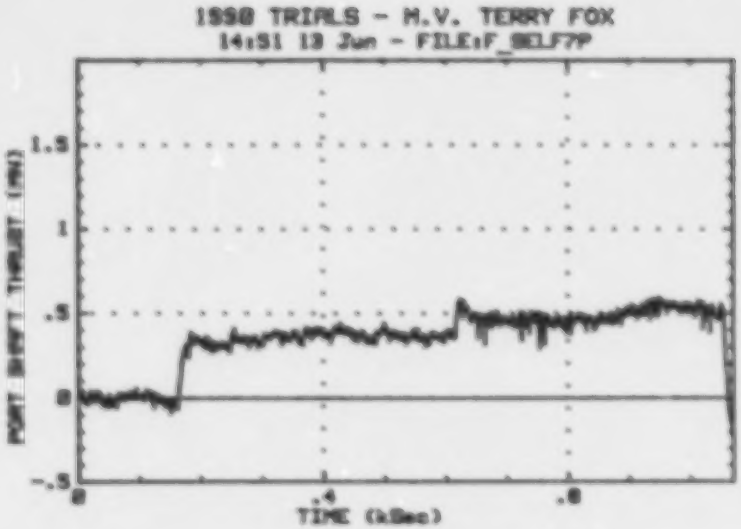

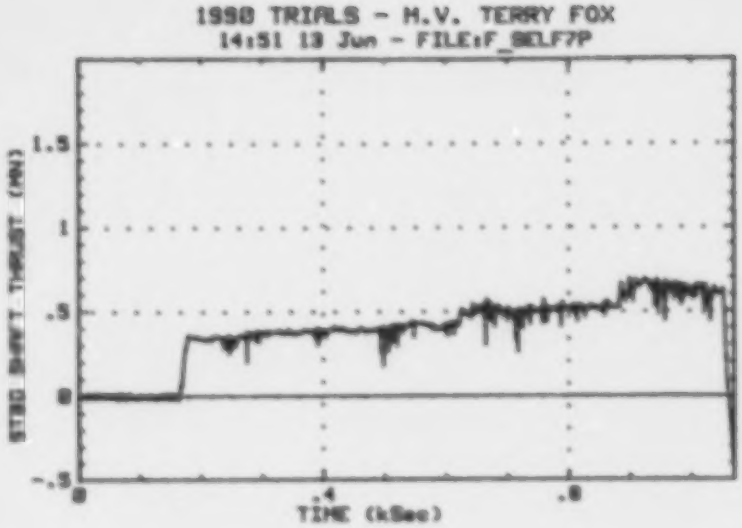

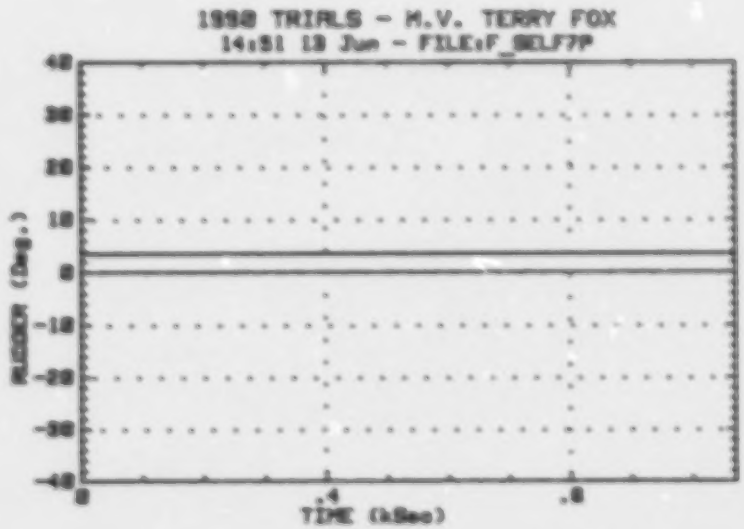

Figure 5.5.8 Port and Starb. Shaft Thrust and Rudder Angle:

MV Terry Fox Self Propulsion Test 7

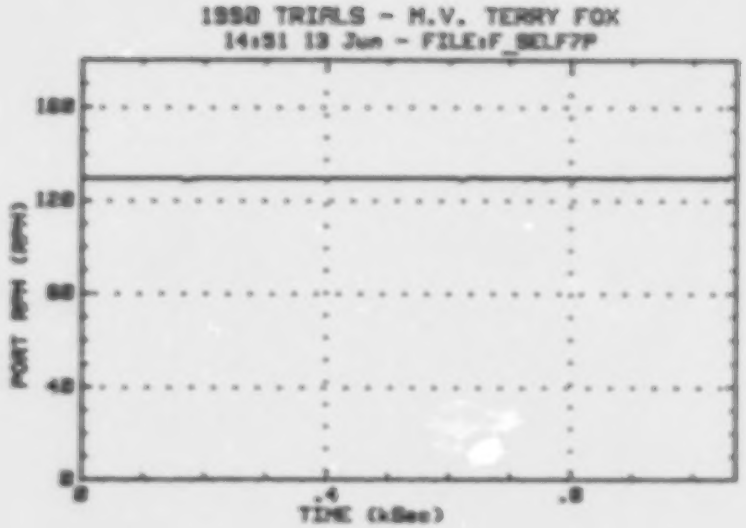

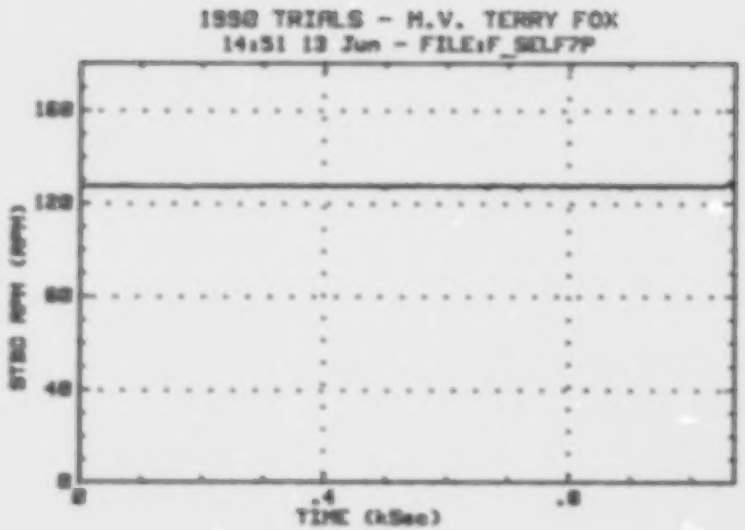

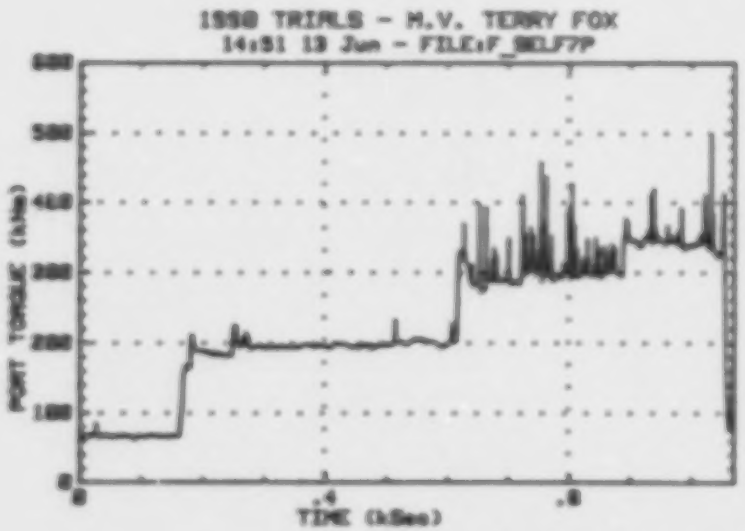

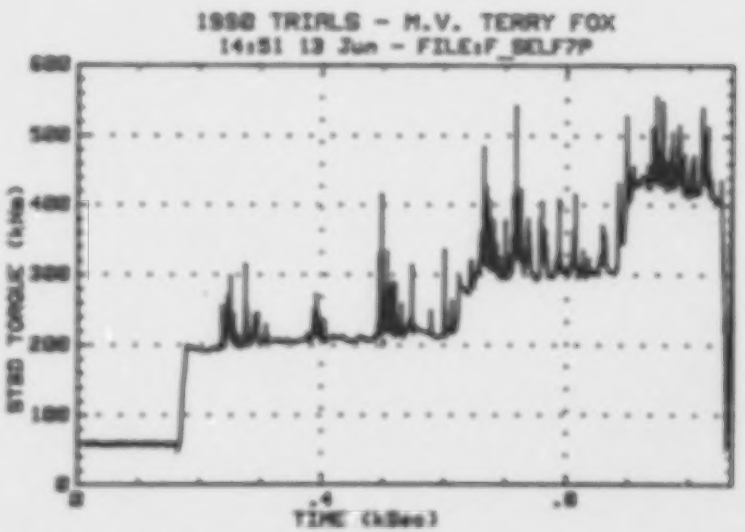

Figure 5.5.9 Port and Starb. Shaft RPM and Torque:

MV Terry Fox Self Propulsion Test 7

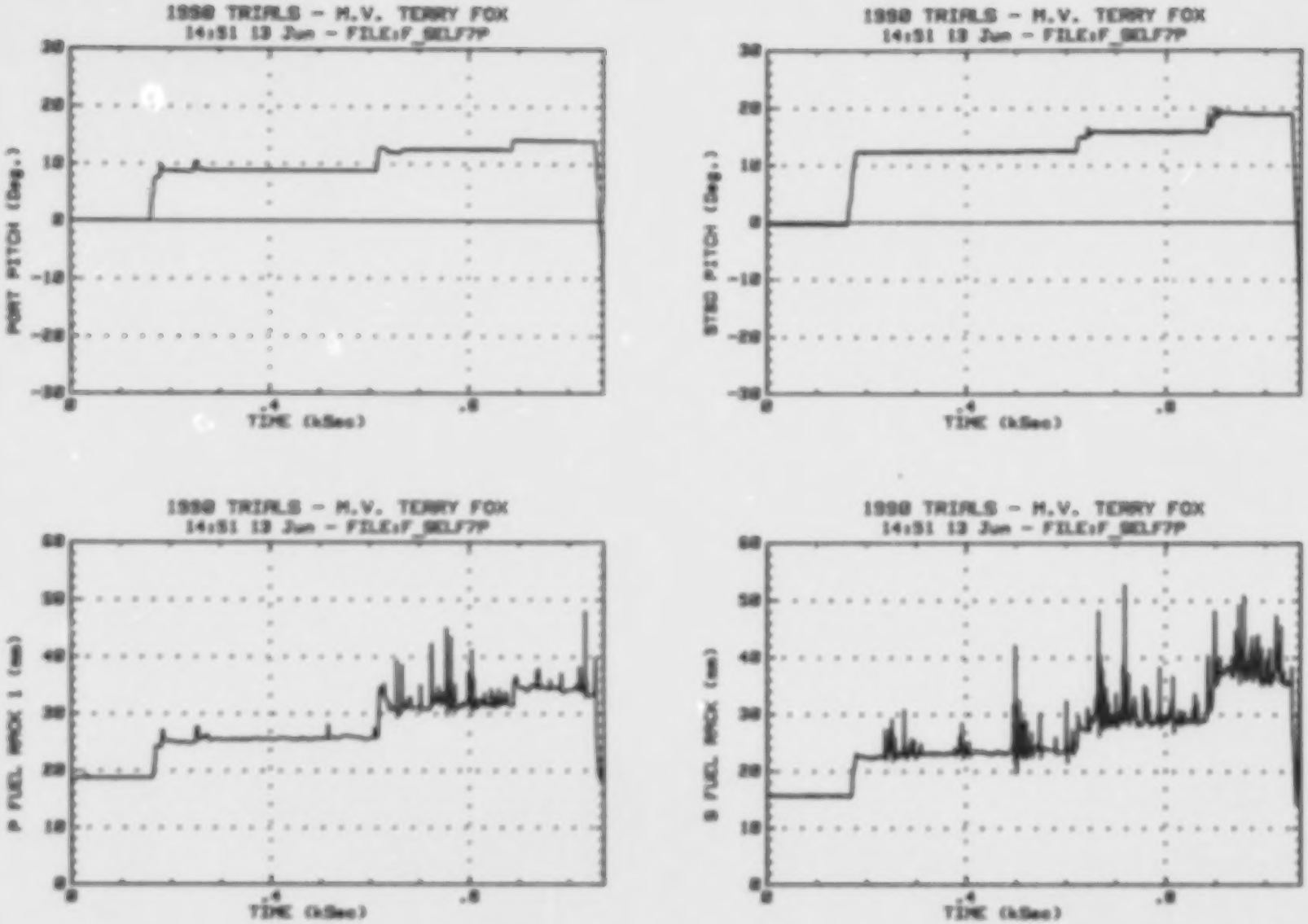

Figure 5.5.10 Port and Starb. Propeller Pitch and Engine Fuel Rack:

MV Terry Fox Self Propulsion Test 7

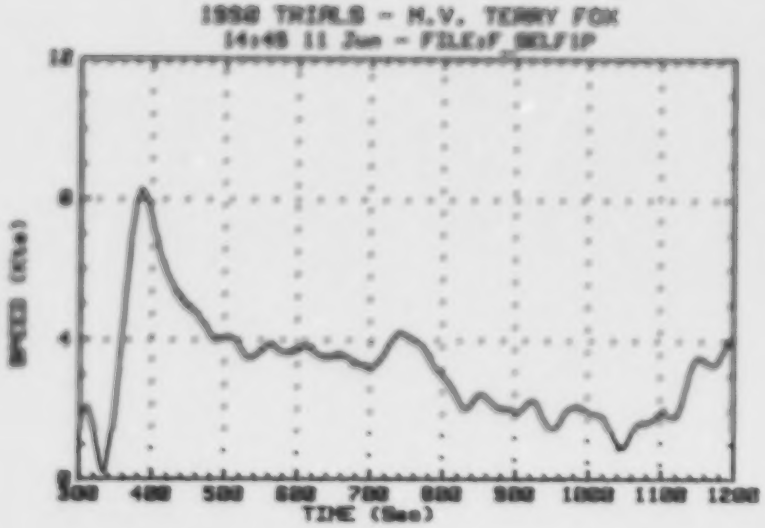

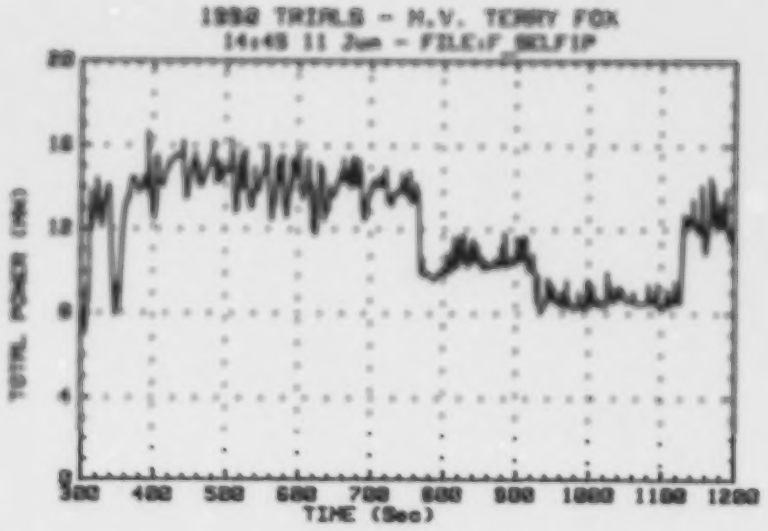

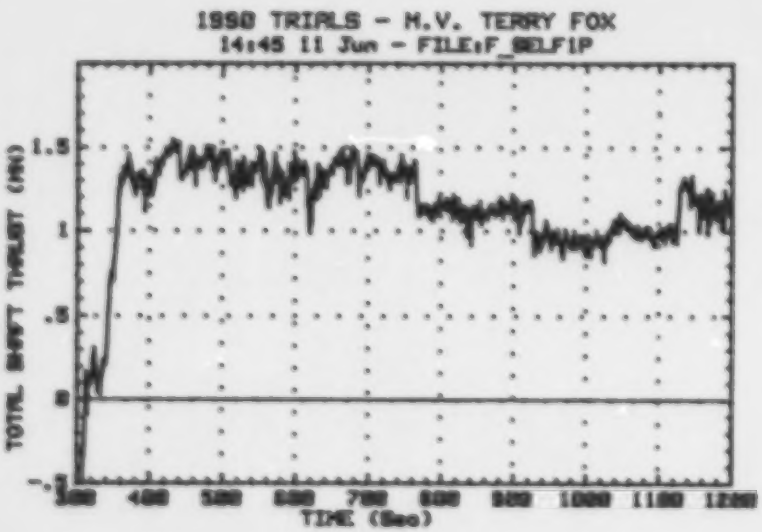

Figure 5.5.11 Ship Speed, Total Power and Total Shaft Thrust:

MV Terry Fox Self Propulsion Test 1

Self Propulsion Test 1: M.V. Terry Fox

Figure 5.5.11 shows the time history plots of the ship speed, total shaft power, and total shaft thrust for the first self-propulsion trial. The initial speed reaches 8 knots prior to entering the uniform ice sheet where a constant speed of 3.6 knots is achieved. This is the highest speed achieved during the self-propulsion trials. Ice is interacting with the propeller almost continuously during this test as indicated by the highly dynamic shape of the shaft power and thrust waveforms.

M.V. Ikaluk Self-Propulsion Test Results

Table 5.5.4 lists a number of the processed data sets from the M.V. Ikaluk self-propulsion trials, along with data are comments regarding the validity of the data. From this data set five tests were selected to be valid and the corresponding measurements are listed in Table 5.5.5. The inertial force (mass x acceleration) calculated, as was done during the towing trials. However, since the data selected consisted of relatively constant speed the inertial forces were negligible and did not effect the resulting thrust (ie. the shaft thrust = total net thrust).

The nozzle thrust was measured with two strain gauges that were mounted on the top of the nozzle for trials that were conducted in the spring of 1989. Table 5.4 lists the measured value and a calculated value (based upon pitch, speed measurements) of the nozzle thrust. It was found that neither of these methods were satisfactory in estimating the nozzle thrust contribution during the self-propulsion trials. The ice interaction with the nozzle and propeller cause erroneous readings. The calculated nozzle thrust assume the vessel in the free running condition, and a satisfactory correction for the overload condition was not found. Therefore, the measured and calculated values of the nozzle thrust are reported but are not included in the presentation of the thrust versus velocity relationship.

Figure 5.5.12 and 5.5.13 illustrate the results in the form of plots of Thrust and Power versus speed. A linear regression line has been drawn through the data points. The fit is good and suggests that the power and thrust varies linearly with speed over the measured speed range of 0.8 to 2.27 knots. If the thrust curve is extrapolated to the vertical axis (zero speed) the thrust is 0.55 MN. This value is approximately the same value as the measured towing force required to start the vessel in motion at the beginning of a towing trial.

Table 5.5.4 Self-Propulsion Data Summary: M.V. IKALUK

Test No.	File	Interval		Speed	Port Shaft				Stbd Shaft				Total shaft		Nozzle		Total		Comments
		Start (sec)	End (sec)	(kts)	Pitch (deg)	Torque (kNm)	Thrust (MN)	Power (MW)	Pitch (deg)	Torque (kNm)	Thrust (MN)	Power (MW)	Thrust (MN)	Power (MW)	Meas. Thrust (MN)	Calc Thrust (MN)	Meas. Thrust (MN)	Calc Thrust (MN)	
1	1P	400	500	2.3	27.4	285	0.44	5.00	27.0	238	0.45	4.14	0.89	9.14	0.34	0.34	1.22	1.23	Good test
2	2P	305	395	0.7	23.0	208	0.41	3.60	23.0	162	0.32	2.81	0.73	6.41	0.30	0.34	1.04	1.07	No cracking, vessel
3	2P	800	870	0.7	25.0	247	0.47	4.32	25.0	207	0.44	3.60	0.91	7.92	0.46	0.37	1 37	1.28	stopped and started,
4	2P	1200	1340	1.0	25.7	256	0.44	4.46	25.4	210	0.43	3.65	0.87	6.60	0.46	0.37	1.33	1.24	rough track
5	3P	1200	1500	1.8	27.4	289	0.36	5.00	27.0	237	0.47	4.12	0.83	9.12	0.29	0.36	1.12	1.19	Variable ice thickness
6	4P	430	475	7.4	27.6	322	0.50	5.60	28.6	233	0.35	4.00	0.85	9.60	0.13	0.10	0.99	0.96	Ice cracking
7	4P	600	700	7.5	28.3	325	0.50	5.60	29.0	238	0.37	4.09	0.87	9.74	0.07	0.11	0.95	0.98	Ice cracking
8	5P	100	600	1.5	26.7	324	0.48	5.65	26.8	232	0.39	3.94	0.87	9.58	0.20	0.37	1.07	1.24	Ice cracking
9	5P	460	580	1.4	26.7	325	0.48	5.65	26.3	230	0.40	3.90	0.87	9.54	0.20	0.37	1.08	1.24	Ice cracking
10	6P	370	545	3.1	22.8	262	0.45	4.60	22.4	205	0.32	3.53	0.77	8.13	0.11	0.21	0.88	0.98	Ice cracking
11	7P	250	370	0.9	18.7	157	3.04	2.78	19.2	122	0.24	2.13	0.54	4.92	0.17	0.24	0.68	0.78	Ice cracking
12	7P	560	920	2.2	19.6	187	0.35	3.30	20.3	145	0.29	2.54	0.64	0.18	0.18	0.20	0.78	0.84	Ice cracking
13	7P	1030	1200	0.9	19.5	201	0.43	3.55	20.0	135	0.26	2.36	0.69	5.91	0.44	0.26	1.09	0.95	Good test
14	8P	0	120	0.9	19.8	190	0.35	3.36	19.6	152	0.30	2.65	0.62	6.00	0.38	0.26	1.00	0.87	Good test
15	8P	200	400	2.2	21.0	214	0.34	3.77	20.6	150	0.28	2.61	0.62	6.38	0.42	0.22	1.04	0.84	Ice cracking
16	8P	540	700	1.2	21.0	206	0.31	3.64	21.1	151	0.28	2.63	0.60	6.27	0.40	0.27	0.95	0.87	Ice cracking
17	9P	300	400	1.5	25.5	293	0.46	5.11	25.2	202	0.34	3.50	0.81	8.60	0.36	0.34	1.20	1.15	Good test
18	9P	500	800	2.2	26.7	321	0.47	5.58	26.5	229	0.37	3.93	0.85	9.51	0.40	0.33	1.20	1.18	Good test
19	10P	250	400	1.9	23.2	250	0.35	4.38	24.2	180	0.36	3.30	0.71	7.68	0.28	0.29	0.99	1.00	Ice Cracking
20	11P	260	400	3.3	26.8	320	0.43	5.56	26.3	227	0.38	3.42	0.81	8.98	0.29	0.28	1.10	1.08	Bad ice but no Cracking
21	11P	580	800	3.2	27.0	322	0.43	5.58	27.1	229	0.40	3.32	0.82	8.91	0.20	0.29	1.02	1.11	Bad ice but no Cracking
22	12P	310	400	4.2	27.0	320	0.50	5.55	26.5	228	0.36	3.90	0.86	9.46	0.22	0.24	1.08	1.09	No good
23	13P	11	500	2.3	26.6	321	0.46	5.58	26.1	230	0.43	3.87	0.88	9.45	0.51	0.32	1.39	1.21	Soft Variable ice

Table 5.5.5 Selected Valid Self-Propulsion Data: M.V. Ikaluk

Data File		Self 7P	Self 8P	Self 9p	Self 9p	Self 1P
Date		Jun-91	Jun-91	Jun-91	Jun-91	Jun-91
Start Time		2:23	2:23	2:44	2:44	2:23
Interval		1030-1200	0 - 120	300 - 400	500 - 600	400 - 500
Port Fuel Rack	(mm)	27.0	27.0	37.0	40.5	41.0
Port Pitch	(Deg.)	19.50	19.70	25.50	26.70	27.30
Port RPM	(RPM)	168.0	168.0	166.0	166.0	166.0
Port Torque	(kNm)	201.0	191.0	293.0	321.0	285.0
Port Thrust	(MN)	0.43	0.35	0.46	0.47	0.44
Stbd Fuel Rack	(mm)	23.0	26.0	31.0	35.0	35.0
Stbd Pitch	(Deg.)	20.20	19.60	25.20	26.50	26.90
Stbd RPM	(RPM)	167.0	166.0	165.0	164.0	165.00
Stbd Torque	(kNm)	135.0	152.0	203.0	228.0	238.0
Stbd Thrust	(MN)	0.26	0.30	0.34	0.37	0.45
Port Rudder	(Deg.)	7.3	1.0	1.3	1.2	2.9
Stbd Rudder	(Deg.)	8.4	1.2	0.6	0.8	-0.7
Port Power	(MW)	3.5	3.4	5.1	5.6	5.0
Stbd Power	(MW)	2.4	2.6	3.5	3.9	4.1
Total Power	**(MW)**	**5.9**	**6.0**	**8.6**	**9.5**	**9.1**
Total Shaft Thrust	(MN)	0.6900	0.6500	0.8100	0.8500	0.8900
Acceleration	(m/s^2)	0.0009	0.0001	0.0017	-0.0003	0.0003
Inertia Thrust (Mass x Acc.)	(MN)	0.0046	0.0006	0.0087	-0.0015	0.0017
Net Thrust	**(MN)**	**0.69**	**0.65**	**0.80**	**0.85**	**0.89**
Velocity	**(knots)**	**0.88**	**0.90**	**1.50**	**2.21**	**2.27**

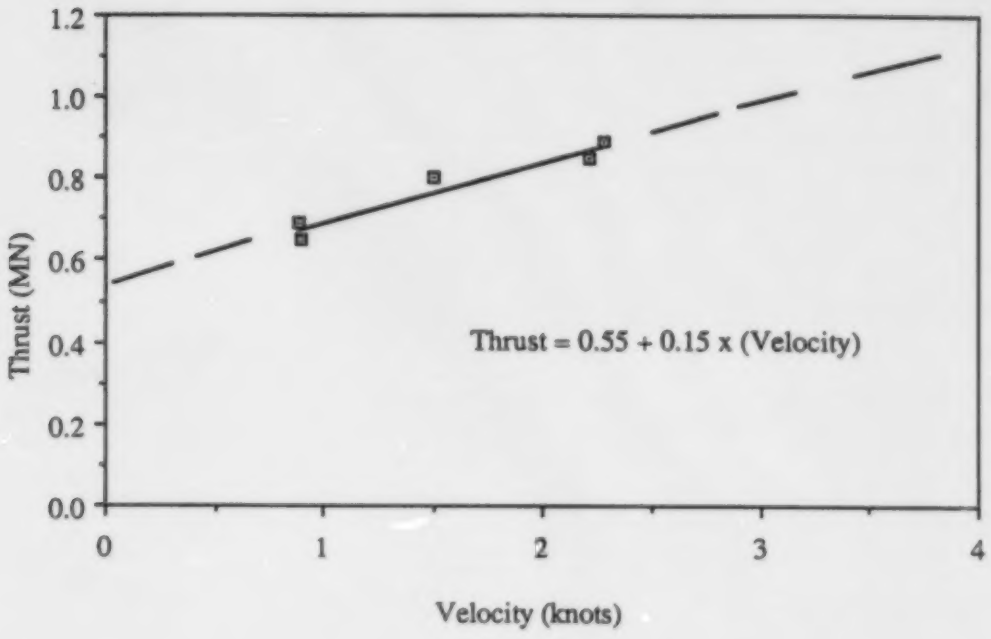

Figure 5.5.12 Thrust vs Velocity: M.V. Ikaluk

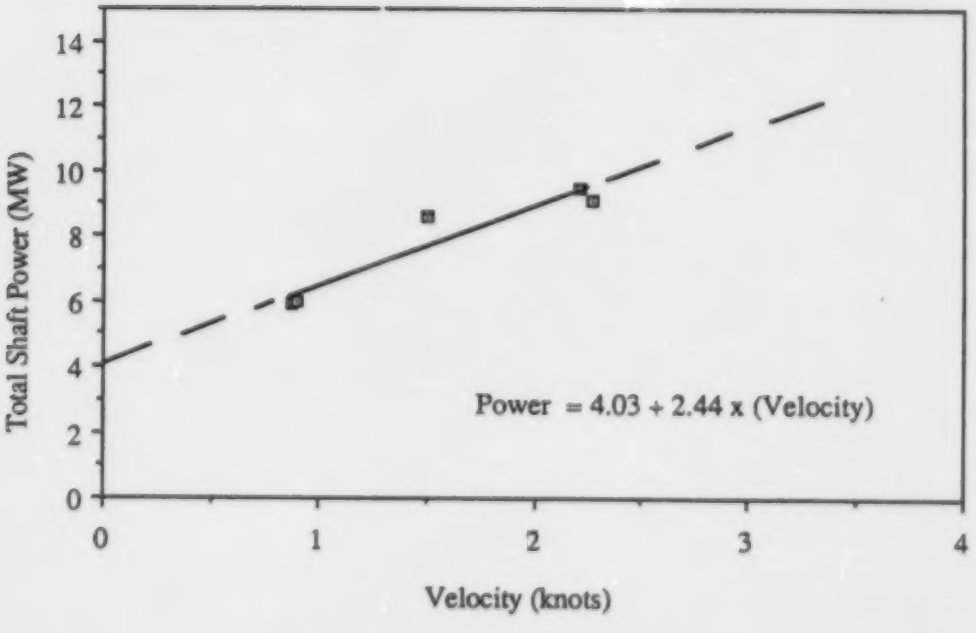

Figure 5.5.13 Shaft Power vs Velocity: M.V. Ikaluk

Self Propulsion Test 7: M.V. Ikaluk

Figure 5.5.14 illustrates the vessel speed, total shaft power, total measured nozzle thrust (not reliable) and total thrust (including nozzle thrust) for the seventh self-propulsion trial. As on the M.V. Terry Fox, the ice interacted with the propeller throughout the test as indicated by the "spikes" in the shaft thrust and power time histories. It is interesting to note that the shaft thrust "spikes" are in the positive direction, which was apposite that of the M.V. Terry Fox. However, the positive thrust "spike" does not result in a positive thrust on the vessel, because the reaction is on the nozzle, as was determined from previous trials.

Figure 5.5.15 shows the speed and total shaft thrust time histories for the time interval of 700-1,300 seconds. There two distinct speeds of which only one was determined to be valid (0.88 knots). Figure 5.5.16 illustrates the corresponding port and starboard shaft torque. Again the ice interaction is illustrated by the "spikes"in the waveforms.

Figure 5.5.17 show the port and starboard rpm and torque time histories. The rpm remains essentially constant, while the torque has torsional "spikes" indicating the ice-propeller interaction again. As with the M.V. Terry Fox the propulsion system configuration is very good at keeping the rpm constant during ice-propeller-nozzle interaction. Figure 5.5.18 shows the port and starboard shaft thrust and rudder angle. The rudder was changed periodical throughout the tests; however care was taken to select time intervals of constant low or near zero rudder angle. Figure 5.5.18 shows the corresponding port and starboard pitch and engine fuel rack for this test.

Figures 5.5.19 and 5.5.20 illustrate the ship speed, port propeller pitch, total thrust (including measured nozzle thrust), and the total power for the 8th and 9th self-propulsion tests.

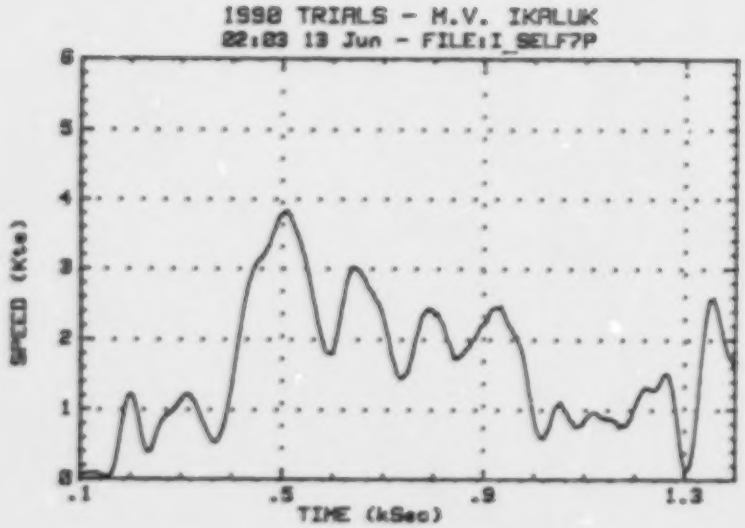

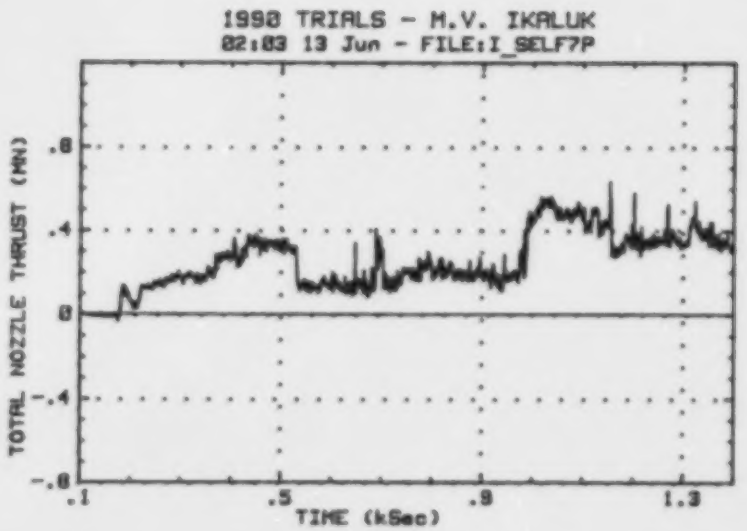

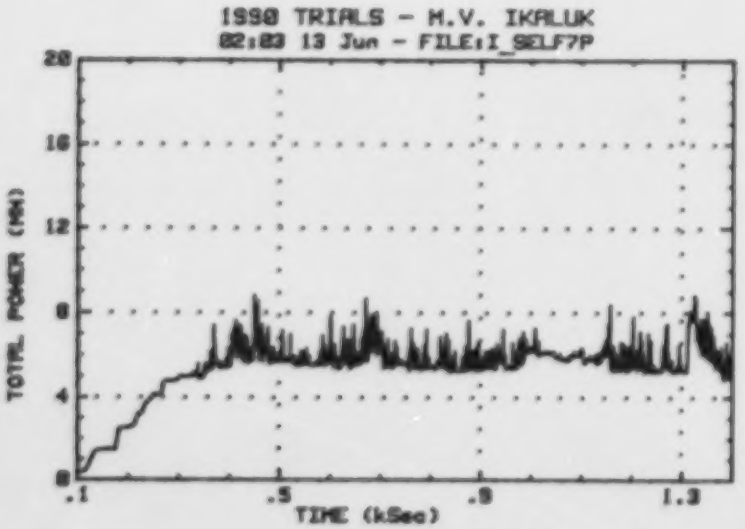

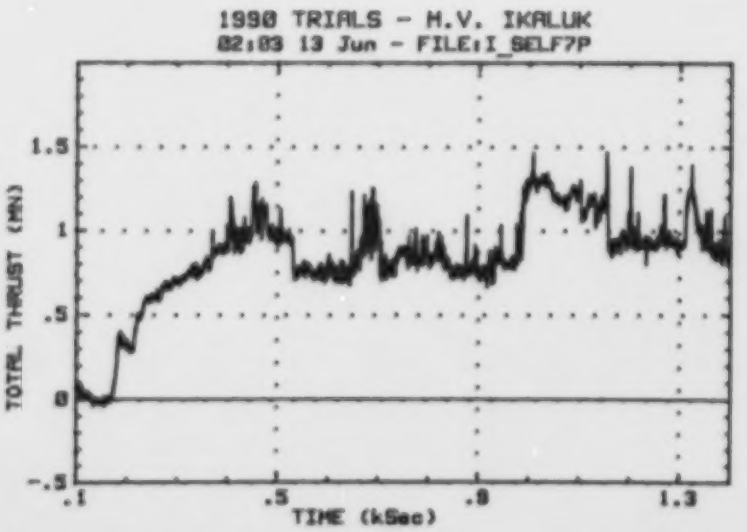

Figure 5.5.14 Ship Speed, Nozzle Thrust, Total Thrust, Total Power:

M.V. Ikaluk Self Propulsion Test 7

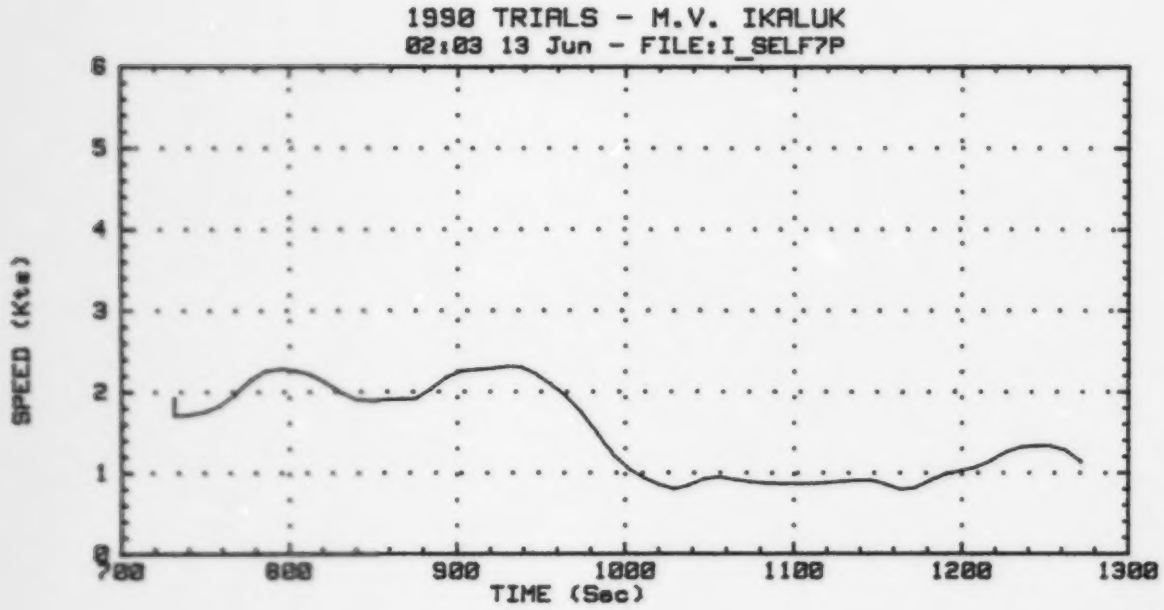

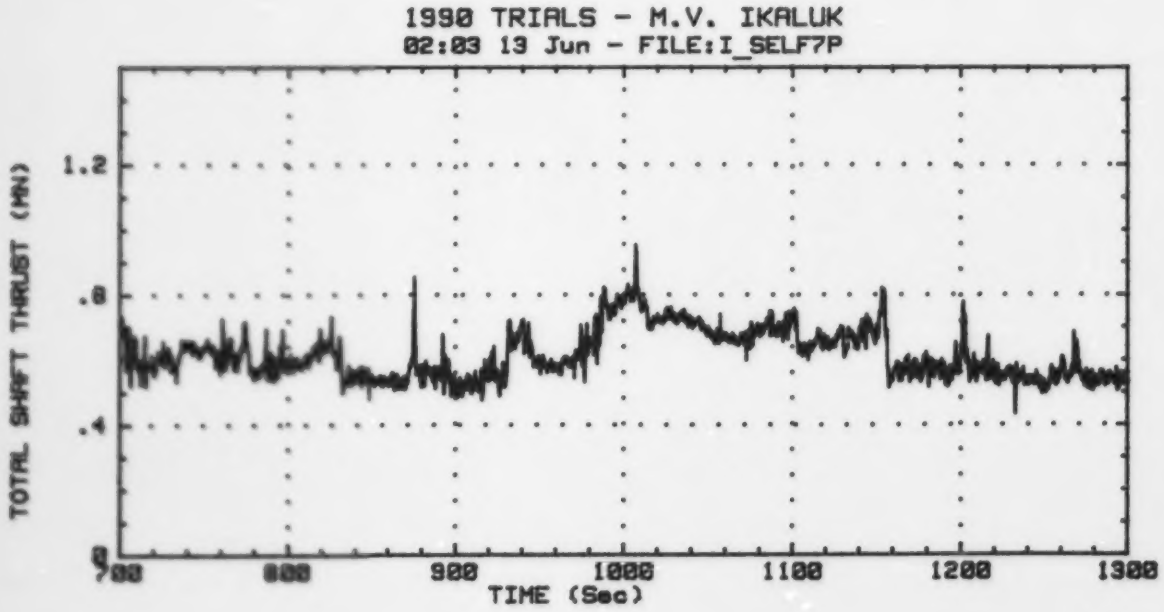

Figure 5.5.15 Ship Speed and Total Shaft Thrust: M.V. Ikaluk Self Propulsion Test 7

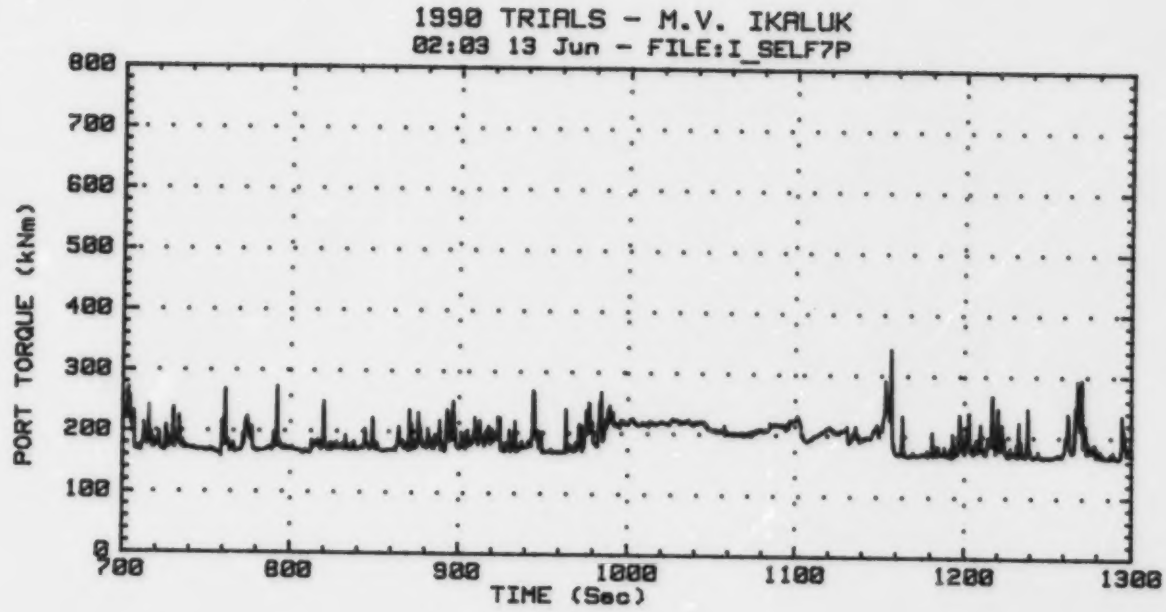

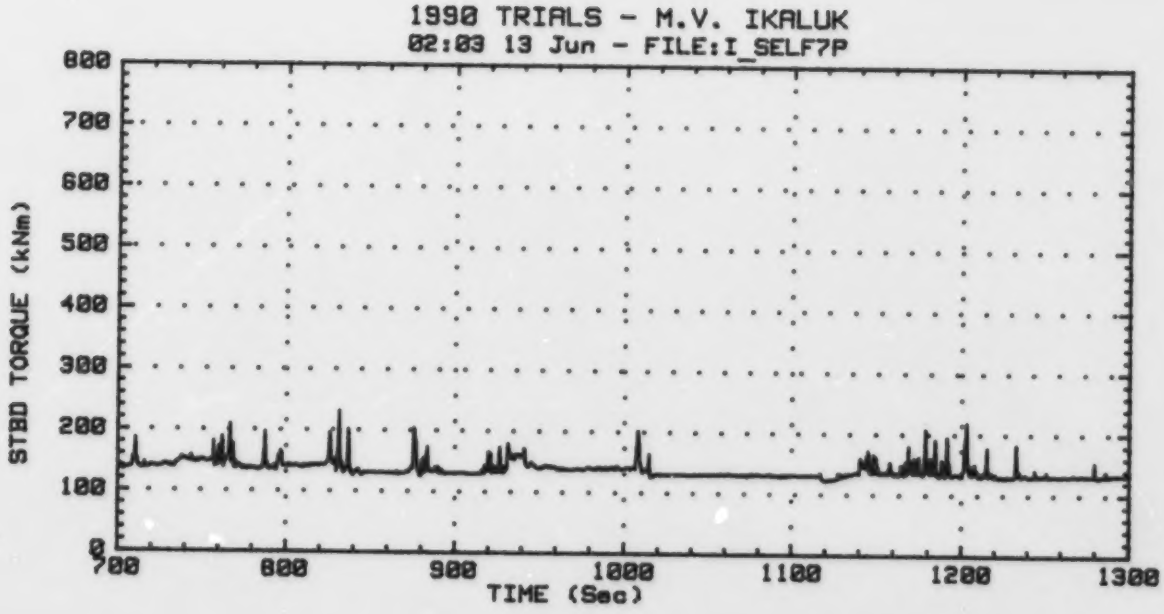

Figure 5.5.16 Port and Starboard Shaft Torque: M.V. Ikaluk Self Propulsion Test 7

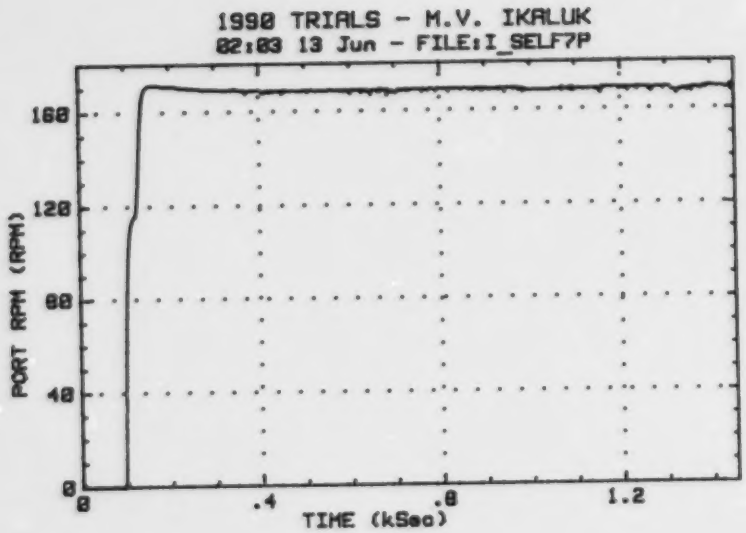

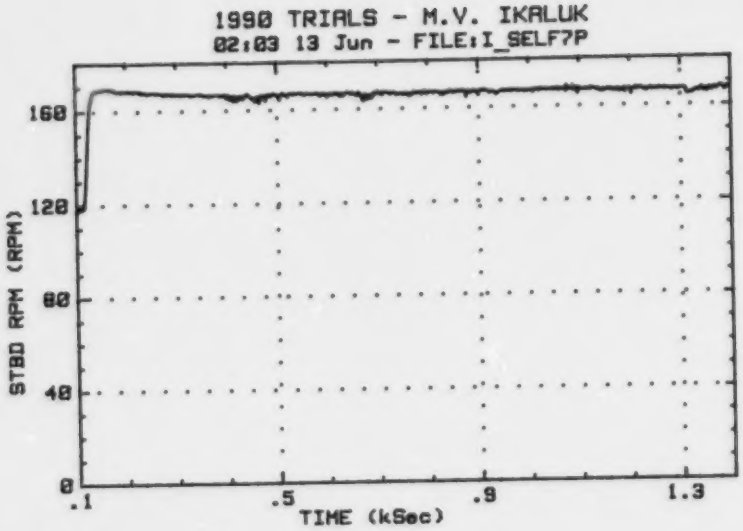

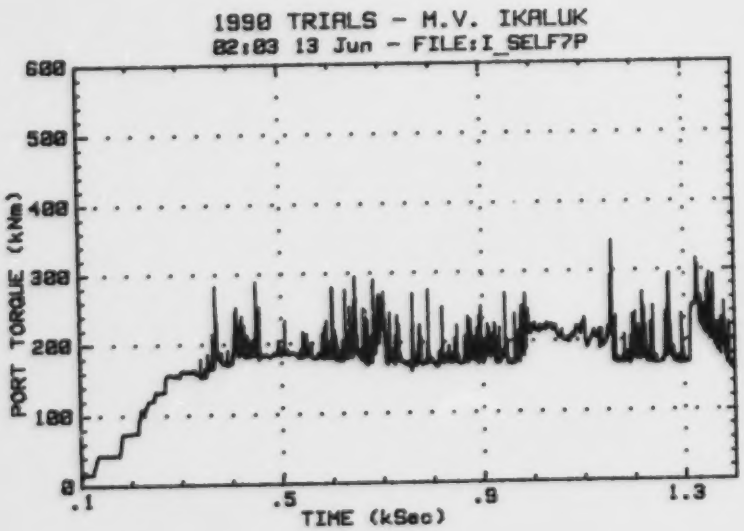

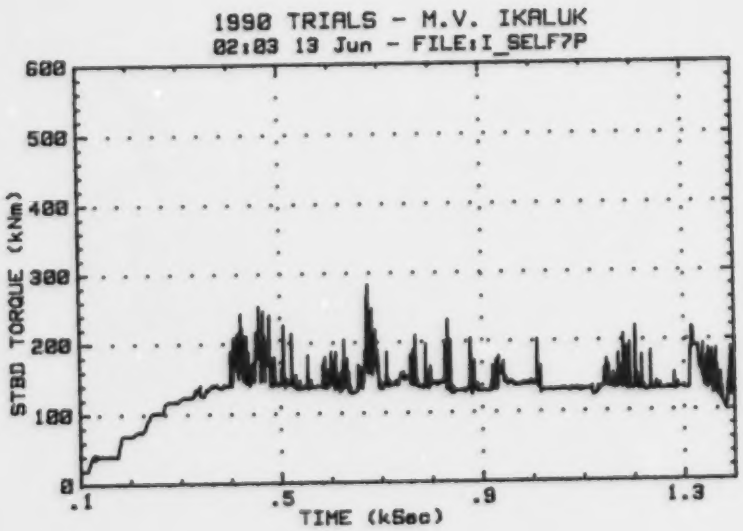

Figure 5.5.17 Port and Starboard Shaft Torque and RPM: M.V. Ikaluk Self Propulsion Test 7

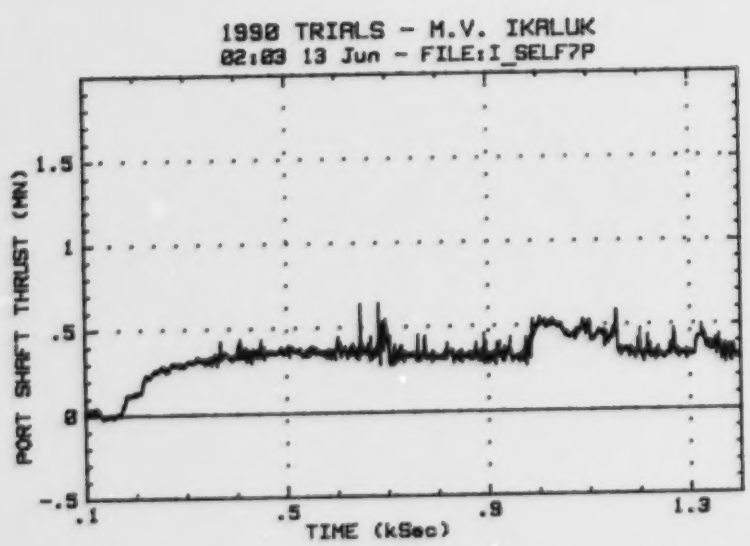

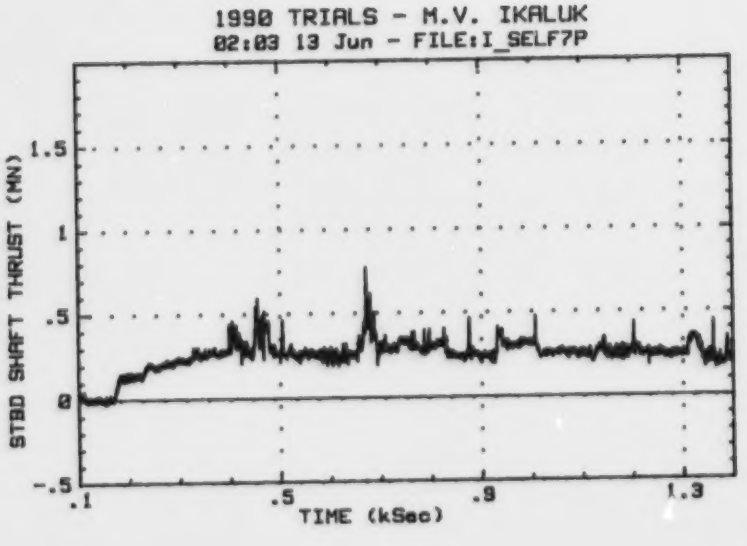

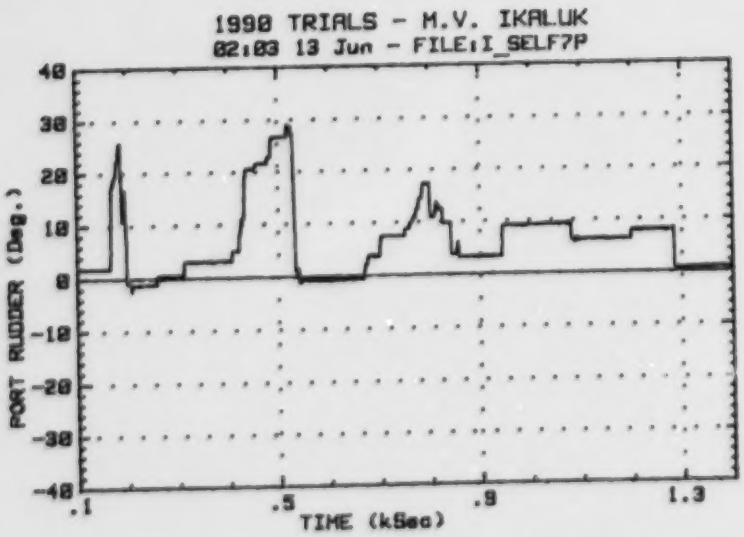

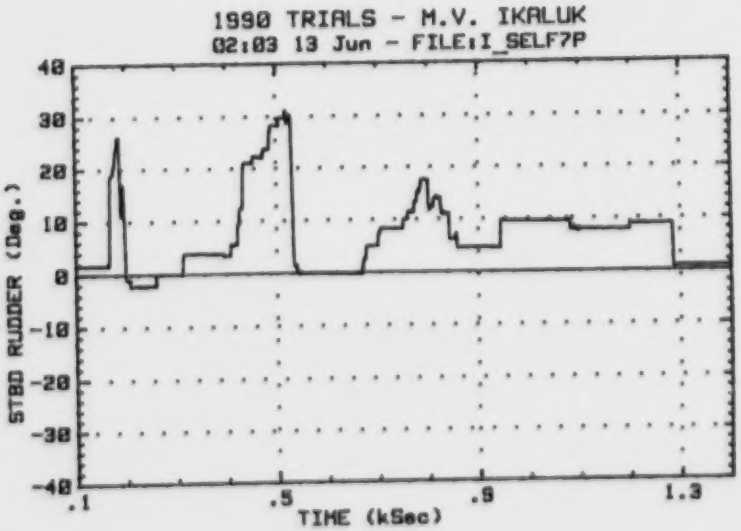

Figure 5.5.18 Port and Starboard Shaft Thrust and Rudder Angle:

M.V. Ikaluk Self Propulsion Test 7

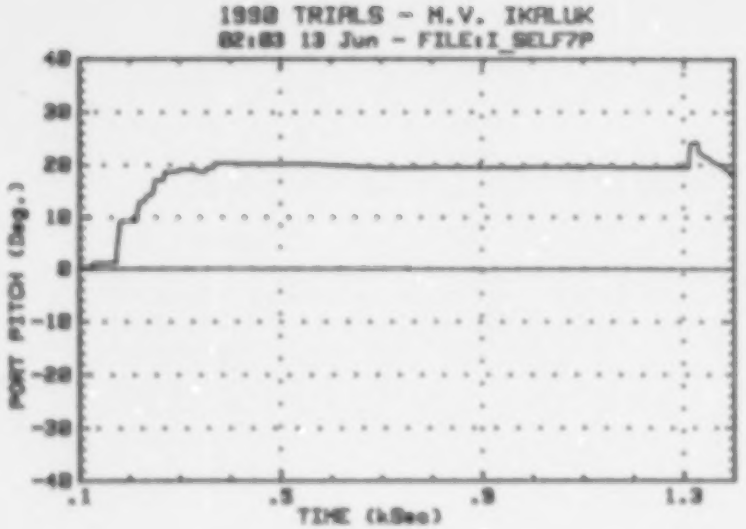

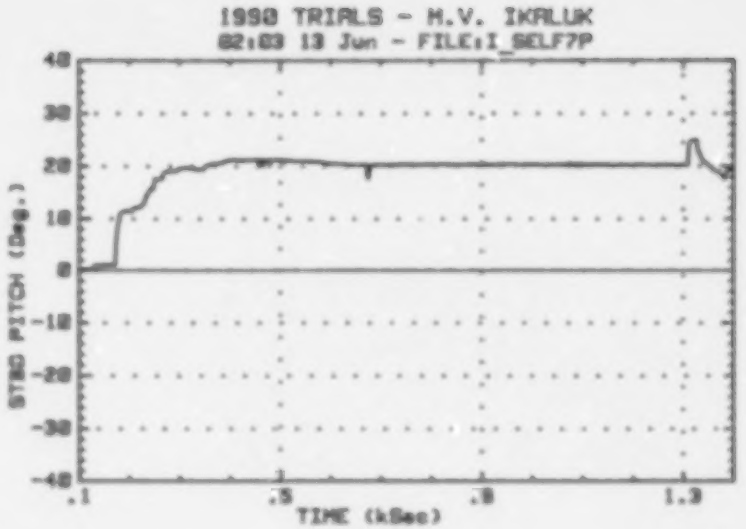

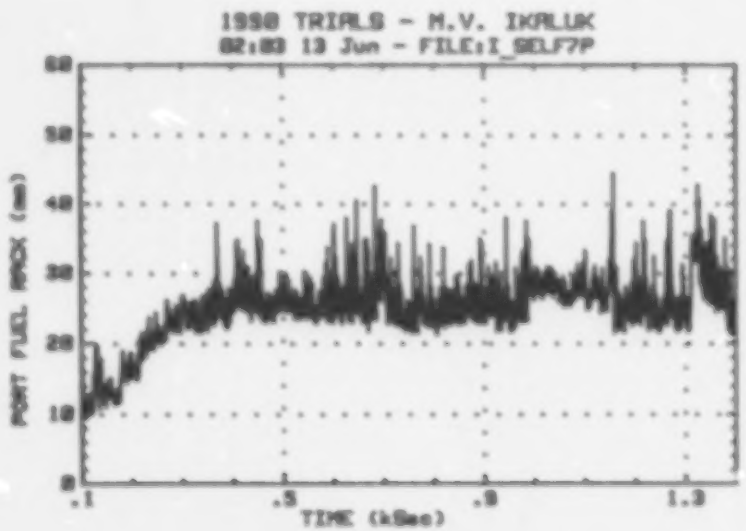

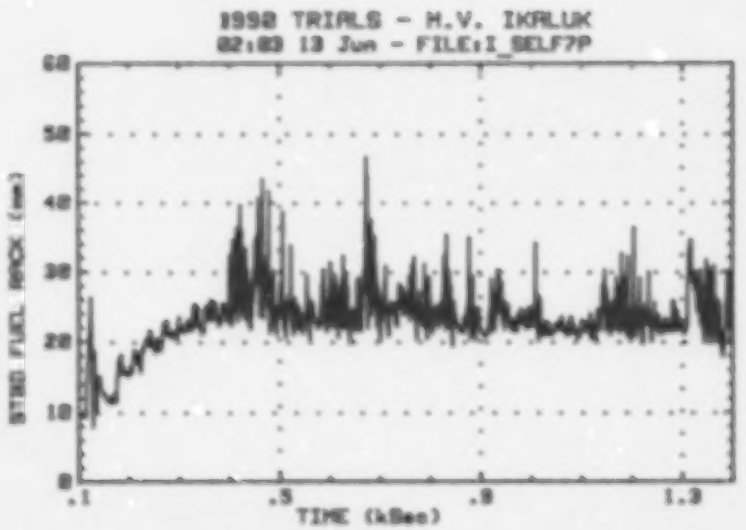

Figure 5.5.19 Port and Starb. Propeller Pitch and Engine Fuel Rack:

M.V. Ikaluk Self Propulsion Test 7

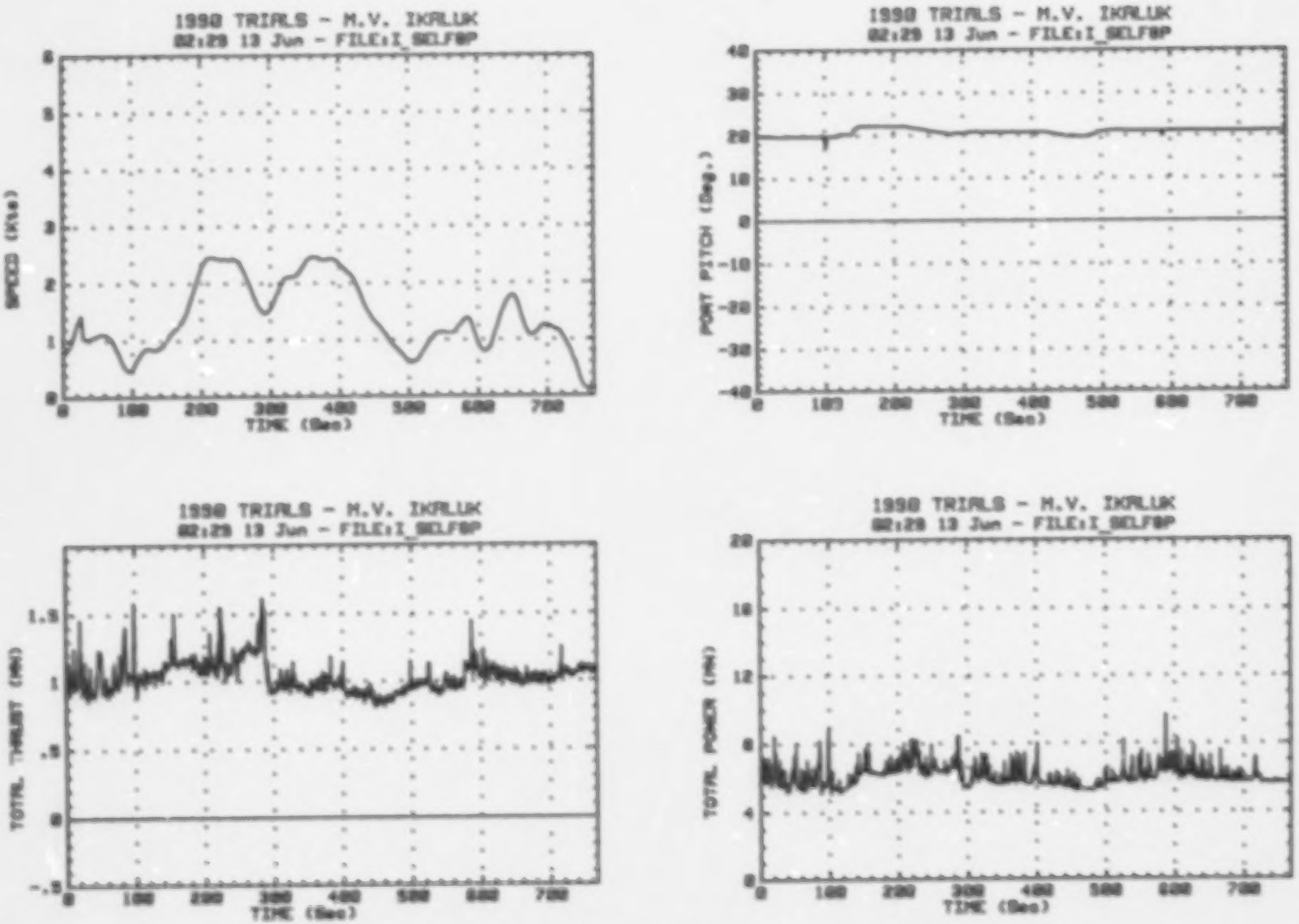

Figure 5.5.20 Ship Speed, Port Pitch, Total Power and Total Shaft Thrust:

M.V. Ikaluk Self Propulsion Test 8

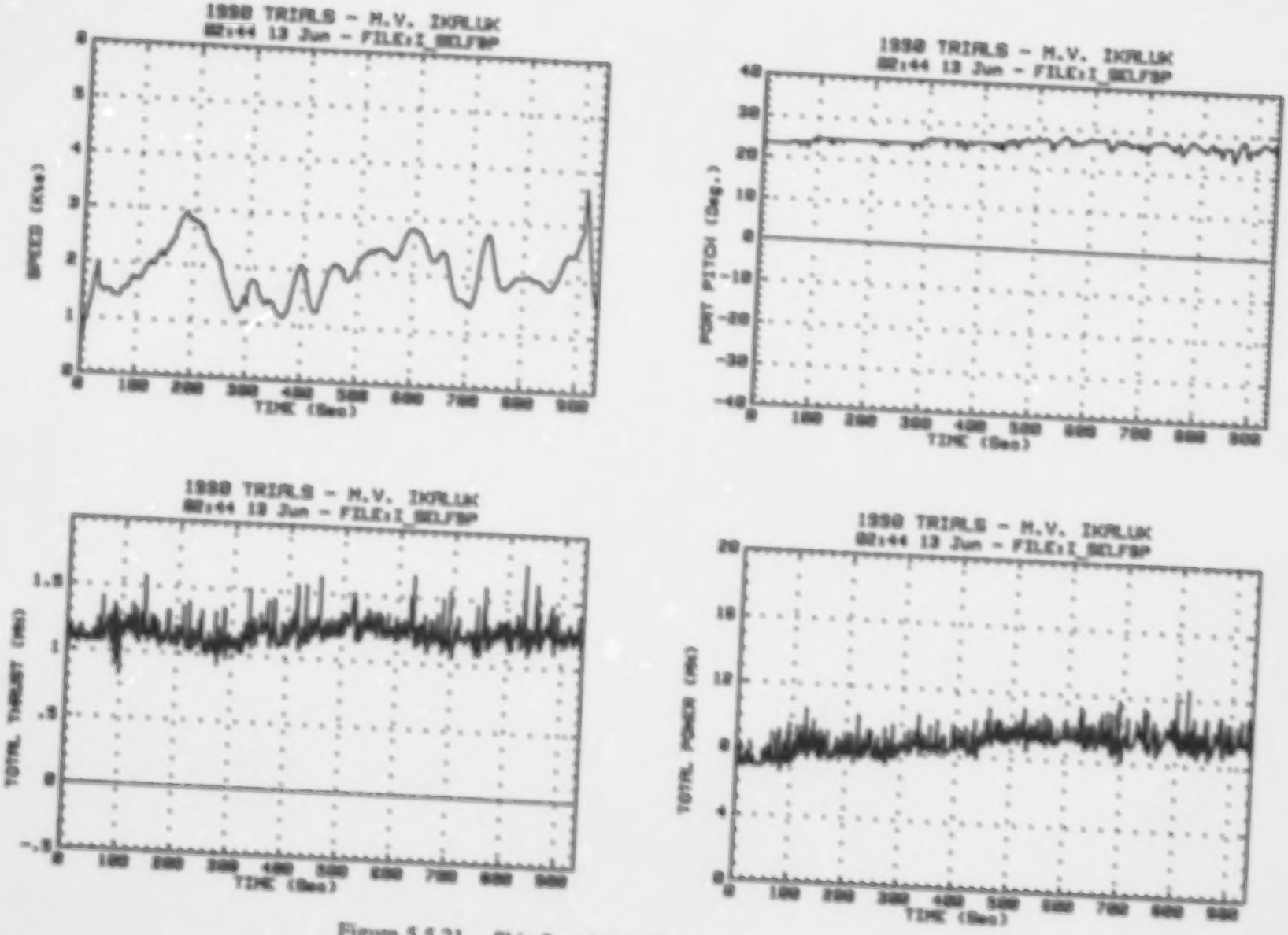

Figure 5.5.21 Ship Speed, Port Pitch, Total Power and Total Shaft Thrust: M.V. Ikaluk Self Propulsion Test 9

5.6 Open Water Overload Tests

This section details the analysis of the data collected during the open water overload trials. The trials were conducted at the end of the towing tests in the clear open water immediately north of the landfast ice. The vessel were positioned stern on stern so that one vessel could provide the required resistance (corresponding ice resistance). Section 4.0 details the test procedure.

Results from the M.V. Terry Fox Tests

Table 5.6.1 lists a summary of the results from open water overload tests on the M.V. Terry Fox, and Figure 5.6.1 is a plot of these results. A linear regression line was computed from the two sets of data points (towline and thrust). The thrust deduction was calculated by taking the difference between the thrust and the resistance values as computed by the linear regression equations. The thrust deduction fraction was computed by taking the ratio of the difference between the thrust and towline forces and the thrust force (see section 4.0 for details). The results are plotted in figures 5.6.2 and 5.6.3. A linear regression curve is also plotted through the computed values of thrust deduction. The thrust deduction varies from 0.05 MN at 1 knots to 0.32 MN at 3.5 knots. The thrust deduction fraction varies from 0.08 at 1 knot and approaches 0.25 asymptotically at 3.5 knots.

Figure 5.6.4 shows the ship speed and towline force time histories that were used to get the above results. The dashed line in the lower figure is the computed vessel resistance for the corresponding velocity in the upper figure (equation derived from towing trials - section 5.4). The solid line in the lower figure is the towline force from the open water overload tests. The measured shaft thrust and towline forces listed in Table 5.6.1 occurred at the same time when these two lines cross (ie. the towline force = the level ice resistance).

Figure 5.6.5 illustrates the vessel acceleration and total shaft thrust time histories for the open water overload tests. The acceleration is higher than that computed when towing the vessel in ice because of the difficulty in achieving a constant velocity. However, the inertial forces (computed by the multiplication of the acceleration by the 110% of the mass - as done before) do effect the results significantly.

Table 5.6.1 Open Water Overload Data Summary: M.V. Terry Fox

Test Id	Elapsed Time (sec)	Velocity (Knots)	Acc. (m/s^2)	FORCES			
				Towline (MN)	Shaft Thrust (MN)	Inertial (MN)	Net Thrust (MN)
OVER2	167.70	0.43	0.00	0.45	0.41	0.02	0.39
OVER2	349.10	1.70	0.01	0.64	0.91	0.05	0.86
OVER2	640.00	3.36	-0.02	0.93	1.11	-0.11	1.22
OVER2	842.10	2.99	0.02	0.89	1.23	0.12	1.11
OVER2	1041.00	2.82	-0.02	0.85	1.05	-0.11	1.16
OVER2	1133.00	1.38	0.00	0.60	0.72	0.01	0.70

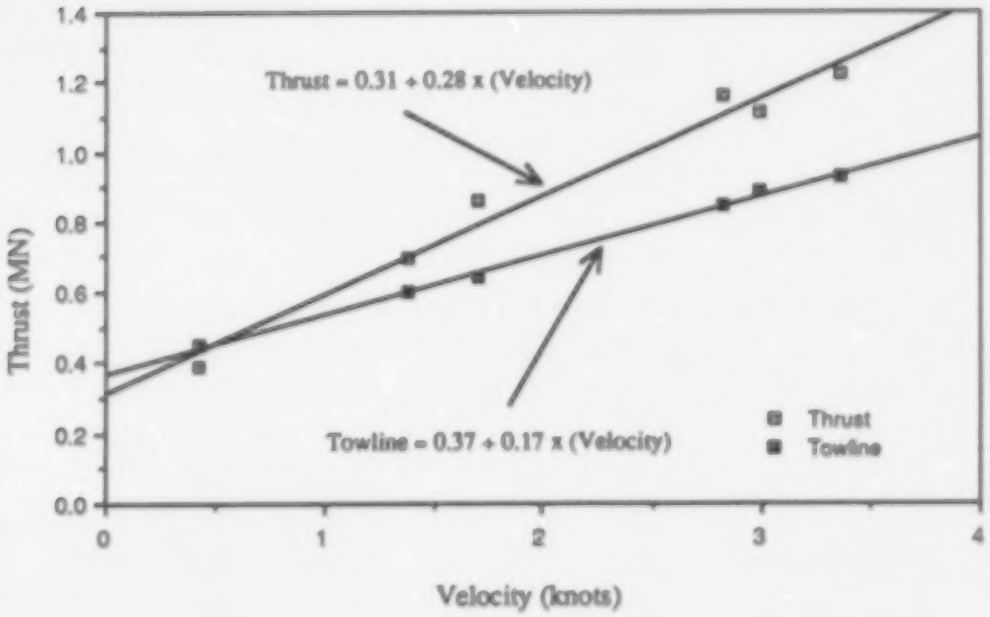

Figure 5.6.1 Open Water Overload Towline and Thrust: M.V. Terry Fox

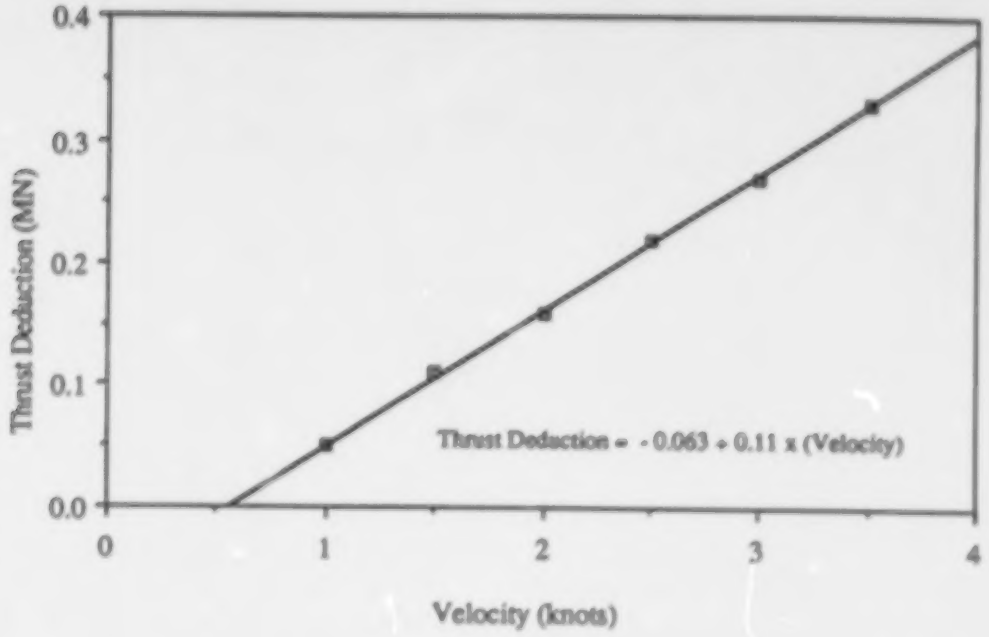

Figure 5.6.2 Open Water Overload Thrust Deduction : M.V. Terry Fox

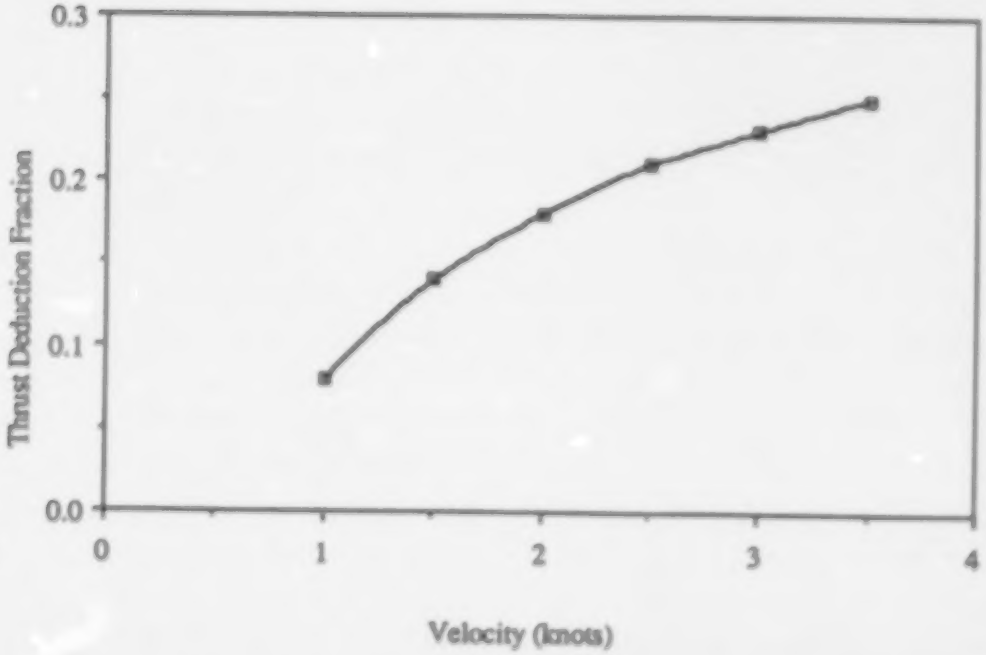

Figure 5.6.3 Open Water Overload Thrust Deduction Fraction: M.V. Terry Fox

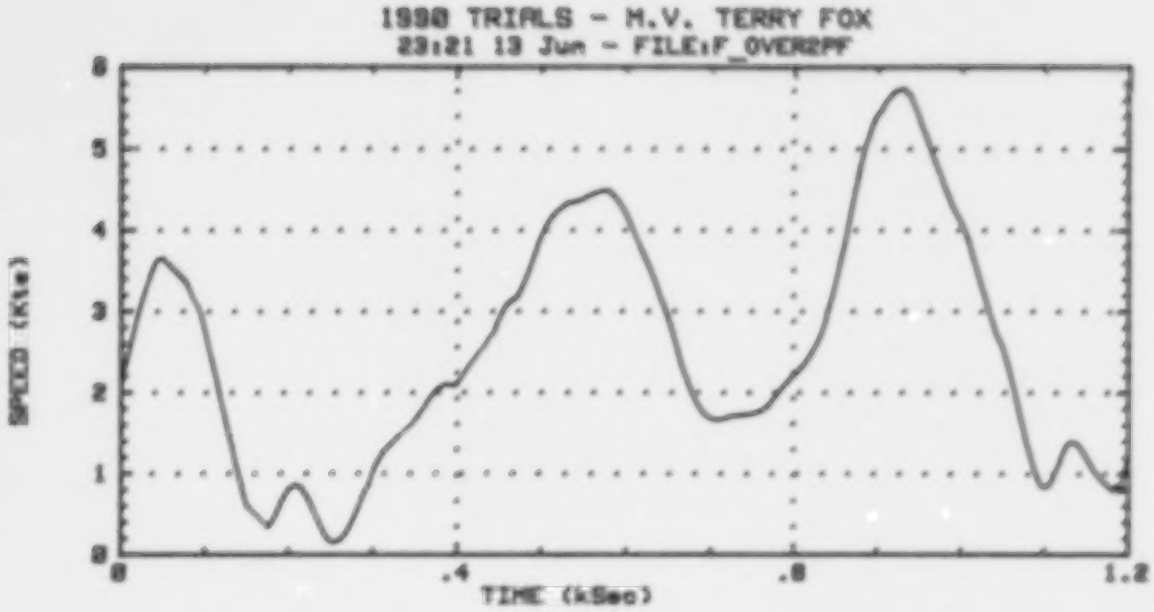

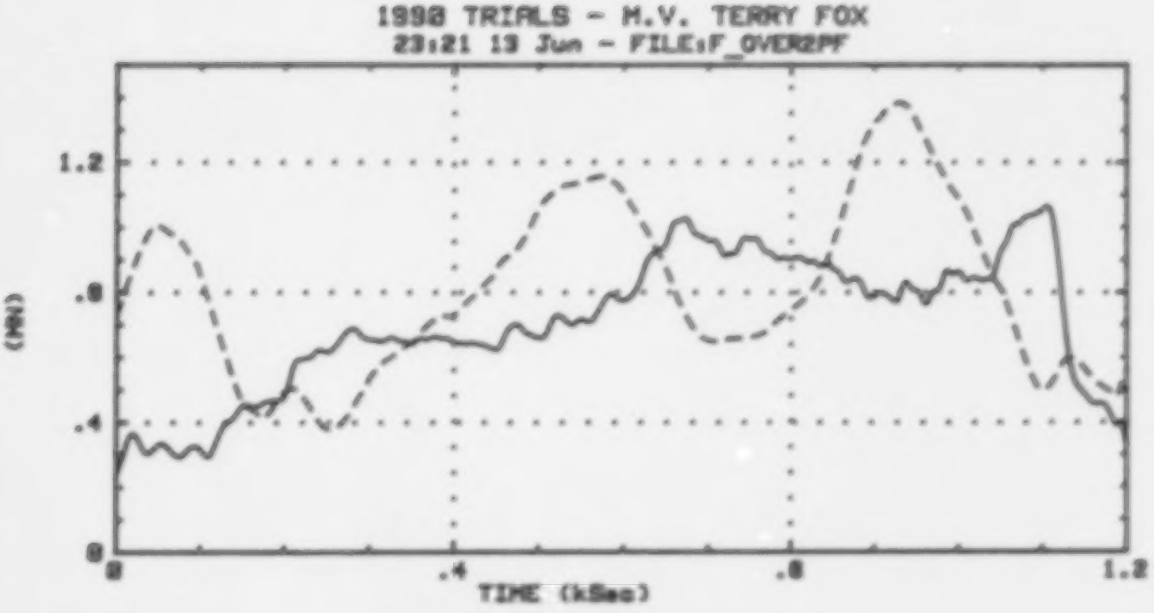

Figure 5.6.4 Towline Force and (Ice Resistance): M.V. Terry Fox O.W. Overload

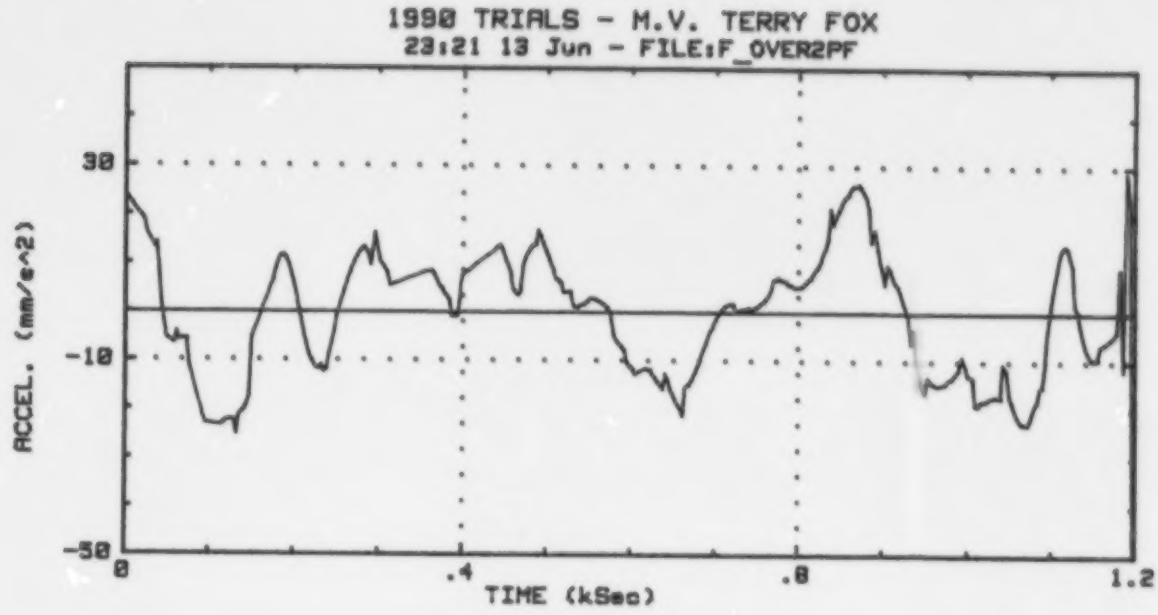

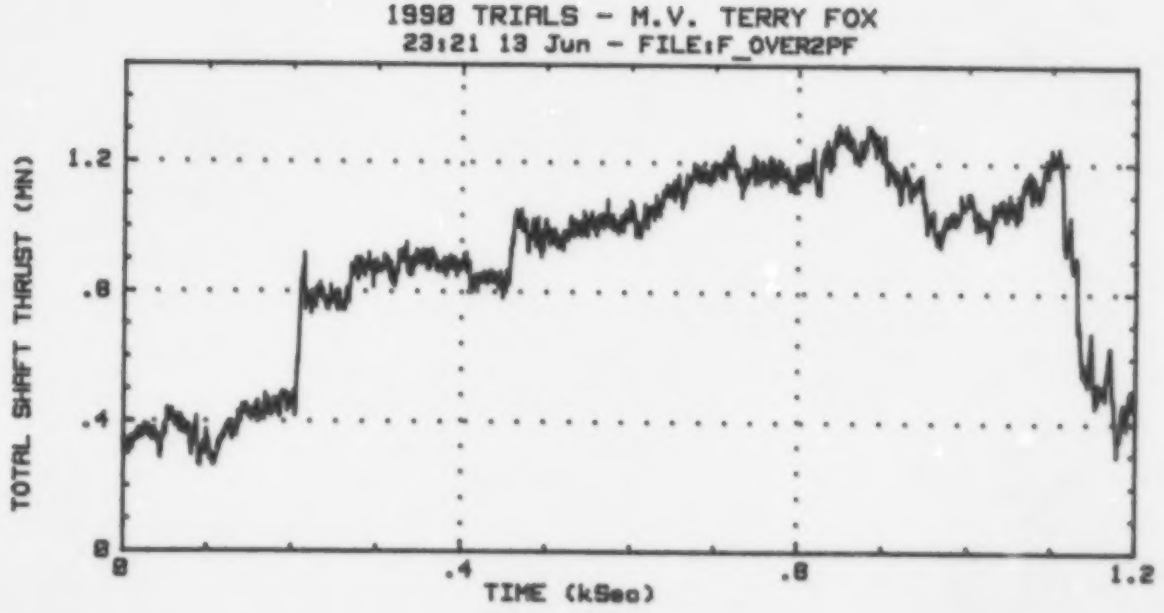

Figure 5.6.5 Ship Accleration and Total Shaft Thrust: M.V. Terry Fox O.W. Overload

Results from the M.V. Ikaluk Tests

Table 5.6.2 lists a summary of the results from open water overload tests on the M.V. Ikaluk, and Figure 5.6.6 is a plot of these results. A linear regression line was computed from the two sets of data points (towline and thrust). The thrust deduction was calculated by taking the difference between the shaft thrust and the resistance values as computed by the linear regression equations. The thrust contribution of the nozzle was not accounted for because of the inaccuracies in the measurement and analytical calculations. Therefore, any comparison with model should take this into account. The thrust deduction fraction was computed by taking the ratio of the difference between the shaft thrust and towline forces and the shaft thrust (see section 4.0 for details). The results are plotted in figures 5.6.7 and 5.6.8. A linear regression curve is also plotted through the computed values of thrust deduction. The thrust deduction is relatively low and varies from 0.02 MN at 1.0 knots to 0.04 MN at 3.0 knots. The thrust deduction fraction is very small and only increases from 0.022 at 0.5 knots to 0.042 at 3 knots. This low figure indicates that the thrust deduction for the M.V. Ikaluk in the open water overload condition is approximately equal to the thrust contribution of the nozzle.

Figure 5.6.9 shows the ship speed and towline force time histories that were used to get the above results. The dashed line in the lower figure is the computed vessel resistance for the corresponding velocity in the upper figure (equation derived from towing trials - section 5.4). The solid line in the lower figure is the towline force from the open water overload tests. The measured shaft thrust and towline forces listed in Table 5.6.2 occurred at the same time when these two lines cross (ie. the towline force = the level ice resistance).

Figure 5.6.10 illustrates the vessel acceleration and total shaft thrust time histories for the open water overload tests. The acceleration is relatively low and therefore, the computed inertial forces did not effect the result significantly.

Table 5.6.2 Open Water Overload Data Summary: M.V. Ikaluk

Test Id	Elapsed Time (sec)	Velocity (Knots)	Acceleration (m/s^2)	FORCES			
				Towline (MN)	Shaft Thrust (MN)	Inertial (MN)	Net Thrust (MN)
2P	160.0	1.4	0.0030	0.67	0.72	0.0195	0.70
2P	324.4	2.5	0.0030	0.76	0.82	0.0195	0.80
2P	613.0	2.4	-0.0024	0.76	0.79	-0.0156	0.81

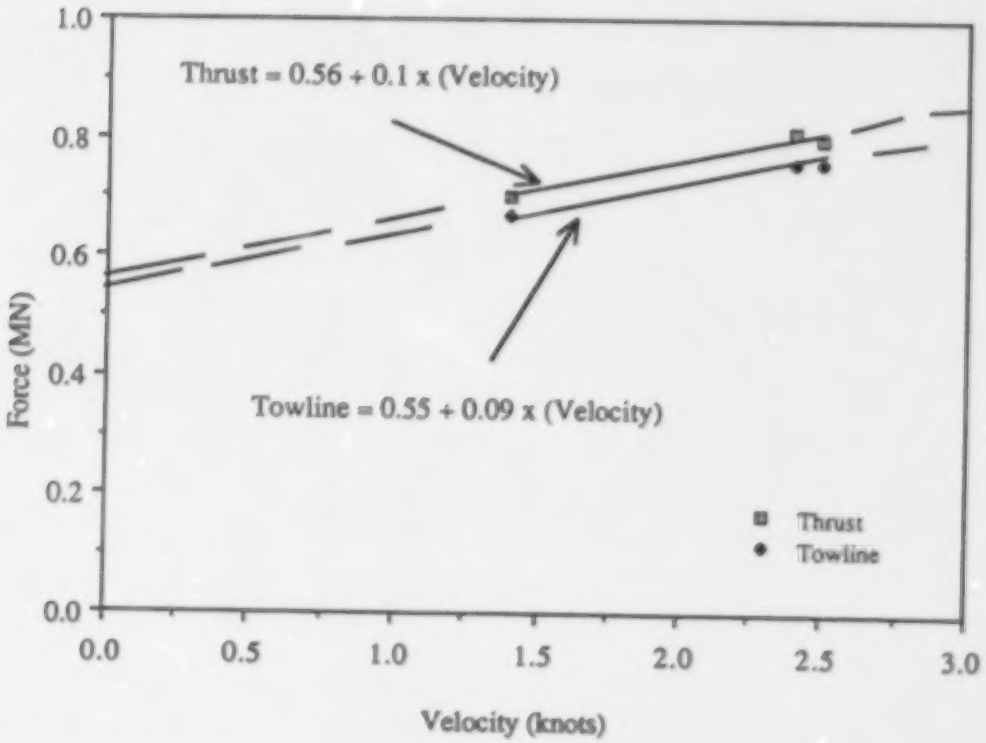

Figure 5.6.6 Open Water Overload Thrust and Towline: M.V. Ikaluk

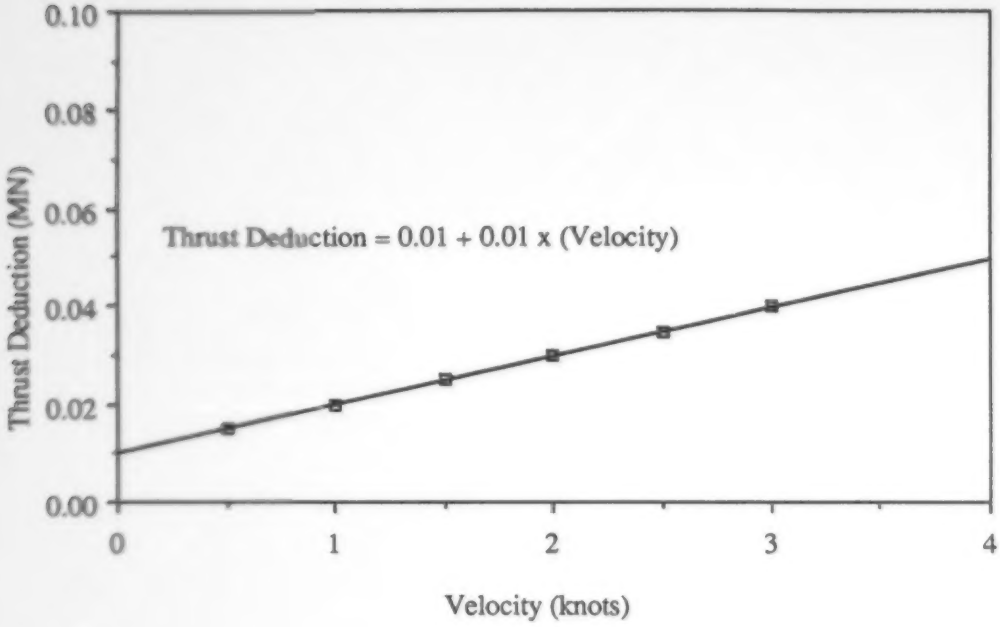

Figure 5.6.7 Open Water Overload Thrust Deduction: M.V. Ikaluk

(Nozzle Thrust not Included)

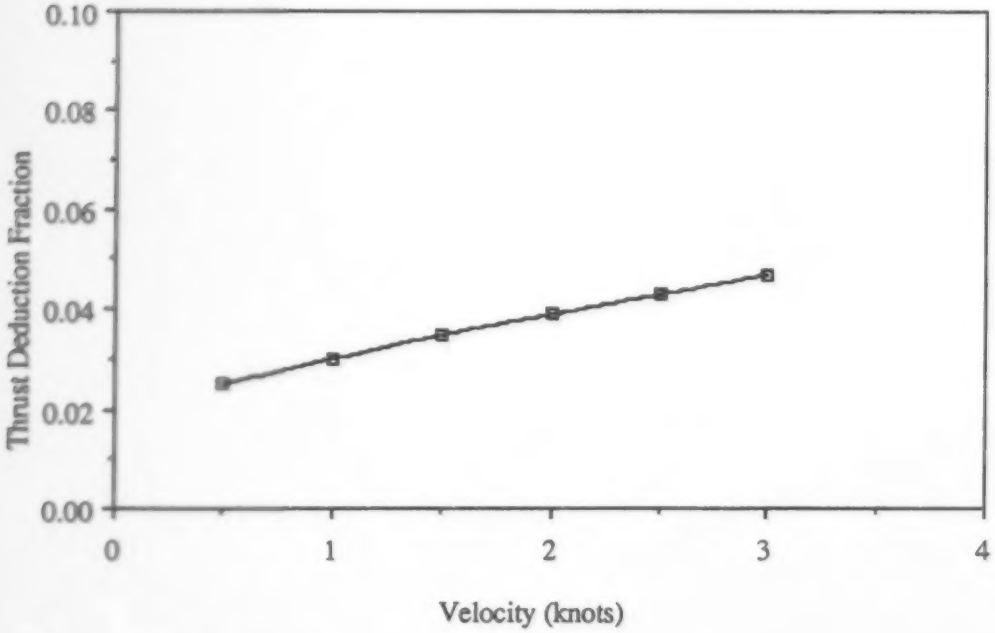

Figure 5.6.8 Open Water Thrust Deduction Fraction: M.V. Ikaluk

(Nozzle Thrust not Included)

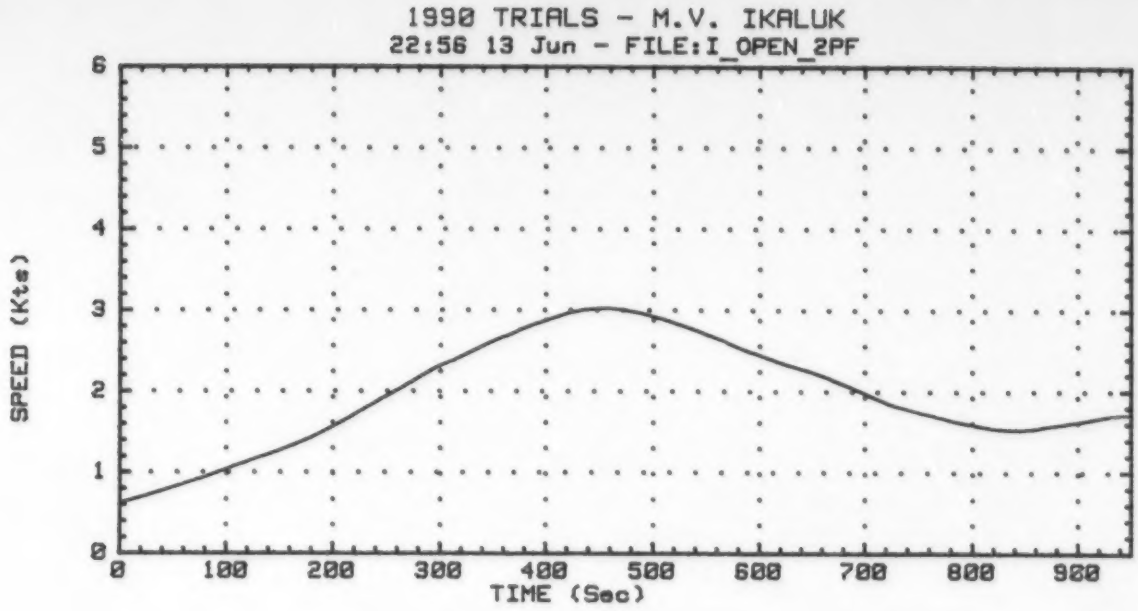

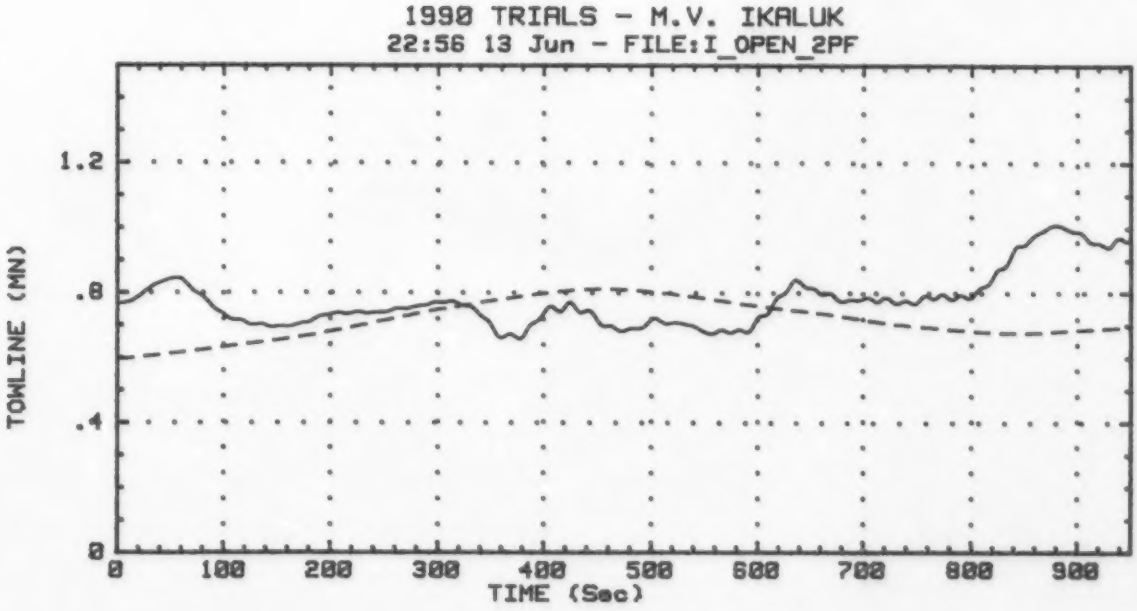

Figure 5.6.9 Towline Force and (Ice Resistance): M.V. Ikaluk O.W. Overload

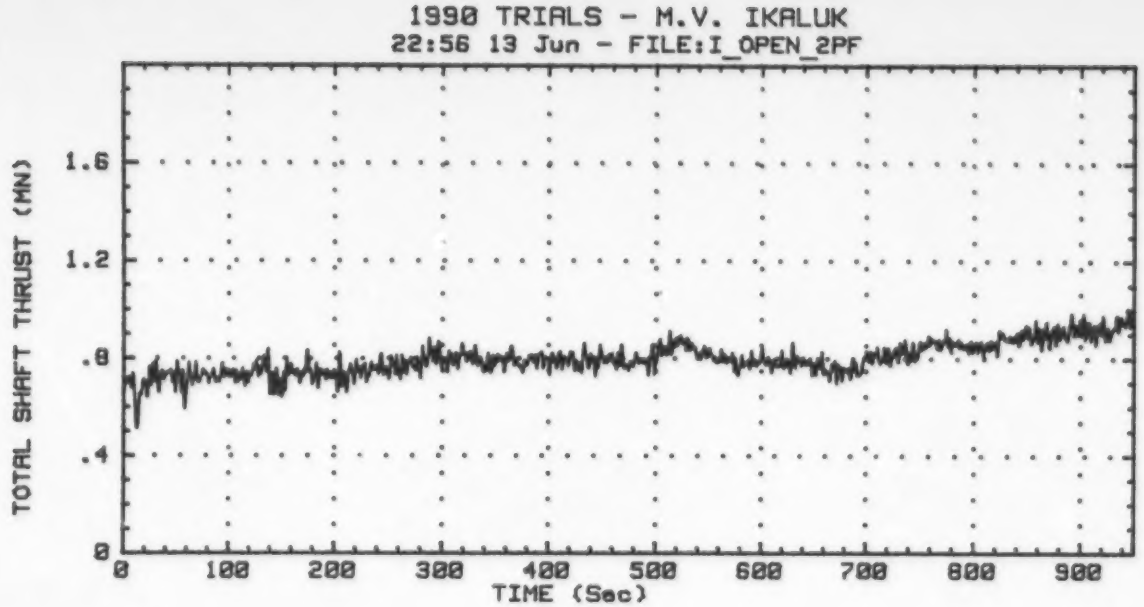

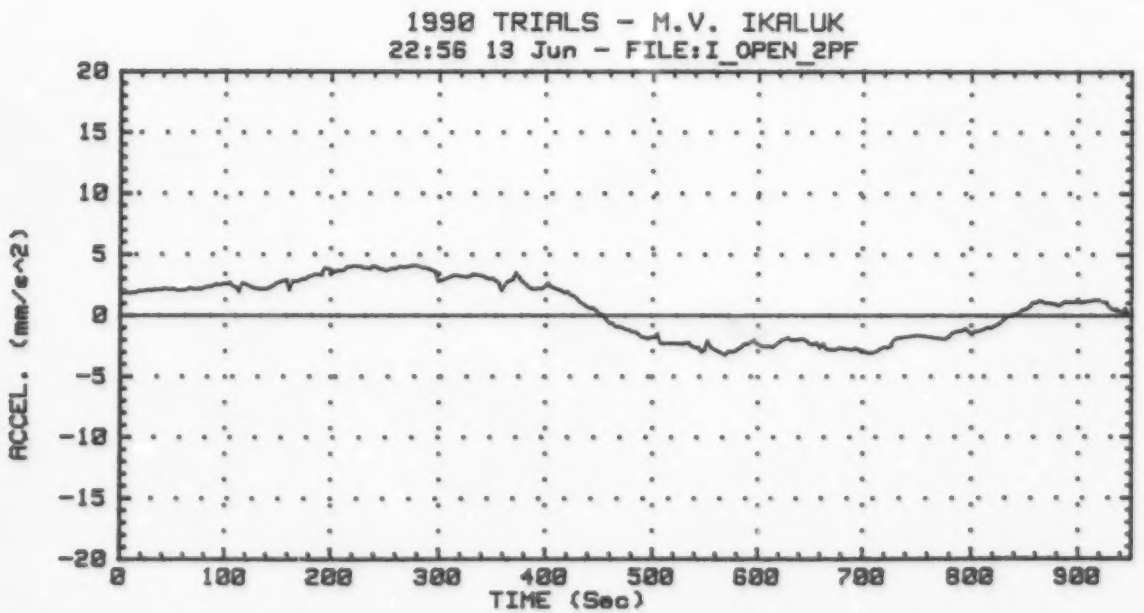

Figure 5.6.10 Ship Accleration and Total Shaft Thrust: M.V. Ikaluk O.W. Overload

5.7 Thrust Deduction Fractions

This section illustrates the results of the thrust deduction computations. The results of the towing and the self-propulsion tests in the level ice are combined to produce the thrust deduction (thrust-resistance) and thrust deduction fraction {(thrust-resistance)/thrust} (see section 4.1). The open water overload thrust deductions and thrust deduction fractions are also presented alongside the corresponding values in ice.

Figures 5.7.1 - 5.7.3 illustrate the primary results of the trials done on the M.V. Terry Fox. In Figure 5.7.1 the self-propulsion thrust and resistance are plotted together against velocity. Linear regression curves are plotted through the data points, and the equations are displayed on the figure. Figure 5.7.2 and 5.7.3 illustrate the thrust deduction and thrust deduction fraction versus velocity relationship. These curves are computed by using the the linear regression equations. The thrust deduction is close to zero at velocities less than 0.5 knots and increases linearly to 0.32 MN (32 tonnes) at 3.5 knots. The corresponding thrust deduction fraction approaches 0.25 asymptotically at 3.5 knots from 0.05 at 0.5 knots.

Figure 5.7.4 and 5.7.5 are plots of the thrust deduction and thrust deduction fractions for the open water overload and the level icebreaking trials. In both figures the open water overload is approximately the same as the icebreaking above 2 knots. The difference in the thrust deduction fraction increases slightly at lower speeds; however, the value is the difference between two relatively small numbers and can be attributed in part to the inaccuracies inherent in the measurement system. This result can prove to be very useful for the scaling of model test data of icebreakers, because the thrust deduction fraction in ice may be equated to that in the open water overload condition. In essence the thrust deduction is more a function of the overloaded condition of the propeller (ie. rpm, local speed) than it is dependent on the presence of ice cover.

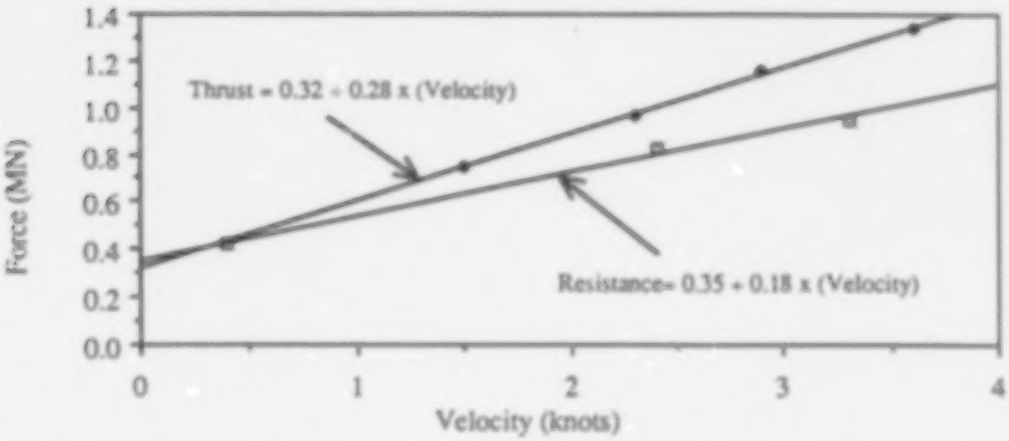

Figure 5.7.1 Resistance and Thrust in Ice: M.V. Terry Fox

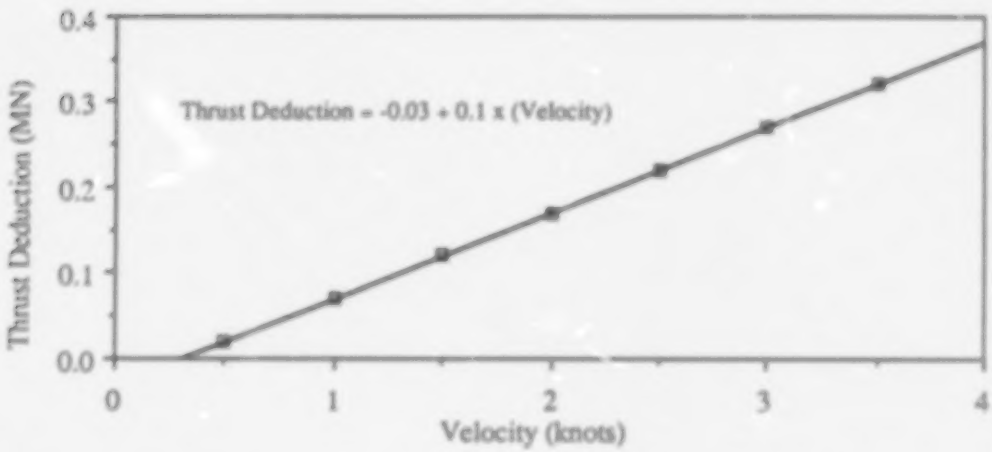

Figure 5.7.2 Thrust Deduction in Ice: M.V. Terry Fox

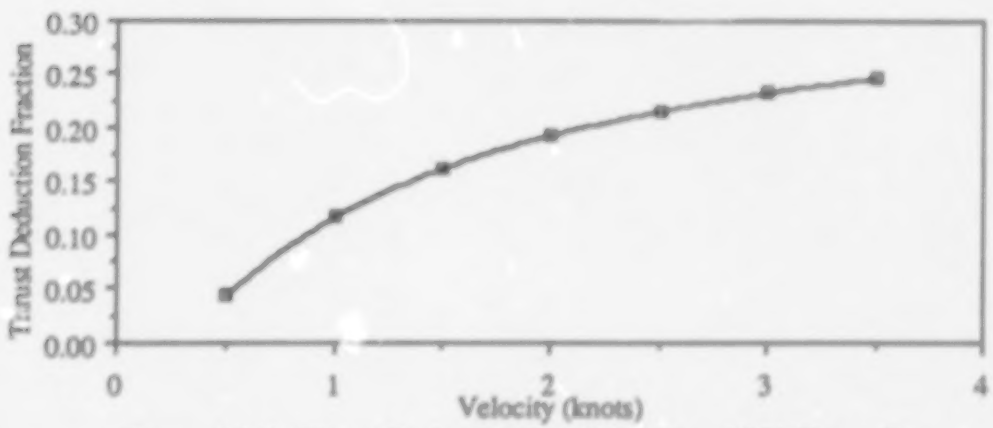

Figure 5.7.3 Thrust Deduction Fraction in Ice: M.V. Terry Fox

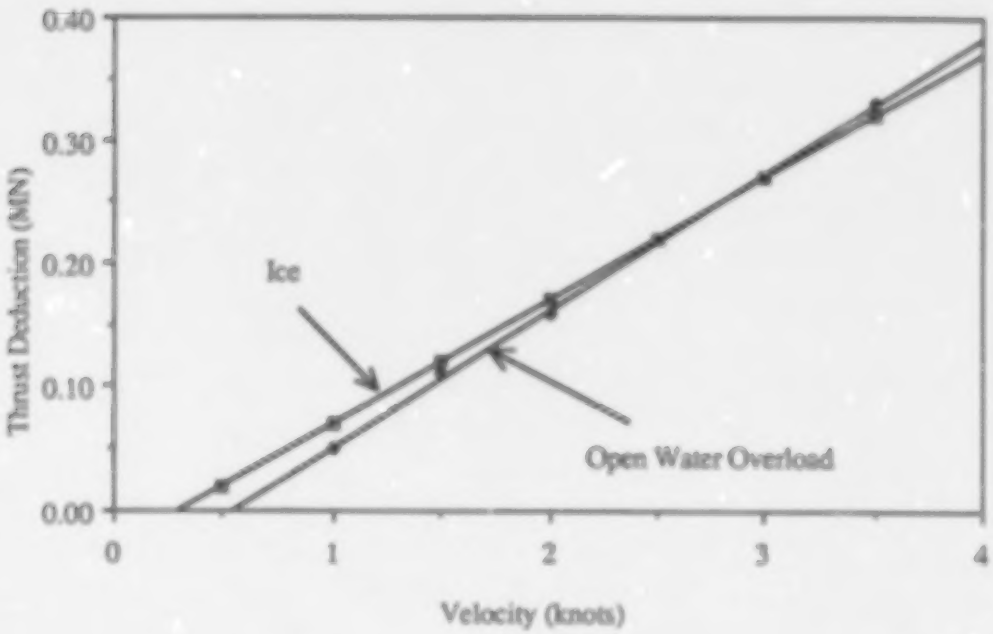

Figure 5.7.4 Thrust Deductions: M.V. Terry Fox
(Open Water Overload and Ice)

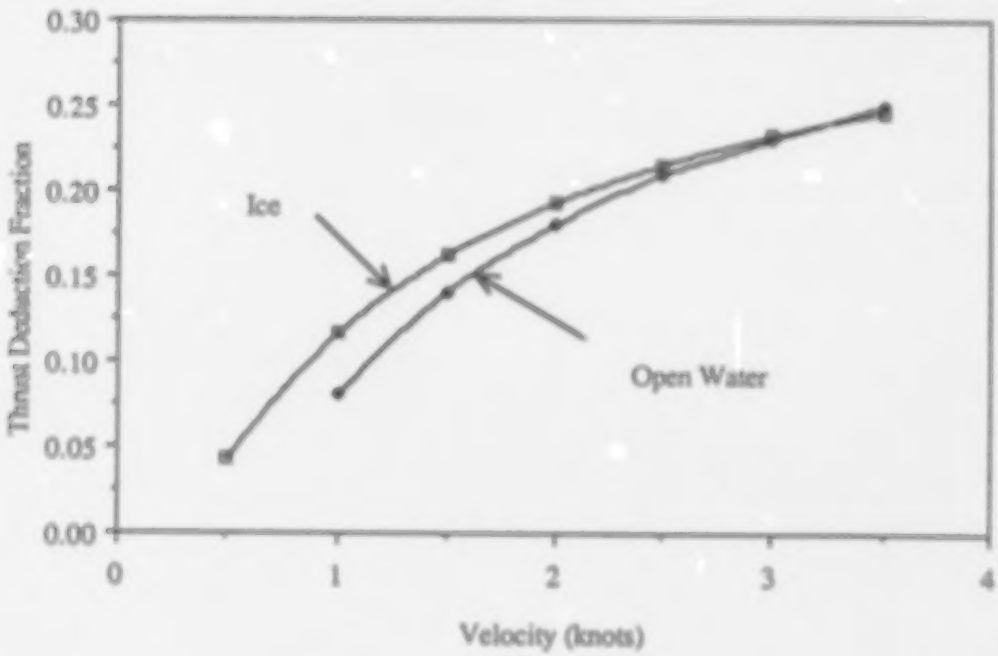

Figure 5.7.5 Thrust Deduction Fractions: M.V. Terry Fox
(Open Water Overload and Ice Breaking)

Figures 5.7.6 - 5.7.8 illustrate the primary results of the trials done on the M.V. Ikaluk. In Figure 5.7.6 the self-propulsion thrust and resistance are plotted together against velocity. Linear regression curves are plotted through the data points, and the equations are displayed on the figure. Figure 5.7.7 and 5.7.8 illustrate the thrust deduction and thrust deduction fraction versus velocity relationship. These curves are computed by using the the linear regression equations. The thrust deduction is zero at a 0.0 knots and increases linearly to 0.23 MN (23 tonnes) at 3.5 knots. The corresponding thrust deduction fraction approaches 0.22 asymptotically at 3.5 knots from 0.05 at 0.5 knots.

Figure 5.7.9 and 5.7.10 are plots of the thrust deduction and thrust deduction fractions for the open water overload and the level icebreaking trials. In both figures the ice condition is much higher than the open water overload, which was not the case for the M.V. Terry Fox. However, the thrust deduction in the open water condition is very low on the M.V. Ikaluk relative to the M.V. Terry Fox. The nozzle thrust is not included in the thrust deduction calculations, due to inaccuracies in the measurement and analytical calculations. Theoretically the nozzle can provide up to 50% of the shaft thrust at bollard conditions. Therefore, if the nozzle thrust was included, the thrust deduction calculations for the M.V. Ikaluk would be considerably higher, and nearer the range of the M.V. Terry Fox for the open water overload condition To accurately measure the nozzle thrust contribution (particularly in ice) of the M.V. Ikaluk the instrumentation would have to be as comprehensive as that installed by in the spring of 1989.

Further work on the comparison of this data along with model data and free running data is warranted but is beyond the scope of this project, and is recommended in future studies.

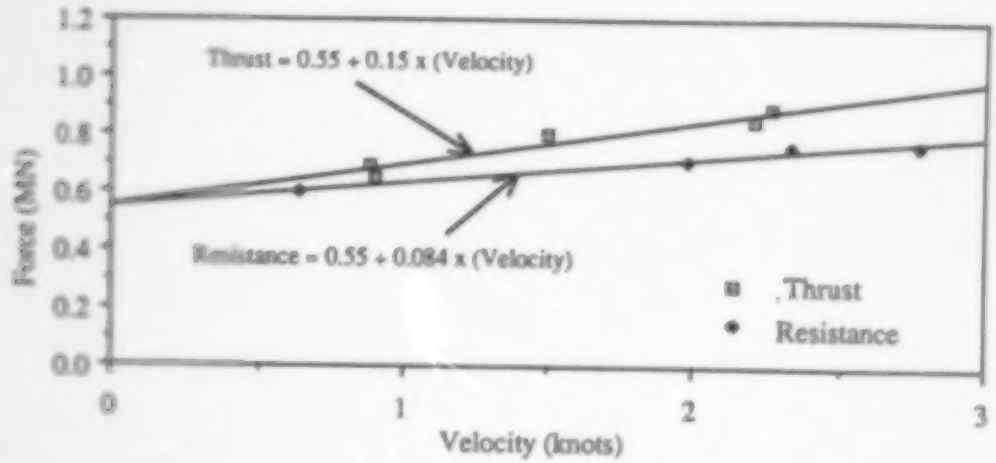

Figure 5.7.6 Resistance and Thrust in Ice: M.V. Ikaluk

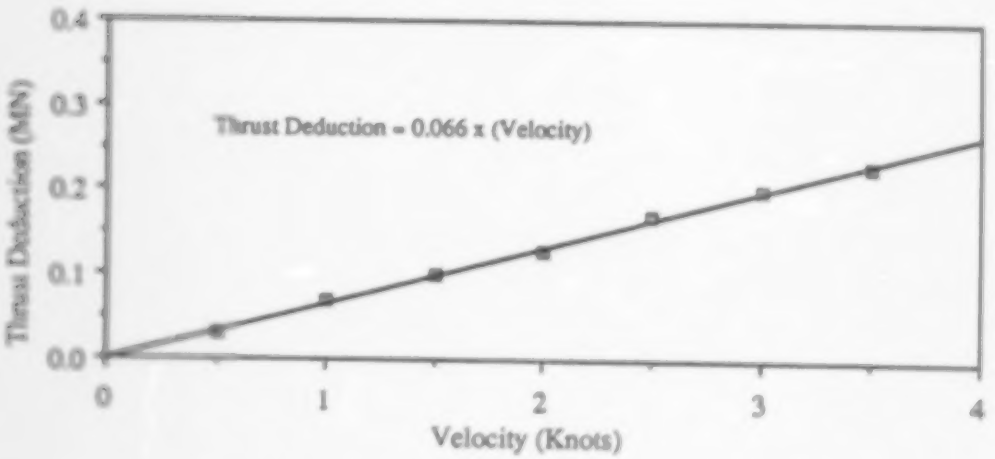

Figure 5.7.7 Thrust Deduction in Ice: M.V. Ikaluk

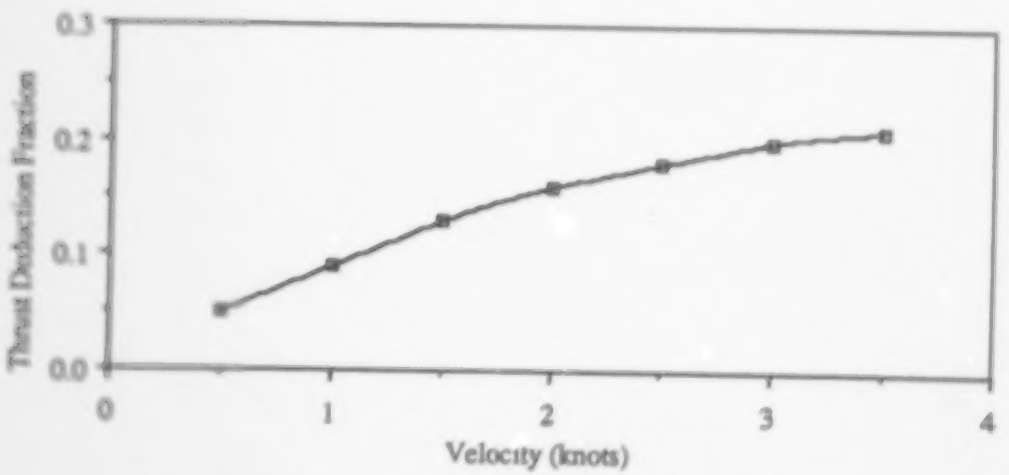

Figure 5.7.8 Thrust Deduction Fraction in Ice: M.V. Ikaluk

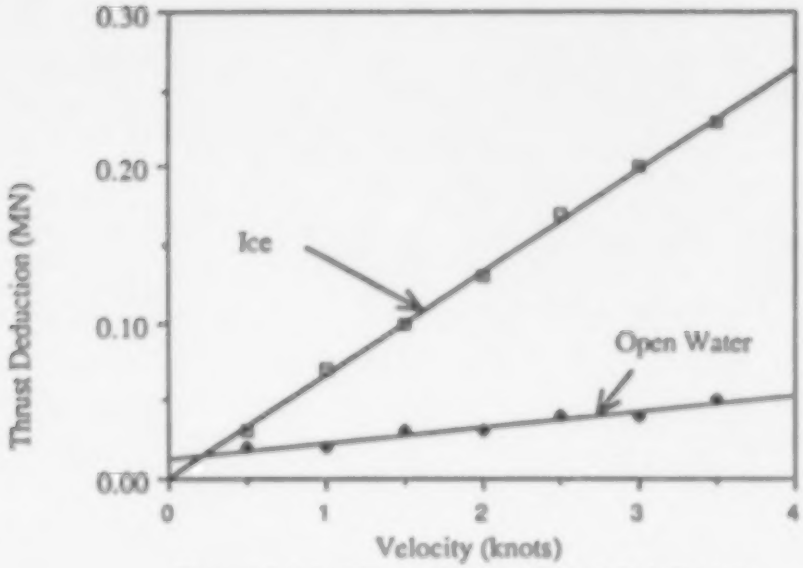

Figure 5.7.9 Thrust Deductions: M.V. Ikaluk
(Nozzle Thrust not Included)

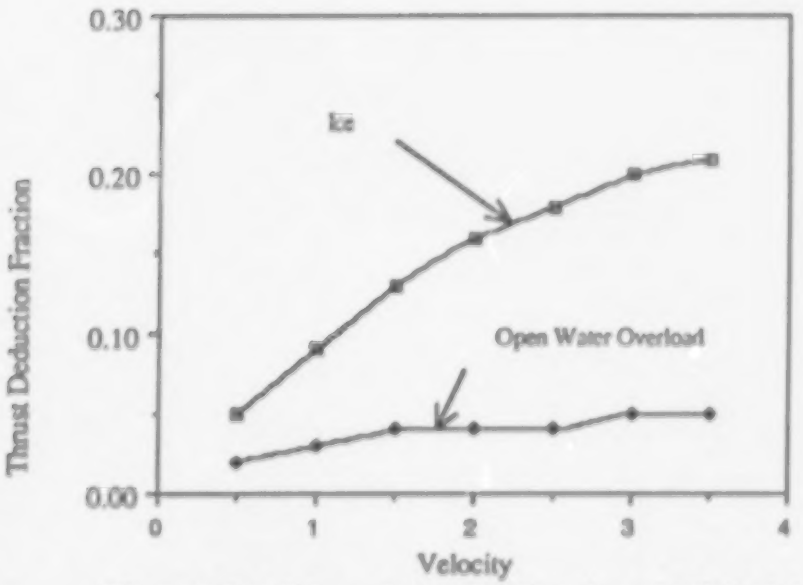

Figure 5.7.10 Thrust Deduction Fractions: M.V. Ikaluk
(Nozzle Thrust not Included)

5.8 Shaftline Response to Ice/Propeller Interaction

Summary

Table 5.8.1. lists a summary of the results from the shaftline response analysis.

Table 5.8.1 Summary of Shaftline Response Analysis

	M.V. Ikaluk	M.V. Terry Fox
Loads:		
Max. Shaft Torque	478 kNm	776 kNm
Max. Dynamic (Ice) Torque	170 kNm	275 kNm
MCR Shaft Torque	317 kNm	595 kNm
Maximum Shaft Thrust	1,400 kN	1,010 kN
Max. Dynamic (Ice) Thrust	900 kN	900 kN
Bollard Shaft Thrust	450 kN	900 kN
Damping:		
(Cycles to dampen to 10% of peak value)		
Torsional	2 - 4	2 - 3
Axial	2 - 3	2 - 3
Response Frequency:		
Torsional	5.5 Hz. (1st. Natural)	3.5 Hz (1st. Natural)
Axial (Thrust)	2.75, 11 and 22 Hz. (Shaft Rate, 1 & 2 x Blade Rate)	8.7 Hz. (Blade Rate)
Ice Condition		
Flexural Strength	1.55 ±0.11 m	1.55 ±0.11 m
Thickness	150 kPa	150 kPa

The following are the main findings of this study:

1. There is not a significant difference in the relative peak torques measured between the nozzled and open screw propellers. The peak shaft torque during ice milling was measured to be 150% and 134% of the MCR torque for the M.V. Ikaluk and the M.V. Terry Fox respectively.

2. The shaftline of the nozzled propeller (M.V. Ikaluk) was measured to have significantly higher axial (thrust) vibrations than the open screw propeller (M.V. Terry Fox). The peak shaft thrust during ice milling was measured to be 310% and 110% of the bollard thrust for the M.V. Ikaluk and the M.V. Terry Fox respectively.

3. Generally more ice-propeller interaction was noticed on the nozzled vessel than the open screw vessel. Both types of shaftlines had approximately the same high damping present in the axial and torsional modes.

Introduction

This section details the data analysis of the shafting response during ice-propeller interaction. A unique feature of these trials was that both vessel's shaftline responses were measured at the same time, in the same operational mode, and in the same ice condition. This testing condition enabled an analysis to be done on the relative shaftline responses to ice-propeller interaction of a nozzled and an open controllable pitch (cp) propeller shaftline, without having to take into account differences in the ice properties. The instrumentation included strain gauges on the shaftline to record thrust. The shaft torque reading was taken from the ASEA torductor. The shaft rpm, engine fuel rack, propeller pitch, and rudder angle were also recorded. The data acquisition system operated at a scan rate of 500 Hz with an analog low pass filters set at 60 Hz. Section 1.0 and 2.0 presented the particulars of the shaftline and the instrumentation employed.

Analysis Procedure and Data Base

The data base consisted of seven events for the M.V. Ikaluk and eight events for the M.V. Terry Fox. Each event consisted of twenty seconds of data with a number of separate ice-propeller interaction events. Time history plots were produced for all of the signals recorded on each vessel (12 - MV Terry Fox, 14 - MV Ikaluk) for each event. In addition plots were produced for specific sections of the time history to display the results at a larger scale. The maximum, minimum and mean values of each of the signals were calculated, as well as the ratios of the peak values to the averages and the difference of the peak values from the average. The dynamic (ice) torque and thrust were computed by the difference between the open water value immediately prior to ice ingestion by the propeller, and the peak value during the propeller ice milling process. A Fourier Transform was computed for selected events and time intervals to determine the dominant axial and torsional response frequencies. The only sensor that did not function properly during the recording of the these events was the starboard shaft thrust on the M.V. Terry Fox. However, the port shaft thrust was working well and it is reasonable to assume that the starboard shaft would experience similar loads, because the shaftlines are positioned symmetrically about the centre line of the vessel.

M.V. Ikaluk Results

Table 5.8.2 lists the maximum, minimum, and mean values of the machinery signals recorded for each 20 second event. In all of the events the M.V. Ikaluk was icebreaking ahead. No events of significance were recorded in the astern mode. The report entitled "Full-Scale Testing and Data Analysis of the Shaftline and Nozzle Dynamics in Ice on the M.V. Ikaluk" (TP 10402E, May 1990) details the response of the shaftline to ice-propeller interaction for a number of manoeuvres including astern and ramming. However, the majority of significant events in that study were recorded with the vessel in the ahead icebreaking mode. Selected events are described in detail below.

Event 1: Milling Ice Full Ahead

Figures 5.8.1 and 5.8.2 illustrate the time history responses of the shaft torque, shaft thrust, engine fuel rack, and propeller pitch for the port and starboard shaftlines respectively. Ice is ingested into the port propeller almost continuously for the first 17 seconds as shown by the highly dynamic response of the shaft torque and thrust. The starboard shaft does not experience as much torsional ice-propeller interaction forces and appears to ingest ice at the time intervals of 0-2, 9-10, 11-12,16-18 seconds. The starboard shaft thrust shows relatively high vibration throughout the event mainly due to hydrodynamic loads. The control system is set to a constant rpm mode, as is the usual case on these vessels when icebreaking. The fuel rack responds to the torsional load on the shaftline such that the rpm remains relatively constant at 165 (time history not shown), for an approximately constant propeller pitch.

The maximum shaft torque occurs on the port shaft at 14.5 seconds as illustrated in Figure 5.8.3 which illustrates the response for the 13-16 second time interval. This figure shows the relatively high damping present in the torsional and axial modes of vibration, as seen by the rapid decrease in dynamic amplitude in both the torque and thrust response time histories.

It is interesting to note that the shaft torque increases from 300 kNm to 450 kNm over a time period of 0.5 seconds with a slight drop at 14.3 seconds. This suggests that ice is continually being milled by the propeller such that the torsional load is not released after each blade passage. This is important to note when designing a propulsion plant for response to dynamic loading conditions. In addition this data can be used for the calibration of simulation programs of propulsion plant responses to dynamic loading.

TABLE 5.8.2
SUMMARY OF SHAFTLINE VIBRATION MEASUREMENTS: M.V. IKALUK

TEST ID	PORT												STARBOARD											
	PITCH			TORQUE			THRUST			RPM			PITCH			TORQUE			THRUST			RPM		
	AVG (deg)	MIN (deg)	MAX (deg)	AVG (kNm)	MIN (kNm)	MAX (kNm)	AVG (MN)	MIN (MN)	MAX (MN)	AVG (RPM)	MIN (RPM)	MAX (RPM)	AVG (deg)	MIN (deg)	MAX (deg)	AVG (kNm)	MIN (kNm)	MAX (kNm)	AVG (MN)	MIN (MN)	MAX (MN)	AVG (RPM)	MIN (RPM)	MAX (RPM)
1	25.4	24.7	26.2	311	230	454	0.45	-0.09	0.95	166	165	167	27.2	26.2	27.9	223	186	307	0.38	-0.05	1.01	164	163	165
2	26	24.8	26.5	313	269	376	0.52	0.066	1.1	166	165	167	23.3	22	24.2	225	160	329	0.50	0.02	1.40	164	161	166
3	25.5	23.6	26.5	297	216	412	0.43	-0.09	1.12	166	165	168	26.6	25.2	27.6	226	178	308	0.37	-0.06	0.96	164	163	166
4	25.7	24.4	26.7	311	245	478	0.48	0.01	0.97	166	165	167	26.9	26.1	27.2	231	197	311	0.43	-0.01	0.85	164	163	165
5	24.9	24.7	25.2	277	241	387	0.45	0.01	0.85	167	166	168	26.1	25.3	27	223	189	288	0.42	-0.02	0.77	164	163	165
6	24.8	23.9	25.2	277	232	369	0.43	-0.05	0.95	167	165	168	26.2	25.7	26.9	223	198	287	0.43	-0.20	1.05	165	163	166
7	4.9	4.7	5.6	47	39	55	0.05	-0.04	0.06	171	171	172	5.4	5.1	6.1	0.04	0.04	0.05	0.05	-0.26	0.39	169	168	170

TEST ID	PORT												STARBOARD											
	PITCH			TORQUE			THRUST			RPM			PITCH			TORQUE			THRUST			RPM		
	MIN AVG	MAX AVG	MAX-MIN (amp.) (deg)	MIN AVG	MAX AVG	MAX-MIN (amp.) (kNm)	MIN AVG	MAX AVG	MAX-MIN (amp.) (MN)	MIN AVG	MAX AVG	MAX-MIN (amp.) (RPM)	MIN AVG	MAX AVG	MAX-MIN (amp.) (deg)	MIN AVG	MAX AVG	MAX-MIN (amp.) (kNm)	MIN AVG	MAX AVG	MAX-MIN (amp.) (MN)	MIN AVG	MAX AVG	MAX-MIN (amp.) (RPM)
1	0.97	1.03	1.50	0.74	1.46	224	-0.20	2.11	1.04	0.99	1.01	2.00	0.96	1.03	1.70	0.83	1.38	121	-0.14	2.69	1.06	0.99	1.01	2.00
2	0.95	1.02	1.70	0.86	1.20	107	0.13	2.12	1.03	0.99	1.01	2.00	0.94	1.04	2.20	0.71	1.46	169	0.04	2.79	1.38	0.98	1.01	5.00
3	0.93	1.04	2.90	0.73	1.39	196	-0.21	2.60	1.21	0.99	1.01	3.00	0.95	1.04	2.40	0.79	1.36	130	-0.17	2.58	1.02	0.99	1.01	3.00
4	0.95	1.04	2.30	0.79	1.54	233	0.02	2.02	0.96	0.99	1.01	2.00	0.97	1.01	1.10	0.85	1.35	114	-0.03	1.98	0.86	0.99	1.01	2.00
5	0.99	1.01	0.50	0.87	1.40	146	0.02	1.89	0.84	0.99	1.01	2.00	0.97	1.03	1.70	0.85	1.29	99	-0.05	1.84	0.79	0.99	1.01	2.00
6	0.96	1.02	1.30	0.84	1.33	137	-0.12	2.21	1.00	0.99	1.01	3.00	0.98	1.03	1.20	0.89	1.29	89	-0.48	2.46	1.25	0.99	1.01	3.00
7	0.96	1.14	0.90	0.83	1.17	16	-0.80	1.20	0.10	1.00	1.01	1.00	0.94	1.13	1.00	1.00	1.25	0	-5.20	7.72	0.65	0.99	1.01	2.00

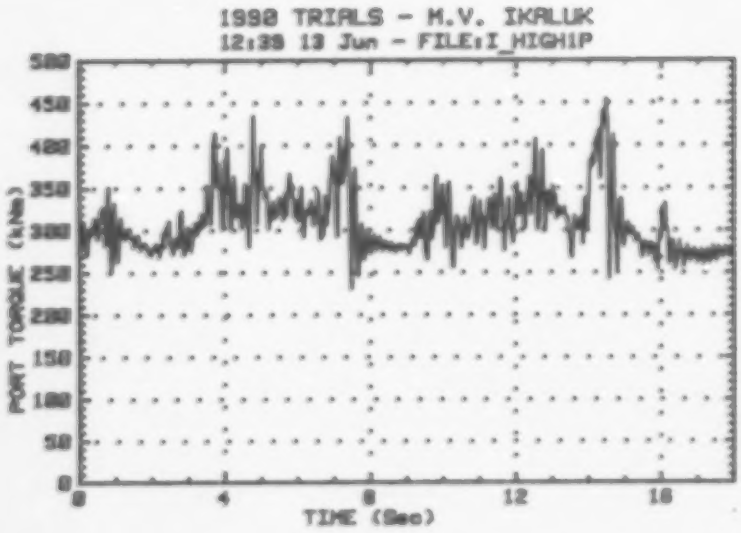

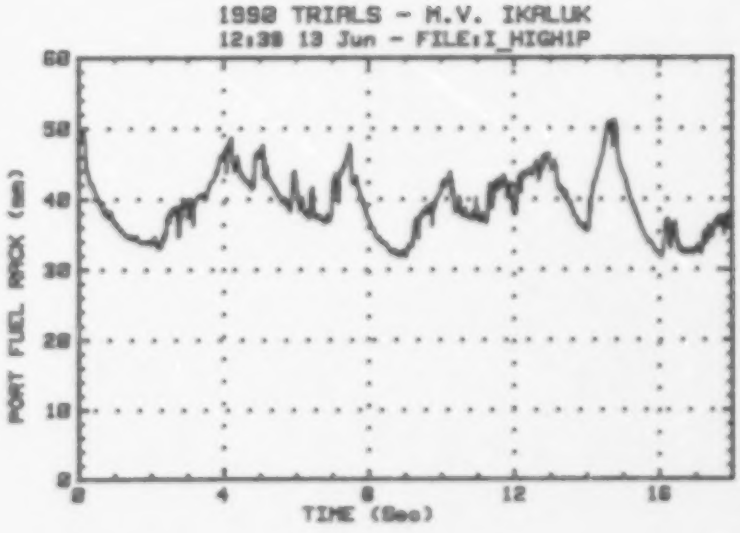

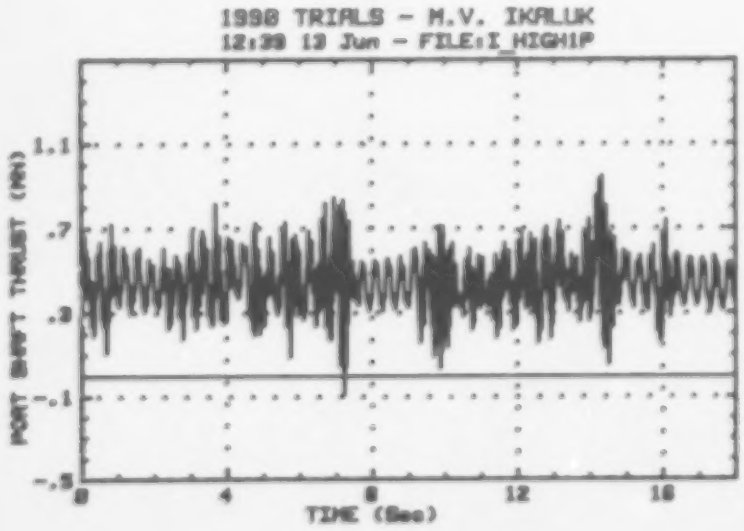

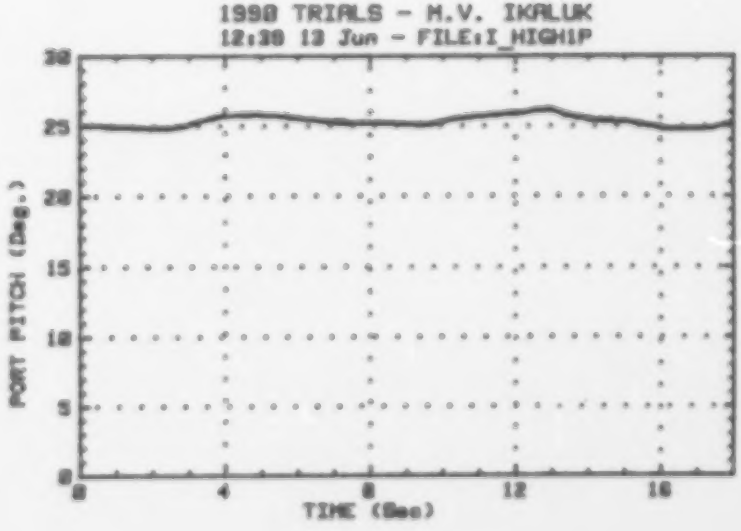

Figure 5.8.1 Port Shaft Torque,Thrust, Pitch, and Fuel Rack: M.V. Ikaluk Test H1

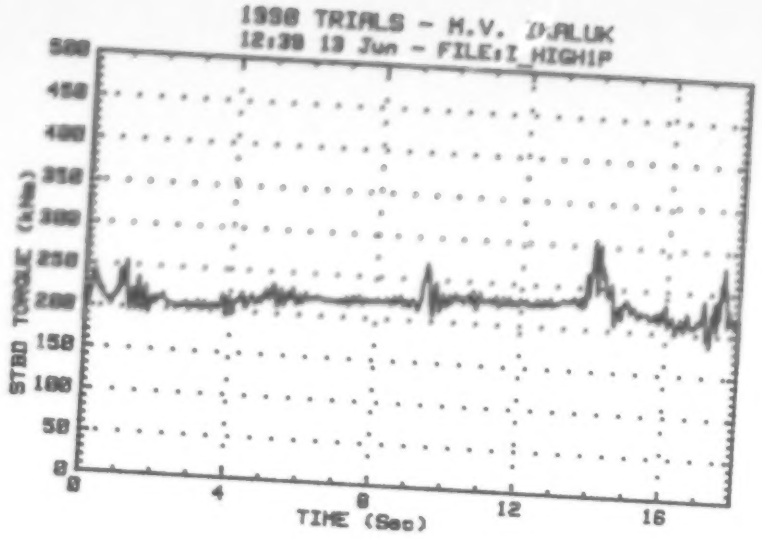

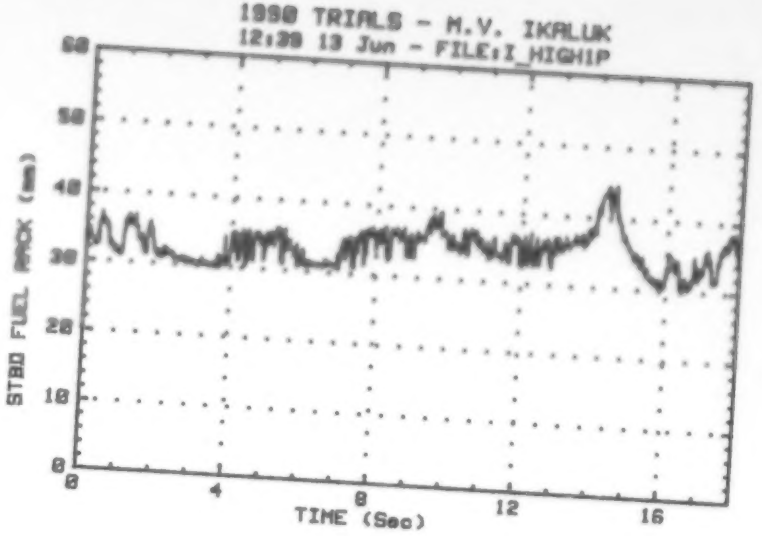

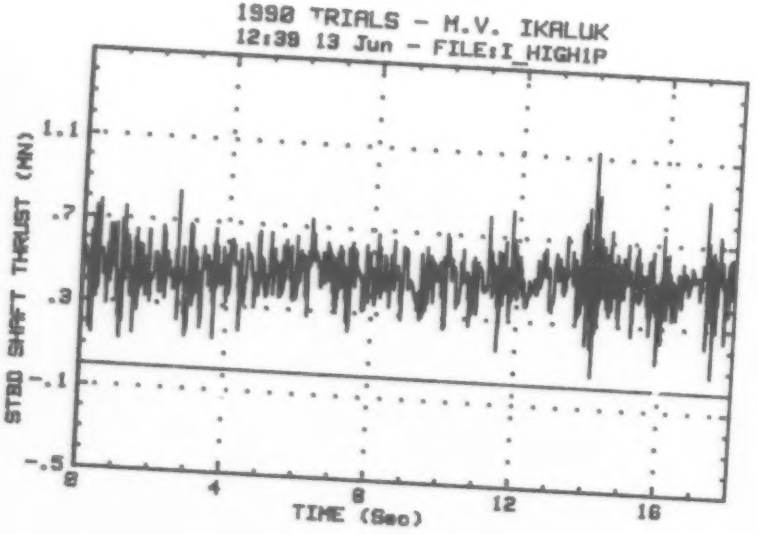

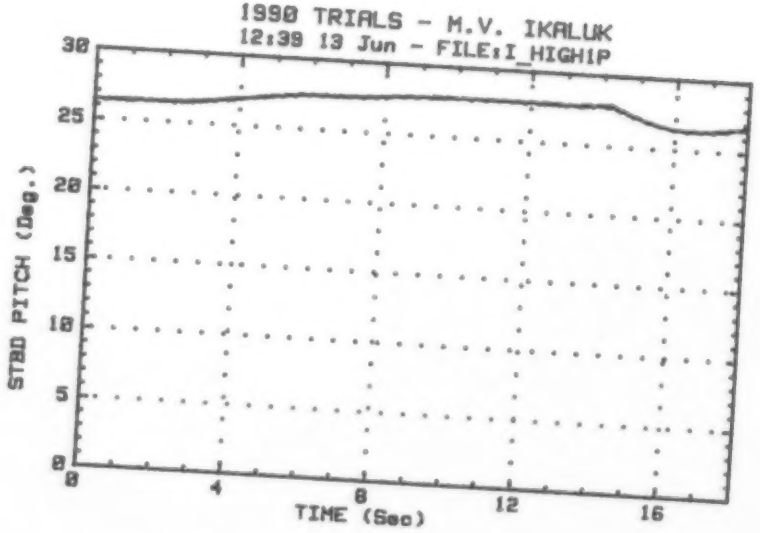

Figure 5.8.2 Stbd. Shaft Torque,Thrust, Pitch, and Fuel Rack: M.V. Ikaluk Test H1

Event 2: Maximum Thrust Vibration and Nozzle Blockage

Figure 5.8.4 illustrates the time history corresponding to the maximum measured shaft thrust (17.32 seconds) and the corresponding shaft torque. The shaft thrust is responding at approximately twice the blade rate (22 Hz). The peak thrust occurs over a time interval of approximately 0.04 seconds or 1/2 of the time for a blade to pass one point. It is interesting to not that there is not a significant vibration in the shaft torque over this time interval. Therefore, it appears as though the nozzle is partially blocked by ice and the face of the propeller is experiencing ice forces but not the leading edge. The shaft torque immediately prior to this time (open water torque) was 200 kNm. Therefore, the increase in torque due to the nozzle blockage is approximately 50 kNm, which is the same figure arrived at in the 1989 trials of the M.V. Ikaluk (TP # 10402E).

Event 3: Milling Ice Full Ahead

Figure 5.8.5 and 5.8.6 illustrate the time history responses of the shaft torque, shaft thrust, engine fuel rack, and propeller pitch for the starboard and port shaftlines respectively. Ice is ingested into the starboard propeller almost continuously for the first 12 seconds as shown by the highly dynamic response of the shaft torque. Between 12 and 14 seconds there is no ice-propeller interaction and then from 14- 18 seconds ice is interacting with the propeller again. The port shaft experiences significant ice-propeller interaction in the first few seconds of the time history. Figure 5.8.7 illustrates the port shaft torque and thrust response for the first 1.5 seconds of this event.

Figure 5.8.8 is a plot of the results from a Fourier analysis of the first 2.5 seconds of the port shaft torque and thrust. The dominant frequency is approximately 4.2 Hz for the torsional response, which corresponds to the estimated first torsional natural frequency. The frequency spectrum for the axial (thrust) response indicates dominant responses at 2.75 Hz (shaft rate), 11 Hz (blade rate), and 22 Hz (2 x blade rate). These results concur with those found in the 1989 propulsion system trials of the vessel.

Event 4: Maximum Shaft Torque

Figure 5.8.9 illustrates the maximum shaft torque measured (478 kNm) on the M.V. Ikaluk, which was recorded on the port shaft. The top plot is the port shaft torque for the first 12 seconds of the event, and the bottom plot is for the time interval from 2.5 to 5.5 seconds. The shaft torque rises from the MCR torque of 317 kNm to the peak of 478 kNm in approximately 0.5 seconds, which corresponds to 1.4 revolutions of the shaft or 5.6 blade passages. Therefore, it is likely that more than one blade is in contact with the ice, and the nozzle is probably clogged with a number of ice block.

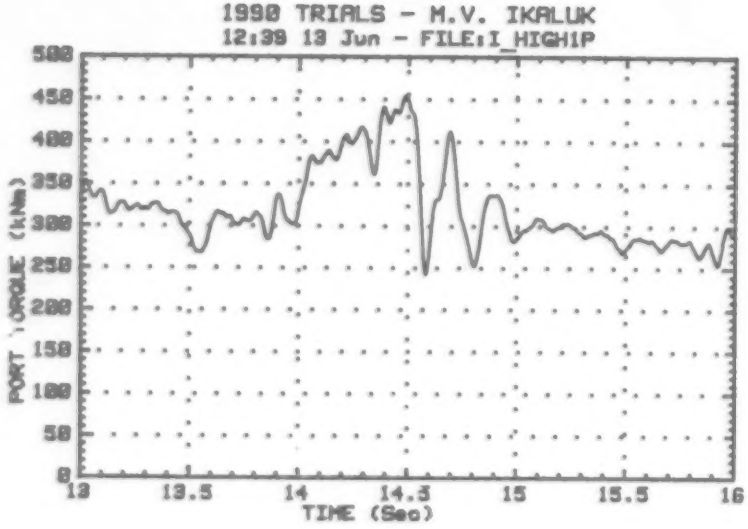

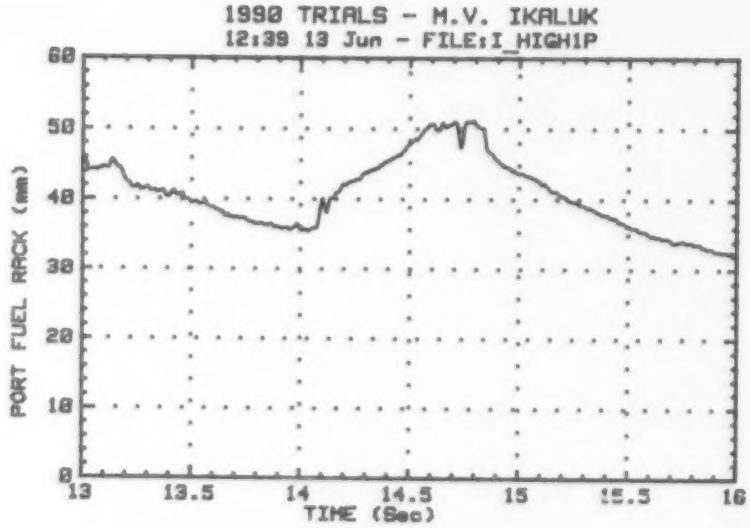

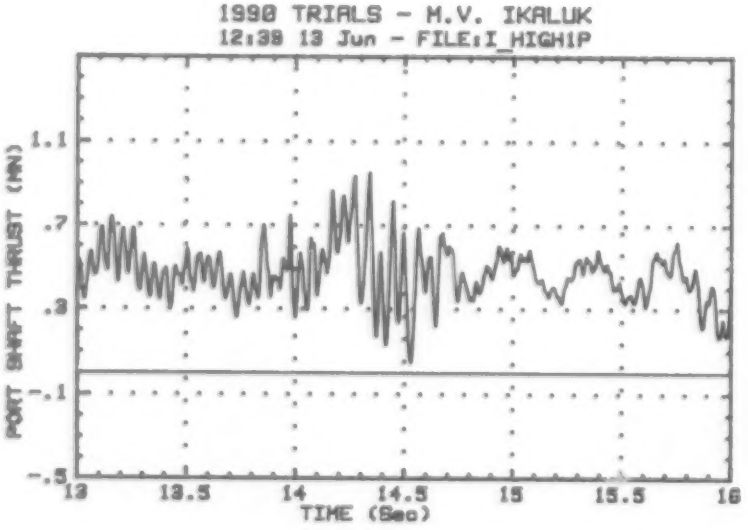

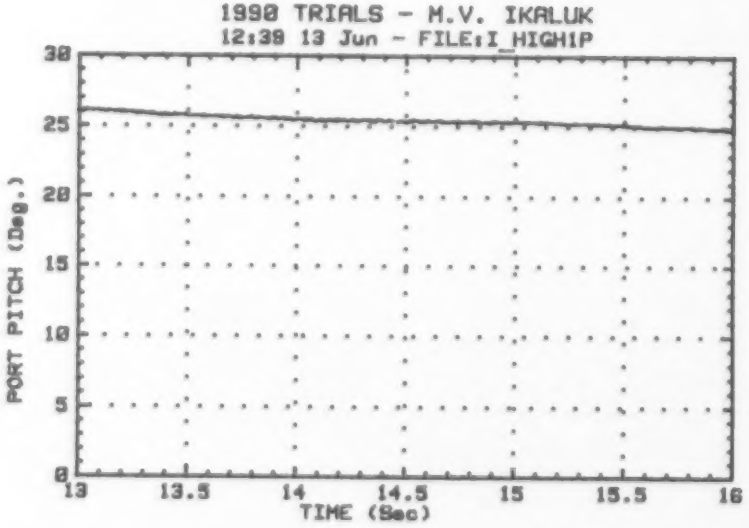

Figure 5.8.3 Port Shaft Torque,Thrust, Pitch, and Fuel Rack: M.V. Ikaluk Test H1

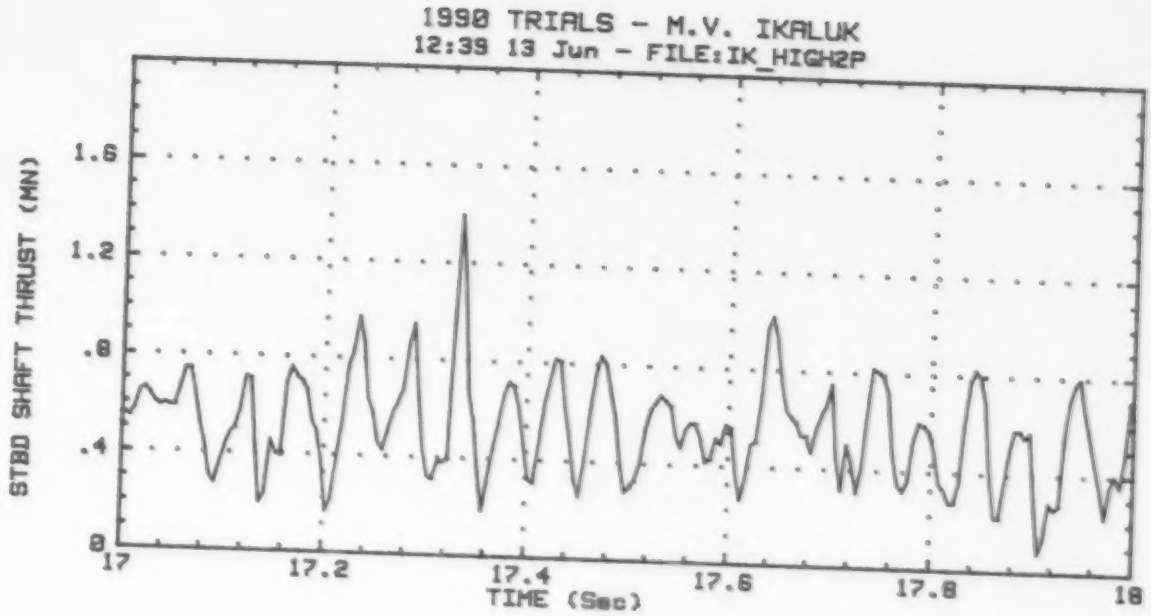

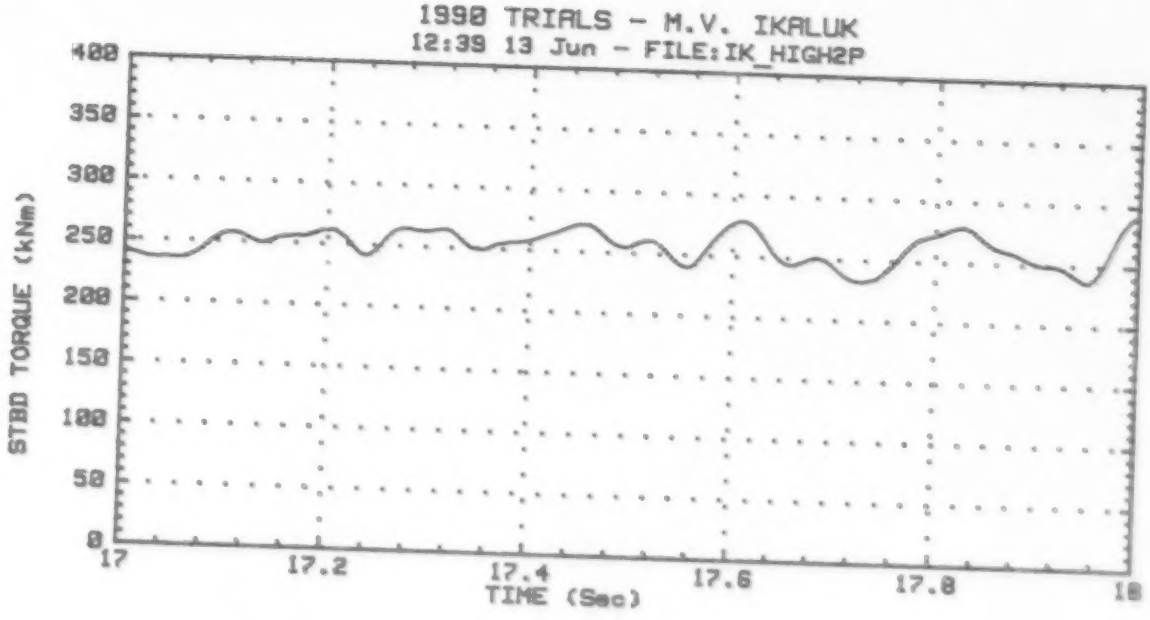

Figure 5.8.4 Starboard Shaft Torque and Thrust: M.V. Ikaluk Test H2

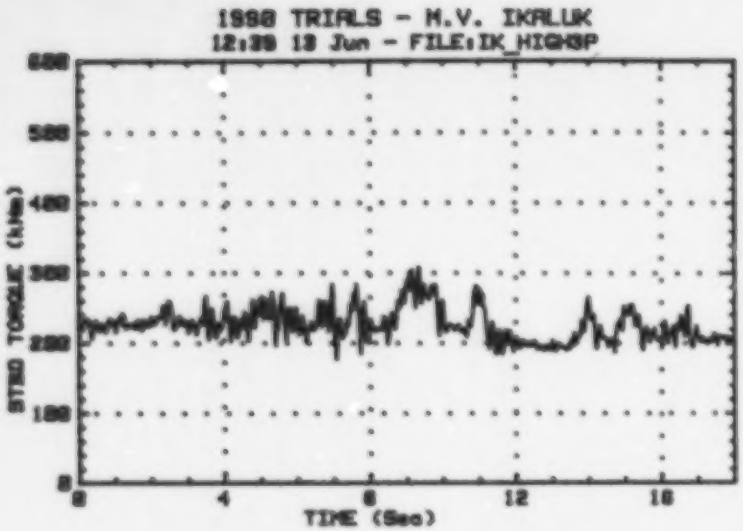

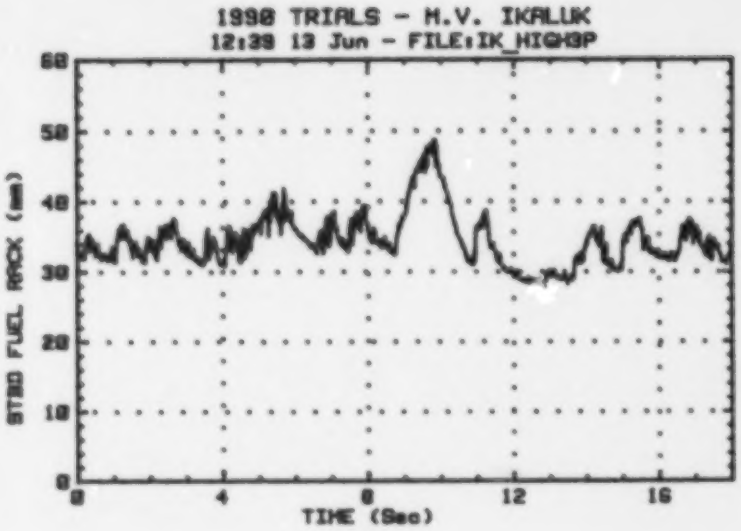

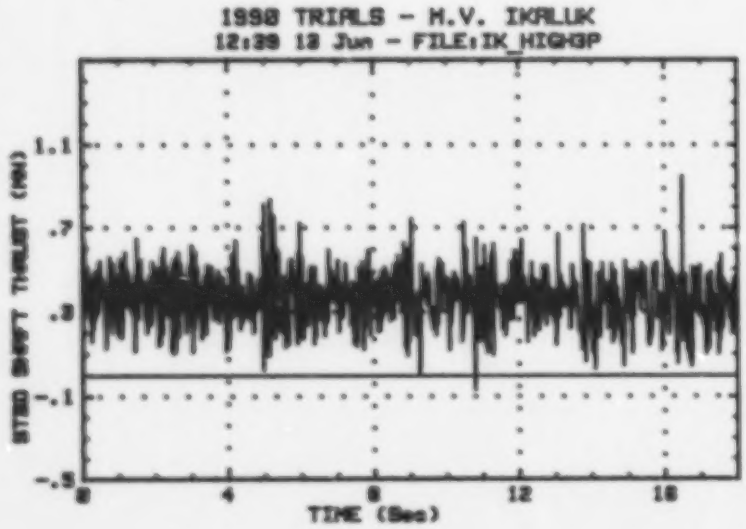

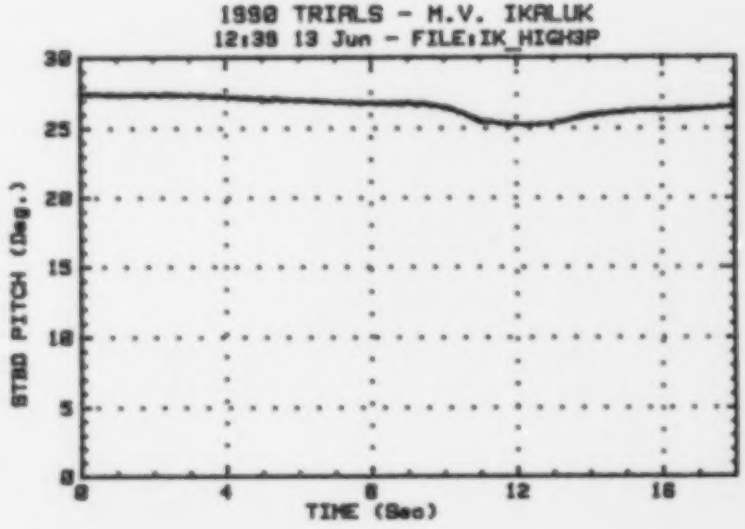

Figure 5.8.5 Stbd. Shaft Torque,Thrust, Pitch, and Fuel Rack: M.V. Ikaluk Test H3

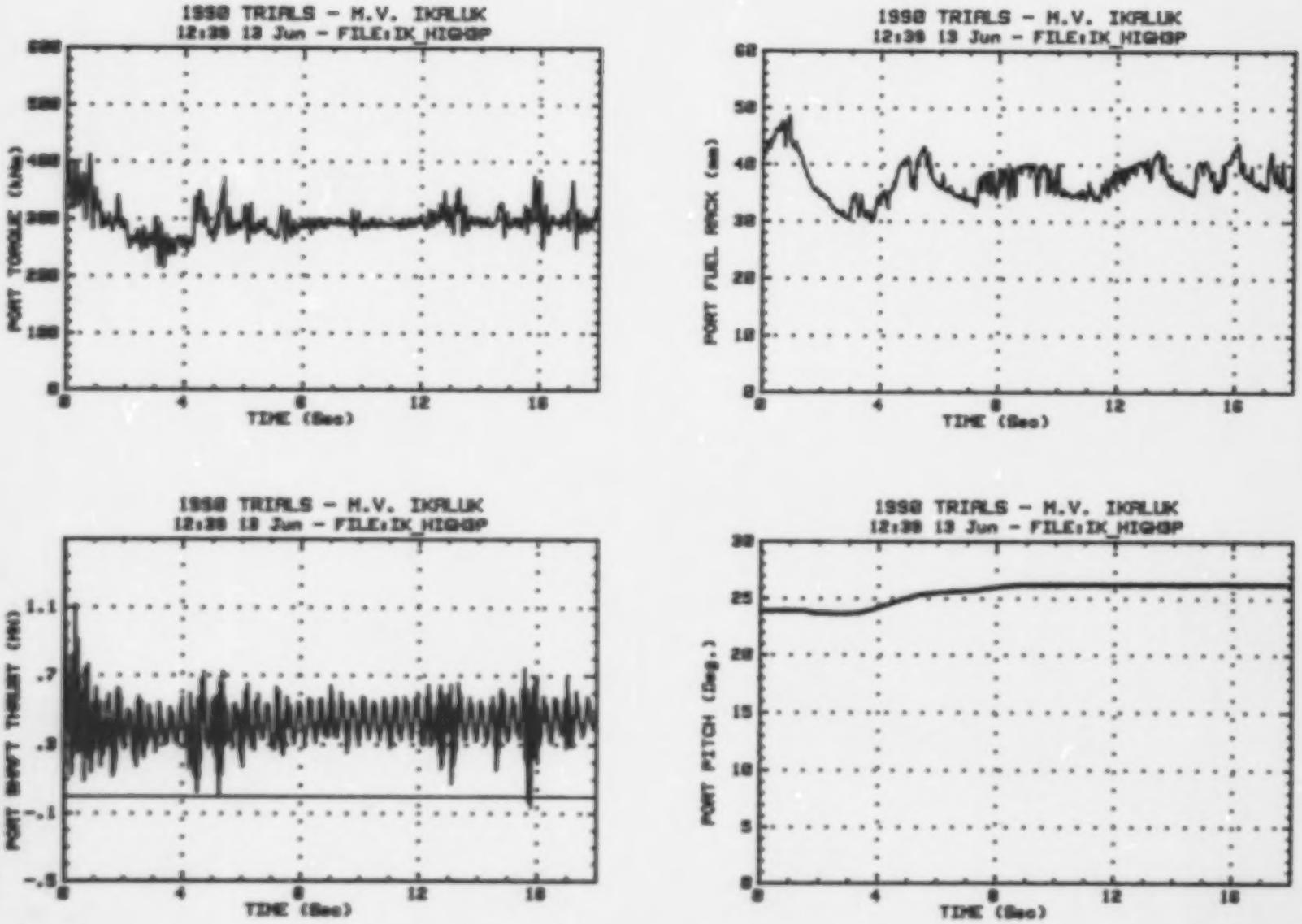

Figure 5.8.6 Port Shaft Torque,Thrust, Pitch, and Fuel Rack: M.V. Ikaluk Test H3

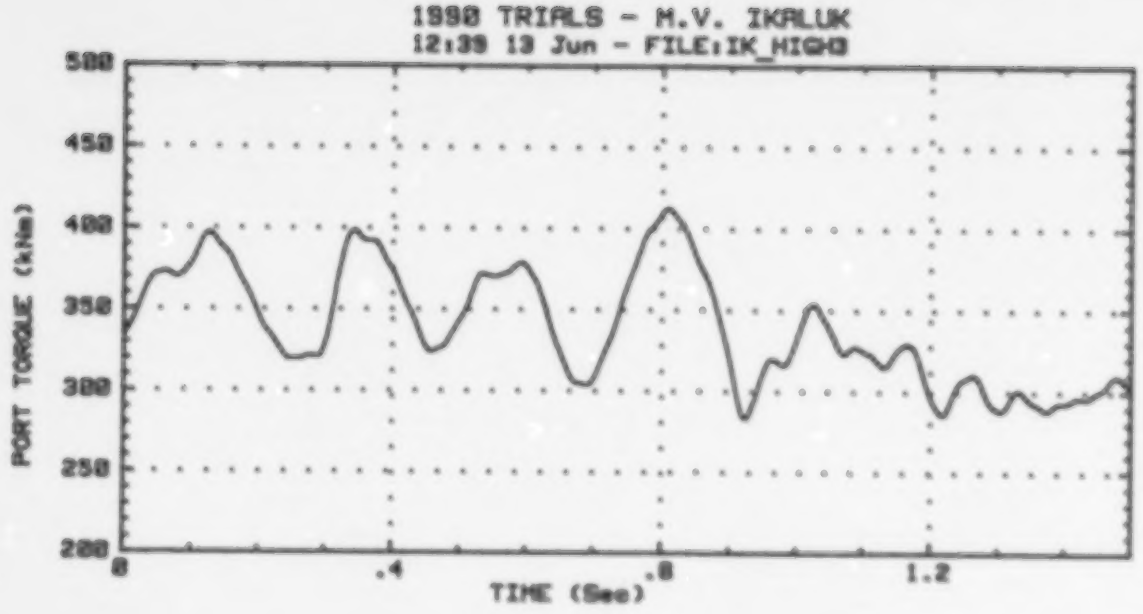

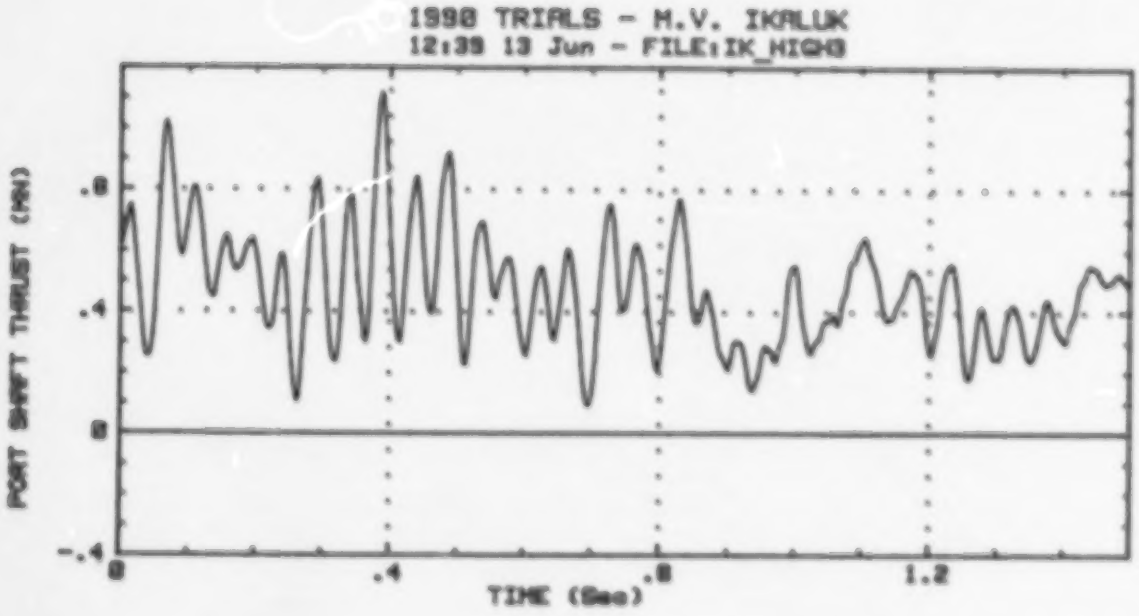

Figure 5.8.7 Port Shaft Torque and Thrust: M.V. Ikaluk Test H3

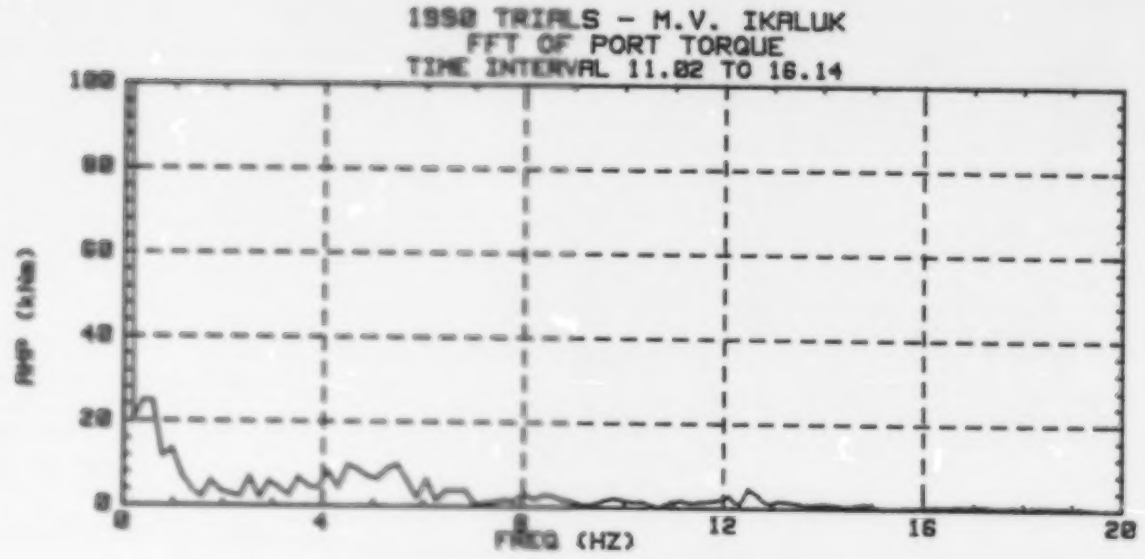

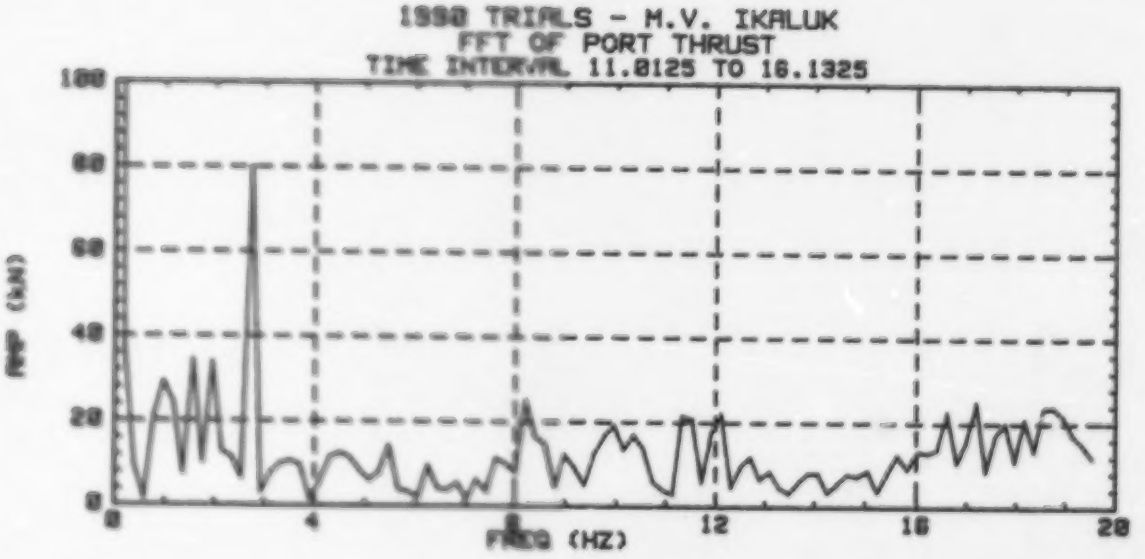

Figure 5.8.8 Fourier Transforms of Port Shaft Torque and Thrust: M.V. Ikaluk Test H3

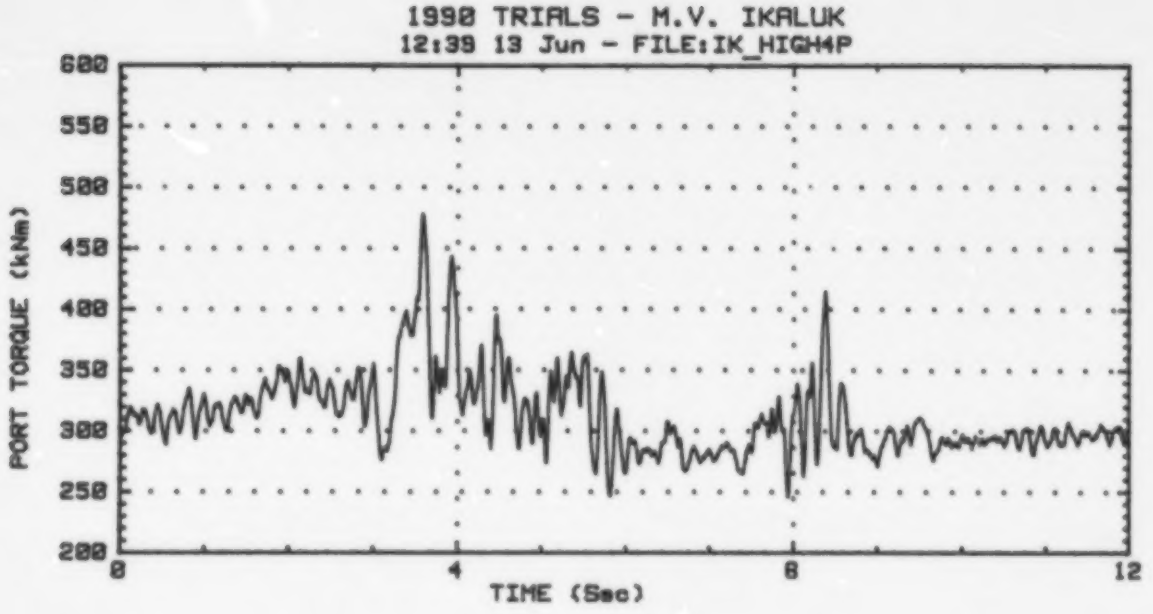

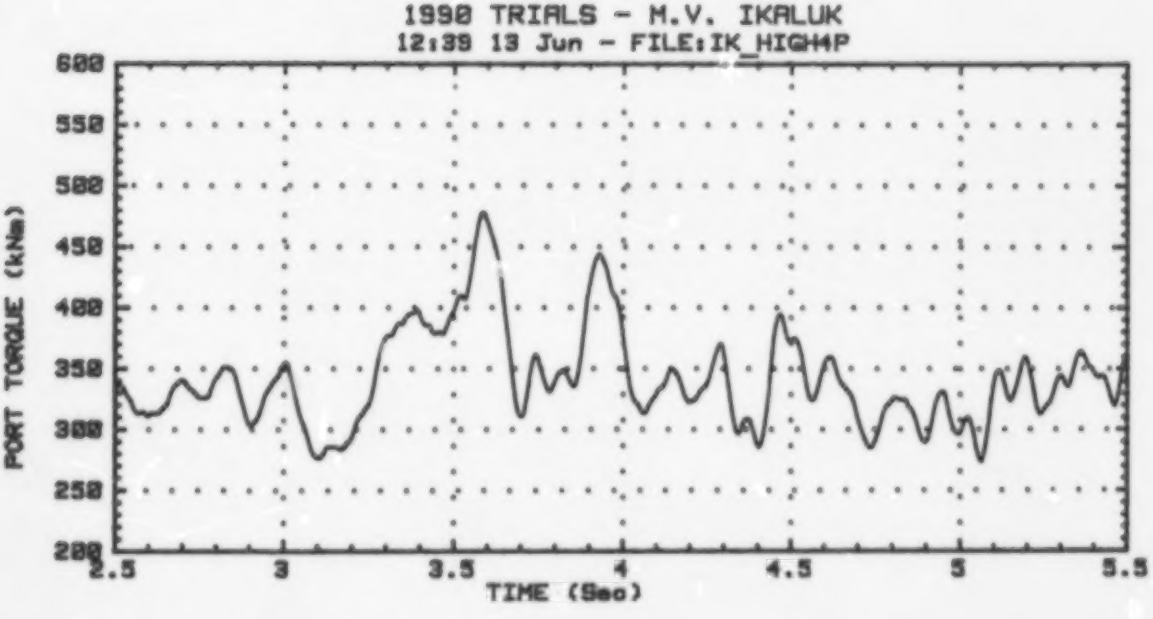

Figure 5.8.9 Port Shaft Torque: M.V. Ikaluk Test H4

M.V. Terry Fox Results

Table 5.8.3 lists the maximum, minimum, and mean values of the machinery signals recorded for each 20 second event. Fleet Technology's report entitled "M.V. Kalvik Propulsion System Full Scale Tests" (TP 8401E, June 1987) details the response of the shaftline to ice-propeller interaction for a number of manoeuvres including astern and ramming. Selected events are described in detail below.

Note:

On all figures and tables port pitch values should be 3° higher than shown.

Event 8: Milling Ice Full Ahead

Figure 5.8.10 illustrate the time history responses of the shaft torque, shaft thrust, engine fuel rack, and propeller pitch for the port shaftline. The vessel is running at full ahead and ice is ingested into the port propeller almost continuously for the first 12 seconds as shown by the highly dynamic response of the shaft torque and thrust. The control system is set to a constant rpm mode, similar to the M.V. Ikaluk. The fuel rack responds to the torsional load on the shaftline such that the rpm remains relatively constant at 130 (time history not shown), during the event. Figure 5.8.11 illustrates the shaftline responses for the time interval from 0 to 6 seconds. In this figure one can distinguish the individual torsional and axial (thrust) vibrations more clearly than Figure 5.8.10. A Fourier Transform was calculated for the shaft thrust and torque from 0.0 to 5.1 seconds and the results are shown in Figure 5.8.12. The dominant response frequency in the torsional mode is at 3.5 Hz which corresponds to the first natural frequency. For the shaft thrust waveform the dominant frequencies are 2.2 Hz (Shaft Rate), 8.8 Hz (Blade Rate), and 12.5 Hz.

Figure 5.8.13 illustrates a 3.0 second time history of the starboard shaft torque and the engine fuel rack. It is interesting to note that the torque increases over a period of approximately 0.3 seconds and reaches a plateau for approximately 0.4 seconds (3 blade passages), after which the ice leaves the propeller and the shaft torque reduces to its previous level within 0.2 seconds. This indicates that the type of loading that the main engine sees and the high torsional damping present in the system.

TABLE 5.8.3
SUMMARY OF SHAFTLINE VIBRATION MEASUREMENTS: M.V. TERRY FOX

TEST ID	PORT												STARBOARD											
	PITCH			TORQUE			THRUST			RPM			PITCH			TORQUE			THRUST			RPM		
	AVG (deg)	MIN (deg)	MAX (deg)	AVG (kNm)	MIN (kNm)	MAX (kNm)	AVG (MN)	MIN (MN)	MAX (MN)	AVG (RPM)	MIN (RPM)	MAX (RPM)	AVG (deg)	MIN (deg)	MAX (deg)	AVG (kNm)	MIN (kNm)	MAX (kNm)	AVG (MN)	MIN (MN)	MAX (MN)	AVG (RPM)	MIN (RPM)	MAX (RPM)
T3	18.5	17.8	19	538	456	673	0.79	0.30	1.07	129	129	130	21.2	19.4	22.0	513	355	715	N.A	N.A	N.A	128	127	129
T5	18.8	17.6	19.4	532	401	618	0.78	0.48	0.97	129	129	130	22.5	22.2	22.8	542	477	598	N.A	N.A	N.A	128	127	129
T6	18.9	18.8	19	551	497	643	0.72	0.52	0.96	129	129	130	21.4	19.2	22.5	506	358	709	N.A	N.A	N.A	128	127	129
T8	18.3	16.6	20.1	496	341	670	0.63	0.25	1.07	129	128	130	21.7	20.6	22.8	486	340	770	N.A	N.A	N.A	128	127	129
T9	17.7	17.6	17.8	466	368	592	0.56	0.35	0.81	129	129	130	21.7	20.2	22.9	499	377	668	N.A	N.A	N.A	128	127	129
T10	11.5	11.4	11.6	190	160	229	0.24	0.10	0.40	130	129	130	23.3	22.7	24.0	469	397	523	N.A	N.A	N.A	128	127	129
T11	-12.5	-18.0	-6.6	232	103	400	-0.42	-0.71	-0.16	130	129	130	20.3	19.1	21.0	513	452	554	N.A	N.A	N.A	128	127	129
T12	-5.0	-13.0	-16	178	171	520	-0.07	-1.00	0.70	129	127	130	-10.0	-15.8	2.3	408	7	776	N.A	N.A	N.A	128	126	130

TEST ID	PORT												STARBOARD											
	PITCH			TORQUE			THRUST			RPM			PITCH			TORQUE			THRUST			RPM		
	MIN AVG	MAX AVG	MAX-MIN (amp.) (deg)	MIN AVG	MAX AVG	MAX-MIN (amp.) (kNm)	MIN AVG	MAX AVG	MAX-MIN (amp.) (MN)	MIN AVG	MAX AVG	MAX-MIN (amp.) (RPM)	MIN AVG	MAX AVG	MAX-MIN (amp.) (deg)	MIN AVG	MAX AVG	MAX-MIN (amp.) (kNm)	MIN AVG	MAX AVG	MAX-MIN (amp.) (MN)	MIN AVG	MAX AVG	MAX-MIN (amp.) (RPM)
1	0.94	1.03	1.80	0.75	1.16	217	0.62	1.24	0.49	1.00	1.01	1.00	0.99	1.01	0.60	0.88	1.10	121	N.A	N.A	N.A	0.99	1.01	2.00
2	0.99	1.01	0.20	0.90	1.17	146	0.72	1.33	0.44	1.00	1.01	1.00	0.90	1.05	3.30	0.71	1.40	351	N.A	N.A	N.A	0.99	1.01	2.00
3	0.91	1.10	3.50	0.69	1.35	329	0.40	1.70	0.82	0.99	1.01	2.00	0.95	1.05	2.20	0.70	1.58	430	N.A	N.A	N.A	0.99	1.01	2.00
4	0.99	1.01	0.20	0.79	1.27	224	0.63	1.45	0.46	1.00	1.01	1.00	0.93	1.06	2.70	0.76	1.34	291	N.A	N.A	N.A	0.99	1.01	2.00
5	0.99	1.01	0.20	0.84	1.21	69	0.42	1.67	0.30	0.99	1.00	1.00	0.97	1.03	1.30	0.85	1.12	126	N.A	N.A	N.A	0.99	1.01	2.00
6	1.44	0.53	11	0.44	1.72	297	1.69	0.38	0.55	0.99	1.00	1.00	0.94	1.03	1.90	0.88	1.08	102	N.A	N.A	N.A	0.99	1.01	2.00
7	2.60	3.20	-3.00	0.96	2.92	349	14.29	-10.00	1.70	0.98	1.01	3.00	1.58	-0.23	18	0.02	1.90	769	N.A	N.A	N.A	0.98	1.02	4.00

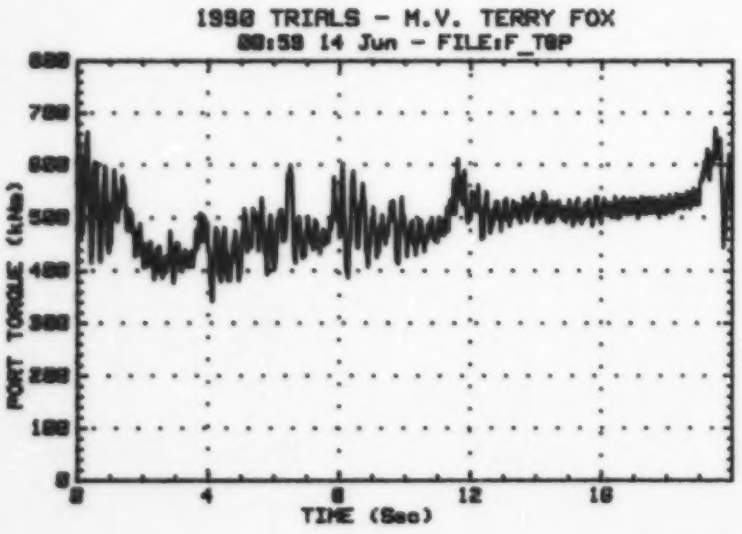

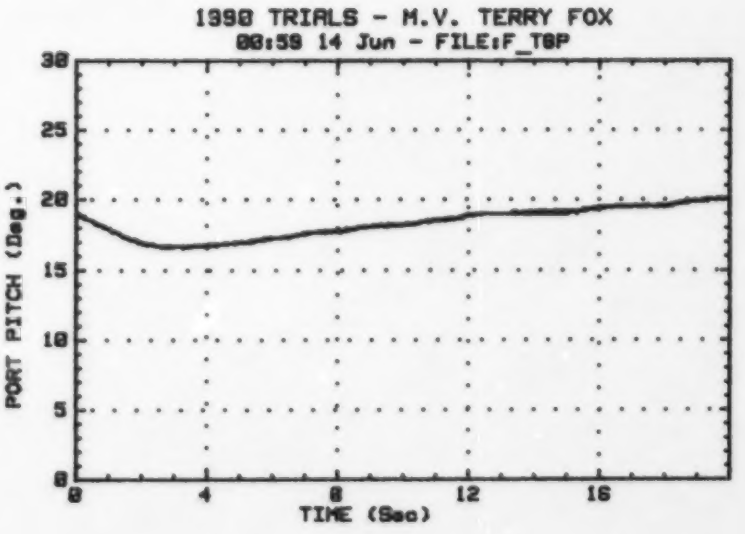

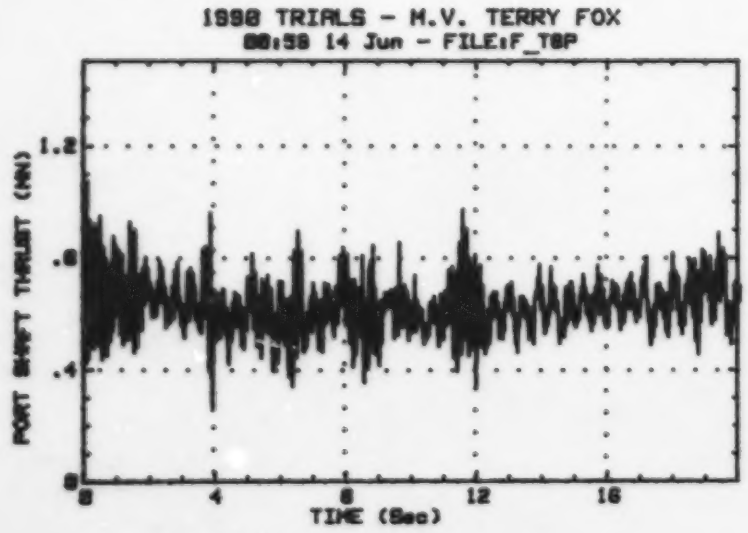

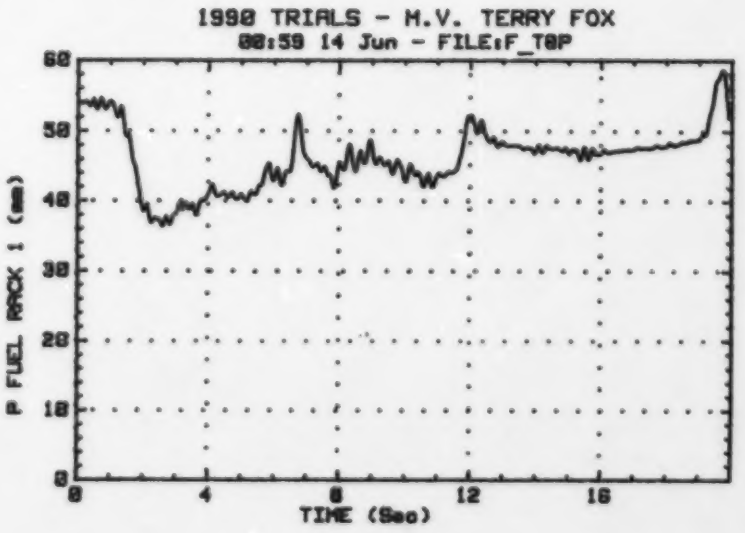

Figure 5.8.10 Port Shaft Torque,Thrust, Pitch, and Fuel Rack:

M.V. Terry Fox Test H8: 0-20 Seconds

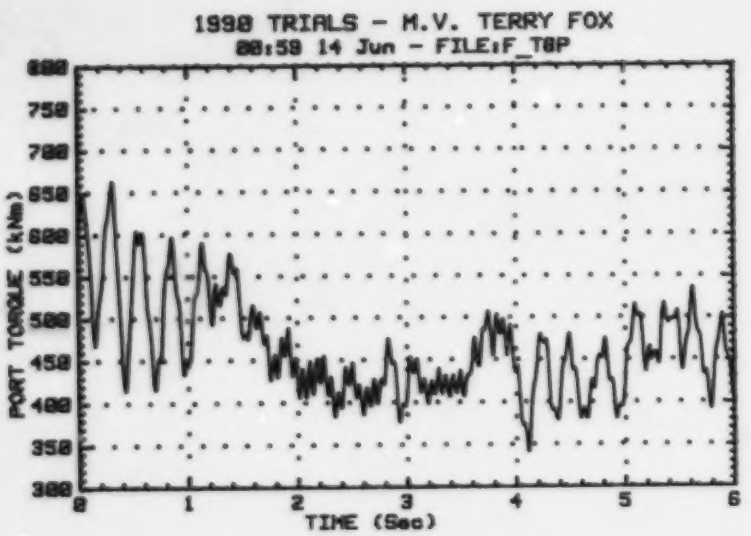

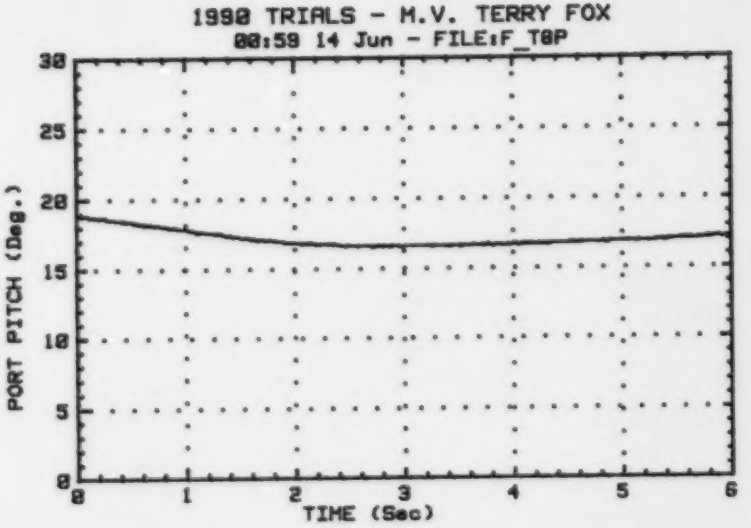

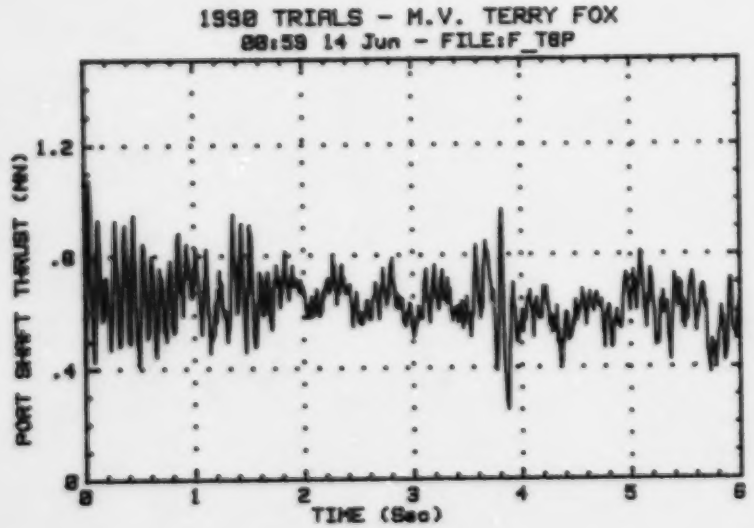

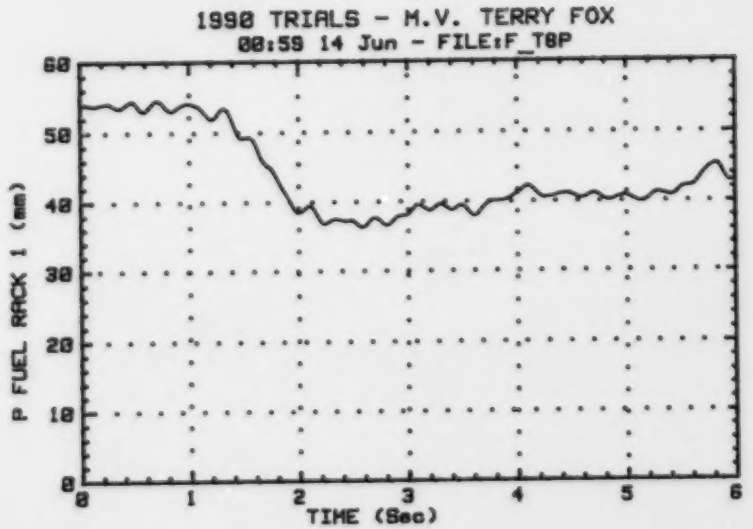

Figure 5.8.11 Port Shaft Torque,Thrust, Pitch, and Fuel Rack:

M.V. Terry Fox Test H8: 0-6 Seconds

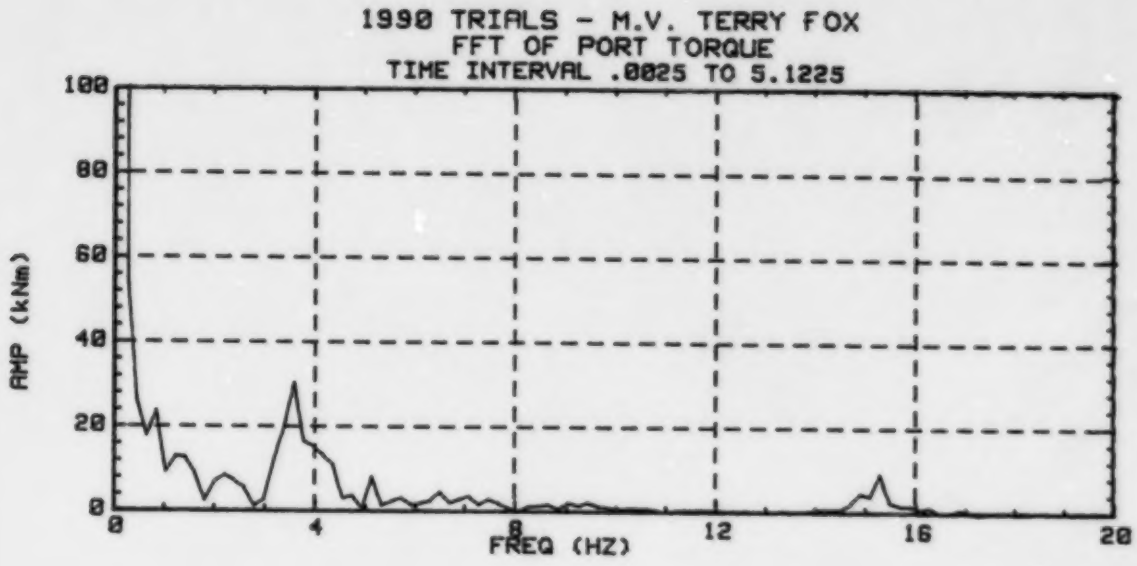

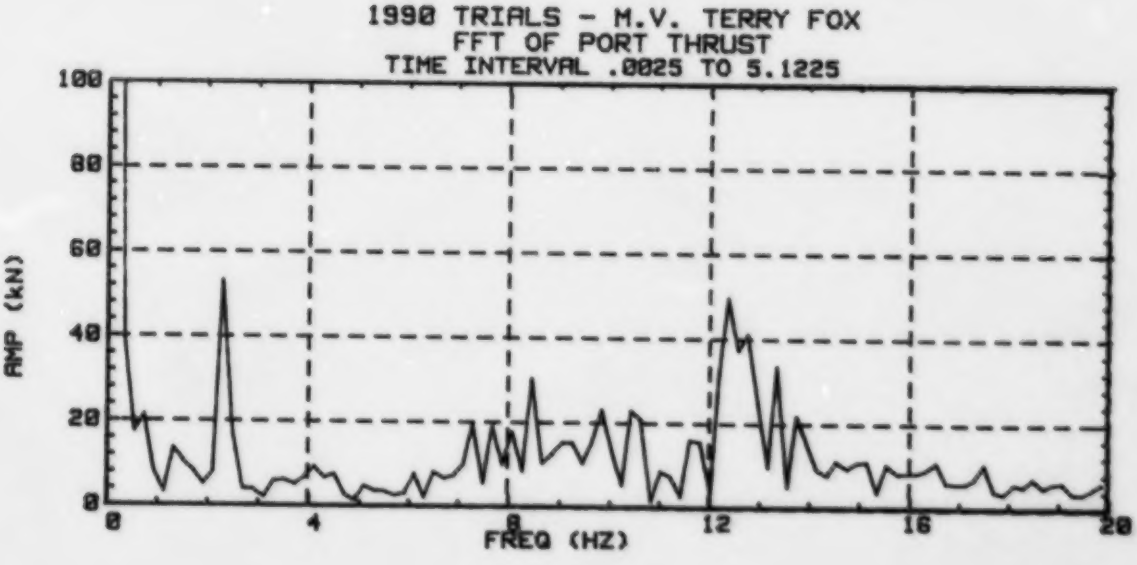

Figure 5.8.12 Fourier Transforms of Port Shaft Torque and Thrust:

M.V. Terry Fox Test H8

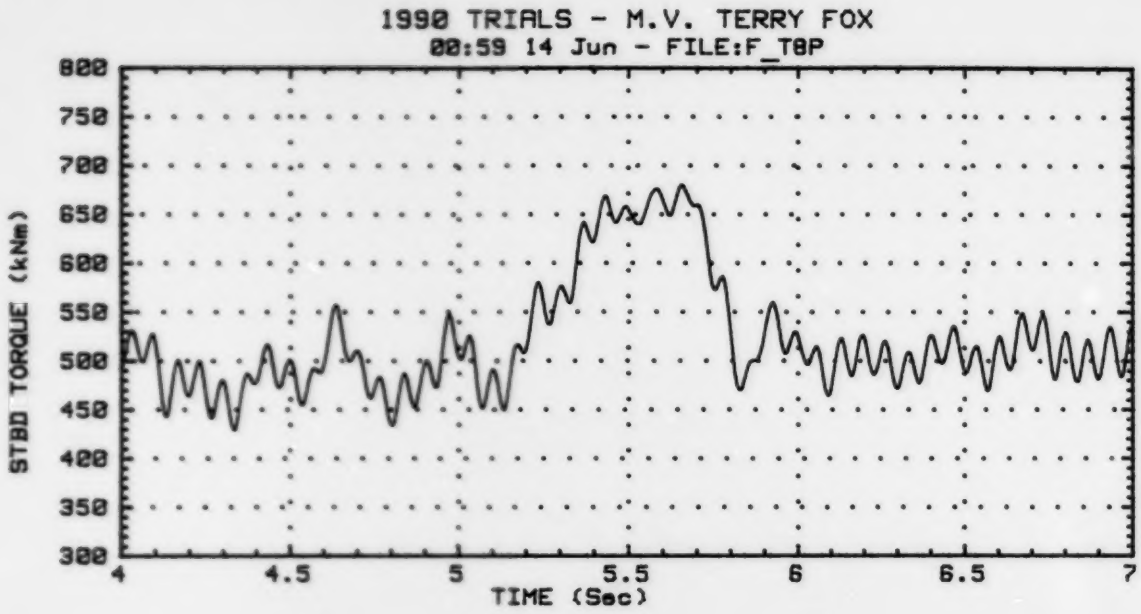

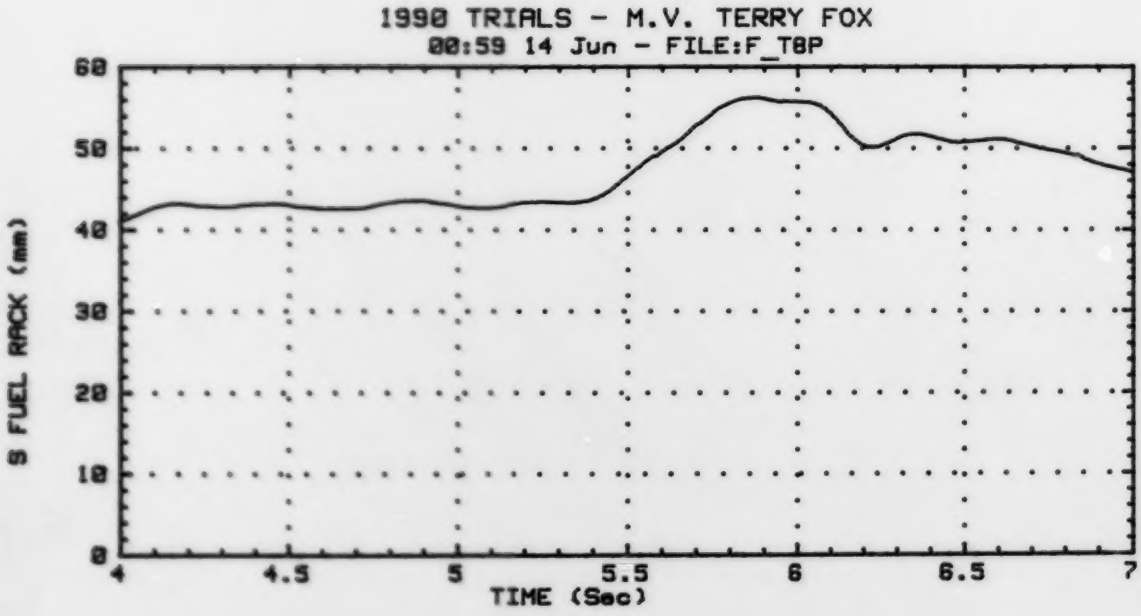

Figure 5.8.13 Starboard Shaft Torque and Fuel Rack: Test H8

Event 12: Milling Ice - Astern Pitch, Maximum Torque

Figure 5.8.14 illustrates the time history response of the port and starboard rpm and propeller pitch for a full 20 second event. The starboard propeller is directed from full astern to zero pitch, and the port propeller is directed to go from zero pitch to full astern during this event. The corresponding port shaft torque and thrust for the entire twenty seconds, and for the time interval of 17 to 20 seconds, are illustrated in Figures 5.8.15 and 5.8.16 respectively. From these figures it is apparent that as the pitch becomes more negative (astern) more ice is ingested into the propeller. The shaft thrust vibrations are relatively more severe than the shaft torque particularly from 17 to 19 seconds. Therefore, there are cases where the axial (thrust) loads are high when the torsional loads are not. This relationship has been measured on other full-scale trials such as the M.V. Robert Lemeur (1984) and the M.V. Kalvik (1986). In addition the reversal of the thrust is seen during the ice propeller interaction such that the thrust magnitude changes from +0.7 MN to - 0.9 MN.

Figure 5.8.17 illustrates the starboard and port shaft torque for the time interval of 5 to 15 seconds. The starboard propeller moving from full astern to ahead during extreme ice-propeller milling. At 10.6 seconds the peak shaft torque of 776 kNm measured during these trials occurs on the starboard propeller of the M.V. Terry Fox.

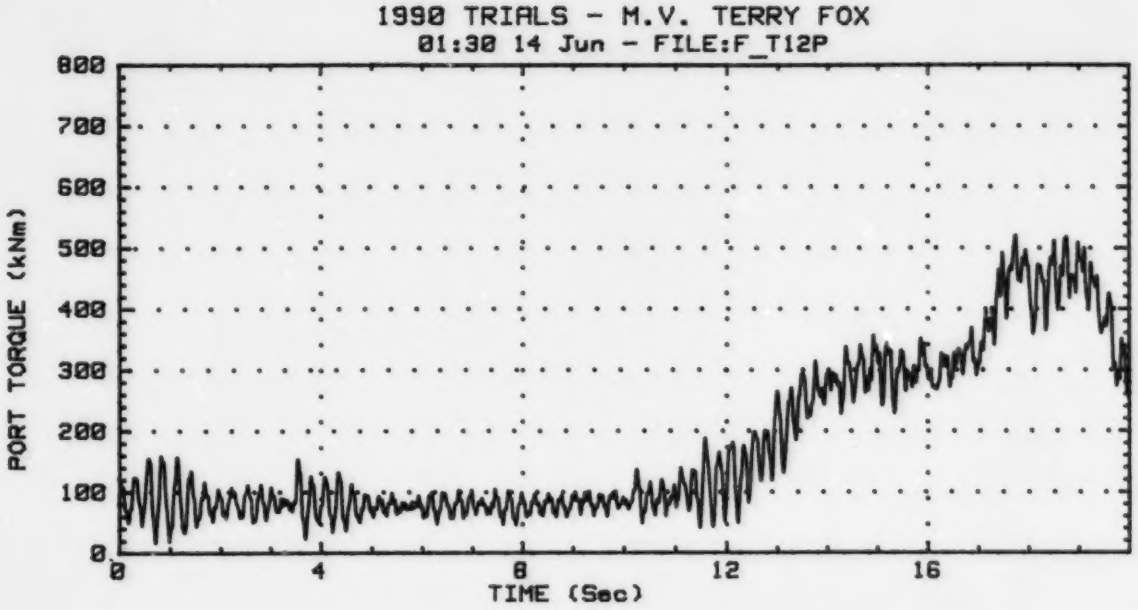

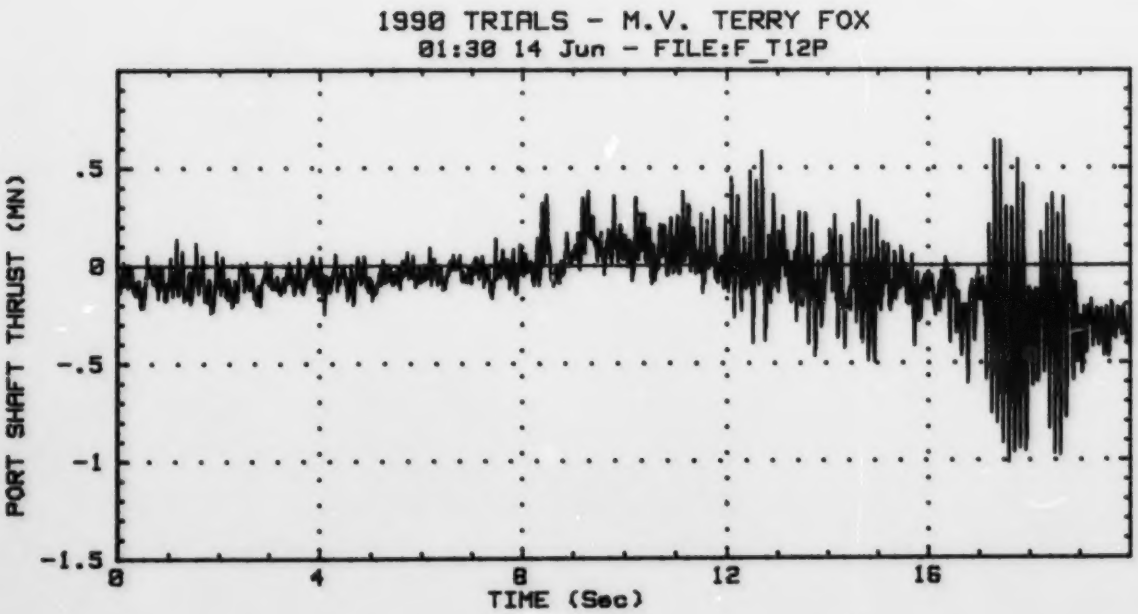

Figure 5.8.14 Starboard and Port Shaft Pitch and RPM: M.V. Terry Fox Test H12

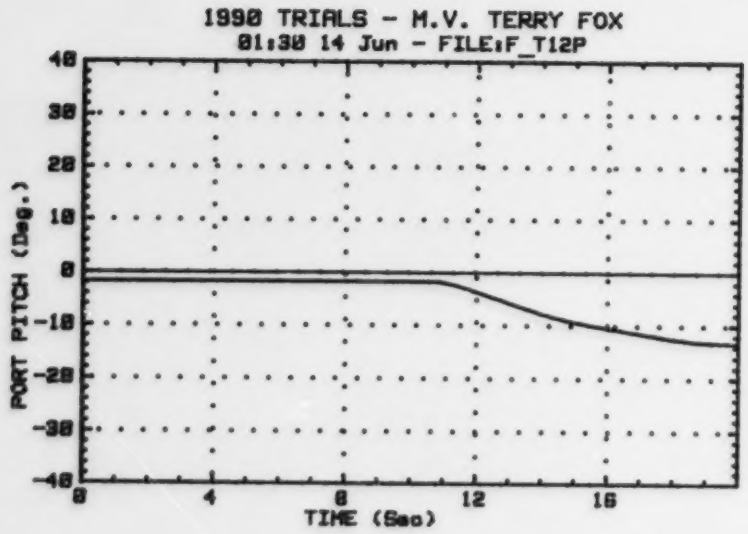

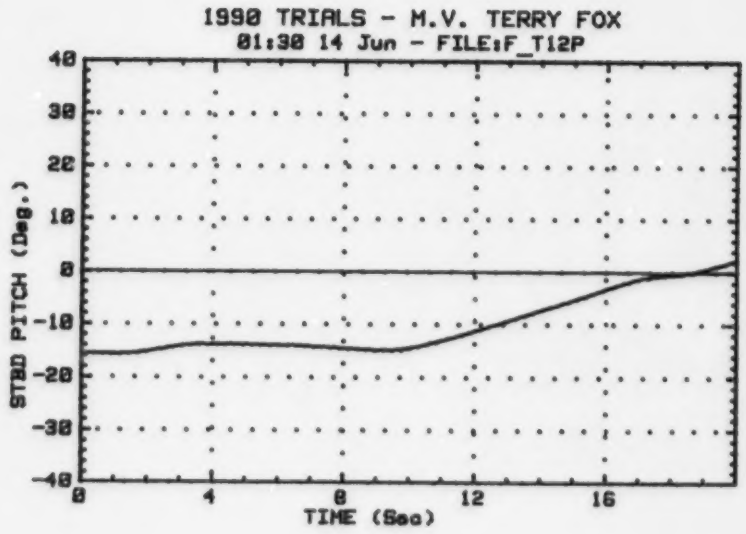

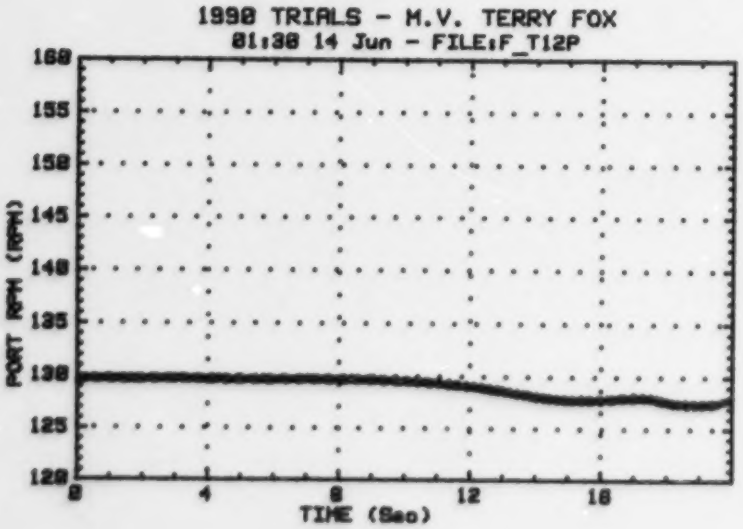

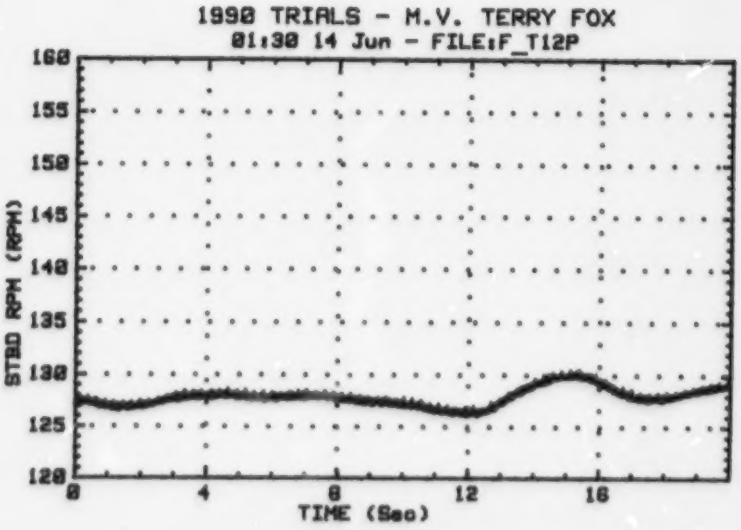

Figure 5.8.15 Port Shaft Torque and Thrust: M.V. Terry Fox Test H12: 0-20 Sec.

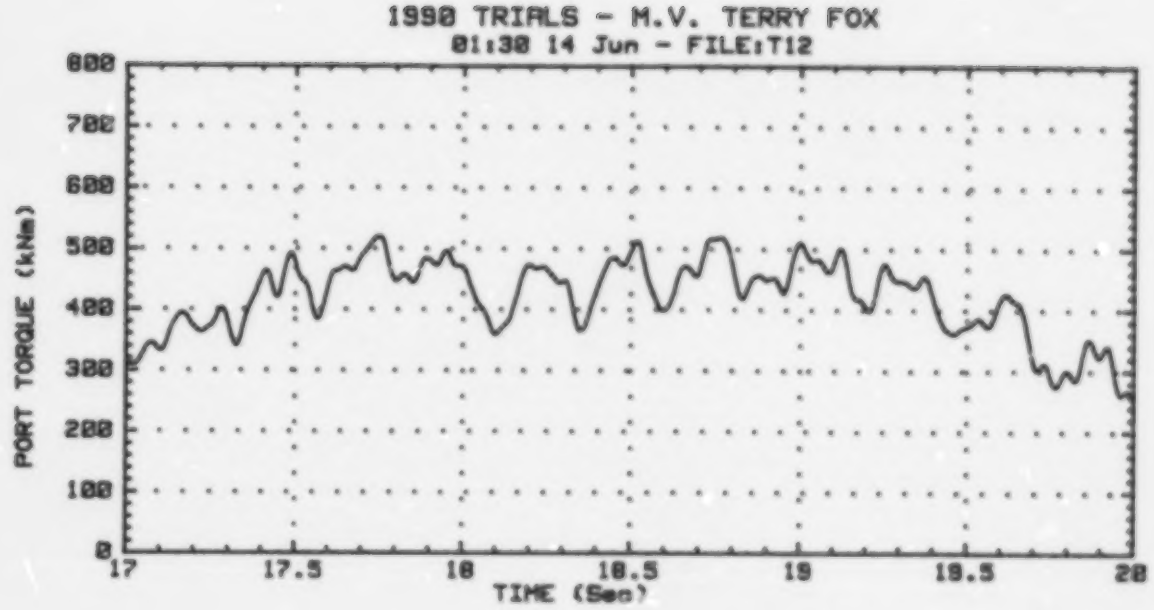

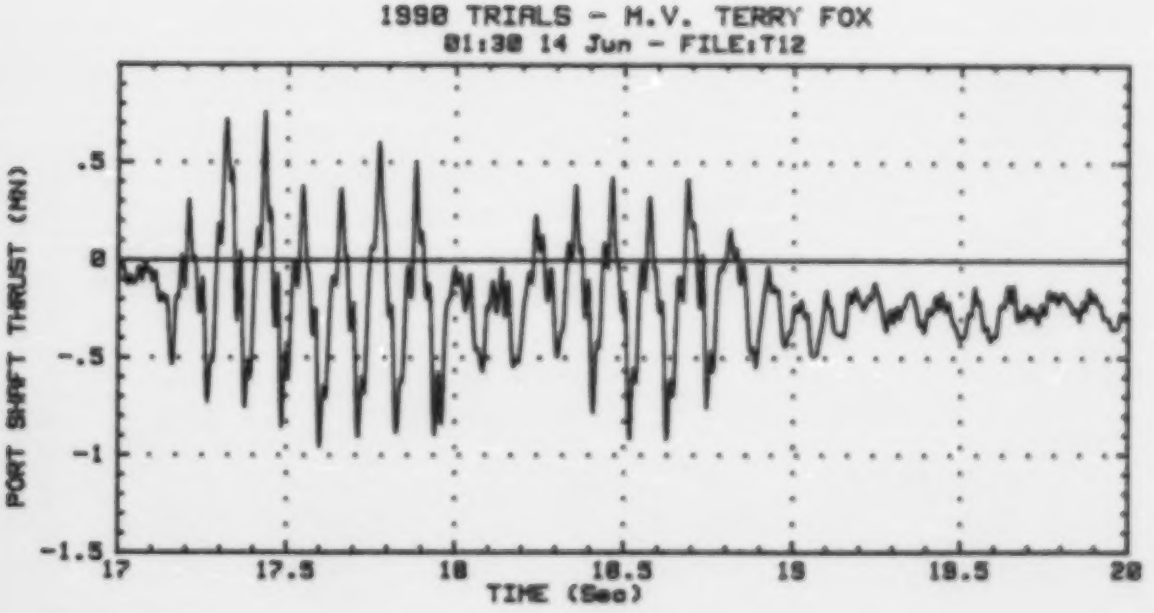

Figure 5.8.16 Port Shaft Torque and Thrust: M.V. Terry Fox Test H12: 17-20 Sec.

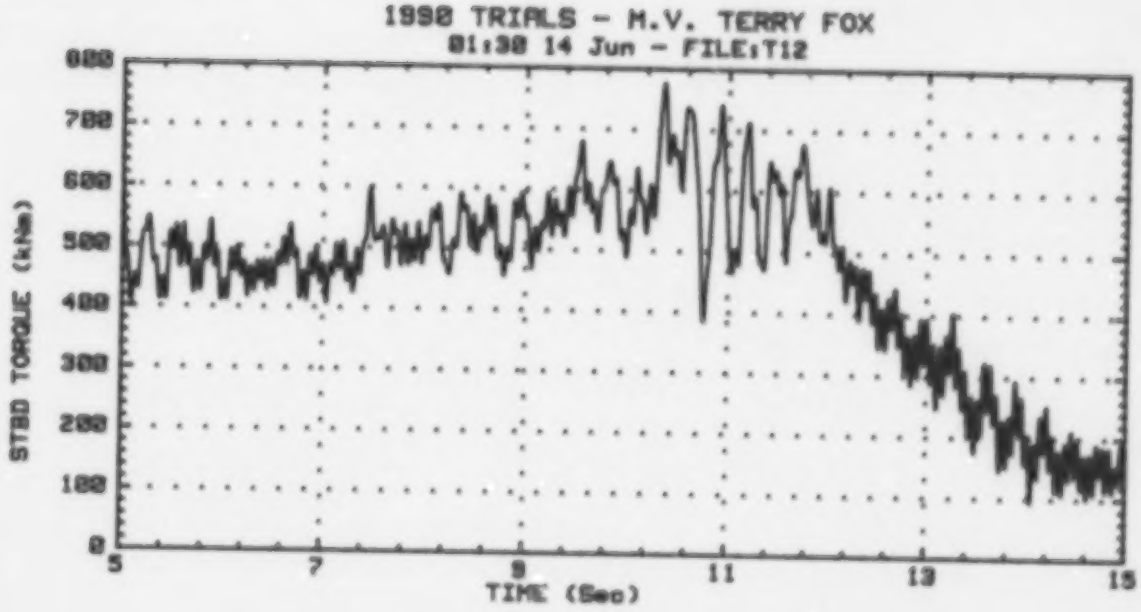

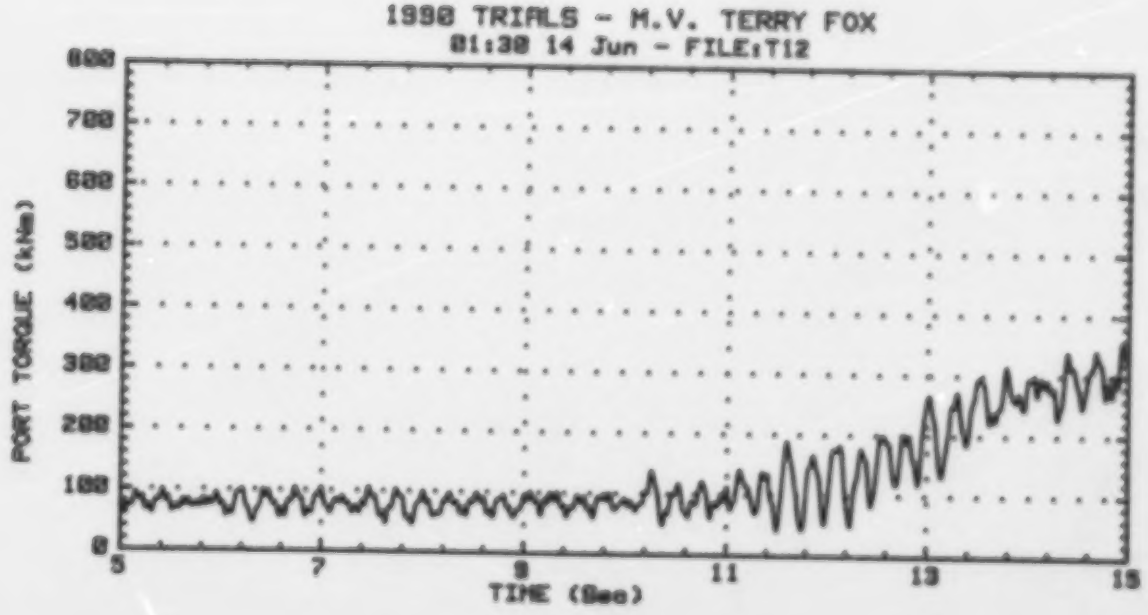

Figure 5.8.17 Port and Starboard Torque: M.V. Terry Fox Test H12: 5-15 Sec.

SECTION 6

CONCLUSIONS

6. CONCLUSIONS

The following main conclusions were made as a result of this work:

1. The maximum resistance for the MV Terry Fox was measured to be 0.95 MN at 3.3 knots. The maximum resistance for the MV Ikaluk was measured to be 0.77 MN at 2.77 knots.

2. The maximum self-propulsion speed attained was 3.6 knots (thrust of 1.34 MN) for the M.V. Terry Fox, and 2.3 knots (thrust of 0.89 MN) for the M.V. Ikaluk.

3. The resistance and power of the two vessels varied linearly with velocity over the tested speed ranges (0.5- 3.6 knots).

4. The thrust deduction fraction in ice is approximately the same as that for the open water overload condition at the corresponding speed and resistance for the M.V. Terry Fox. It ranged from 0.05 at 0.5 knots to 0.25 at 3.6 knots.

5. The thrust deduction fraction for the M.V. Ikaluk was much higher in ice than in open water. It ranged from 0.05 at 0.5 knots to 0.16 at 2.0 knots in ice, and was low (in the range of 0.02 to 0.05) in the open water overload condition. In the open water overload condition the thrust deduction was approximately equal to the hydrodynamic thrust provided by the nozzle.

6. The shaftline of the ducted propeller (M.V. Ikaluk) was measured to have significantly higher axial (thrust) vibrations than the open screw propeller (M.V. Terry Fox).

7. There was not a significant difference in the relative peak shaft torques measured between the nozzled and open screw propellers. The peak shaft torque during ice milling was measured to be 150% and 134% of the MCR torque for the M.V. Ikaluk and the M.V. Terry Fox respectively.

8. Generally more ice-propeller interaction was noticed on the nozzled vessel than on the open screw vessel. Both types of shaftlines had approximately the same high damping present in the axial and torsional modes.

The results from the full scale towing tests and the self-propulsion tests can be used to verify or revise scaling laws for icebreaker powering performance. In addition the results provide data for the calibration of empirical, model test, and numerical model methods of performance prediction. Further insight into the phenomenon surrounding ice/propeller interaction and the corresponding shaftline response was also attained for both open and ducted controllable pitch propellers, by direct, side by side operation of the vessels.

SECTION 7

BIBLIOGRAPHY

7. BIBLIOGRAPHY

American Bureau of Shipping, Rules for Building and Classing Steel Vessels Under 61 Meters (200 Feet) in Length, 1983.

American Bureau of Shipping, Rules for Building and Classing Steel Vessels Over 61 Meters (200 Feet) in Length, 1988.

Antonides, G., Hagen, A., Langrock, D., Full Scale Icebreaking Stresses on Propellers of the Polar Star, SNAME New York Section, 1981.

Arctic Water Pollution Prevention Act, Arctic Shipping Pollution Prevention Regulations, C.R.C. 1978, c. 353, No. 1- January 1985.

Arctec Canada Limited, Experimental Determination of Factors Affecting Loads Imposed on Propellers in Ice, TDC Report TP 6812E for Transport Canada, July 1985.

Arctec Canada Limited, Methods for Predicting Forces Encountered by Propellers During Interactions With Ice, Report 75C-1 for Transport Canada, March 22, 1976.

Arctec Canada Limited, M.V. Arctic Machinery Vibration, Report 1146c.1 for Canadian Coast Guard and Canarctic Shipping Limited, October, 1982.

Arctec Canada Limited, Results of Trials In Ice & Open Water of CCGS Pierre Radisson, Report 245C-8 for Canadian Coast Guard Fleet Systems - Technical, November, 1979.

Arctec Canada Limited, Polar Class Antarctic 1984 Level Ice Resistance Tests, TDC Report TP 7813E for Transport Canada, March, 1985.

Arctec Canada Limited, Consolidation of Previous Years of Polar Class Work, Report I723-C for Transport Canada, October, 1985.

Arctec Canada Limited, Design of Rudders, Rudder Stocks and Steering Systems, Preliminary Regulation Outline,Task 7, Kanata, Ontario, March, 1986.

Arctec Canada Limited, Evaluation of the Performance of a Modern Commercial Icebreaker, The Report on the 1986 Trials of M.V. Kalvik, Volume 1, Main Report, Kanata, Ontario, February 1987, TP 8269E.

Arctec Canada Limited, M.V. Kalvik Propulsion System Full Scale Tests, TDC Report TP 8401E for Transport Canada, March, 1987.

Babanin V.F. and Sokov E.V., Abstract: Stern Tube Bearings - Operational Experience in the Icebreaker " Lenin ", USSR Ministry of Shipbuilding, 1980.

Bathe, K.J. and Wilson, E.L., Numerical Methods in Finite Element Analysis, 1976
Bathe, K.J., Wilson, E.L., Peterson, F.E., SAP IV - A Structural Analysis Program for Static and Dynamic Response of Linear System, Earthquake Engineering Research Centre Report No. 73 -11, University of California, Berkeley, California, 1974.

Belyashov, V.A., and Shpakov, V.S., On Mechanics of Ice Crushing by Propeller Blades, Nauka, Academy of Science of the USSR., Ice Mechanics and Physics

Bulat, V., and Glen, I.F., The Testing of a Ship Model in Ice for the National Research Council, Arctec Canada Limited Reportr No. 335C-3, Kanata, Ont 1981.

Bureau Veritas, Rules and Regulations for the Classification of Steel Ships, August 1985

Canarctic Shipping Limited, M.V. Arctic, Statistical Measurement of Structural Propulsion and Steering System Loads, Report TP-8289E for Canadian Coast Guard Northern, February, 1987.

Cheronov S., Abstract: Trials of the Main Shafts of the Icebreaker.," Kaptain Evdokimov ", Ministry of Inland Waterways Shipping, USSR, 1984.

Chernov S. and Merkulov V. , Loads in the shaft of River Icebreakers, The Journal of the RSFSR Ministry of River Shipping, No. 6, 1986.

Cheung, Y.K. and Yeo, M.G., A Practical Introduction to Finite Element Analysis, Pitman Publishing Ltd., London, 1979.

Cowper, D.N.B., Murray, Dr. A., Modeling of Ice Class Shafting Systems, Ice Tech '90, SNAME Arctic Section, March 1990.

Cowper, D.N.B., Murray, Dr. A., The Shaft Modeling Tool Kit (A Software Package for the Dynamic and Static Analysis of Marine Shaftlines), Spring Meeting, SNAME Pacific Northwest Section, March 1989.

Cowper, D.N.B., Dynamic Torsional Analysis of the Polar 8 Icebreaker Shaft Line, for Polar 8 Icebreaker Consructors, August, 1988.

Cowper, D.N.B., Edgecombe M.H., System Design and Evaluation of the USCGC "Polar Sea", 1985 Global Ice Impact Tests, SNAME Arctic Section, November 1986.

Cowper, D.N.B., Edgecombe M.H. , Ritch R. and Semery Pierre L., The 1986 M.V. Kalvik Propulsion System Full Scale Tests: Bearing Instrumentation and Data, SNAME Propeller's 88 Symposium, Virginia Beach, Virginia, USA, September 1988.

Cowper, D.N.B , "M.V. Robert Lemeur", Propulsion System Torsional Response to Ice Loads and Operator Commands , Canmar Internal Report, May 1983

Dally J., Riley, W., Experimental Stress Analysis, McGraw Hill, 1978.

Dashnaw, F.J., Winn, L.W., Evaluation of Selected Lip Seals/Liners for Propulsion Shafts of Merchant Ships, SNAME, Propellers '81 Symposium, Virginia, 1981.

DeBord, F.W., Voelker, R.P., Geisel, F.A., Coburn, J.L. and Dane, K.E., Winter 1981 Trafficability Tests of the USCGC Polar Sea: Volume V - Bollard and Tow-Rope Pull Tests, Arctec Incorporated Report No. 583C-3, Columbia, Md., 1981.

DeGeorge, V.A., Combined Effect of Vertical and Horizontal Lineshaft Alignment on Main Reduction Gear, SNAME, 1981.

Edwards, R.Y., Major R.A., Kim, J.K., German, J.G., Lewis, J.W. and Miller, D.R., Influence of Major Characteristics of Ice-breaker Hulls on Their Powering Requirements and Maneuverability in Ice, TRANS SNAME Vol 84, 1976.

Edwards, R.Y., Lewis, J.W., Wheaton, J.W., and Coburn, J.L., Full Scale and Model Tests of Great Lakes Icebreaker, TRANS SNAME, Vol 80, 1972.

Edwards, R.Y., Johnson, B., Dunne, M., Comfort, G., and Bulat, V., Results of Full Scale Trials in Ice of CCGS Pierre Radisson, Proceedings, SNAME Sixth Ship Technology and Research (STAR) Symposium, Paper No. 23, 1981.

Forrest Jr., A.W., Labasky, R.F., Shaft Alignment Using Strain Gages, SNAME Philadelphia Section, 1980.

Freathy, R.G., Developments in Ducted Propulsion Technology.

Harvald, S.A., Tug Propulsion: Wake, Thrust Deduction, and R.P.M., European Shipbuilding, Vol 12, No. 3, 1963.

Harvald, S.A., Wake and Thrust Deduction at Extreme Propeller Loadings, Swedish State Shipbuilding Experimental Tank, Publication No. 61, Gotegorg, 1967.

Johansson, B.M. and Revill C.R., Future Icebreaker Design, International Polar Transportation Conference, Vancouver, 4-8 May, 1986.

Juurmaa, K. and Segercrantz, H., On Propulsion and its Efficiency in Ice, SNAME Spring/Star Symposium, June 1981.

Jussila, M., Ice Loads on the Propulsion System of an Ice Breaking Tug, Technical Research Centre of Finland.

Kashtelyan, V.I. and Faddeev, O.V., Problems and Tendencies in Studies of Ice Propulsion of Ships, Nauka, Academy of Sciences of the USSR., Ice Mechanics and Physics, 1983.

Kashteljan, V.I., Poznjak, I.I., and Ryylin, A.J., Ice Resistance to Motion of a Ship (Translation), Sudostroenie, Leningrad, 1968.

Kolotygin, V.V., Results of the Trial Operation of Plastic Propellers Under Ice Conditions, Sudostroenie, USSR, 1981.

Kotras, T., Humphreys, D., Baird, A., Morris, G., Morley, G., Determination of Propeller-Ice Milling Loads

Laskow V., Spencer P.A., Bayly I.M., The M.V. Robert Lemeur Ice-Propeller Interaction Project: Full Scale Data, SNAME, 1985.

Langrock D.G., Wuehrer W., Vassilopoulos L.,The Performance of the Controllable Pitch Propellers on the U.S. Coast Guard Polar Class Icebreakers, SNAME, 1981.

Laskey, N.V., Design of Steering Gears, Rudders, Rudderstocks, and Propeller Protection for Canadian Arctic Class Vessels, SNAME New England Section, 1979.

Lecourt, E.J., Major, R.A., Thomas, H.L. and Naegle, J.N., Recent United States Coast Guard Efforts to Improve Icebreaking Efficiency, Proceedings, SNAME Spring Meeting (STAR) Symposium, 1978.

Lewis, J.W., DeBord, F.W., Bulat, V.A., Resistance and Propulsion of Ice-Worthy Ships, SNAME, November 1982

Lewis, J.W. and Edwards, R.Y., Jr., Methods for Predicting Icebreaking and Ice Resistance Characteristics of Icebreakers, TRANS SNAME, Vol 78, 1970.

Lloyd's Register, Rules and Regulations for the Classification of Ships, January, 1989

Malyi, P. and Segal, Z., Determining the Propulsive Performance of Ships in Ice, Rechnoi Transport, USSR, 1980

McKernan, J., Propulsion Shafting Installation and Alignment Procedures, SNAME Spring Meeting Star Symposium, 1986.

Milano, V.R., Ship Resistance to Continuous Motion in Ice, TRANS SNAME, Vol 81, 1973.

Milano, V.R., Ship Resistance to Continuous Motion in Ice, PhD Dissertation, Stevens Institute of Technology, Hoboken, J.J., 1972.

Ministry of Defence UK, Naval Engineering Standard (NES) 304 Part 2, Issue 1, May 1982 (CONFIDENTIAL)

Ministry of Defence UK, Naval Engineering Standard (NES) 304 Part 1, Issue 2, July 1983 (CONFIDENTIAL)

Murdey, D.C., Resistance and Propulsion Experiments with Model 327-1 and Propellers 66C and 66R, National Research Council MDSL Report LTR-SH-269, 1980.

Narbut, F.L., Factors Affecting the Selection of a Controllable-Pitch Propeller, SNAME New England Section, 1974.

Parsons, M.G., Mode Coupling in Torsional and Longitudinal Shafting Vibrations, Marine Technology, 1983.

Parsons, M.G., Vorus, W.S., Added Mass and Damping Estimates for Vibrating Propellers, SNAME, Propellers '81 Symposium, Virginia, 1981.

Paz, M., Structural Dynamics Theory and Computation, second edition, Van Nostrand Reinhold Company, New York, 1985.

Shigley, Joseph E., Mechanical Engineering Design, McGraw Hill, Copyright 1977.

SNAME Panel, Results of a Survey on Shaft Alignment Procedures used by American Shipyards, Panel, M-16, March 1978

SNAME Panel, Longitudinal Stiffness of Main Thrust Bearing Foundations, Panel M-20, September 1972.

Thomson, W.T., Theory of Vibration with Applications, Second Edition, Prentice-Hall, Inc., Englewood Cliffs, New Jersey, 1981, pp. 296 - 339.

Vance, G.P., Gracewski, A.S., and Goodwin, J.J., Full-Scale Icebreaking Tests of the USCGS Katmai Bay, Proceedings, SNAME Sixth Ship Technology and Research (STAR) Symposium, Paper No 25, 1981.

Vassilopoulos, L., The Use of Proximity Probes for Sterntube Boring Verification and Tailshaft Monitoring on Trails and In Service, SNAME International Maritime Innovation Symposium, New York, 1984.

Vassilopoulos,L., Hamilton, F.M., Longitudinal Stiffness Analyses for the Propulsion Shafting Systems of the Polar Class Icebreakers, ASNE Day, May, 1980.

Volcy, G.C., Interaction and Compatibility Between Machinery and Hull from a Static and Vibratory Point of View, SNAME, 1978.

Wind J., The Dimensioning of High Power Propeller Systems for Arctic Icebreakers and Ice Breaking Vessels., 5th Lips Propeller Symposium, 19-20 May 1983.

Wu, Jong-Shyong, Chen, Wen-Hsiang, Computer Method for Forced Torsional Vibration of Propulsive Shafting System of Marine Engine With or Without Damping, SNAME Headquarters, 1981.

Wuehrer, W., The Polar Class Controllable Pitch Propellers and their Impact on Vessel Performance, Escher Wyss Inc. W. Germany, SNAME, LSAC 83.6.

Mourelatos Zissimos P. and Parsons Michael G., Finite - Element Analysis of Elastohydrodynamic Stern Bearings, SNAME Transactions, Vol. 93, 1985.

Ice Property

Edwards, R.Y., Dunne, M.D., Comfort, G., Tam, G., Nawwar, A., Balat, V., and Steele, M., 1979, Results of Trials in Ice and Open Water of CCGS Pierre Radisson, contractor report 245 submitted by Arctec Canada Ltd to the Canadian Coast Guard.

Frankenstein, G.E., and Garner, R., 1967, Equations for Determining the Brine Volume of Sea Ice From -0.5°C to -22.9°C, Journal of Glaciology, Vol. 6, No. 48.

Lainey, L., and Tinawi, R., 1984, The Mechanical Properties of Sea Ice - A Compilation of Available Data, Canadian Journal of Civil Eng., Vol. 11, no. 4, p. 884-923.

Lane, J.F., 1980, On the Strengths of Sea Ice and a Correlation Between the Various Strength Tests, NRC Internal Report LTR-LT-104.

Lee, J., Ralston, R., and Petrie, D.H., 1986, Full-Thickness Sea Ice Strength Tests, proc. IAHR Symposium on Ice Problems, Iowa City, Iowa, USA.

Mellor, M., 1983, Mechanical Behaviour of Sea Ice, CRREL Monograph 83-1.

Michel, B., 1978, Ice Mechanics, Laval University Press, Quebec City.

Noble, P., and Comfort, G., 1979, Ice Trials to Evaluate Low Friction Coating on CCGS LOUIS S. ST. LAURENT, contractor report 357 submitted by Arctec Canada Ltd to the Canadian Coast Guard.

Petrie, D.H., and Poplin, J.P., 1986, Comparison of Small-Scale and Large-Scale Sea Ice Strengths, proc. IAHR Symposium, Iowa City, Iowa, USA.

Tabata, T., 1966, Studies of the Mechanical Properties of Ice IX - Measurement of the Flexural Strength In-Situ (3), Low Temperature Science Ser. A., V.24, p. 259-268.

Tabata, T., Fujino, K., and Aota, M., 1966, Studies of the Mechanical Properties of Sea Ice XI. The Flexural Strength of Sea Ice In-Situ. Physics of Snow and Ice, International Conference on Low Temperature Science, Sapporo, Japan.

Timco, G., and Frederking, R., 1989, Seasonal Compressive Strength of Beaufort Sea Ice Sheets, proc. IUTAM Symposium on Ice-Structure Interaction, St. John's, Newfoundland.

Timco, G., and Frederking, R., 1989, Compressive Strength of Sea Ice Sheets, Cold Regions Science and Technology.

Wang, Y.S., and Piplin, J.P., 1986, Laboratory Compressive Tests of Sea Ice at Slow Strain Rates from a Field Test Program, Proc. OMAE 86, Tokyo, Japan, Vol. 4., pp 379-384.

Weeks, W.F., and Anderson, D.L., 1958, An Experimental Study of the Strength of Young Sea Ice, Trans. of American Geophysical Union, vol. 39, no. 4., p. 641-647.

Weeks, W.F., and Assur, A., 1967, The Mechanical Properties of Sea Ice, CRREL Monograph, MP-467.

APPENDIX

MV TERRY FOX AND MV IKALUK TRIALS LOG

M.V.TERRY FOX/IKALUK TOWING TRIALS

TRIALS LOG ON BOARD M.V.IKALUK

SUNDAY 10 JUNE 1990

20.03 IKALUK MOVES AWAY FROM WINTER MOORING. RUNNING IN NEW LINERS AT 40% POWER.
21.00 RUNNING IN FINISHED. IKALUK CONTINUES TO OVERNIGHT LOCATION BY TEST AREA. MAKES STEADY SPEED OF CLOSE TO 1 M/S AT MAX POWER IN 1.5 - 2.0 M OF DETERIORATED ICE.
22.00 ON LOCATION. T.FOX YET TO MOVE.
24.00 T.FOX MOVES UP.
24.45 CLOSE DOWN.

MONDAY 11 JUNE 1990

08.00 LIGHT SNOW. VISIBILITY 0.5 - 1 KM.
ICE PARTY TAKES CORE NEXT TO IKALUK. 1.6 M THICK.
MEASURES ICE THICKNESS EVERY 100 M FROM VESSELS TO ICE EDGE.
09.00 ICE PARTY RETURNS ON BOARD.
T.FOX RECALIBRATING SEVERAL CHANNELS.
09.00 T.FOX POSITION INDICATOR NOT WORKING.
SPARE EQUIPMENT TAKEN OVER TO FOX.
ADJUSTING DRAFTS ON IKALUK.
10.00 LIGHT SNOW, VISIBILITY 1 KM.
IKALUK CLUTCHING IN.
10.30 WEATHER SUDDENLY CLEARS. VISIBILITY 3 KM.
11.05 READY TO BREAK ICE.
DRAFT 8.03 M. HEADING 105 DEG.
11.19 RUN SELF PROPULSION TEST NO. IK-SELF 1 .
100% POWER. STRAIGHT RUN OF ABOUT 5 SHIP LENGTHS. INITIALLY AT ABOUT 2.8 KNOTS, THEN REDUCING TO A STEADY 2.2 KNOTS. NO RADIAL CRACKS GENERATED IN THE ICE. WIND SPEED 26 KNOTS.
DATA PRINTED OUT. LOOK GOOD EXCEPT PORT TORQUE A LITTLE HIGH.
12.30 RUN SELF PROPULSION TEST NO. IK-SELF 2.
RUN STARTS WITH ABOUT 70% POWER. SPEED FLUCTUATES FROM 0.3 - 0.8 KNOTS WITH A STEADY PORTION OF ABOUT 0.6 KNOTS FOR 1 SHIP LENGTH. VESSEL THEN STOPPED BY ICE. POWER MAINTAINED AND VESSEL EVENTUALLY MOVES AGAIN. INCREASE POWER TO 85% FOR NEXT RUN.
12.50 RUN SELF PROPULSION TEST NO. IK-SELF 3.
NOTED THAT THE SIDE OF THE BROKEN TRACK FOR RUNS 2 AND 3 IS MORE JAGGED THAN FOR RUN 1. POSSIBLY MORE VARIATION IN THE ICE IN THIS AREA.
12.57 RUN SELF PROPULSION TEST NO. IK-SELF 4.
100% POWER. STOPPED AFTER ABOUT 2 MINS - DATA DISC FULL. CANCEL RUN.
DECIDED TO HEAD FOR THE ICE EDGE AND CUT OUT THIN ICE AT THE END OF THE INTENDED TOWING TRACKS.
T.FOX SORTING OUT RANGE PROBLEMS.
13.50 ARRIVE AT ICE EDGE. HEADING TO TEST AREA TO CUT OUT

WEAK ICE EDGE.
FOX NOT MOVING YET BUT INSTRUMENTATION PROBLEMS ARE SORTED OUT.

14.18 STOPPED IN ICE EDGE AT TEST ZONE FOR SELIDAS POSITION CHECK.

14.30 WIND 29 KNOTS.

15.50 FOX SORTING OUT DATA STORE PROGRAM.
READY AT END OF FIRST MARKED TRACK FOR OFFLOADING ICE PARTY AND RUNNING LINE.

16.10 ICE PARTY SET DOWN ON ICE.

17.05 ICE PARTY DRILLING ALONG FIRST TOW TRACK. CHECKING VALUES MEASURED DAY BEFORE.
PORT TORQUE CALIBRATION CONSTANT FOUND TO BE IN ERROR. CORRECTED.

17.25 ICE PARTY BACK ON BOARD.
FOX TURNING INTO POSITION AT BEGINNING OF FIRST TOW TRACK.

19.00 ICE CORE TAKEN NEXT TO IKALUK.
LINKING MOORING LINE LEADER FROM FOX TO IKALUK'S LEADER.

21.00 ATTACHING TOW CABLE TO FOX'S BRIDLE.
A CRACK IS NOTED FOR ABOUT 100 M FORWARD OF FOX'S BOW.

21.06 START FIRST TOWING TEST. IK-PU-FOX 1.
IKALUK PULLS AHEAD VERY SLOWLY, PAYING OUT SOME CABLE. FOX HOLDS WITH ASTERN THRUST.

21.19 FOX MOVES AT SLOW SPEED WITH PULL OF 30-35 TONNES. FOLLOWED BY HIGHER SPEEDS AT PULLS OF ABOUT 50 TONNES AND 90-100 TONNES. SPEED AT END OF RUN ABOUT 4.5 KNOTS. LAST PART OF ICE WAS SOFTER OR CRACKING OCCURED SINCE FOX CONTINUED TO MOVE WELL AFTER TOW FORCE DROPPED.

21.31 TOWING TEST COMPLETE.

22.30 CABLE RECOVERED.
IKALUK MOVES TO TRIM ICE EDGE.
FOX TO CARRY OUT SP TESTS 300 M NORTH OF TOWED TRACK. THEN POSITION FOR NEXT TOW TEST.

TUESDAY 12 JUNE 1990

00.00 IKALUK AND FOX ON LOCATION FOR RUNNING TOW WIRE OVERNIGHT.

08.30 CABLE ATTACHED AND READY TO TOW.

08.45 START SECOND TOWING TEST. IK-PU-FOX 2.
70% POWER, APPROX. 2.5 KNOTS.
100% POWER, APPROX. 3 KNOTS.

08.56 TOWING TEST COMPLETED.
VESSELS MOVE INTO OPEN WATER WITH TOWLINE ATTACHED FOR OPEN WATER OVERLOAD TESTS.

09.30 COMMENCE OPEN WATER OVERLOAD TEST IK-OV-FOX 1.
IKALUK PULLS AHEAD AT DIFFERENT FORWARD SPEEDS AND TOW ROPE PULLS WHILE FOX PROVIDES THE BRAKE USING REVERSE THRUST.
WHEN IKALUK HAD ABOUT 3 KNOTS FORWARD SPEED AT ABOUT 75% POWER, T.FOX STARTED TO FISHTAIL AND WAS VERY DIFFICULT TO CONTROL. SOME OVERLOAD DATA OBTAINED FOR IKALUK. DECIDED TO MOVE AHEAD WITH NEXT TOW AND

	COMPLETE PROPULSION OVERLOAD LATER WITH VESSELS PULLING BACK TO BACK.
10.00	REELING IN TOW CABLE.
	ICE PARTY COMPLETES MEASURING THIRD TOW TRACK.
10.20	TOW DISCONNECTED.
10.50	LINES TRANSFERRED FROM FOX TO IKALUK.
12.40	ICE PARTY BACK ON BOARD.
	FOG SURROUNDS VESSELS.
13.08	POSITIONED FOR PROPULSION RUN BETWEEN TOW TRACKS 1 & 2.
13.12	START SELF PROPULSION RUN IK-SELF-4.
	FULL POWER. VISIBILITY 1 KM. WIND CALM.
	RADIAL CRACKS GENERATED ALONG RUN.
13.40	STOPPED TO REPLACE LEAKY FUEL VALVE.
	INTEND FULL POWER RUN TO START OF FIRST IKALUK TOW TEST.
14.00	TURNING FOR START OF SELF PROPULSION RUN.
14.40	READY FOR RUN.
14.45	START SELF PROPULSION RUN IK-SELF-5.
	100% POWER. PROCEEDED ABOUT 3 SHIP LENGTHS AT ABOUT 1.6 KNOTS.
	NO RADIAL CRACKING.
15.40	FOX POSITIONING HERSELF FOR TOWING IKALUK.
16.20	READY FOR FURTHER SELF PROPULSION RUN TO START OF TOW TEST.
16.27	START SELF PROPULSION RUN IK-SELF-6.
	60% POWER. CRACK STARTED RUNNING AHEAD OF VESSEL FOR ABOUT 4 SHIP LENGTHS AND THEN MOVED OFF ON PORT BOW.
	REACHED SPEED OF ABOUT 4 KNOTS.
	STOPPED AT END OF RUN IN POSITION FOR TOW TEST.
	CRACK ON PORT BOW. SMALL CRACK AHEAD.
16.55	READY TO RUN LINES.
18.45	STILL PULLING LINES - ONE PARTED PREVIOUSLY.
19.45	CABLE RUN AND CONNECTED.
20.00	READY FOR FIRST TOW OF IKALUK.
20.21	START FIRST TOW TEST OF IKALUK. FOX-PU-IK1.
	FOX PULLS ABOUT 50 TONNES. IKALUK REVERSE THRUST ABOUT 35 TONNES. TOW BLOCK APPEARS TO READ HIGH.
	CANCEL TEST START AND CHECK INSTRUMENTATION.
23.00	INSTRUMENTATION CORRECTED. RESUME RUN IK-TOW-1.
	3 SPEEDS ON THE RUN. FIRST TWO WITH ABOUT 45 AND 75 TONNES PULL. INITIAL CRACK ON PORT SIDE RAN AWAY TO 3 BEAMS AFTER 1-2 SHIP LENGTHS, ABOUT HALF WAY THROUGH FIRST SPEED. NO ADDITIONAL CRACKS GENERATED DURING FIRST 2 SPEEDS. THIRD SPEED WITH ABOUT 100 TONNES PULL. RADIAL CRACKS GENERATED ON STARBOARD BOW.
23.04	END OF FIRST IKALUK TOW.

JUNE 13 1990

01.25	TOWLINE DISCONNECTED
	LEAVING TRACK 3 FOR SELF PROPULSION IN TRACK 4.
02.00	READY FOR SELF PROPULSION ON TRACK 4.

FOUND NECESSARY TO GO NEARER TO SHORE THAN PREVIOUS TRACKS IN ORDER TO FIND GOOD FAST ICE WHICH DID NOT CRACK.

02.03 DATA RECORDED ALMOST CONTINUOUSLY FROM THIS TIME TO ABOUT 03.00. TWO GOOD RUNS WITH NO RADIAL CRACKING TOWARDS THE END OF THIS PERIOD. MARKERS PUT ON ICE AT BEGINNING OF FAST ICE RUNS FOR LATER ICE MEASUREMENT. RUNS IK-SELF-7/8/9 CARRIED OUT.
GOOD RUNS AT SPEEDS OF 1.3-1.4 KNOTS AND ABOUT 2.3 KNOTS.

03.00 IKALUK TURNING FOR RUN TO TOW PICK UP POINT.

04.07 START SELF PROPULSION RUN IK-SP-10 TO TOW PICK UP POINT. SPEED 1.6-2.1 KNOTS. NO RADIAL CRACKING.

09.00 READY FOR SECOND TOW TEST OF IKALUK.

09.05 START TOWING TEST. FOX-PU-IK2.
IKALUK TOWED AT THREE SPEEDS WITH PULLS OF APPROX. 60, 75 AND 95 TONNES. NO RADIAL CRACKING UNTIL VERY END OF RUN NEAR ICE EDGE.

09.20 COMPLETE TOW TEST.

10.30 VESSELS MOVE TO OPEN WATER WITH TOWLINE ATTACHED.
START OPEN WATER TOWING TEST FOX-PU-IK3.
SPEED OF ABOUT 5 KNOTS WITH ABOUT 15 TONNES PULL.
SHAFT DECLUTCHED. FULL AHEAD PITCH. NO FREEWHEELING.

11.00 MOVE INTO BROKEN CHANNEL.
START TOWING TEST FOX-PU-IK4.

11.20 SPEED IN BROKEN CHANNEL 2 KNOTS.

11.26 HIGHER SPEED. DECLUTCHED SHAFT.

11.48 FOX CONTINUES INTO UNBROKEN ICE TOWING IKALUK.

12.03 TESTS COMPLETED.
FREIGHT COMING IN FOR FOX AND IKALUK.

13.09 CHANGING COURSE FOR FULL POWER SELF PROPULSION TEST.

13.25 TAKING ZEROS FOR SELF PROPULSION TEST.
STARBOARD RPM SIGNAL LOST. RPM FROM GAUGE 160.

13.30 START SELF PROPULSION TEST IK-SELF-11.
HEADING TO POSITION FOR NEXT TOW.
THE ICE APPEARS DIFFERENT TO THAT FOR EARLIER TESTS. ICE BREAKS AND CRUMBLES INTO SMALL PIECES OF 1 M^3 OR SO. VERY LITTLE PROP/ICE INTERACTION. OCCASIONALLY ICE IS HARDER, LARGER PIECE SIZE AND MORE PROP/ICE INTERACTION. NO RADIAL CRACKING.
SPEED IS HIGHER THAN 2-3 KNOTS PREVIOUSLY. TYPICALLY 3-3.5 KNOTS BUT UP TO 6 KNOTS AT END OF RUN.

13.50 END RUN AND CHANGE HEADING FOR RUN TO START OF NEXT TOW TEST.
CREW CHANGES.

14.40 START SELF PROPULSION TEST IK-SP-12.

14.43 STOP RUN TO RETRIEVE CARGO NETS FROM ICE.

14.57 RESUME RUN AS IK-SP-13.
ICE IS FAIRLY SOFT AND VARIABLE. NO RADIAL CRACKING.

15.10 END RUN.

18.49 CABLE HOOKED UP FOR TOW.
ICE PARTY FINISHING MEASURING TRACK.
SLIGHTLY OVERCAST CONDITIONS.
LIGHT WIND ON PORT BEAM.
THE ICE IN THIS AREA AND FOR SP TESTS IMMEDIATELY BEFORE IS SAID TO BE A LITTLE THICKER THAN AVERAGE OF LAST FEW DAYS.

19.22 START TOW TEST OF IKALUK FOX-PU-IKS.

19.30 IKALUK HOLDS POSITION UP TO ABOUT 60 TONNES PULL. TOW ROPE PULL GOES UP TO 100 TONNES - DIFFICULT TO START IKALUK MOVING. ONCE IKALUK MOVES, SHE GOES UP TO ABOUT 3 KNOTS, THEN MEETS HEAVIER ICE. RADIAL CRACKING OCCURS AND CONTINUES TO THE END OF THE RUN. FOR A GOOD PART OF THE RUN, IKALUK MAKES ABOUT 3 KNOTS WITH A TOW ROPE PULL OF ABOUT 75 TONNES AND NO RADIAL CRACKING.

19.37 TOW TEST COMPLETED.

20.15 PREPARE FOR OPEN WATER PROPULSION OVERLOAD TESTS. DISCONNECT TOWLINE AND RECONNECT BACK TO BACK WITH T.FOX.

21.15 IKALUK TOWED ASTERN INTO OPEN WATER.

21.30 PROPULSION OVERLOAD TESTS WITH IKALUK TOWING AHEAD.

LOAD TONNES	SPEED KNOTS
30	1.5
60	1.5
55	2.5
85	2.5
80	3.5
110	2.5

23.12 IKALUK OVERLOAD TESTS COMPLETE.

23.15 PROPULSION OVERLOAD TESTS WITH T.FOX TOWING AHEAD.

23.45 FOX OVERLOAD TESTS COMPLETE.
TRIALS PROGRAM COMPLETE.

M.V. TERRY FOX/IKALUK TOWING TRIALS

TRIALS LOG ON BOARD M.V. TERRY FOX

MONDAY 11 JUNE 1990

11.30	IKALUK MOVES OFF FOR SELF PROPULSION TESTS IN ICE	
12.00	AIR TEMP +1°C WIND DIR 33 SPEED 20K	
14.25	BRIDGE CONTROL FOX	
14.30	M.V. TERRY FOX MOVES OUT - CHECK DATA ACQUISITION SYSTEM	
14.45	MANOEUVERING FOR SELF PROPULSION TESTS IN ICE FOR M.V. TERRY FOX	
14.50	SP1 FULL POWER (10)	
	SP2 SETTING (8)	
	SP3 SETTING (6)	
	SP4 SETTING (5P/6S)	
	SP5 SETTING (6.5S/7.55P)	CRACKS TO STBD IN ICE
15.05	COMPLETED SELF PROPULSION TESTS FOR M.V. TERRY FOX MOVE TO TEST SIGHT FOR TOWING	
16.00	AIR TEMP +3°C WIND DIR 31 SPEED 26K	
16.20	MANOUVRE FOR SELF PROPULSION IN ICE	
16.24	SP6 FULL POWER (10)	
16.27	SP7 SETTING (7P/7.5S)	
16.30	SP8 SETTING (5.5P/6.5S)	
16.35	SP9 SETTING (4P/5S)	
16.37	STOP MANOUVRE	
16.55	SP10 SETTING (5P/6S) 300 300 1.7	
17.05	COMPLETE MANOEUVRE FOR TOW TEST	
18.25	MESSENGER OUT FROM IKALUK PROCEEDING WITH HOOK UP	
20.00	AIR TEMP +2°C WIND DIR 33 SPEED 15K	
21.00	HOOK UP COMPLETE	
21.15	TIGHTENING UP TOWLINE	
21.20	T1 FIRST TOW FOR M.V. TERRY FOX	0.5 KNOTS
21.30	TOW TEST COMPLETE	
22.37	TOWLINE DISCONNECTED AND PENNANT IN MANOEUVERING TO CARRY OUT ADDITIONAL SELF PROPULSION IN ICE	
22.47	IN POSITION HDG 250 Ha 8.2m Hf 8.0m	
22.50	SP11 SELF PROPULSION	ABORT (ALARM)
23.03	SP12	CRACKING TO OL CHANNEL
23.11	CROSSED CHANNEL	
23.12	SP13 POWER INCREASE	3.1 KNOTS
23.14	SP14 POWER INCREASE	4.2 KNOTS
23.15	SP15 POWER INCREASE	5.0 KNOTS
23.17	STOP	
23.20	MANOUVRING FOR TOW PICKUP	
24.00	AIR TEMP -1°C WIND DIR 32 SPEED 8K	

M.V. TERRY FOX/IKALUK TOWING TRIALS
TRIALS LOG ON BOARD M.V. TERRY FOX
PAGE 2

TUESDAY 12 JUNE

00.15	ICE MILLING ASTERN
00.31	IN POSITION FOR SELF PROPULSION TO TOW PICKUP
00.34	SP16 SETTING ABT (5)
00.40	STOP
00.43	IN POSITION FOR TOW
01.00	COMMENCE TO PULL MESSENGER TO IKALUK
03.15	TOWLINE COUPLED TO MESSENGER
04.00	AIR TEMP +1°C WIND DIR 12 SPEED 10K
05.15	TOW WIRE CONNECTED
08.00	AIR TEMP +1°C WIND DIR 09 SPEED 10K
08.38	TIGHTEN UP ON TOW LINE
08.45	T2 ABT 70% POWER OF M.V. IKALUK 2.5 KNOTS
08.52	FULL POWER OF M.V. IKALUK 3.1 KNOTS
08.56	COMPLETE TOW TEST
10.33	TOWLINE DISCONNECTED
	MANOEUVERING TO PASS PENNANT TO IKALUK
11.50	PENNANT PASS COMPLETE
12.00	AIR TEMP +1°C WIND - LIGHT AIRS FOG
12.31	MANOUVRING TO SELF PROPULSION TESTING
12.51	SP17 COMMENCE HDG 256 CRACKING P&S 6.5 KNOTS
12.58	CROSSING CHANNEL
13.00	MANOUVRING TO SOLID ICE SHEET HDG 225
13.04	SP18 STILL SOME CRACKING 4.5 KNOTS
13.05	SP19 SLOWING TO 2.5 KNOTS
	CRACKING STOPPED
13.07	SP20 INCREASE TO 2.9 KNOTS
13.09	COMPLETE SELF PROPULSION TESTS
13.12	HIGH SPEED DATA ACQUISITION - BACKING IN ICE
13.38	MANOUVRING TO TOW IKALUK
14.03	STOPPED CREW CHANGE
	MANOUVRING FOR TOW TEST
16.00	IN POSITION FOR TOW
	AIR TEMP 0°C WIND DIR 08 SPEED 12K
	FOG LIFTING FAST
17.00	ONGOING CREW CHANGES
18.46	COMMENCE RUNNING MESSENGER FOR TOW
19.50	MESSENGER CONNECTED
20.00	HOOK UP COMPLETE
20.15	TENSIONING
23.50	M.V. TERRY FOX TOWING M.V. IKALUK 1.8 KNOTS
22.56	2.7 KNOTS
2300	ACCEL
23.05	COMPLETED FIRST TOWING OF M.V. IKALUK
	PROCEEDING TO DISCONNECT TOW
23.47	TOW LINE DISCONNECTED
24.00	AIR TEMP +1°C WIND DIR 110 SPEED 12K
24.00	MANOUVRING TO PICK UP MESSENGER

	BRING IN TOW LINE
20.00	AIR TEMP +3ºC WIND DIR 08 SPEED 10K
20.25	TOW LINE DISCONNECTED
	MANOUVRING FOR OPEN WATER OVERLOAD TESTS
21.05	LOAD CELL HOOKED UP FOR OVERLOAD TESTS
21.15	TOWING IKALUK STERN FIRST TO OPEN WATER
21.30	OVERLOAD TESTS IKALUK TOWING
23.12	IKALUK TESTS COMPLETE
	FOX OPEN WATER OVERLOAD
	46T @ 0.5K
	66T @ 2.2K
	85T @ 1.8K
	100T @ 4.0K
	103T @ 2.5K
23.38	FOX OPEN WATER OVERLOAD TESTS COMPLETE
23.46	AIR TEMP +5ºC WIND DIR 170 SPEED 1K
	HIGH SPEED DATA ACQUISITION SETUP
	RECORDED SHAFTLINE VIBRATIONS IN SAME ICE SHIFT AS M.V. IKALUK

THURSDAY 14 JUNE 1990

01.30	FINISHED TESTING
02.00	STARTED TO DECOMMISSION INSTRUMENTATION
06.00	FINISHED DECOMMISSIONING
10.00	FLIGHT TO INUVIK

Library and Information Centre /
Centre de documentation (GSC)
RECEIVED / REÇU LE
AUG 27 199
Transport Canada / Transports Canada